Title
Heme oxygenase-1: a host enzyme that limits immune activation during chronic HIV disease

Author
Seu, Lillian

Publication Date
2011

Peer reviewed|Thesis/dissertation

Heme oxygenase-1: A host enzyme that limits immune activation during chronic HIV disease

by

Lillian Seu

DISSERTATION

Submitted in partial satisfaction of the requirements for the degree of

DOCTOR OF PHILOSOPHY

in

Pharmaceutical Sciences and Pharmacogenomics

in the

GRADUATE DIVISION

of the

UNIVERSITY OF CALIFORNIA, SAN FRANCISCO

Power without love is reckless and abusive

Love without power is sentimental and anemic

Martin Luther King Jr.

Dedicated to all HIV positive individuals, their families, and friends

Acknowledgements

Publication reprints:

I. The text of this dissertation/thesis contains a reprint of material as it appears in:

Tryptophan catabolism by indoleamine 2,3-dioxygenase 1 alters the balance of T_H17 to regulatory T cells in HIV disease

David Favre*, Jeffrey Mold*, Peter W. Hunt, Bittoo Kanwar, P'ng Loke, **Lillian Seu**, Jason D. Barbour, Margaret M. Lowe, Anura Jayawardene, Francesca Aweeka, Yong Huang, Daniel C. Douek, Jason M. Brenchley, Jeffrey N. Martin, Frederick M. Hecht, Steven G. Deeks, Joseph M. McCune

Science Translational Medicine 2010 May 19;2(32):32ra36.

*Co-equal first authors

II. The text of this dissertation/thesis contains a reprint of material as it appears in:

Naïve human T cells are activated and proliferate in response to the heme oxygenase-1 (HO-1) inhibitor tin mesoporphyrin (SnMP)

Trevor D. Burt, **Lillian Seu**, Jeffrey E. Mold, Attallah Kappas, Joseph M. McCune, *Journal of Immunology* 2010 Nov 1;185(9):5279-88

III. The text of this dissertation/thesis contains a reprint of material as it appears in:

Variations in the heme oxygenase-1 microsatellite polymorphism are associated with plasma CD14 and viral load in HIV-infected African Americans

Lillian Seu, Trevor D. Burt, John S. Witte, Jeffrey N. Martin, Steven G. Deeks, Joseph M. McCune

Genes and Immunity, In Review

IV. The text of this dissertation/thesis contains a reprint of material as it will appear in:

Circulating myeloid subpopulations differentially predict CD4 recovery in patients during early HAART

Lillian Seu*, Gabriel M. Ortiz*, Steven G. Deeks, Jeffrey N. Martin, Joseph M. McCune

Journal of Infectious Diseases, In Preparation

Co-equal first authors

V. The text of this dissertation/thesis contains a reprint of material as it will appear in:

Inhibition of heme oxygenase-1 in SIV-infected AGMs causes increased immune activation and viremia

Trevor D. Burt, **Lillian Seu**, Rebecca Botelho, David Favre, Yong Hong, Richard M. Dunham, Kristina Abel, Atallah Kappas, Joseph M. McCune

Manuscript in preparation

Pre-doctoral Dissertation/Training Funding:

1) National Institute of Health: T32 GM 07175

   Principal Investigator: Deanna L. Kroetz

   Name: Pharmaceutical Sciences and Pharmacogenomics

   Project Narrative: There is an increasing need for the development of new and effective drug therapies for the treatment of disease that can be tailored for individual patients. Students in the Pharmaceutical Sciences and Pharmacogenomics Graduate Program are trained to be future scientific leaders in this area. Their training will prepare them to develop effective treatment strategies for existing and newly developed drugs that consider the principles of pharmacology and our advancing knowledge of personal genetics.

2) California HIV Research Program: D09-SF-313

   Principal Investigator: Lillian Seu

   Name: Inactivation of HIV-1 by Metalloporphyrin compounds

   Project Narrative: Due to issues such as escape mutations and long-term side effects of existing anti-retroviral medications, it becomes important and necessary to explore alternative drug candidates- particularly ones with a favorable bioavailability and metabolic profiles such as metalloporphyrins. The studies outlined in this proposal will elucidate whether metalloporphyrin compounds could represent a new class of antiretroviral drugs in the treatment of chronic HIV-1 infection.

Personal Acknowledgements

To my thesis advisor, **Mike McCune**: Your encouragement and guidance over these formative years has been such an integral component of my scientific journey. You lead by example, you motivate others with positive feedback, you sincerely want the best for your advisees, and your passion for seeking the bigger picture through focused scientific inquiry is truly an inspiration. It is a bittersweet moment to be leaving the lab- what I will miss the most is knocking on your door and being greeted with a friendly smile and an anecdote (and impromptu kittens). I am happy to know that I have a lifelong mentor and a great friend even after I leave, and I look forward to many fruitful collaborations and interactions in the future.

To my thesis committee member, **Deanna L. Kroetz**: I appreciate all of your encouragement and support over the years as my qualifying exam chair and thesis committee member. Your scientific insights, your positive outlook, and your advice for collaborating with specific researchers for project considerations have enabled many milestones. Thank you for being so supportive, particularly at the moments when they are needed the most.

To my thesis committee member, **Steven G. Deeks**: thank you for many years of lending your clinical expertise in HIV immunology. As a new student of clinical HIV research, much of my initial time in lab was spent on "herding cats." The one important lesson I learned in this field is that the course of HIV disease has many moving parts. But after many meetings with you, I've finally appreciated the nuances of studying a complex disease like HIV. Through your training, I am equipped with understanding the important difference between "statistically significant" versus "clinically significant."

To **Trevor D. Burt** (Trevor-"Perfect Ten"-Burt): It's hard to imagine that it has been 4

years now from when I joined the lab. Back then, I had the great fortune of being in the right place at the right time to be able to receive guidance from a talented, patient, and fabulous physician-scientist. As Mike told me back then "Isn't Trevor a wonderful human being?!" I would only add that you are super-human in many ways for wearing so many hats in the clinic as well as in the lab. Thank you for all that you do, and for being such a great role model (a 10!) as I transition to the next phase of my career.

To **Gabriel M. Ortiz** ("faaancy"): Mix one part detailed clinical infectious disease expertise. Mix one part careful and inquisitive scientific exploration. Mix another part compassion for global health disease burdens. Shake it all up and add a little bit of latin flair while busting a salsa move on the Copacabana dance floor and that's a vignette of what the world gets from GMO. Thank you for being such an inspiring mentor in the lab.

To **McCune Lab:** There are so many role models in lab to make me a more motivated, creative, and honest scientist. Thank you all for leading by example, and for helping me push back the boundaries of my scientific knowledge on a daily basis.

To the **Division of Experimental Medicine**: Some of the most inspiring, empathic, and talented group of scientists and clinicians are found in our hallways and in the 5th floor conference room on Mondays at noon. Thank you all for contributing to the alleviation of global disease burdens, for all of the great collaborative interactions, and friendly chats.

Positive Health Program patients: Thank you to all the patients enrolled in the SCOPE studies for your continued support and contribution to the scientific progresses made in our division. With your dedication and support, we hope to continue advancing better HIV diagnostic measures and therapeutics.

Pharmaceutical Sciences and Pharmacogenomics Graduate Division: Thank you to

Debbie Acoba for all of her support over the years as well as to the incredibly talented and enthusiastic students that I continue to learn from and get motivated by. Special thanks to Anita Grover for organizing the AAPS bi-monthly field trips to Medshare in San Leandro.

University of California San Francisco: It was in the summer of 2004 that I had the great opportunity to work as an undergraduate researcher at UCSF. I knew from the first day that I worked on the Mission Bay campus that this was truly a unique research institution- where collaboration was encouraged and scientists thrived. I feel so fortunate to have been a part of so many more gems offered: working with the SF Unified School District through the Science and Health Education Partnership and being a graduate advisor in the Summer Research Training Program were some of the greatest highlights. UCSF constantly feels like a scientific amusement park for interdisciplinary, progressive, and translational research.

Tenderloin Health: To the Sunday afternoon crew at TLH, it was so valuable to learn about sustainable harm reduction models of health service provision from you all. I am so inspired by your passion for public health (and particularly in serving marginalized communities), and I will take these lessons with me as I continue my studies in public health.

NIH Fogarty International Center: After dreaming about pursuing sustainable global health research for many years now, it is still feels unreal that I am part of the cohort of Fogarty International Clinical Research Fellows. At the NIH Fogarty orientation, it was so inspiring and humbling to meet talented scholars from all over the world that are so committed to bridging global health resource gaps. The past 10 years of my scientific training feels like it has led me to this point now, and I am so thankful to the FICRS-F program administrators for appreciating my passion and for giving me this amazing opportunity (and for giving me the best motivation to finish my dissertation at UCSF).

Judy Seu: To my mom, my greatest role model in life, my best friend, and someone who always had faith in my abilities- thank you for your continued support over the past 27 years. You make me want to be a better person all the time and I love and appreciate you so much. 나는 엄마가 있어서 행복한 사람이 되었어요.

Christina Oh- thank you for always believing in my abilities and for being an unwavering support from many miles away. **Boram Kim**- your beautiful energy, generous spirit, and commitment to global health research are daily inspirations that I am so appreciative for. **Caro Chung-** to my partner in crime, thank you for never failing to brighten up my day. **Claimes Lee**- thank you for your continued support and for all your generosity. **April Suwalsky**- you are such an incredible role model for the work that you do in your community in Richmond, and there's really nothing more to say than "thank you for being you." **Carina Perez**- thank you for today, and for everyday- you taught me to never aim for what's possible because that wouldn't be aiming high enough.

San Francisco: San Francisco has made these last 5 years the most creative, happy, and enlightened years of my life. The amount of street art per capita in this city is unparalleled to any other in the world, and illustrates the community-driven mindset of the inhabitants in our beautiful bubble. I have fallen in love with the misty mornings, the urban farms permeating these city blocks, the Free Farm Stand that donates weekly organic produce, the unyieldingly resilient and collaborative attitude of city residents, the impromptu musical sessions on porches, weekly pickup ultimate Frisbee with 13 of your new best friends, and the culture of sharing surplus and minimizing waste. "But of course there's no logic to San Francisco generally, a city built with putty and pipe cleaners, rubber cement and colored construction paper. It's the work of fairies, elves, happy children with new crayons." (David Eggers)

Abstract

Immune activation and inflammation are predictive of a rapid pace of HIV disease progression, and host immunoregulatory factors that blunt immune activation and inflammation may contribute to delayed disease progression.

We hypothesized that host factors controlling HIV-associated inflammation might be protective during the course of disease and that amongst such factors, heme oxygenase-1 (HO-1) was a good candidate as an important stress-response enzyme. It is the rate-limiting enzyme that initiates heme degradation and maintains cellular homeostasis during stress through its depletion of pro-oxidant heme, via generation of cytoprotective carbon monoxide, and biliverdin.

The experiments discussed in this thesis aim to explain how the activity of HO-1 controls harmful immune activation in HIV-positive individuals primarily through its function in blood monocyte populations.

We show that HO-1 plays an important role in dampening nonspecific T cell activation in murine and human studies. Pharmacological alteration of HO-1 in mice as well as in circulating immune cells of humans leads to altered T cell proliferation, maturation, and survival profiles. This discovery sets the important groundwork for establishing HO-1 pharmacological agents as potential therapies for HIV disease.

Next, we show that inter-individual genetic variability in the HO-1 promoter region influences its transcriptional regulation. We conducted a candidate genotyping analysis of the HO-1 promoter polymorphisms during HIV-disease to show that African Americans with greater HO-1 GT_n polymorphic repeats had higher plasma CD14 levels and viral loads on and off therapy, respectively.

HO-1 is regulated to a variable extent in the blood monocyte populations as defined by CD14 and CD16 expression, and we show that these circulating monocytes differentially predict HIV disease parameters.

Lastly, we determined how pharmacological inhibition of HO-1 influences virological and immunological consequences during pathogenic SIV disease. We administered the HO-1 inhibitor, tin mesoporphyrin (SnMP), to AGMs infected with the simian immunodeficiency virus (SIV). Treated animals had higher peak viral load during seroconversion, higher T cell activation, and higher absolute $CD4^+$ T cell counts.

The results from this thesis show the importance of HO-1 activity in regulating homeostatic T cell activity as well as T cell function during inflammatory conditions such as HIV infection.

2. Aims:

The aims of this thesis are summarized in four main studies that explain how the activity of HO-1 controls harmful immune activation in HIV-positive individuals primarily through its function in blood monocyte populations:

Chapter I: To determine the effect of HO-1 inhibition with a pharmacological inhibitor, SnMP, on $CD4^+$ and $CD8^+$ T cell homeostasis and its role in $CD14^+$ monocyte biology in mice and humans

Chapter II: To determine how the GT microsatellite polymorphism variation in the HO-1 promoter region is associated with plasma CD14 levels and set point viral load in HIV-infected patients

Chapter III: To determine how circulating myeloid subpopulations differentially predict CD4 recovery in early HAART patients

Chapter IV: To determine how the inhibition of HO-1 influences virological and immunological consequences in AGMs (AGM)

Table of Contents

1. List of abbreviations

HIV/SIV	Human immunodeficiency virus, type I
SIV	Simian immunodeficiency virus
APC	Antigen presenting cell
HLA-DR	Human leukocyte antigen-DR (MHC class II receptor)
MHC	Major histocompatibility complex
HMOX1	Heme oxygenase-1 (HGNC nomenclature for gene)
HO-1	Heme oxygenase-1 (HGNC nomenclature for transcript and protein)
CO	Carbon monoxide
Mo	Monocyte
Fe^{2+}	Iron cation
CoPP	Cobalt protoporphyrin IX
SnMP	Tin mesoporphyrin IX
FePP	Iron protoporphyrin IX
CD38	Cluster of Differentiation 38 (cyclic ADP-ribosylase)
CD14	Cluster of Differentiation 14 (Lipopolysaccharide receptor)
CD16	Cluster of Differentiation 16 (FcγIII receptor)
CD86	Cluster of Differentiation 86 (co-stimulatory receptor on APCs)
Ki67	An antigen in cell line localized to the nucleus of proliferating cells (MK167)
T_N	T naïve cell
T_{CM}	T central memory cell
PBMC	Peripheral blood mononuclear cell
TNFα	Tumor necrosis factor alpha

IFNα/γ	Interferon alpha/gamma
IL-1/2/6/10	Interleukin 1/2/6/10
SNP	Single nucleotide polymorphism
GWAS	Genome wide association study
LD	Linkage disequilibrium
GT_n	Guanidine-thymidine dinucleotide repeat
HAART	Highly active antiretroviral therapy
ART	Antiretroviral therapy
NHP	Non-human primate
AGM	AGM
GALT	Gut-associated lymphoid tissue
CCR5	C-C chemokine receptor type 5
LTNP	Long term non-progressor
INR	Immunological non-responder
IDO	Indoleamine-2,3 dioxygenase (HGNC nomenclature for transcript and protein)
T_H17	T helper 17 cell
Treg	T regulatory cell
LPS	Lipopolysaccharides
16s rDNA	16S ribosomal DNA
ROS	Reactive oxygen species
RCT	Randomized clinical trial

3. Literature Review

3.1. HIV immunopathogenesis

High levels of immune activation and inflammation are predictive of a more rapid pace of HIV disease progression, and host immunoregulatory factors that blunt immune activation and inflammation may contribute to delayed disease progression (1). HO-1, the rate-limiting enzyme in heme catabolism, is a potent anti-inflammatory protein that may represent one such factor (2).

Infection with the human immunodeficiency virus (HIV) typically results in chronic disease that, in most cases, cripples the host immune system (3). Thirty years of intense research on HIV have delivered definitive achievements such as the development of antiretroviral medications (4), a better understanding of HIV-induced pathogenesis (5), a small animal model for HIV infection (6), and a non-human primate model of SIV infection (7).

Although development of antiretroviral therapies has reduced the global burden of the disease, limited availability as well as clinical complications resulting from these medications necessitates research into effective vaccine strategies (8). The experiments outlined in this proposal are aimed at understanding how certain host immune responses may contribute to effective control of the virus. Previous research has shown that antigen-nonspecific pro-inflammatory responses are associated with enhanced replication and spread of virus and more rapid disease progression after HIV infection (9-13). Studies in non-human primates (NHP) and in infected humans have revealed that inflammation during SIV/HIV infection is tightly correlated with the generation of pro-inflammatory cytokines (14), T cell activation

(15), increased microbial translocation of lipopolysaccharide products from the gut flora (16), and increased frequencies of inflammatory monocyte populations (17,18).

3.1.1. Natural history of HIV/SIV infection and immune activation

The natural history of HIV disease is marked by $CD4^+$ T lymphocyte depletion and immune dysregulation that predicts an individual's risk for infection with opportunistic pathogens and development of other complications. During the acute phase of HIV infection, there is widespread dissemination of the virus in the periphery as well as in secondary lymphoid sites that is concordant with a rapid decline of circulating $CD4^+$ T lymphocytes. (13) This period is followed by a prolonged period of clinical latency (lasting as long as 10 years) during which time cellular and humoral immune responses to HIV are observed and there is a decrease in plasma viral levels. During this time, the $CD4^+$ T-cell count continues to gradually decrease until it drops below the level of 200 $CD4^+$ T cells/μL, at which time the risk of developing opportunistic diseases substantially increases and a diagnosis of AIDS is assigned (Figure 1). In the absence of therapy, clinical disease often develops and death may follow within several years.

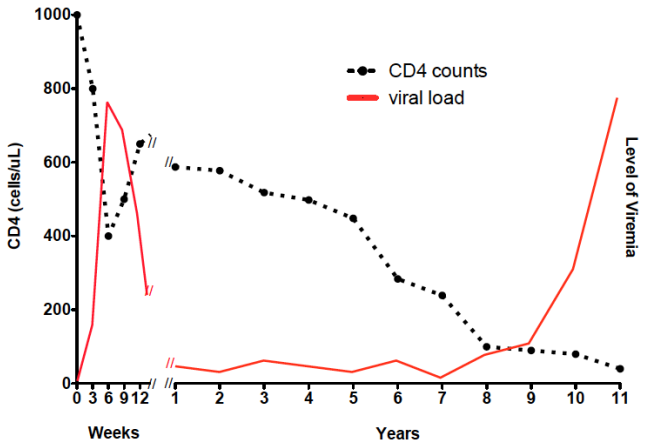

Figure 1: Natural history of untreated HIV infection (Adapted from (13))

Although host immune activation in response to pathogens is critical for their eradication, the inflammatory response can paradoxically enhance pathogenesis. HIV pathogenesis is an example of this delicate balance, where progressive and pathogenic infection is associated with chronic immune activation, including heightened destruction and diminished production of T lymphocytes (19,20), increased serum levels of pro-inflammatory cytokines such as TNFα, IL-1 and IL-6 (21,22), and of various chemokines (23), and increased levels of the pro-inflammatory transcription factors, NFκB, and NF-AT (24). These signs of host immune activation are not only associated with pathogenic HIV disease, but are actually predictive of the pace of HIV disease progression, even more so than plasma viral load. In particular, studies have shown that $CD8^+$ T cell expression of the surface "immune activation marker," CD38, predicts survival times in chronic HIV disease, independently of viral load (25). Another study demonstrated that the "immune activation set point" early in the course of HIV disease is predictive of the ability to maintain peripheral $CD4^+$ T cell counts (26). From our own studies, we measured these markers in cryopreserved PBMCs from seronegative individuals (n=30), highly active antiretroviral therapy (HAART) patients virally suppressed for >2 years (n=44), HIV-infected patients off therapy for ≥1 year with viral loads <2,000 copies/mL (n=54), and HIV-infected patients with viral loads >10,000 copies/mL (n=20). We showed that HIV-infected patients with viral loads >10,000 copies/mL had the highest percentages of $CD38^+$ and $HLA\text{-}DR^+$ double positive $CD4^+$ and $CD8^+$ T cells (Figure 2).

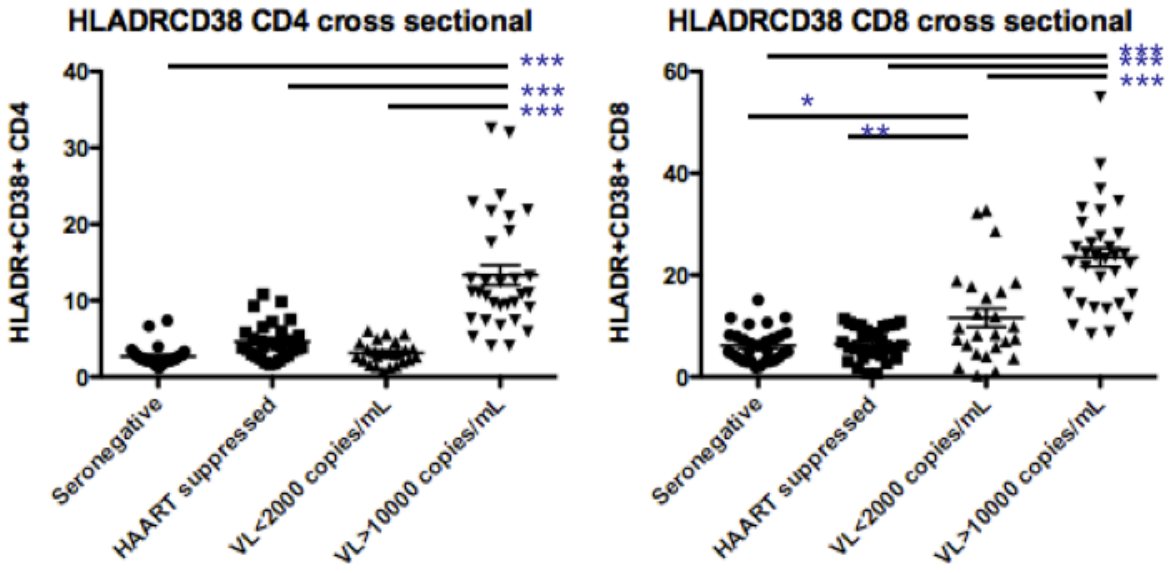

Figure 2: Cross sectional analysis of T lymphocyte activation during HIV disease as measured by HLA-DR and CD38 expression on $CD4^+$ and $CD8^+$ T cells (1-way ANOVA). (*p<0.05, **p<0.01, ***p<0.001)

Similar associations are pertinent to the course of simian immunodeficiency virus (SIV) infection of non-human primates (NHP). For instance, in some NHP species (e.g., the AGM, sooty mangabey, and chimpanzees), SIV infection is non-pathogenic and is consistently associated with lower levels of bystander immune activation than in species that develop pathogenic SIV disease (e.g., pigtail or rhesus macaques) (27). In one study, necropsy samples from SIV-infected pigtail macaques displayed increased expression of Ki67, a marker of cell proliferation and activation, compared to SIV-infected AGMs (28). These studies suggest that increased immune activation during the chronic stage of HIV and SIV infection can contribute to disease pathogenesis, and is consistent with the fact that the pro-inflammatory environment during chronic infection leads to the promotion of anergy and

apoptosis of activated T lymphocytes as well as to increased proviral transcription via the transcription factors, NFκB and NF-AT (29).

3.1.2. Sources of immune activation during HIV infection

During the first few weeks of pathogenic (and non-pathogenic) HIV and SIV infection, substantial $CD4^+$ T-cell depletion occurs in the gastrointestinal tract (30-32). In pathogenic (but not non-pathogenic) infections, the ensuing loss of intestinal epithelial integrity and damage to the gastrointestinal mucosal surface enhances systemic immune activation during the chronic phase of HIV infection via the increased translocation of luminal microbial products. Lipopolysaccharides (LPS), the cell wall component of gram-negative bacteria such as E. *coli*, stimulate the immune system by triggering monocyte activation via CD14 and TLR4-mediated signaling, resulting in the release of pro-inflammatory cytokines (33).

Recent studies have shown that circulating lipopolysaccharide, LPS-binding protein (LBP), and soluble CD14 are significantly increased in the context of progressive disease in HIV-infected patients and in SIV-infected rhesus macaques. Increased levels of circulating LPS were correlated with the levels of plasma IFNα and to the percentage of activated $CD8^+$ T lymphocytes (34). Furthermore, microbial translocation was found to be diminished in HIV-infected patients treated with antiretroviral drugs and absent in SIV-infected sooty mangabey hosts with non-pathogenic infection. A similar study related the levels of circulating LPS, sCD14, and LBP to the degree of activation of circulating monocytes (as measured by surface expression of CCR5 and CD69), to serum levels of IL-6, and to the degree of HIV-associated dementia in AIDS patients (35).

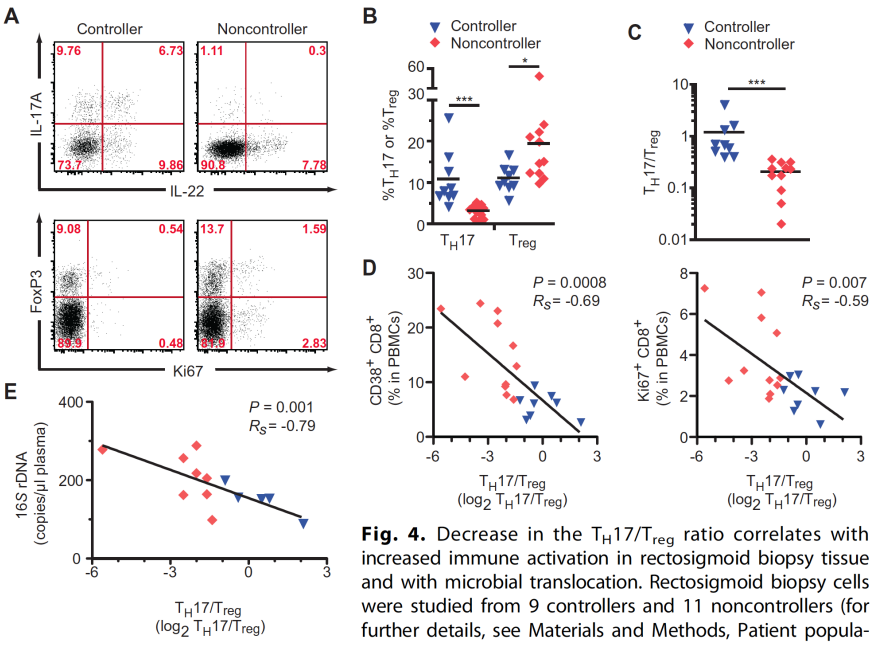

Fig. 4. Decrease in the T_H17/T_{reg} ratio correlates with increased immune activation in rectosigmoid biopsy tissue and with microbial translocation. Rectosigmoid biopsy cells were studied from 9 controllers and 11 noncontrollers (for further details, see Materials and Methods, Patient populations, Study D, and table S1). (**A**) Example of intracellular FACS detection of IL-17A and IL-22 (top panels) and of FoxP3 and Ki67 (bottom panels) in $CD4^+$ T cells from rectosigmoid biopsies in representative examples of viral controller and noncontroller subjects. (**B**) Frequency of T_H17 and $FoxP3^+$ T_{reg} cells in rectosigmoid biopsies from noncontrollers compared to controllers. (**C**) T_H17/T_{reg} ratio in patient groups. (**D**) Correlation between T_H17/T_{reg} ratio in rectosigmoid biopsies (expressed as $\log_2$ T_H17/T_{reg}) and systemic T cell activation as measured by CD38 and Ki67 expression in $CD8^+$ T cell from paired PBMCs. (**E**) Plasma concentration of 16*S* rDNA (a marker of bacterial translocation) in samples within the linear range of detection. Mann-Whitney *U* test was used for group comparisons (*$P < 0.05$, **$P < 0.005$, ***$P < 0.0005$). The Spearman rank correlation test was used for the correlations (R_s, Spearman correlation coefficient).

Figure 3: Increased immune activation caused by dysregulation of T_H17/Treg cell ratio and subsequent microbial translocation products (36)

One recent study showed that a potential source of mucosal barrier breakdown may be due to the up-regulation of indoleamine-2,3 dioxygenase (IDO), an IFN type I responsive gene. In the GALT, IDO enzymatic activity leads to a loss of T_H17 cells and a relative increase in Tregs that contributes to the breakdown of epithelial barriers and the ensuing microbial translocation of immune-activating bacterial products (Figure 3) (36). These studies showed that progressive HIV infection is marked by an increase in circulating bacterial products as a result of impaired mucosal integrity and increased microbial

translocation. The increase in circulating bacterial components may contribute to the systemic immune activation observed during progressive HIV/SIV disease.

3.2 Host genetics and HIV

The era of human genomics has vastly expanded thanks to efforts of Celera and the Human Genome Project completed 10 years ago (37,38). Many HIV biologists have pursued candidate genotyping projects as well as genome-wide association studies (GWAS) to determine host genetic factors that may involve virological and immunological correlates of protection against HIV.

3.2.1. *Summary of recent candidate genotyping studies*

Since the advent of high throughput genomics sequencing, there have been many studies looking at polymorphisms of various host genetic factors that influence the transmission and the course of HIV disease both on and off therapy. A list of recent candidate genotyping studies is summarized in Table 1. Only studies with a clearly defined effect size as well as a statistically significant association for candidate genes are reported (39-53).

A recent study analyzed the expression levels of the top genes that are comparatively up-regulated in $CD3^+$ T cells from HIV patients who are Long-Term Non Progressors (LTNPs) (mean years since seroconversion =17.6 years, with mean CD4 levels=638.2 cells/mL) compared to progressors (mean years since seroconversion =2.4 years, with mean CD4 levels=488 cells/mL). Using a "t-statistic," the pooled standard deviation value is determined using empirical Bayes methods across both progressors and LTNP. Analysis comparing progressors versus LTNP revealed over-expression of 322 genes in progressors and 136 in

LTNP. Up-regulated genes in progressors were mainly involved in regulation of DNA replication, cell cycle, and DNA damage. In contrast, most up-regulated genes in LTNP were involved in cytokine-cytokine receptor interaction, negative control of apoptosis, or regulation of actin cytoskeleton (54).

3.2.2. Genome-wide association studies (GWAS)

Many complex diseases with complex etiologies have been hypothesized to be explained by the "common disease, common-variant" (CD-CV) model (55). This model takes into account the human allelic spectrum, where diseases with more complex etiologies may be influenced by the nature of interaction of these variations with environmental factors. Lately, in a rebuttal to this model, scientists have recently advocated for sequencing first to identify rare causal variants that may be contributing to a greater aggregate disease outcome measure (56).

The study of CD-CV has been made a reality for many complex diseases by the bounty of human genomic information now available with the Human Genome Project (aimed at sequencing an entire human genome), the International HapMap Project (aimed at measuring genetic linkage between commonly occurring genetic polymorphisms in world populations), and the 1000 Genomes Project (aimed at identifying both common and rare variation in multiple world populations) (57). The most current record of all published GWAS are available on http://www.genome.gov/gwastudies/, and publications using platforms with at least 100,000 single nucleotide polymorphisms (SNPs) and p-values $< 1.0 \times 10^{-5}$ are reported. Additionally, The Human Genome Epidemiology Network (HuGENet™) (58) is an international collaboration that assesses the role of human genome variation in health and

Table 1: Selected Candidate Genotyping studies for parameters of HIV disease

HIV Disease Outcome Measure	Candidate Gene and Polymorphism	(Reference) Details	Sample Population	Sample Size	Statistical test	Effect size	Association strength
AIDS progression in high risk group off therapy	2 SNPs CX_3CR1: 249 GC +280 CT	(39) Faure S et al. Science 2000	Caucasians from SEROCO	426	Kaplan-Meier survival of AIDS progression	Relative Hazard=2.13 for CX3CR1 -280 TT	p=0.039
HIV+ Long Term Non-Progressor status	CCR5 59029AG + CCR5 59353CT	(40) Clegg, AO et al. AIDS 2000	The Australian Long-Term Non-Progressor Study Group	71 LTNP 75 Progressors	Chi Square Analysis LTNP (CD4>500cells/uL, >8 years) vs. Progressors (AIDS or death <8 years)	Genotypes CCR5 59209AA + CCR5 59353CC is 34.7% of HIV progressors and 19.7% of LTNP	Fisher's Exact p=0.043
HIV acquisition and AIDS progression in high risk group off therapy	RANTES promoter SNP haplotype G1: -403G/G -28C/C G4: -403G/A. -28C/C	(41) McDermott DH et al. AIDS 2000	Caucasians from MACS	200	(1) Chi Square for acquisition (2) Kaplan-Meier for AIDS-free duration	(1) HIV acquisition with G4 versus G1: OR=1.72 (w/o CCR5del32 OR=2.13) (2) G4 vs. G1: Rel. Hazard: 0.65	(1) G4 haplotype p value: 0.016 (without CCR5del32 p=0.005) (2) Relative Hazard: p=0.007
Meta Analysis of 19 cohort studies of HIV disease progression off therapy	CCR5-del32, CCR2-64I, and SDF-1 3'A Alleles	(42) Ioannidis JPA et al. Ann. Int. Med. 2001	19 prospective cohort studies and case–control studies from the United States, Europe, and Australia.	Meta analysis	(1) Kaplan-Meier for progression to AIDS/death (2) Mean difference in Log10 HIV-1 RNA	Relative Hazard AIDS-free (1) CCR5del32: 0.74 (2) CCR2-64I: 0.76 Mean Log10 HIV-1 RNA (1) CCR5del32: -0.18 log10 copies/mL (2) CCR2-64I: -0.14 log10 copies/mL	AIDS-free (1) CCR5del32 p value=0.01 (2) CCR2-64I p value=0.01 MeanLog10 HIV-1 RNA (1) CCR5del32 p value<0.05 (2) CCR2-64I p value<0.05
Disease progression off therapy	KIR3DS1 and HLA-B Bw4-80Ile SNPs	(43) Martin MP et al. Nature Genetics 2002	Caucasians and African Americans from MACS, MHCS, HGDS, SFCC, ALIVE	631 Caucasians 234 African Americans	Kaplan-Meier survival of AIDS progression	Relative Hazard proportion AIDS-free (>200 CD4 cells/uL) KIR3DS1+Bw4-80Ile: =0.60 in Caucasians =0.18 in African Americans	p=0.006 in Caucaisans p=0.01 in African Americans
Highly Exposed Persistently Seronegative (HEPS)	CCR2 and CCR5 haplotypes	(44) Tang J et al. JVI 2002	Caucasians and African Americans from MACS, MHCS, HGDS, SFCC, ALIVE	703	Chi Square (HEPS vs. Seroconverters)	CCR2-CCR5 haplotype: G*2/any, E/E, and Reference yields a 0.54 Odds Ratio in Seroconverters vs. HEPS	P=0.004
Rate of CD4 decline in HIV disease off therapy	64 SNPs spanning IL2, IL4, IL6, IL10, IL12p35 and p40, IL13 and IFNg	(45) Vasilescu, A et al. Genes and Immunity 2003	Caucasians from GRIV cohort	337	Chi Square Slow Progressors (>8 yrs w/o ARV and >500 cells/uL) vs. Rapid progressors (CD4 <300cells/uL <3 years after last seronegative test)	OR=0.5 for presence of H2 haplotype in IL4	p=0.035
AIDS progression in high risk group off therapy	7 SNPs spanning APOBEC3G	(46) An P et al. JVI 2004	Caucasians and African Americans from MACS, MHCS, HGDS, SFCC, ALIVE	290 African Americans	Kaplen-Meier survival of AIDS progression (CD4<200cells/uL)	Relative Hazard for presence of 186RR allele =2.94	p=0.005
Disease progression off therapy	CCR5 haplotypes	(47) Li, M et al. ARHR 2005	Caucasians from North America and Spain	188	(1) Chi Square: Rapid (CD4<200 cells/ul in 5 yrs) and Slow progressors (CD4>500 cells/ul, >8 yrs) (2) Kaplan-Meier of AIDS	(1) CCR5-HHE haplotype is represented 48.2% in RP vs. 22.9% in SP (2) CCR5-HHE haplotype has 3.12 Relative Hazard proportion AIDS-free (>200 CD4 cells/uL)	(1) Chi Square p = 0.002 (2) Relative Hazard p=0.037

Table 1 continued: Selected Candidate Genotyping studies for parameters of HIV disease

HIV Disease Outcome Measure	Candidate Gene and Polymorphism	Reference	Sample Population	Sample Size	Statistical test	Effect size	Association strength
High Risk Exposed Uninfected (HREU) and AIDS progression off therapy	21 SNPs spanning CCL3, CCL4, and CCL18	(48) Modi, WS et al. AJHG 2006	African Americans from ALIVE Caucasians from MACS	238 (ALIVE) 403 (MACS)	(1) Chi Square (HREU vs. Seropositive) (2) Kaplan-Meier survival of AIDS progression (CD4<200cells/uL)	(1) 3 SNPs in CCL18 haplotype block (OR=0.47) (2) CCL4 1931 T/- Relative Hazard: 1.51	(1) Chi square p=0.02-0.03 (2) Rel. Haz. P value=0.0072
CD4+ T cell recovery from HAART initiation to 48 weeks	137 SNPs analyzed across IL-2, IL-2Rβ, IL-2Rγ, IL-15, IL-15Rα, TRAIL, Bim, TNF-α, and IFN-γ	(49) Haas, DW et al. JID 2006	AIDS Clinical Trials Group (U.S. and Puerto Rico)	837	Multivariate logistic regression analyses	CD4 cells/4 years gain after HAART (homozygous protective genotype) (1) TRAIL (-1674 G/T): TT (378 cells/uL) (2) TNFa (-488 A/G): GG (279cells/uL) (3) BIM (26368 T/C): CC (198 cells/uL) (4) IL15RA (13994 A/G): AA (403 cells/uL) (5) IL15 (83125 A/G): GG (396 cells/uL)	(1) TRAIL: Adj. p= 0.0019 (2) TNFa: Adj. p=0.0052 (3) BIM: Adj. p=0.0216 (4) IL15RA: Adj. p=0.0305 (5) IL15: Adj. p=0.048
AIDS progression in high risk group off therapy	12 SNPs spanning CUL5	(50) An P et al. PLoS Gen 2007	Caucasians and African Americans from MACS, MHCS, HGDS, SFCC, ALIVE	239 African Americans	Kaplan-Meier survival of AIDS progression (CD4<200cells/uL)	Relative Hazard= 2.57 for presence of Haplotype 10 in Cul5	p=0.001
Time to CD4 T cell decline to <400 cells/uL off therapy	ZNRD1, HLA-C, and HCP5 alleles with HLAB*57 and HLA-A10	(51) Catano et al. PLoSone 2008	US army medical: Natural History Study cohort at BAMC and WHMC	664	Kaplan-Meier survival curves for AIDS progression (>400 CD4 cells/uL)	Relative Hazard AIDS-free (>400 CD4 cells/uL) (1) ZNRD1 CT + HLA-A10: RH=0.37 (2) HLAB*57 + HCP5 CC: RH=0.17	(1) ZNRD1 (C/T) + HLA-A10: p=0.004 (not sig w/o HLA-A10) (2) HLAB*57 + HCP5 CC: p= 7.5×10^{-5} (not sig w/o HLAB*57)
CD4+ T cell recovery during HAART	CCL3L1-CCR5 Genetic Risk Group (GRG) (1) High: low CCL3L1 + detrimental CCR5 (2) Mod.: low CCL3L1 + nondetr. CCR5 or high CCL3L1 + detr. CCR5 (3) Low: high CCL3L1 + nondetr. CCR5	(52) Ahuja, S. et al. Nat. Med. 2008	US army medical: Natural History Study at WHMC and AIEDRP	1,235	Linear GEE (Generalized Estimating Equation)	CD4 cells/month gain after HAART (1) GRG Low: 2.89 ± 0.13 (2) GRG Moderate: 1.42 ± 0.20 (3) GRG High: –0.85 ± 0.76	(1) GRG Low: p= 1.7×10^{-9} (2) GRG Mod: p= 4.3×10^{-3} (3) GRG High: p= 3.1×10^{-6}
Survival	Apolipoprotein E (ε3 and ε4)	(53) Burt TD et al. PNAS 2008	US army medical: Natural History Study at WHMC	1,251	Kaplan-Meier survival curves	Relative Hazard for survival with possession of ApoE ε3/ε3: 2.16	p=0.002
Markers of inflammation during HAART and Viral load off HAART	Heme Oxygenase-1 promoter (GT)n microsatellite polymorphism	Seu L et al.	African Americans and Caucasians from SCOPE at UC San Francisco	74 African Americans 177 Caucasians	Multiple Linear Regression for soluble CD14 levels and viremia against additive (GT)n repeat	(1) β coefficient for sCD14=2.3 (10^4pg/mL) (2) β coefficient for mean viral load= 3,805.13 (copies/mL)	(1) p=0.007 (2) p=0.04

SEROCO (French Agence Nationale de la Recherche sur le SIDA), MACS (Multicenter AIDS Cohort Study), MHCS (Multicenter Hemophilia Cohort Study), HGDS (Hemophilia Growth & Development Study)
SFCC (San Francisco City Clinic), ALIVE (AIDS Linked to Intravenous Experience), GRIV (Genetic Resistance to infection by HIV-1), BAMC (Brooke Army Medical Center) and WHMC (Wilford Hall Medical Center)
AIEDRP (Acute Infection and Early Disease Research Program), SCOPE (Study of the Consequences of Protease Inhibitors Era)

disease at the population level and integrates data from the NHGRI GWAS Catalog, HapMap (59), the Human Genome Epidemiology (HuGE) Navigator, the Broad Institute's SNP Annotation and Proxy Search (SNAP), and University of California Santa Cruz (UCSC) genome browser. The data are posted on the GWAS Integrator website http://hugenavigator.net/HuGENavigator/gWAHitStartPage.do (60)

LTNPs of HIV-1 are individuals who are able to maintain normal levels of $CD4^+$ T cells (> 500 cells/μL) for ten or more years after presumed infection, even in the absence of antiretroviral therapy (ART), and who remain asymptomatic. It is estimated that about 5-10% of all individuals infected by HIV-1 are LTNPs (61,62). "Elite controllers" make up a subset of the LTNP group and are defined by their ability to control levels of viremia to < 50 viral copies per milliliter of plasma (below the level of detection). It has been estimated that anywhere from 0.3 to 1% of the HIV-infected patient population meet these criteria (63).

In this era of widely available human genomic technologies and genotyping platforms, studies have examined the role that host genetics may play on the ability of an individual to control the progression of HIV disease. GWAS of HIV disease parameters use genetic markers to elucidate which combinations of genes are important in a phenomenon that is most likely multifactorial and polygenic. These GWAS on HIV disease have focused on the control of viral load as the primary outcome measure; however, recent GWAS have included disease progression as measured by CD4 T cell counts, the development of carotid atherosclerosis during HAART, and mother-to-child-transmission of HIV. A summary of the most current GWAS for HIV disease outcome is shown in Table 2 (64-77).

A recent GWAS conducted by the International Controllers Study (70) comparing HIV positive "viral controllers" (patients with viral control <2000 copies/mL in the absence of

Table 2: HIV Disease Genome Wide Association Studies Summary

HIV Disease Outcome Measure	Array	(Reference) Details	Consortium	Sample Population	Variant Allele	Chromosomal Region	Gene (LD genes)	Effect Size: either (A) Odds Ratio [OR], (B) β coeff. from Logistic Regression [LR] (C) Hazard Ratio [HR] of Cox Proportional Hazards	Association strength
Mean log setpoint VL	Illumina HumanHap 550K SNP chip	(64) Fellay et al. Science 2007	CHAVI	486 HIV positive Europeans & African Americans	1) rs2395029-G 2) rs9264942-C	1) 6p22.33 2) 6p22.33	1) HCP5 2) HLA-C 5'	1) LR: β=-1 log10 (cp/mL) 2) LR: β=-0.4 log10 (cp/mL)	1) $p=9.36\times10^{-12}$ 2) $p=3.77\times10^{-9}$
Mean log setpoint VL	Illumina HumanHap550 & Human1M Beadchip	(65) Fellay et al. PLoS Genetics 2009	Euro-CHAVI MACS	2,362 HIV positive Caucasian subjects	1) rs2395029-G 2) rs7758512-C	1) 6p21.33 2) 6p21.33	1) HCP5 (HLA-B*5701) 2) HLA-C	1) LR: β=-0.06 log10 (cp/mL) 2) LR: β=-0.053 log10 (cp/mL)	1) $p=5x10^{-35}$ 2) $p=6x10^{-32}$
HIV Disease Progression: CD4 <500cell/ul	Illumina HumanHap550 & Human1M Beadchip	Fellay et al. PLoS Genetics 2009	Euro-CHAVI MACS	1071 HIV+ Caucasians	1) rs2395029-G 2) rs9264942-C 3) rs9261174-C 4) CCR5del32	1) 6p22.33 2) 6p22.33 3) 6p22.33 4) 3p21.31	1) HCP5, HLA-B 2) HLA-C 3) ZNRD1 4) CCR5	1) HR=0.39 2) HR=0.68 3) HR=0.65 4) HR=0.62	1) $p=1.2x10^{-11}$ 2) $p=7.4x10^{-12}$ 3) $p=3.8x10^{-8}$
Long Term Non-Progression (no ARVs, CD4 T cell count >500 cells/uL for >8 years)	Illumina Infinium II HumanHap300 BeadChips	(66) Limou et al. JID 2009	GRIV Euro-CHAVI & MACS	275 LTNP Europeans (France) 1352 seronegative Europeans (France)	rs2395029-G	6p21.33	HCP5 (HLA-B, MICB, MCCD1, BAT1, LTB, TNF)	OR=3.47	$p=6.79x10^{-10}$
Rapid Progression (≥2 CD4 T cell counts <300 cells/uL within 3 years after last seronegative test)	Illumina Infinium II HumanHap300 BeadChips	(67) Le Clerc et al. JID 2009	GRIV	85 rapid progressor Europeans (France) 1352 seronegative Europeans (France)	1) rs4118325-G 2) rs1522232-C 3) rs10800098-A 4) rs1020064-G	1) 1p13.3 2) 12p12.1 3) 1q23.3 4) 2q12.1	1) Intergenic (PRMT6) 2) SOX5 3) RXRG 4) TGFBRAP1	1) OR=0.24 2) OR=0.45 3) OR=3.29 4) OR=0.34	1) $p=6x10^{-7}$ 2) $p=2x10^{-6}$ 3) $p=4x10^{-6}$ 4) $p=7x10^{-6}$
Mother-to-Child-Transmission of HIV (followed up to 12 weeks)	Illumina HumanHap650Y Genotyping BeadChip	(68) Joubert BR et al. Genome Med 2010	Queen Elizabeth Central Hospital in Blantyre	100 Malawian HIV+ infants 126 Malawian HIV- infants	NA	NA	NA	NA	NA
CD4:CD8 Ratio	Illumina 610-Quad BeadChip	(69) Ferreira MAR et al. Am J Hum Gen 2010	QIMR, Twins UK Study	2,538 adolescent twins from 1,089 Australian families	rs2524054-A	6p21.33	HLA-B	1) LR: β= 0.37 (Standard Deviation for transformed CD4:CD8 units)	$p=2 \times 10^{-28}$
Viral Control (<2000 copies/mL in absence of therapy)	Illumina 610-Quad BeadChip	(70) Ferreira MAR et al. Am J Hum Gen 2010	International HIV Controllers Study, ACTG A5128	445 HIV+ European controllers 733 HIV+ European non-controllers	rs2524054-A	6p21.33	HLA-B	OR= 0.32	$p=9.1x10^{-11}$

Table 2 continued: HIV Disease Genome Wide Association Studies Summary

HIV Disease Outcome Measure	Array	Reference	Consortium	Sample Population	Variant Allele	Chromosomal Region	Gene (LD genes)	Effect Size: either (A) Odds Ratio [OR], (B) β coeff. from Logistic Regression [LR] (C) Hazard Ratio [HR] of Cox Proportional Hazards	Association strength
Viral Control (<2000 copies/mL, 3 collections, no ARVs, over 12 month period)	Illumina HumanHap 650Y	(70) IHCS et al. Science 2010	International HIV Controllers Study	European- 516 cases, 1,196 controls Af_American- 341 cases, 892 controls Hispanic- 117 controls, 560 controls	1) rs9264942-C 2) rs4418214-C 3) rs2395029-G 4) rs2523608-G 5) rs3131018-C	1) 6p21.33 2) 6p21.33 3) 6p21.33 4) 6p21.33 5) 6p21.33	1) HLA-C (European) 2) MICA (Af_American) 3) HLA-B (European) 4) HLA-B (Af_American) 5) PSORS1C3 (European)	1) OR=2.9 2) OR=4.4 3) OR=5.3 4) OR=2.6 5) OR=2.1	1) $p=3x10^{-33}$ 2) $p=1x10^{-34}$ 3) $p=1x10^{-25}$ 4) $p=9x10^{-20}$ 5) $p=4x10^{-16}$
Viral Load set point (copies/mL)	Illumina 1M, 1M-Duo, 550K	(71) Pelak et al. JID 2010	DoD HIV NHS, MACS	285 HIV+ African American	rs2523608-C	6p21.33	HLA-B*5703	1) LR: β= 0.10 (copies/mL)	$p=5.6x10^{-10}$
LTNP (same criteria as Limou et al. 2009, excluding VL <100 copies/mL)	Infinium II HumanHap300 BeadChips	(72) Limou et al. JID 2010	GRIV	186 LTNP Europeans 697 HIV-1 seronegative healthy Europeans	rs2234358	3p21.31	CXCR6	OR=1.85	$p=2.5x10^{-7}$
AIDS progression (1987 CDC classification)	Affymetrix SNP array 6.0 genotyping (700K)	(73) Troyer JL et al. JID 2011	MACS MHCS HGDS SFCC ALIVE	755 European American HIV seroconverters	1) rs11884476-? 2) rs6467710-? 3) rs477687-? 4) rs7217319-? 5) rs1015164-? 6) rs6441975-?	1) 2q33.3 2) 7q33 3) 5q31.1 4) 17p13.3 5) 3p21.31 6) 3q21.31	1) PARD3B 2) DGKI 3) H2AFY 4) RPH3AL 5) LTF 6) CCRL2	1) HR= 0.3 2) HR= 4.3 3) HR=1.55 4) HR=1.48 5) HR=1.46 6) HR=1.48	1) $p=3x10^{-9}$ 2) $p=6x10^{-7}$ 3) $p=6x10^{-6}$ 4) $p=4x10^{-6}$ 5) $p=9x10^{-6}$
common Intima Media Thickness (cIMT) in HIV-infected HAART patients	Illumina HumanCNV370-quad beadchip	(74) Shrestha S et al. AIDS 2010	FRAM	177 Caucasian HIV-infected HAART patients (male)	1) rs2229116-G 2) rs17691394-G 3) rs13053817-A	1) 15q14 2) 7q31.33 3) 22q12.2	1) RYR3 2) GRM8 3) RFPL1 (AP1B1, THOC5, NF2)	1) LR: β=1.15 (log IMT) 2) LR: β=1.32 (log IMT) 3) LR: β=1.21 (log IMT)	1) $p=3x10^{-8}$ 2) $p=9x10^{-7}$ 3) $p=2x10^{-6}$
in vitro HIV replication in monocyte-derived macrophages	Illumina 610 Quad 500K	(75) Bol SM et al. PLoS One 2011	Amsterdam blood bank donors	96 cases (high p24=-0.65 log10 copies/mL) 96 controls (low p24=0.49 log10 copies/mL)	rs12483205-A	21q22.13	DYRK1A	LR: β not provided	$p=2.16x10^{-5}$ (not significant)
HIV-1 susceptibility (30% of sample population are HIV+)	Illumina Human 1M or 1M-Duo DNA Analysis BeadChips	(76) Petrovski S et al. AIDS 2011	CHAVI Clinical Care	848 Malawian cases 531 Malawian controls	NA	NA	NA	NA	NA
Progressions: LTNP versus Rapid Progressors	Illumina HumanHap300 BeadChips	(77) Le Clerc et al. JAIDS 2011	GRIV ACS MACS	365 HIV+ European LTNP 147 European Rapid Progressors	1) rs2395029-C 2) rs9368699-G 3) rs8192591-T 4) rs2072255-A	1) 6p21.33 2) 6p21.33 3) 6p21.32 4) 17p12	1) HCP5 (intergenic, MICB) 2) C6orf48 (RDBP, TNXB) 3) NOTCH4 (GPSM3) 4) RICH2	1) OR=3.41 2) OR=2.9 3) OR=2.32 4) OR=0.43	1) $p=8.54x10^{-15}$ 2) $p=3.03x10^{-10}$ 3) $p=9.08x10^{-7}$

CHAVI: Center for HIV/AIDS Vaccine Immunology, MACS: Multicenter AIDS Cohort Study, GRIV: Genetic Resistance to Immunodeficiency Virus, FRAM: Fat Redistribution And Metabolic change in HIV infections
ACTG: AIDS Clinical Trials Group, DoD HIV NHS: Department of Defense Human Immunodeficiency Virus Natural History Study, MHCS: Multicenter Hemophilia Cohort Study, ACS: Amsterdam Cohort Studies
HGDS: Hemophilia Growth and Development StudySFCC: San Francisco City Clinic, ALIVE: AIDS Linked to the IntraVenous Experience, QIMR: Queensland Institute of Medical Research, IHCS: International HIV Controller

ARTs for at least 1 year) to HIV non-controllers found four SNPs in chromosome 6p21.33 that, in aggregate, explain 19% of the variance between cases and controls. This region of the genome displays high linkage disequilibrium, but these four SNPs do not show direct functionality. In addition to using data from their GWAS platform (Illumina HumanHap 650Y), they also imputed HapMap haplotype data to link their tagging SNP with known HLA class I alleles. By doing this, they found associations that B*57:01, B*27:05, B*14/Cw*08:02, B*52, and A*25 were associated with protection and B*35 and Cw*07 were associated with risk.

This region of chromosome 6 is overwhelmingly overrepresented in many HIV GWAS, whether the outcome measure is viral control, immune control, or even the more recent study showing association with the control of CD4:CD8 ratios in healthy donors. These results underscore the importance of early and robust CD8 and/or NK cell responses influenced by peptide presentation by MHC receptors on APCs that influence viral control from the early to the chronic stage of infection.

3.3. HO-1

Heme oxygenase is a key enzyme in the catabolic conversion of intracellular heme and the overall maintenance of iron stores and carbon monoxide release. It is the rate limiting enzyme in the breakdown of heme to its stoichiometric reaction products CO, Fe^{2+}, and biliverdin (78). Given the determinative impact of immune activation/inflammation on the pace of HIV disease progression, we hypothesized that differential up-regulation of HO-1 in response to HIV infection may play an important role in HIV pathogenesis. In particular, increased levels of HO-1 upregulation may provide an anti-inflammatory state that serves to

prevent disease progression. If so, certain HO-1 promoter polymorphisms may segregate between HIV-infected subjects with slow versus rapid disease progression.

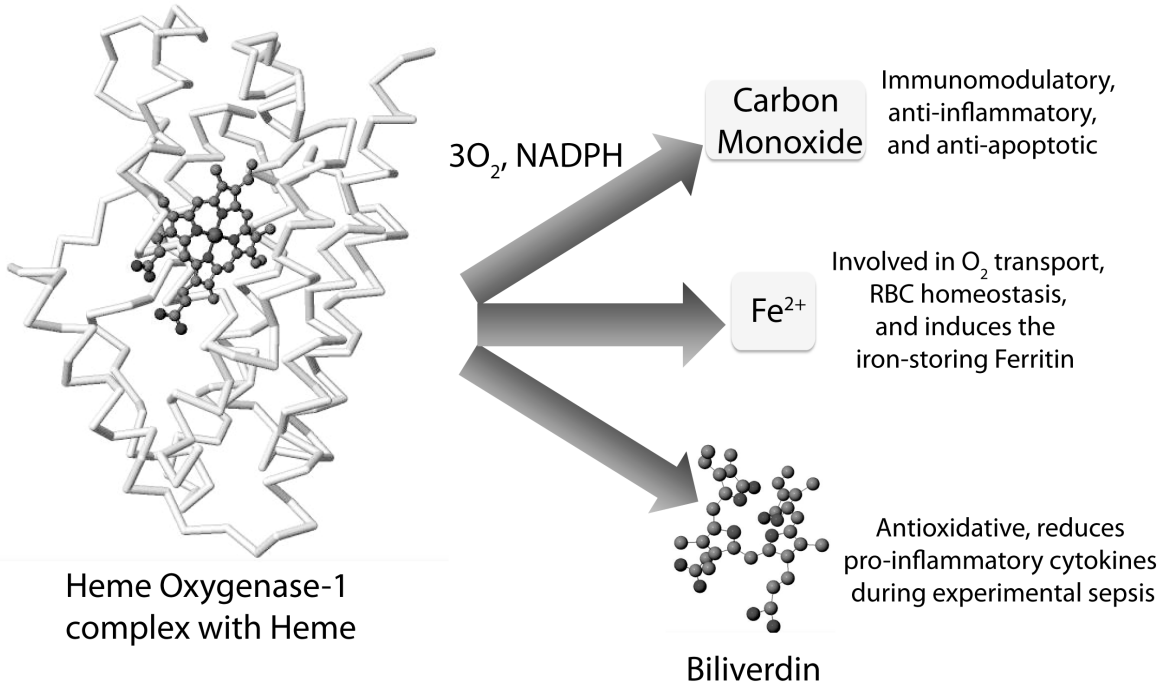

Figure 4: HO-1 structure and enzymatic activity

(Generated from Protein Data Base ID #1N45 and #1S8C)

3.3.1. *Role during cellular stress*

Of the three isoforms of heme oxygenase (HO-1, HO-2, and HO-3), HO-1 is constitutively expressed in the spleen but is the only isoform that has been shown to be induced by a myriad of stress signals, e.g., oxidative stress, UVA radiation, the pro-inflammatory cytokines (IL-1, IL-6, TNFα), nitric oxide, heavy metal exposure, hypoxia and hyperoxia, heme itself, and other metalloporphyrins. Through its depletion of the pro-oxidant molecule, heme, and the generation of its three cytoprotective factors (carbon monoxide,

biliverdin, and the ferritin-inducing Fe^{2+}), HO-1 is an important house-keeping enzyme that maintains homeostasis during cellular stress (Figure 4) (78).

Recently, HO-1 has been implicated as an immune modulator, with anti-proliferative, anti-oxidant, and anti-apoptotic effects (79). Studies on the *Hmox1*$^{(-/-)}$ mouse show that during activation (with either LPS or αCD3/αCD28), mouse macrophages deficient in HO-1 displayed increased production of TNFα, IFNα, IL-6, and IL-2 (80). Furthermore, *Hmox1*$^{(-/-)}$ mice displayed splenomagaly, lymphadenopathy, leukocytosis, hepatic inflammatory infiltrates, glomerulonephritis, as well as iron overload.

Studies have shown that HO-1 inhibits the expression of the pro-inflammatory cytokine TNFα while maintaining or augmenting the expression of the anti-inflammatory cytokine, IL-10. Notably, these observations were made in the myeloid lineage cells such as dendritic cells and macrophages (81-83). The mechanism of cytoprotection by HO-1 is primarily attributed to the actions of carbon monoxide, and exogenous administration of CO most closely mimics its effects. Administration of CO to *Mkk3*$^{(-/-)}$ mice augmented IL-10 expression and inhibited TNFα expression via a mitogen-activated protein kinase pathway within macrophages (84).

In the NOD mouse model of type-1 diabetes, induction of HO-1 with cobalt protoporphyrin IX (CoPP) resulted in the rescue of normal insulin production well after autoimmune pancreatitis and islet destruction. This effect was attributed to HO-1 activity, as administration of the HO-1 inhibitor, SnMP (85).

One reported clinical case study of an individual who was deficient for HO-1 reported growth retardation, anemia, leukocytosis, thrombocytosis, elevated serum haptoglobin, ferritin, and heme, low bilirubin concentration, hemolysis, an abnormal coagulation system,

inflammation, high levels of heme, high levels of cold reactive protein, dysmorphic monocytes, lymphadenopathy and persistent endothelial damage with an increase in adhesion molecules such as von Willebrand factor, ICAM1, and selectins (86,87).

3.3.2. HO-1 Candidate Genotyping

Given the important role that HO-1 has as an anti-inflammatory mediator, numerous case-control studies have linked proximal promoter region *HMOX1* polymorphisms to disease states that are driven by inflammation. In particular, the -413AT (rs2071746) and the -1195AG (rs3761439) SNPs as well as the dinucleotide GT_n microsatellite repeat have been implicated in many pathologies affected by inflammation. Prior studies of the HO-1 promoter region examined the association between the -413AT (rs2071746) SNP and coronary artery disease outcomes (88), and the -1195AG (rs3761439) SNP and cardiac function during exercise (89).

The GT_n microsatellite repeat is the best characterized of the three polymorphisms, and have been analyzed in diseases such as graft versus host disease, ischemia, emphysema, cardiovascular diseases, and idiopathic recurrent miscarriage are some of the few that has been studied in the past decade (90) (Figure 5).

Previous studies using promoter-luciferase assays in cell lines have shown an association between GT_n microsatellites with a small number of repeats and enhanced transcription of the HO-1 gene (88,91-93). The alternating purine-pyrimidine repeats within the GT_n microsatellite form a left-handed helical Z-DNA conformation and may affect gene transcription through the inhibition of RNA polymerase-mediated transcription (94). The HO-1 GT_n microsatellite locus is unique in being able to influence gene transcription under

multiple cellular stress conditions. A recent study using primary endothelial cells isolated from newborns showed that HO-1 induction was more robust in the context of fewer ($GT_{n<23}$) than greater ($GT_{\geq 29}$) repeats with CoPP, H_2O_2, and LPS stimulation (95). The central mediator implicated in this pathway is the Nrf2 transcription factor during HO-1 induction with CoPP and H_2O_2 (96,97) and HO-1 down-regulation with LPS stimulation (98).

Although many candidate gene studies have detected associations between the short HO-1 GT_n microsatellite variant and control of inflammatory disease states, no study has examined its functional role in regulating gene expression in primary immune cells (e.g., myeloid cells) that directly influence pathogenic outcomes in HIV-infected subjects.

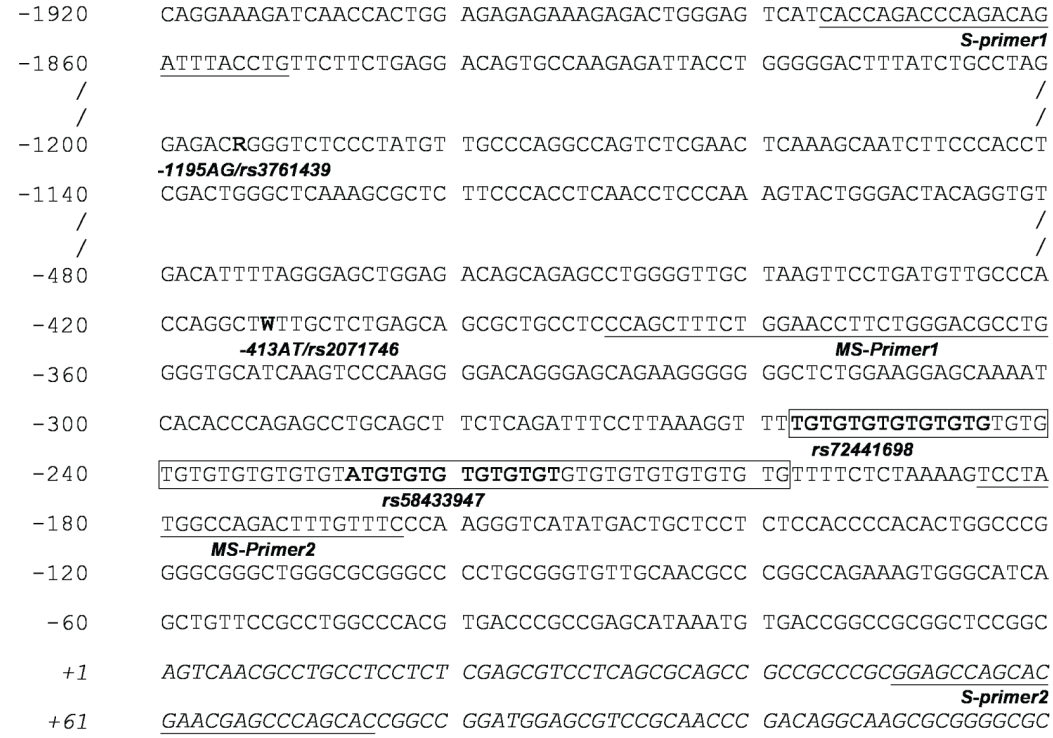

Figure 5: HO-1 promoter region polymorphisms. SNPs are labeled with dbSNP reference numbers and the GT_n microsatellite repeat is shown in the boxed area. S-primer-1/2 refer to subcloning primers for gene-expression assays.MS-Primer1/2 refer to primers for the GT_n repeat number PCR-capillary electrophoresis.

3.4. Circulating myeloid subpopulations

Neutrophils and monocytes comprise two members of circulating blood phagocytes. Both cell types are recruited to sites of infection where they recognize and can be induced to ingest microbes for intracellular killing. Of the two, circulating monocytes are less abundant (about 3-8% of leukocytes compared to the neutrophil abundance of 50-70%) and respond less rapidly to extracellular pathogens. Blood monocytes have a lifespan of 1-3 days: they then enter extravascular tissues and, unlike neutrophils, survive for long periods of time as tissue macrophages (99). Human $CD14^+$ monocytes are phagocytic, and produce reactive oxygen species (100) and inflammatory cytokines in response to a broad range of microbial cues (101).

3.4.1. Classical and non-classical blood monocyte populations

In humans, blood monocytes have been characterized on the basis of morphology, the activity of monocyte-specific esterase, and by flow cytometric detection of distinguishing light scatter properties and cell-surface markers such as CD14. The latter technology has also enabled the identification of a CD16 subpopulation that comprises about 10% of $CD14^+$ cells and about 13% of $CD16^+$ cells (102). This latter population is characterized by higher basal major histocompatibility complex (MHC) class II expression and higher TNFα production after stimulation by Toll-like receptor (TLR) ligands (103). Based on the fact that this latter $CD14^+CD16^+$ monocyte population expresses surface markers resembling those found on tissue macrophages, it was designated the "non-classical monocyte" while the $CD14^+CD16^-$ was designated a "classical monocyte."

Further studies have characterized the $CD14^+CD16^+$ monocyte population to show that,

upon stimulation, it has low to absent IL-10 expression and high levels of TNFα, interleukin-12, and inducible nitric oxide synthase (104). The $CD14^{+}CD16^{+}$ monocyte was also shown to develop into $CD1b^{+}$ dendritic cells that preferentially migrates and that have superior antigen-presenting capabilities (105). $CD14^{+}CD16^{+}$ monocytes were shown to adhere to activated endothelium more strongly and to undergo trans-endothelial migration across unstimulated human umbilical vascular (HUVEC) and brain microvascular endothelial (BMVEC) cell monolayers in response to soluble fractalkine (FKN/CX3CL1) (106). These cells were also shown to exhibit pro-inflammatory and pro-atherosclerotic activity, with shortened telomere length as compared to the $CD14^{+}CD16^{-}$ monocyte (107). A recent study showed that human $CD14^{dim}CD16^{+}$ monocytes have the functional role of patrolling the endothelium of blood vessels and are weak phagocytes that do not produce reactive oxygen species (ROS) or cytokines upon signaling across Toll-like receptors. Instead, they are involved in the innate local surveillance of tissues and may contribute to the pathogenesis of autoimmune diseases (108).

Studies have shown that the absolute number of circulating $CD14^{+}CD16^{+}$ monocytes is higher in males (59.1cells/μL) than in females (45.4cell/μL), and that it is also elevated during inflammatory diseases such as sepsis, coronary artery disease, rheumatoid arthritis, and HIV (109).

3.4.2. *Circulating myeloid subpopulations during HIV infection*

Blood monocytes and tissue macrophages can be infected by HIV (110) and represent a source of the viral reservoir in HIV-infected patients (111). These cells may also be involved in the shuttling of virus to tissue sites where they can serve to establish productive infection

and contribute to the basal amounts of immune activation observed, even in the context of maximally suppressive combination ART regimens (112,113). During HIV infection, there are elevated levels of the monocyte pro-inflammatory cytokines such as IL-1, IL-6, and TNF-α (114,115). Infected blood monocytes may also function as the causative link to observed co-morbidities during treated and un-treated HIV disease, such as increased risk of thrombosis (116), cardiovascular diseases (117), and HIV-associated dementia (118).

It has long been recognized that individuals with HIV have 2 to 8-fold percent higher $CD14^{dim}CD16^{+}$ inflammatory monocytes than uninfected controls (119-121). In an animal model of pathogenic HIV infection, rhesus macaques infected with SIV were shown to have significantly elevated absolute numbers of monocytes expressing CD16 during acute and chronic infection. Also, a significant positive correlation was evident between the number of monocytes expressing CD16 and plasma viral load in the infected cohort (122).

Shedding of CD14 from the surface of non-inflammatory $CD14^{hi}$ monocytes upon exposure to an activating stimulus (e.g., LPS) may represent an important part of their transition into pro-inflammatory $CD14^{dim}CD16^{+}$ monocytes (123,124).

3.4.3. *HO-1 expression in circulating myeloid subpopulations*

The first glimpse that HO-1 may have a role in the control of HIV disease came from a study showing elevated HO-1 mRNA levels in PBMCs from AIDS patients (125). The motivation for this study was to understand the development of hematological abnormalities commonly found in AIDS patients. PBMCs from AIDS patients showed marked bilirubin formation as well as HO-1 mRNA levels. The authors did not address whether this association was causal or coincident, but speculated that elevated HO-1 activity in cells of

AIDS patients could produce a decrease in cellular heme needed for transductional signaling for the growth factor network.

Previous studies reported that pharmacological alterations of HO-1 induced a tolerogenic profile in antigen presenting cells of the monocytic lineage (126). Another study showed that blood monocytes that were $CD16^{+}CCR2^{-}$ had a preferential production of HO-1 at steady state (127). A more exhaustive microarray analysis (with 16,328 probe sets for expressed genes) showed that 2,759 genes were differentially expressed between $CD16^{+}$ and $CD16^{-}$ monocytes from healthy donors. In $CD16^{+}$ compared to $CD16^{-}$ monocytes, 228 and 250 genes were >2-fold up-regulated and down-regulated, respectively. $CD16^{+}$ monocytes up-regulated transcripts for dendritic cell markers, macrophage markers, DC-T cell interaction, cell activation, and negative regulation of the cell cycle. $CD16^{-}$ monocytes were distinguished by up-regulation of transcripts for myeloid and granulocyte markers. HO-1 was found to be up-regulated in $CD16^{+}$ monocytes, corroborating the previous study showing that HO-1 was expressed to a higher extent in $CD16^{+}CCR2^{-}$ monocytes (128).

More recently, LPS has been shown to suppress HIV replication in human monocytes by protein kinase C-dependent HO-1 induction (129). These studies all underscore the importance of determining the nature of HO-1 up-regulation within subpopulations of blood monocytes in the context of HIV disease.

3.5. Targeting HO-1 as a potential for HIV therapy

3.5.1. *Existing Clinical Use*

Neonatal jaundice is still a health burden in resource-poor settings where phototherapy may not be available (130). Bilirubin in large amounts can act as a potent

neurotoxin and leads to neurological encephalopathies (131). Inhibitors of heme-oxygenase-1 such as SnPP have been successfully used to treat neonates with a reduced capacity to naturally clear their biliverdin and bilirubin levels (132).

A recent clinical study reported that the synthetic metalloporphyrin, hematin (Fe^{2+} protoporphyrin IX) (Panhematin ®, Lundbeck Inc.), can induce a 15-fold increase in HO-1 activity (133). Further investigations into how GT_n repeat polymorphisms influence the inducibility of HO-1 by pharmacological metalloporphyrins may help us better understand the clinical pharmacogenetics properties of these medicines. Pharmacological augmentation of HO-1 may represent a strategy for the treatment of diseases such as HIV, in which unchecked immune activation results in deleterious clinical outcomes (85,134-139). The HO-1 GT_n microsatellite genetic locus may represent an informative marker to predict the efficacy of therapeutic agents targeted at inducing HO-1 for treatment of pathologic inflammatory diseases.

3.5.2. *Potential therapeutic for HIV disease*

It has been reported that human monocytes and PBMCs treated with FePP are much less susceptible to infection with CCR5, CXCR4, and dual-tropic lab strains, as well as with multiple drug-resistant, patient-derived isolates (140). In this study, the authors also used a NOD SCID PBMC mouse model to show that upon IP injection of hemin four days after HIV infection, the viral load in the serum of these mice was reduced. This suppression was apparently mediated by HO-1, as it was reversed upon administration of SnMP. This study did not, however, examine the cells on which HO-1 was acting on or analyze the immune response that was induced.

Given the observation that immune activation contributes to enhanced and accelerated pathogenesis in the setting of HIV infection (5,141), one therapeutic strategy to combat disease progression would be to utilize agents that lead to a reduced level of immune activation. The drive to develop immunosuppressive agents was put on the back burner in the mid 1990s with the availability of HAART (defined as treatment with at least three active anti-retroviral medications, typically two nucleoside or nucleotide reverse transcriptase inhibitors plus a non-nucleoside reverse transcriptase inhibitor or a protease inhibitor) (4). The beneficial effects of such agents in the context of HIV disease progression have been shown in the instance of cyclosporin A (142) (via inhibition of NF-ATc) and glucocorticoids (a broad anti-inflammatory hormone shown to cause sustained increases in peripheral $CD4^+$ T cell counts) (143). A recent trial of ART-naïve HIV patients (13 treated, 14 control) using a celecoxib, a cyclooxygenase type 2 (COX-2) inhibitor, down-modulated immune activation related to clinical progression of chronic HIV infection and improved T cell-dependent functions. In the 13 treated patients, CD38 and PD-1 expression on $CD8^+$ T cells were reduced, while the numbers of T regulatory cells was increased over the course of 12 weeks (144). Through its activity as a specific COX-2 inhibitor, celecoxib may be limiting the availability of cAMP in circulation that may then lead to priming of monocytes to secrete various pro-inflammatory cytokines capable of activating T lymphocytes (101).

These studies warrant further work to identify broad range immunosuppressant agents that might limit HIV disease progression in infected individuals. In addition to the use of antiretroviral drugs, further characterization of available immunomodulating agents in the context of HIV pathogenesis might be beneficial in the face of increased viral escape mutants as well as the relative low cost of therapeutic production and distribution. Pharmacological

augmentation of HO-1 enzymatic therapies may be a viable option to combat disease states where unchecked immune activation cause deleterious clinical outcomes such as in the setting of chronic HIV infection.

4. Summary of important findings

The experiments of this thesis address the relationship between HO-1 activity (particularly as it is expressed in blood myeloid subpopulations) and immune activation in the context of HIV disease.

Pharmacological alteration of HO-1 with SnMP and CoPP is analyzed in murine peripheral lymphoid organs as well as in circulating immune cells of humans. The results from these studies are summarized in **Chapter I**.

An analysis of how HO-1 promoter polymorphisms can influence inter-individual variability in transcriptional regulation as well as a candidate genotyping analysis of the HO-1 promoter polymorphisms during HIV disease (association with plasma CD14 levels and set point viral load in HIV-infected patients on and off-therapy, respectively) is summarized in **Chapter II**.

HO-1 expression in different monocyte populations and an analysis of the circulating blood monocyte populations during HIV disease as well as the relationship of these parameters to CD4 reconstitution in HAART patients is summarized in **Chapter III**.

Lastly, to determine how the pharmacological inhibition of HO-1 influences virological and immunological consequences in AGMs (AGM) infected with SIV, results from a longitudinal trial are shown in **Chapter IV**.

Additional materials related to the specific aims of this thesis are included in the Appendix. To determine the potential role for HO-1 in preserving GALT epithelial integrity during untreated HIV infection, HO-1 immunohistochemistry in colon biopsy samples of HIV patients is summarized in **Appendix A**. A protocol for a candidate genotyping study for the HO-1 GT_n microsatellite repeat in cerebral malaria patients is included in **Appendix B.**

Additionally, a proposal for a randomized clinical trial of HO-1 induction in HAART patients is summarized in **Appendix C.**

4.1. HO-1 functional studies

4.1.1. *HO-1 in murine peripheral lymphoid organs*

To determine how HO-1 pharmacological agents affected peripheral lymphoid tissue, wild-type female Balb/c mice (3 months) were injected intraperitoneally with either saline, the HO-1 inducer, CoPP (8 μmoles/kg), or the HO-1 antagonist, SnMP (6 μmoles/kg). Mice were sacrificed at days 1, 3, and 7 and lymph nodes (pooled inguinals, axillaries, and brachials) and spleen were harvested (Figure 6). Animals injected with either metalloporphyrin displayed increased $CD3^+$ T cell apoptosis (Annexin V^+) in their lymph nodes, and had fewer naïve $CD4^+$ and $CD8^+$ T cells in both lymph nodes and spleen. Animals injected with either metalloporphyrin displayed decreased levels of the co-stimulatory marker, CD86 and the murine major histocompability class II receptor on $CD11c^+$ cells in the spleen but not the lymph node. These results demonstrate that pharmacological inhibition of HO-1 results in enhanced T cell maturation and apoptosis, as well as decreased expression of co-stimulatory markers on antigen-presenting cells.

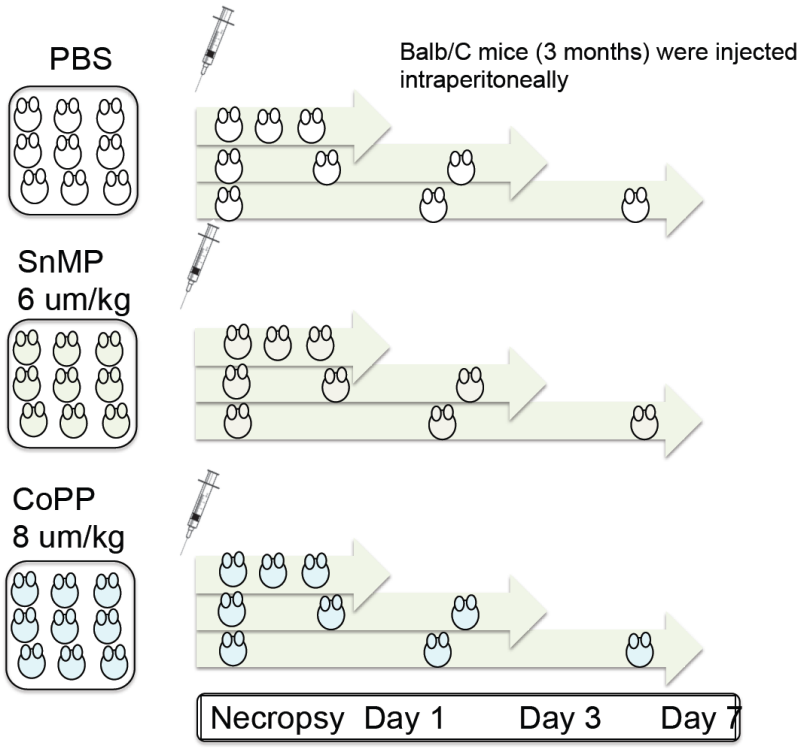

Figure 6: Schematic of HO-1 pharmacological study in mice. Balb/c mice were injected intraperitoneally and were sacrificed at the indicated timepoints

4.1.2. *HO-1 in circulating immune cells of humans*

We tested the possibility that pharmacologic effects on HO-1 by metalloporphyrin influenced the activation of human T cells. Specifically, we hypothesized that inhibition of HO-1 in PBMCs *in vitro* by SnMP would result in T cell activation and proliferation. We determined that SnMP induces activation, proliferation, and maturation of naive $CD4^+$ and $CD8^+$ T cells via interactions with $CD14^+$ monocytes in vitro. This response is dependent upon interactions of T cells with MHC class I and II on the surface of $CD14^+$ monocytes. Furthermore, $CD4^+CD25^+FoxP3^+$ regulatory T cells were able to suppress this proliferation, even though their suppressive activity was itself impaired by SnMP. Given the magnitude of the antigen-independent T cell response induced by SnMP, we speculate that HO-1 plays an

important role in dampening nonspecific T cell activation. Based on these findings, we proposed a potential role for HO-1 in the control of naive T cell homeostatic proliferation (Figure 7). We also showed that treatment of PBMCs with SnMP and CoPP alter monocyte expression of multiple markers of myeloid differentiation and activation such as CD11c, CD16, CD86, CD163, HLA-DR, and BDCA-2 (145).

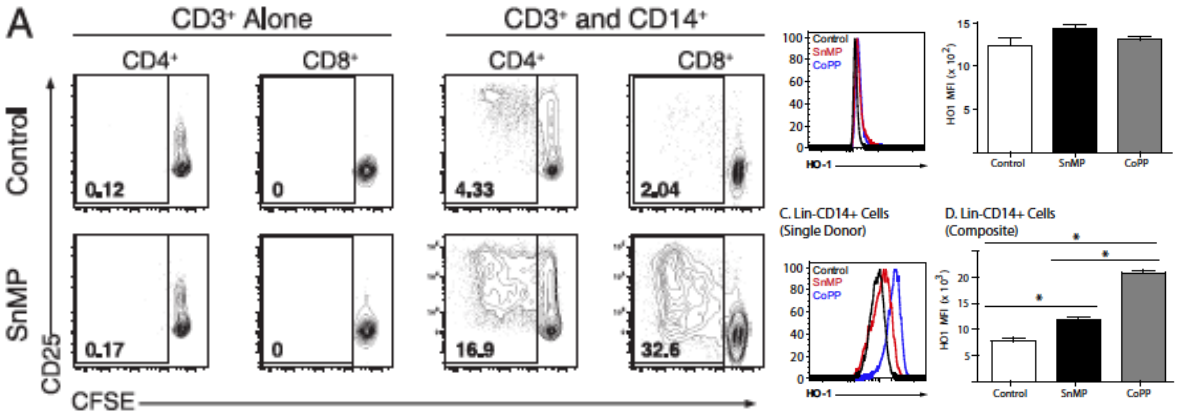

Figure 7: The HO-1 inhibitor Tin mesoporphyrin (SnMP) induces activation, proliferation, and maturation of naive $CD4^+$ and $CD8^+$ T cells via interactions with autologous $CD14^+$ monocytes in vitro and is induced in $CD14^+$ monocytes

4.2. HO-1 GTn microsatellite promoter polymorphism

4.2.1. *Primary cell functional analysis and phenotyping in healthy donors*

Given previous findings that shorter length variants of a HO-1 promoter-region GT_n microsatellite polymorphism are associated with increased HO-1 expression in cell lines, we hypothesized that shorter variants would also be associated with increased levels of HO-1 expression, less inflammation, and lower levels of inflammation-associated viral replication in HIV-infected subjects. Healthy donors (n=20) with shorter GT_n repeats had higher HO-1

mRNA transcript in peripheral blood mononuclear cells stimulated with lipopolysaccharide (LPS) (r= -0.38, p=0.05) (Figure 8).

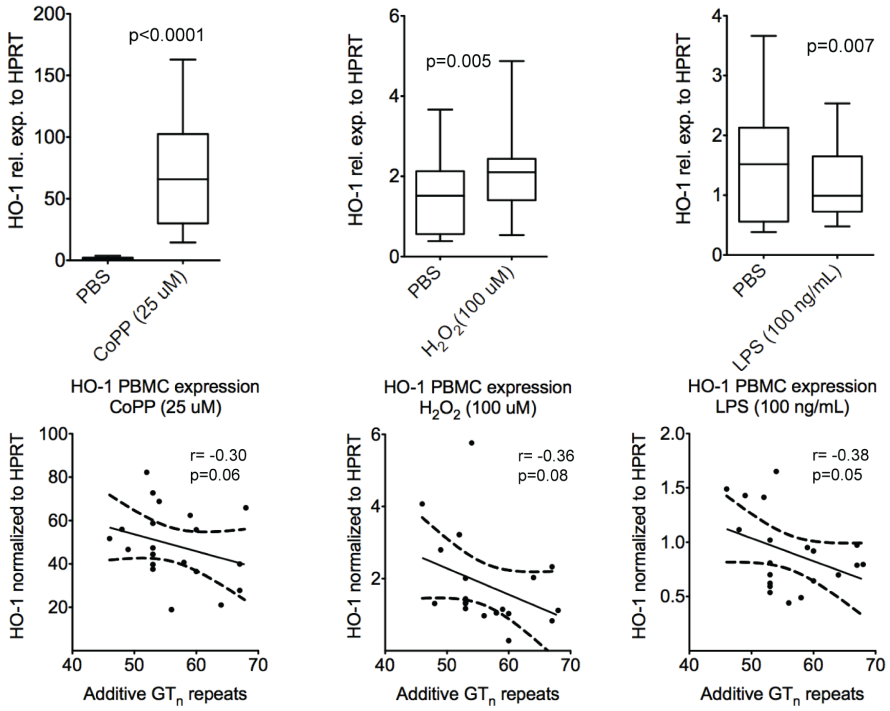

Figure 8: GT_n microsatellite polymorphism numbers are associated with increased HO-1 expression in PBMCs from healthy donors. (Pearson r correlation coefficient and corresponding P-value are reported)

4.2.2. *Candidate genotyping*

The presence of fewer GT_n repeats in subjects with untreated HIV disease was associated with higher HO-1 mRNA levels in peripheral blood (r= -0.41, p=0.02); similar observations were made in $CD14^+$ monocytes from antiretroviral-treated subjects (r= -0.36, p=0.04). In African-Americans, but not Caucasians, greater GT_n repeats were correlated with higher soluble CD14 (sCD14) levels during highly active antiretroviral therapy (HAART) (r=

0.38, p=0.007) as well as higher mean viral load off-therapy (r= 0.24, p=0.04). These data demonstrate that the HO-1 GT_n microsatellite polymorphism is associated with higher levels of HO-1 expression and that this pathway may have important effects on the association between inflammation and HIV replication (Figure 9).

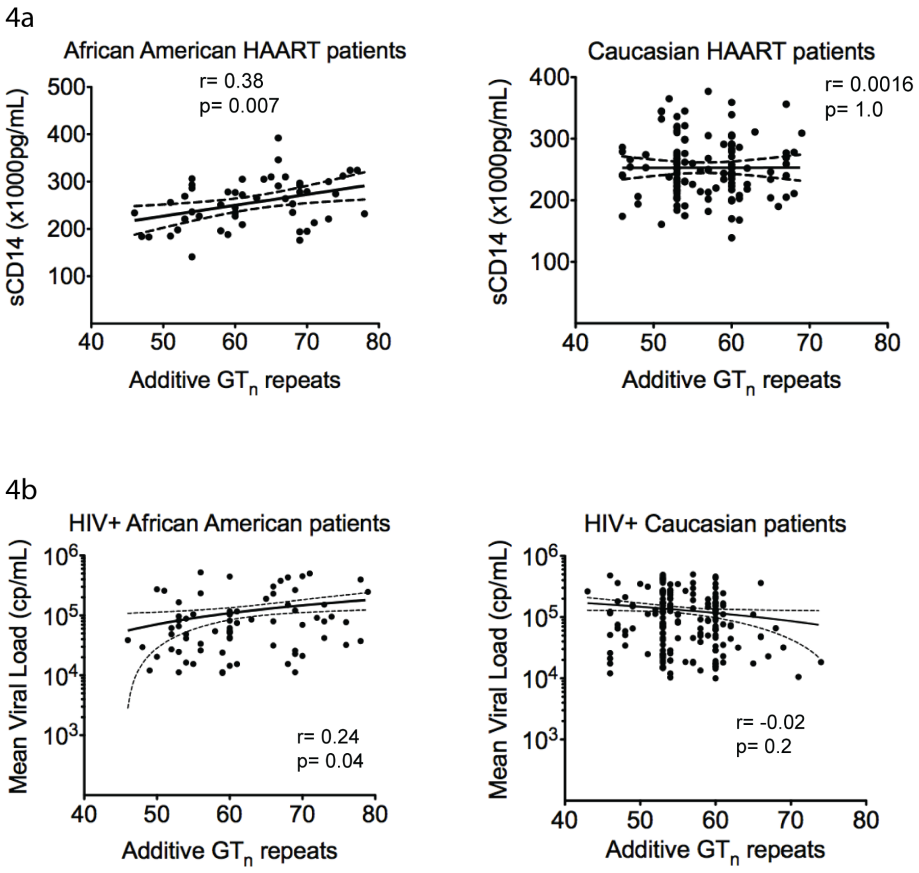

Figure 9: HO-1 candidate genotyping in HIV patients on and off therapy. (Pearson r correlation coefficient and corresponding P value are reported)

4.3. Circulating myeloid subpopulations and HIV infection

4.3.1. *Classical, intermediate, and non-classical subpopulations*

Peripheral blood mononuclear cells from HIV patients of the SCOPE cohort were analyzed for their myeloid/monocyte compartments: $CD14^{hi}CD16^{neg}$, $CD14^{hi}CD16^{pos}$, and $CD14^{dim}CD16^{pos}$ were analyzed. First, a cross-sectional phenotyping study of seronegative controls, HIV viral non-controllers (viral load >10,000 copies/mL), HIV viral controllers (viral load <1000 copies/mL), and HAART suppressed (viral control to <75 copies/mL) was executed. We found that the frequency of $CD14^{dim}CD16^{pos}$ cells followed the same pattern as that of other commonly used markers of activation (e.g., CD38 and HLA-DR expression on T lymphocytes), with the highest levels in the HIV viral non-controllers and the lowest in HIV-seronegative individuals. The population of $CD14^{hi}$ monocytes showed a pattern that was reciprocal to that of $CD14^{dim}CD16^{pos}$ monocytes. These results confirm and extend existing reports (119,121,146,147) and suggest that blood monocyte populations may play a regulatory role in the extent of immune reconstitution and T cell activation during HIV disease (Figure 10).

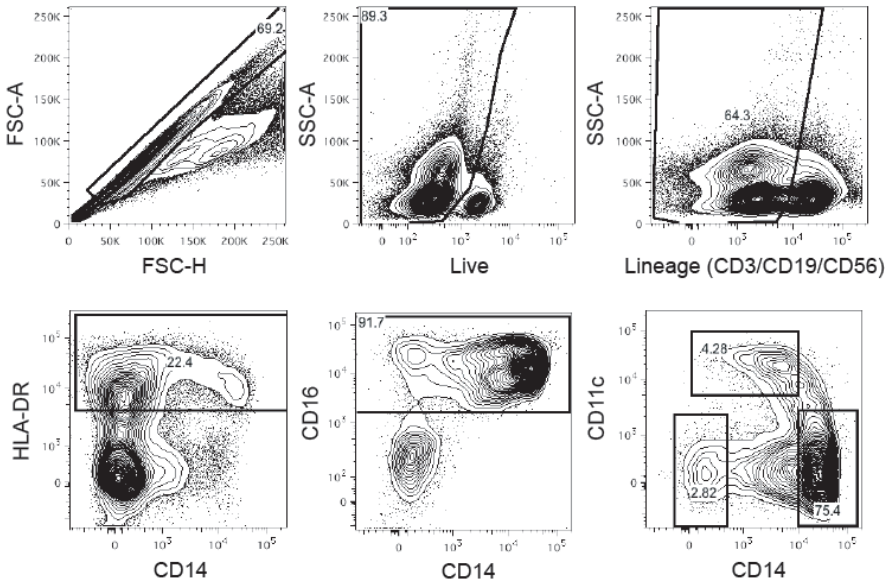

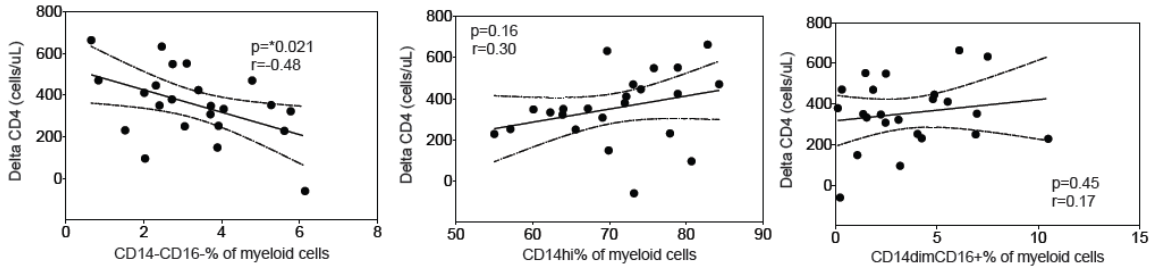

Figure 4c: HO-1 expression in myeloid populations and Delta CD4 (Peak-Nadir)

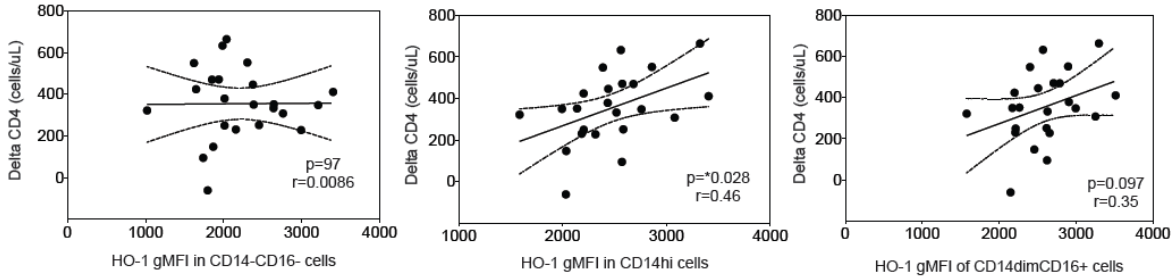

Figure 10: Blood monocytes during HIV infection- characterization of myeloid cells by flow cytometry gating analysis and association with CD4 reconstitution in HIV HAART patients (Pearson r correlation coefficient and corresponding P-value are reported)

4.3.2. HO-1 expression in monocytes

To determine the extent of HO-1 expression in blood monocyte populations, PBMCs were isolated by density gradient centrifugation of whole blood on cell separation medium. They were then cultured with CoPP for two days and stained for cell surface markers and HO-1. Lineage $(Lin)^+$ ($CD3^+$, $CD19^+$, $CD56^+$) cells were gated separately from Lin^-CD14^+ cells and the mean fluorescence intensity (MFI) of HO-1 was determined. HO-1 was most induced in $CD14^{hi}$ monocytes in PBMCs compared to the $CD14^{dim}CD16^{pos}$ population (Figure 11).

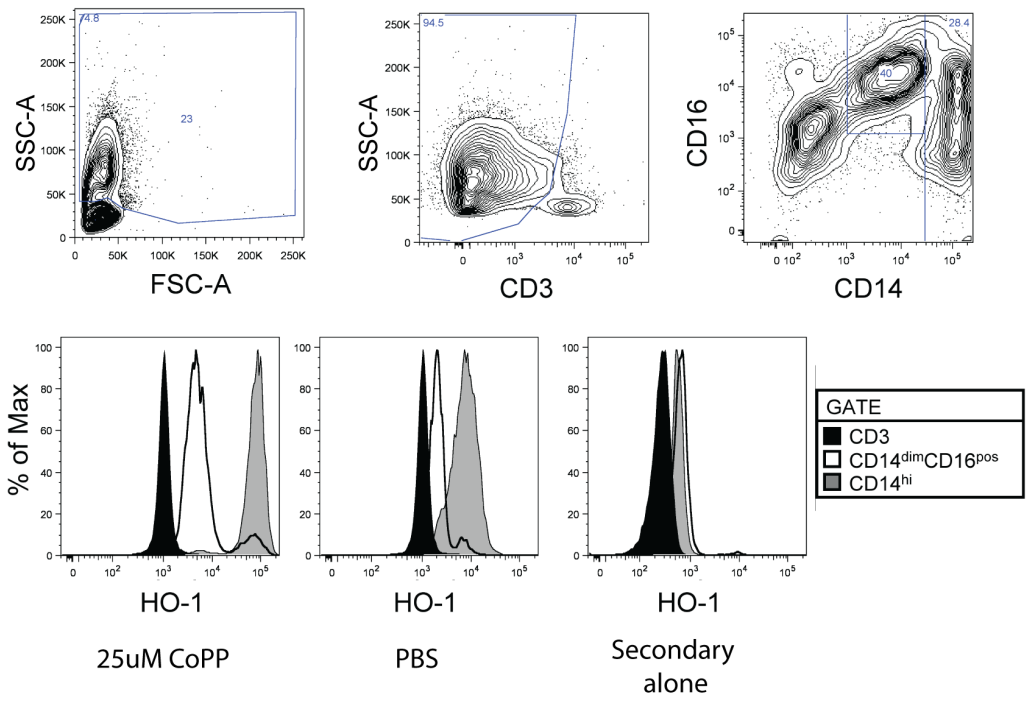

Figure 11: HO-1 expression in blood monocyte populations of PBMCs cultured with CoPP.

4.4. HO-1 and GALT epithelial integrity during untreated HIV infection

4.4.1. *HO-1 immunohistochemistry in colon biopsy samples of HIV patients*

To determine the potential role for HO-1 function in preserving GALT epithelial integrity during untreated HIV infection, HO-1 immunohistochemistry in colon biopsy samples of HIV patients was conducted. Staining results were consistent with previous reports: there was staining of HO-1 in macrophage-like cells interspersed throughout the lamina propria of the colon in healthy human tissue (148-150).

HO-1 is up-regulated in epithelial cells of colonic crypts during conditions of inflammation (e.g., viremic HIV and during inflammatory bowel disease). Notably, this epithelial expression shows a pattern of higher staining in regions that are adjacent to inflammatory infiltrates in the lamina propria. HO-1 induction in these regions could exert its

cytoprotective mechanisms by combating inflammation and apoptosis in these tissue sites. These data have implications for HIV GALT biology: up-regulation of HO-1 may be a mechanism to protect epithelial cells from destruction that ultimately leads to microbial translocation and subsequent systemic immune activation (Figure 12).

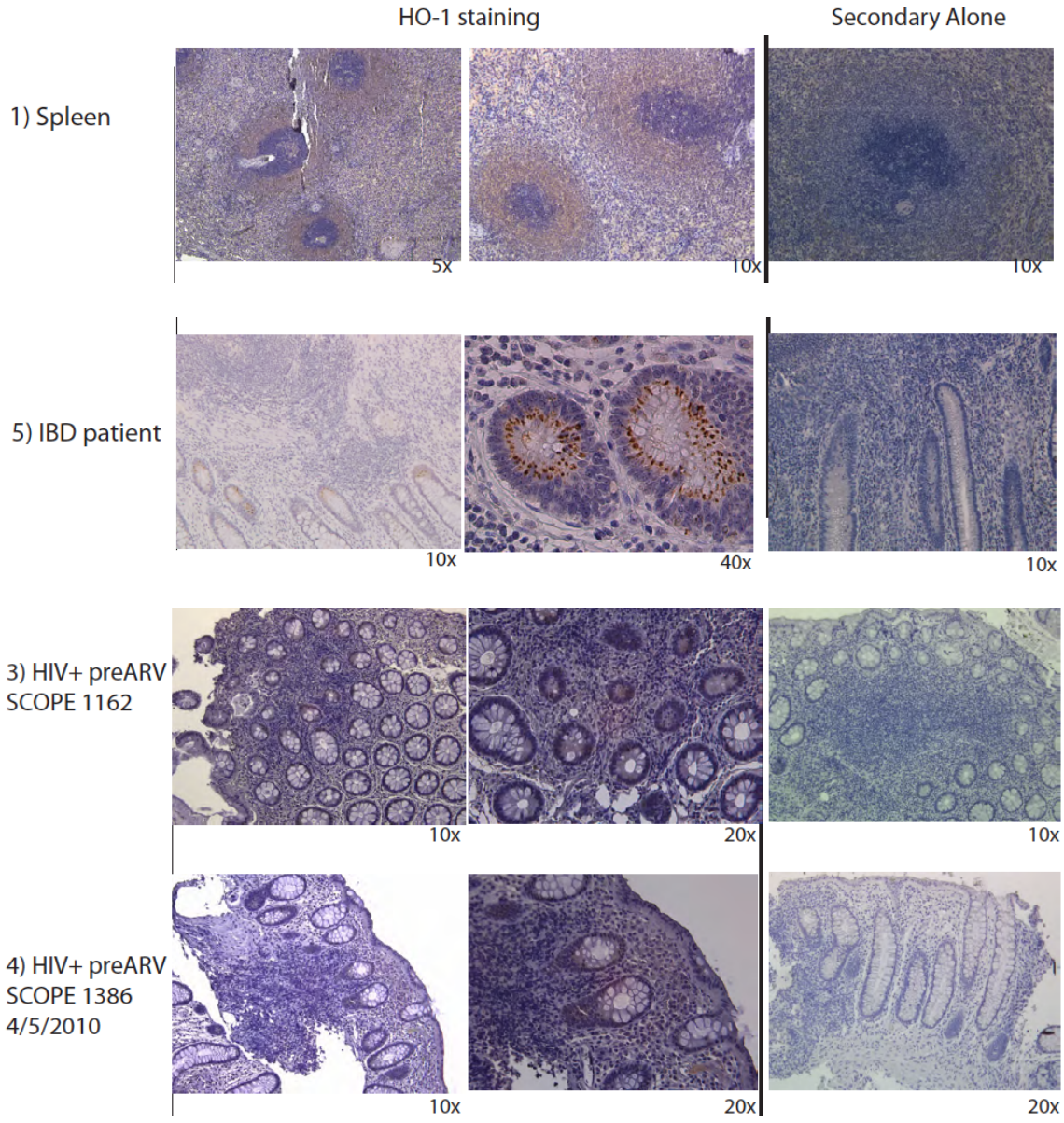

Figure 12: HO-1 immunohistochemistry from human tissues: healthy spleen, colon resection

from IBD patient, and colon biopsy from two ART-naïve HIV patients

4.4.2. HO-1 and microbial translocation products in HAART patients

We hypothesized that the extent of HO-1 induction during HIV disease may contribute to the extent of harmful microbial translocation. We examined the correlation between HO-1 induction in circulating immune cells of HIV-infected patients on suppressive HAART regimens and the extent of microbial translocation observed in these patients as measured by plasma sCD14 (34). PBMCs from 14 HAART-suppressed HIV patients were analyzed for HO-1 transcript while their concurrent sCD14 plasma levels were measured. From this limited sample size, there was a trend towards a positive association between relative HO-1 transcript of PBMCs and plasma sCD14 levels in HAART-suppressed HIV patients. With a β coefficient of 0.2548, these results suggest that for every relative unit increase of HO-1 transcript in PBMCs, there is a concomitant 0.25 ($x10^4$ pg/mL) increase in plasma sCD14 levels in these patients. Although these results did not reach significance, greater sample numbers may show that there is a positive correlation between the extent of HO-1 induction in circulating immune cells and the extent of microbial translocation (Figure 13).

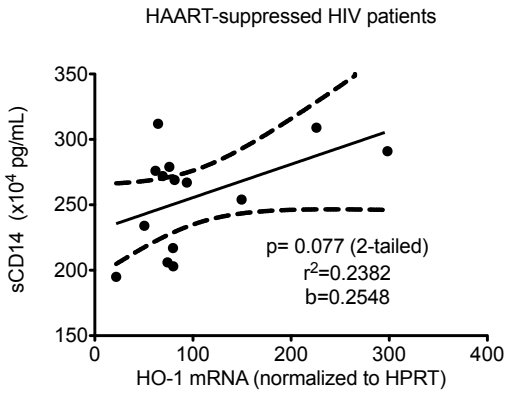

Figure 13: HO-1 relative expression in PBMCs from HAART suppressed HIV patients (14 total) Results reported in median ± I.Q.R. (months on HAART: 17.3 ± 13.5, viral load in RNA copies/mL: ± I.Q.R.= 75 ± 25, CD4 counts in cells/μL: 349 ± 127)

4.5. HO-1 clinical studies in non-human primate SIV infection

SIV-infected AGMs (natural non-human primate hosts that do not normally show SIV disease progression (151) were treated with SnMP (5 animals) or saline (3 animals) longitudinally to determine effects of HO-1 inhibition on viral pathogenesis. SnMP-treated animals were found to have higher peak viral loads during seroconversion and higher levels of T cell activation ($CD8^+$ Ki-67% and HLA-DR%), consistent with the hypothesis that HO-1 activity normally plays a role in suppressing disease progression in this species (Figure 14). Interestingly, SnMP-treated animals had higher absolute $CD4^+$ T cell counts both prior to and during SIV infection. This study is similar to a recent study that experimentally induced immune activation in AGMs with LPS and with a Treg inhibitor (Ontak: Diphtheria toxin-Interleukin-2 fusion protein). In this study, animals treated with LPS had a minor transient increase in viral load as well as an increase in $CD4^+$ and $CD8^+$ cells that were $Ki67^+$ (152).

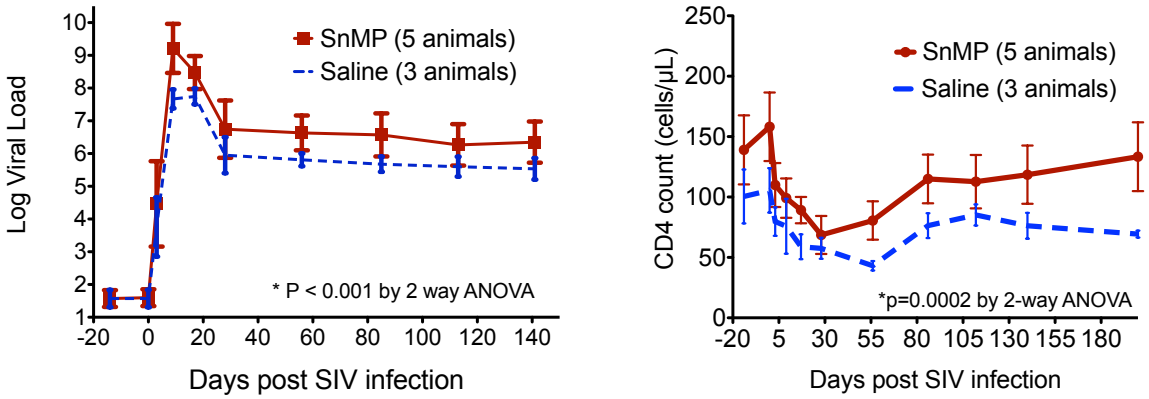

Figure 14: Inhibition of HO-1 by SnMP leads to elevated viral load and increased absolute $CD4^+$ T cell counts in AGMs (AGM) infected with Simian Immunodeficiency Virus (SIV)

4.6. *HO-1 protocol drafts for human clinical studies*

Based on our findings that HO-1 inhibition leads to heightened T cell activation, increased viral loads, and general immune dysfunction, we propose a randomized controlled trial (RCT) for an intervention in Immunological Non-responder (INRs) patients. INRs are HIV patients that fail to restore CD4 counts above a level of 500 cells/μL despite years of suppressive HAART. Based on large cohort studies, INRs represent about 30% of HAART patients (153). More specifically, one publication reported that 44% of HIV-infected individuals who started therapy with a $CD4^+$ cell count of 100 cells/mm3 and 25% of those with 100-200 cells/μL were unable to achieve a $CD4^+$ cell count >500 cells/μL by year ten (154).

We propose an RCT for HIV INRs using metalloporphyrin compounds that are known to alter the activity of HO-1. The metalloporphyrin heme (synthesized endogenously and obtained through diet) and the xenobiotic, CoPP, have been shown to induce greater levels of HO-1 expression from *in vivo* and *in vitro* studies (138,155). The first randomized controlled clinical study using hematin to induce HO-1 expression increased plasma HO-1 protein concentration four- to five-

fold and HO-1 activity ~15-fold relative to baseline at 24 and 48 hours in treated patients (156). Another randomized controlled trial showed that administration of heme arginate led to increased HO-1 mRNA and protein over 48 hours (133).

We hypothesize that efficient up-regulation of HO-1 may be associated with enhanced CD4 recovery in HIV patients undergoing HAART. Our research question is as follows: Does administration of iron protoporphyrin IX enhance CD4 recovery among HIV immunological non-responders receiving (HAART)?

5. Concluding remarks and future perspectives

Given the evidence that immune activation contributes to HIV pathogenesis (9,10,17,157), one therapeutic strategy to combat continued HIV progression would be to utilize agents that lead to a reduced level of immune activation. Previous efforts have been made to develop immunosuppressive agents as potential therapeutics for HIV disease, e.g., cyclosporine A (142), glucocorticoids (143), and Cox-2 inhibitors (144), and all have been tested for their ability to combat HIV-associated immune activation.

The work outlined in this thesis explores the potential for pharmacological augmentation of HO-1 enzymatic therapies as a viable therapeutic option in states where unchecked immune activation causes deleterious clinical outcomes, such as in the setting of chronic HIV infection. We show that HO-1 plays an important role in dampening nonspecific T cell activation in both murine and human studies as well as in an exploratory clinical study in SIV disease. We also show that inter-individual genetic variability in the HO-1 promoter region influences its transcriptional regulation and is important for controlling harmful disease parameters during HIV infection. Such regulation becomes critical when taking into account where HO-1 is regulated. Different blood monocyte populations (defined by CD14 and CD16 expression) differentially express HO-1, and we show that these circulating monocytes also differentially predict HIV disease parameters.

After 30 years of intensive biomedical research in HIV and AIDS, we have arrived at an important and exciting new frontier of discovery. These past five years have been notable for many aspects of HIV therapies, and it is with a hopeful outlook in the future of HIV therapies that I submit this dissertation.

At the most current date, several beacons of light in HIV therapeutics have emerged

during the last two years of my doctorate at UCSF.

First, a historical HIV vaccine trial showed that, for the first time, a vaccine regimen could cut the risk of infection. In a randomized controlled trial of the efficacy of a priming canarypox vector vaccine (ALVAC-HIV [vCP1521]) plus two booster injections of a recombinant glycoprotein 120 subunit vaccine (AIDSVAX B/E), there was a 31.2% decrease in transmission rate in the vaccine versus the placebo arm. Although modest, this study was landmark in showing for the first time that a vaccine could potentially be used as preventative in HIV acquisition (158,159).

Next, a study was published demonstrating the effectiveness and safety of tenofovir gel, an antiretroviral microbicide, for the prevention of HIV infection in women (160). This discovery was important in that it addresses both an unmet therapeutic need while also empowering women to address the behavioral challenges for implementing harm-reduction approaches to combat the spread of HIV (161).

Early this year, it was reported that antiretroviral chemoprophylaxis before exposure was a promising approach for the prevention of HIV acquisition. A randomized controlled trial of HIV-seronegative men or transgender women was designed to have subjects receive a combination of two oral antiretroviral drugs, emtricitabine and tenofovir disoproxil fumarate (FTC–TDF), or once-daily placebo (162,163).

To continue this theme of HIV "treatment as prevention," it was reported this month that antiretroviral therapy that reduces viral replication could limit the transmission of HIV in serodiscordant couples. These two studies highlight that fact that there are both personal and public health benefits from such therapy (164).

Additionally, a study of the first person ever cured of HIV disease has been published

(165). Dubbed “the Berlin patient,” this individual was an HIV-infected patient in whom viral replication remained absent despite discontinuation of antiretroviral therapy after transplantation with CCR5Δ32/Δ32 stem cells. The “Berlin patient” has since made his identity known- Timothy Ray Brown is a Bay Area resident and an important face to help drive the hope and inspiration needed around the world to continue fighting this deadly disease (166).

It is truly an inspiring and encouraging time to be a biomedical researcher of HIV, and it is with a hopeful heart that I continue in my journey as a National Institute of Health post-doctoral researcher at the Center for Infectious Disease Research in Lusaka, Zambia. As a Fogarty International Clinical Research Fellow, my research will focus on characterizing founder HIV quasispecies in mother-to-child (MTCT) HIV infection and correlating these viral signatures to an infant’s clinical and virological outcome. I am excited to apply the knowledge that I have gained in clinical HIV immunology to better understand how the virus evades host immune responses during pregnancy.

6. References

1. Deeks SG. HIV infection, inflammation, immunosenescence, and aging. Annu Rev Med 2010, Jan 27.

2. Ryter SW, Choi AM. Heme oxygenase-1/carbon monoxide: From metabolism to molecular therapy. Am J Respir Cell Mol Biol 2009, Sep;41(3):251-60.

3. Centers for Disease Control (CDC). Update on acquired immune deficiency syndrome (AIDS)--united states. MMWR Morb Mortal Wkly Rep 1982, Sep 24;31(37):507-8, 513-4.

4. Stephenson J. The art of'HAART': Researchers probe the potential and limits of aggressive HIV treatments. JAMA: The Journal of the American Medical Association 1997;277(8):614.

5. McCune JM. The dynamics of CD4+ t-cell depletion in HIV disease. Nature 2001, Apr 19;410(6831):974-9.

6. McCune J, Kaneshima H, Krowka J, Namikawa R, Outzen H, Peault B, et al. The scid-hu mouse: A small animal model for HIV infection and pathogenesis. Annu Rev Immunol 1991;9(1):399-429.

7. Daniel MD, Desrosiers RC, Letvin NL, King NW, Schmidt DK, Sehgal P, Hunt RD. Simian models for AIDS. Cancer Detection and Prevention. Supplement: Official Publication of the International Society for Preventive Oncology, Inc 1987;1:501.

8. Girard MP, Osmanov S, Assossou OM, Kieny MP. Human immunodeficiency virus (HIV) immunopathogenesis and vaccine development: A review. Vaccine 2011, Jun 28.

9. Douek DC, Roederer M, Koup RA. Emerging concepts in the immunopathogenesis of AIDS. Annu Rev Med 2009;60:471-84.

10. Boasso A, Shearer GM. Chronic innate immune activation as a cause of HIV-1 immunopathogenesis. Clin Immunol 2008, Mar;126(3):235-42.

11. Lawn SD, Butera ST, Folks TM. Contribution of immune activation to the pathogenesis and transmission of human immunodeficiency virus type 1 infection. Clin Microbiol Rev 2001, Oct;14(4):753-77, table of contents.

12. Cannavo' G, Paiardini M, Galati D, Cervasi B, Montroni M, De Vico G, et al. Abnormal intracellular kinetics of cell-cycle-dependent proteins in lymphocytes from patients infected with human immunodeficiency virus: A novel biologic link between immune activation, accelerated t-cell turnover, and high levels of apoptosis. Blood 2001, Mar 15;97(6):1756-64.

13. Pantaleo G, Fauci AS. Immunopathogenesis of HIV infection. Annu Rev Microbiol 1996;50:825-54.

14. Manches O, Bhardwaj N. Resolution of immune activation defines nonpathogenic SIV infection. J Clin Invest 2009, Dec;119(12):3512-5.

15. Barbour JD, Ndhlovu LC, Xuan Tan Q, Ho T, Epling L, Bredt BM, et al. High CD8+ T cell activation marks a less differentiated HIV-1 specific CD8+ T cell response that is not altered by suppression of viral replication. Plos One 2009;4(2):e4408.

16. Pandrea I, Apetrei C. Where the wild things are: Pathogenesis of SIV infection in african nonhuman primate hosts. Curr HIV/AIDS Rep 2010, Feb;7(1):28-36.

17. Sodora DL, Allan JS, Apetrei C, Brenchley JM, Douek DC, Else JG, et al. Toward an AIDS vaccine: Lessons from natural simian immunodeficiency virus infections of african nonhuman primate hosts. Nat Med 2009, Aug;15(8):861-5.

18. Hasegawa A, Liu H, Ling B, Borda JT, Alvarez X, Sugimoto C, et al. The level of monocyte turnover predicts disease progression in the macaque model of AIDS. Blood 2009, Oct 1;114(14):2917-25.

19. Hazenberg MD, Stuart JW, Otto SA, Borleffs JC, Boucher CA, de Boer RJ, et al. T-Cell

division in human immunodeficiency virus (HIV)-1 infection is mainly due to immune activation: A longitudinal analysis in patients before and during highly active antiretroviral therapy (HAART). Blood 2000, Jan 1;95(1):249-55.

20. Hellerstein M, Hanley MB, Cesar D, Siler S, Papageorgopoulos C, Wieder E, et al. Directly measured kinetics of circulating T lymphocytes in normal and hiv-1-infected humans. Nat Med 1999, Jan;5(1):83-9.

21. Poli G, FAUCI AS. The effect of cytokines and pharmacologic agents on chronic HIV infection. AIDS Res Hum Retroviruses 1992;8(2):191-7.

22. Matsuyama T, Kobayashi N, Yamamoto N. Cytokines and HIV infection: Is AIDS a tumor necrosis factor disease? AIDS 1991;5(12):1405.

23. Valdez H, Lederman MM. Cytokines and cytokine therapies in HIV infection. AIDS Clinical Review 1997:187.

24. Kinoshita S, Su L, Amano M, Timmerman LA, Kaneshima H, Nolan GP. The T cell activation factor nf-atc positively regulates HIV-1 replication and gene expression in T cells. Immunity 1997;6(3):235-44.

25. Giorgi JV, Hultin LE, McKeating JA, Johnson TD, Owens B, Jacobson LP, et al. Shorter survival in advanced human immunodeficiency virus type 1 infection is more closely associated with T lymphocyte activation than with plasma virus burden or virus chemokine coreceptor usage. J Infect Dis 1999;179:859-70.

26. Deeks SG, Kitchen CM, Liu L, Guo H, Gascon R, Narváez AB, et al. Immune activation set point during early HIV infection predicts subsequent CD4+ t-cell changes independent of viral load. Blood 2004, Aug 15;104(4):942-7.

27. Silvestri G, Paiardini M, Pandrea I, Lederman MM, Sodora DL. Understanding the

benign nature of SIV infection in natural hosts. J Clin Invest 2007, Nov;117(11):3148-54.

28. Favre D, Lederer S, Kanwar B, Ma ZM, Proll S, Kasakow Z, et al. Critical loss of the balance between th17 and T regulatory cell populations in pathogenic SIV infection. Plos Pathog 2009, Feb;5(2):e1000295.

29. Rosenberg ZF, Fauci AS. Immunology of AIDS: Approaches to understanding the immunopathogenesis of HIV infection. International Journal of Clinical & Laboratory Research 1989;19(1):189-209.

30. Mattapallil JJ, Douek DC, Hill B, Nishimura Y, Martin M, Roederer M. Massive infection and loss of memory CD4+ T cells in multiple tissues during acute SIV infection. Nature 2005, Apr 28;434(7037):1093-7.

31. Guadalupe M, Reay E, Sankaran S, Prindiville T, Flamm J, McNeil A, Dandekar S. Severe CD4+ t-cell depletion in gut lymphoid tissue during primary human immunodeficiency virus type 1 infection and substantial delay in restoration following highly active antiretroviral therapy. The Journal of Virology 2003;77(21):11708.

32. Brenchley JM, Schacker TW, Ruff LE, Price DA, Taylor JH, Beilman GJ, et al. CD4+ T cell depletion during all stages of HIV disease occurs predominantly in the gastrointestinal tract. J Exp Med 2004, Sep 20;200(6):749-59.

33. Visintin A, Mazzoni A, Spitzer JH, Wyllie DH, Dower SK, Segal DM. Regulation of toll-like receptors in human monocytes and dendritic cells. The Journal of Immunology 2001;166(1):249.

34. Brenchley JM, Price DA, Schacker TW, Asher TE, Silvestri G, Rao S, et al. Microbial translocation is a cause of systemic immune activation in chronic HIV infection. Nat Med 2006, Dec;12(12):1365-71.

35. Ancuta P, Kamat A, Kunstman KJ, Kim EY, Autissier P, Wurcel A, et al. Microbial translocation is associated with increased monocyte activation and dementia in AIDS patients. Plos One 2008;3(6):e2516.

36. Favre D, Mold J, Hunt PW, Kanwar B, Loke P, Seu L, et al. Tryptophan catabolism by indoleamine 2,3-dioxygenase 1 alters the balance of TH17 to regulatory T cells in HIV disease. Sci Transl Med 2010, May 19;2(32):32ra36.

37. Olivier M, Aggarwal A, Allen J, Almendras AA, Bajorek ES, Beasley EM, et al. A high-resolution radiation hybrid map of the human genome draft sequence. Science 2001, Feb 16;291(5507):1298-302.

38. Genomics C. The sequence of the human genome. Science 2001;291(5507):1304-51.

39. Ahuja SK, Kulkarni H, Catano G, Agan BK, Camargo JF, He W, et al. CCL3L1-CCR5 genotype influences durability of immune recovery during antiretroviral therapy of hiv-1-infected individuals. Nat Med 2008, Apr;14(4):413-20.

40. Burt TD, Agan BK, Marconi VC, He W, Kulkarni H, Mold JE, et al. Apolipoprotein (apo) E4 enhances HIV-1 cell entry in vitro, and the APOE epsilon4/epsilon4 genotype accelerates HIV disease progression. Proc Natl Acad Sci U S A 2008, Jun 24;105(25):8718-23.

41. Faure S, Meyer L, Costagliola D, Vaneensberghe C, Genin E, Autran B, ALT F. Rapid progression to AIDS in HIV+ individuals with a structural variant of the chemokine receptor CX3CR1. Science 2000;287(5461):2274.

42. Clegg AO, Ashton LJ, Biti RA, Badhwar P, Williamson P, Kaldor JM, Stewart GJ. CCR5 promoter polymorphisms, CCR5 59029A and CCR5 59353C, are under represented in hiv-1-infected long-term non-progressors. The australian long-term non-progressor study group.

AIDS 2000, Jan 28;14(2):103-8.

43. McDermott DH, Beecroft MJ, Kleeberger CA, Al-Sharif FM, Ollier WE, Zimmerman PA, et al. Chemokine RANTES promoter polymorphism affects risk of both HIV infection and disease progression in the multicenter AIDS cohort study. AIDS 2000, Dec 1;14(17):2671-8.

44. Ioannidis JP, Rosenberg PS, Goedert JJ, Ashton LJ, Benfield TL, Buchbinder SP, et al. Effects of ccr5-delta32, CCR2-64I, and SDF-1 3'A alleles on HIV-1 disease progression: An international meta-analysis of individual-patient data. Ann Intern Med 2001, Nov 6;135(9):782-95.

45. Martin MP, Gao X, Lee JH, Nelson GW, Detels R, Goedert JJ, et al. Epistatic interaction between KIR3DS1 and HLA-B delays the progression to AIDS. Nat Genet 2002, Aug;31(4):429-34.

46. Tang J, Shelton B, Makhatadze NJ, Zhang Y, Schaen M, Louie LG, et al. Distribution of chemokine receptor CCR2 and CCR5 genotypes and their relative contribution to human immunodeficiency virus type 1 (HIV-1) seroconversion, early HIV-1 RNA concentration in plasma, and later disease progression. J Virol 2002;76(2):662.

47. Vasilescu A, Heath SC, Ivanova R, Hendel H, Do H, Mazoyer A, et al. Genomic analysis of th1-th2 cytokine genes in an AIDS cohort: Identification of IL4 and IL10 haplotypes associated with the disease progression. Genes Immun 2003, Sep;4(6):441-9.

48. An P, Bleiber G, Duggal P, Nelson G, May M, Mangeat B, et al. APOBEC3G genetic variants and their influence on the progression to AIDS. J Virol 2004, Oct;78(20):11070-6.

49. Li M, Song R, Masciotra S, Soriano V, Spira TJ, Lal RB, Yang C. Association of CCR5 human haplogroup E with rapid HIV type 1 disease progression. AIDS Res Hum Retroviruses 2005, Feb;21(2):111-5.

50. Modi WS, Lautenberger J, An P, Scott K, Goedert JJ, Kirk GD, et al. Genetic variation in the CCL18-CCL3-CCL4 chemokine gene cluster influences HIV type 1 transmission and AIDS disease progression. Am J Hum Genet 2006, Jul;79(1):120-8.

51. Haas DW, Geraghty DE, Andersen J, Mar J, Motsinger AA, D'Aquila RT, et al. Immunogenetics of CD4 lymphocyte count recovery during antiretroviral therapy: An AIDS clinical trials group study. J Infect Dis 2006, Oct 15;194(8):1098-107.

52. An P, Duggal P, Wang LH, O'Brien SJ, Donfield S, Goedert JJ, et al. Polymorphisms of CUL5 are associated with CD4+ T cell loss in HIV-1 infected individuals. Plos Genet 2007, Jan 26;3(1):e19.

53. Catano G, Kulkarni H, He W, Marconi VC, Agan BK, Landrum M, et al. HIV-1 disease-influencing effects associated with ZNRD1, HCP5 and HLA-C alleles are attributable mainly to either HLA-A10 or HLA-B*57 alleles. Plos One 2008;3(11):e3636.

54. Salgado M, López-Romero P, Callejas S, López M, Labarga P, Dopazo A, et al. Characterization of host genetic expression patterns in hiv-infected individuals with divergent disease progression. Virology 2011, Mar 1;411(1):103-12.

55. Reich DE, Lander ES. On the allelic spectrum of human disease. Trends in Genetics 2001;17(9):502-10.

56. Need AC, Goldstein DB. Whole genome association studies in complex diseases: Where do we stand? Dialogues Clin Neurosci 2010;12(1):37-46.

57. Wellcome Trust Case Control Consortium. Genome-Wide association study of 14,000 cases of seven common diseases and 3,000 shared controls. Nature 2007, Jun 7;447(7145):661-78.

58. Little J, Hawken S. On track? Using the human genome epidemiology roadmap. Public

Health Genomics 2010;13(4):256-66.

59. Gibbs RA, Belmont JW, Hardenbol P, Willis TD, Yu F, Yang H, et al. The international hapmap project. Nature 2003;426(6968):789-96.

60. Yu W, Yesupriya A, Wulf A, Hindorff LA, Dowling N, Khoury MJ, Gwinn M. GWAS integrator: A bioinformatics tool to explore human genetic associations reported in published genome-wide association studies. Eur J Hum Genet 2011, May 25.

61. Pantaleo G, Fauci AS. New concepts in the immunopathogenesis of HIV infection. Annu Rev Immunol 1995;13:487-512.

62. Buchbinder S, Vittinghoff E. Hiv-Infected long-term nonprogressors: Epidemiology, mechanisms of delayed progression, and clinical and research implications. Microbes and Infection 1999;1(13):1113-20.

63. Deeks SG, Walker BD. Human immunodeficiency virus controllers: Mechanisms of durable virus control in the absence of antiretroviral therapy. Immunity 2007, Sep;27(3):406-16.

64. Fellay J, Shianna KV, Ge D, Colombo S, Ledergerber B, Weale M, et al. A whole-genome association study of major determinants for host control of HIV-1. Science 2007, Aug 17;317(5840):944-7.

65. Fellay J, Ge D, Shianna KV, Colombo S, Ledergerber B, Cirulli ET, et al. Common genetic variation and the control of HIV-1 in humans. Plos Genet 2009, Dec;5(12):e1000791.

66. Limou S, Le Clerc S, Coulonges C, Carpentier W, Dina C, Delaneau O, et al. Genomewide association study of an aids-nonprogression cohort emphasizes the role played by HLA genes (ANRS genomewide association study 02). J Infect Dis 2009, Feb 1;199(3):419-26.

67. Le Clerc S, Limou S, Coulonges C, Carpentier W, Dina C, Taing L, et al. Genomewide association study of a rapid progression cohort identifies new susceptibility alleles for AIDS (ANRS genomewide association study 03). J Infect Dis 2009, Oct 15;200(8):1194-201.

68. Joubert BR, Lange EM, Franceschini N, Mwapasa V, North KE, Meshnick SR, the NIAID Center for HIV/AIDS Vaccine Immunology. A whole genome association study of mother-to-child transmission of HIV in malawi. Genome Med 2010, Mar 1;2(3):17.

69. Ferreira MA, Mangino M, Brumme CJ, Zhao ZZ, Medland SE, Wright MJ, et al. Quantitative trait loci for CD4:CD8 lymphocyte ratio are associated with risk of type 1 diabetes and HIV-1 immune control. Am J Hum Genet 2010, Jan;86(1):88-92.

70. Pereyra F, Jia X, McLaren PJ, Telenti A, de Bakker PI, Walker BD, et al. The major genetic determinants of HIV-1 control affect HLA class I peptide presentation. Science 2010, Dec 10;330(6010):1551-7.

71. Pelak K, Goldstein DB, Walley NM, Fellay J, Ge D, Shianna KV, et al. Host determinants of HIV-1 control in african americans. J Infect Dis 2010, Apr 15;201(8):1141-9.

72. Limou S, Coulonges C, Herbeck JT, van Manen D, An P, Le Clerc S, et al. Multiple-Cohort genetic association study reveals CXCR6 as a new chemokine receptor involved in long-term nonprogression to AIDS. J Infect Dis 2010, Sep 15;202(6):908-15.

73. Troyer JL, Nelson GW, Lautenberger JA, Chinn L, McIntosh C, Johnson RC, et al. Genome-Wide association study implicates pard3b-based AIDS restriction. J Infect Dis 2011, May 15;203(10):1491-502.

74. Shrestha S, Irvin MR, Taylor KD, Wiener HW, Pajewski NM, Haritunians T, et al. A genome-wide association study of carotid atherosclerosis in hiv-infected men. AIDS 2010, Feb 20;24(4):583-92.

75. Bol SM, Moerland PD, Limou S, van Remmerden Y, Coulonges C, van Manen D, et al. Genome-Wide association study identifies single nucleotide polymorphism in DYRK1A associated with replication of HIV-1 in monocyte-derived macrophages. Plos One 2011;6(2):e17190.

76. Petrovski S, Fellay J, Shianna KV, Carpenetti N, Kumwenda J, Kamanga G, et al. Common human genetic variants and HIV-1 susceptibility: A genome-wide survey in a homogeneous african population. AIDS 2011, Feb 20;25(4):513-8.

77. Le Clerc S, Coulonges C, Delaneau O, Van Manen D, Herbeck JT, Limou S, et al. Screening low-frequency SNPS from genome-wide association study reveals a new risk allele for progression to AIDS. J Acquir Immune Defic Syndr 2011, Mar 1;56(3):279-84.

78. Ryter SW, Alam J, Choi AM. Heme oxygenase-1/carbon monoxide: From basic science to therapeutic applications. Physiol Rev 2006, Apr;86(2):583-650.

79. Wagener FA, Volk HD, Willis D, Abraham NG, Soares MP, Adema GJ, Figdor CG. Different faces of the heme-heme oxygenase system in inflammation. Pharmacol Rev 2003, Sep;55(3):551-71.

80. Kapturczak MH, Wasserfall C, Brusko T, Campbell-Thompson M, Ellis TM, Atkinson MA, Agarwal A. Heme oxygenase-1 modulates early inflammatory responses: Evidence from the heme oxygenase-1-deficient mouse. Am J Pathol 2004, Sep;165(3):1045-53.

81. Tamion F, Richard V, Renet S, Thuillez C. Protective effects of heme-oxygenase expression against endotoxic shock: Inhibition of tumor necrosis factor-alpha and augmentation of interleukin-10. J Trauma 2006, Nov;61(5):1078-84.

82. Rémy S, Blancou P, Tesson L, Tardif V, Brion R, Royer PJ, et al. Carbon monoxide inhibits tlr-induced dendritic cell immunogenicity. J Immunol 2009, Feb 15;182(4):1877-84.

83. Lee TS, Chau LY. Heme oxygenase-1 mediates the anti-inflammatory effect of interleukin-10 in mice. Nat Med 2002, Mar;8(3):240-6.

84. Otterbein LE, Bach FH, Alam J, Soares M, Tao Lu H, Wysk M, et al. Carbon monoxide has anti-inflammatory effects involving the mitogen-activated protein kinase pathway. Nat Med 2000, Apr;6(4):422-8.

85. Li M, Peterson S, Husney D, Inaba M, Guo K, Kappas A, et al. Long-Lasting expression of HO-1 delays progression of type I diabetes in NOD mice. Cell Cycle 2007, Mar 1;6(5):567-71.

86. Yachie A, Niida Y, Wada T, Igarashi N, Kaneda H, Toma T, et al. Oxidative stress causes enhanced endothelial cell injury in human heme oxygenase-1 deficiency. J Clin Invest 1999, Jan;103(1):129-35.

87. Koizumi S. Human heme oxygenase-1 deficiency: A lesson on serendipity in the discovery of the novel disease. Pediatr Int 2007, Apr;49(2):125-32.

88. Ono K, Mannami T, Iwai N. Association of a promoter variant of the haeme oxygenase-1 gene with hypertension in women. J Hypertens 2003, Aug;21(8):1497-503.

89. He Z, Hu Y, Feng L, Lu Y, Bao D, Xi Y, et al. Association between HMOX-1 genotype and cardiac function during exercise. Appl Physiol Nutr Metab 2008, Jun;33(3):450-60.

90. Exner M, Minar E, Wagner O, Schillinger M. The role of heme oxygenase-1 promoter polymorphisms in human disease. Free Radic Biol Med 2004, Oct 15;37(8):1097-104.

91. Hirai H, Kubo H, Yamaya M, Nakayama K, Numasaki M, Kobayashi S, et al. Microsatellite polymorphism in heme oxygenase-1 gene promoter is associated with susceptibility to oxidant-induced apoptosis in lymphoblastoid cell lines. Blood 2003, Sep 1;102(5):1619-21.

92. Chen YH, Lin SJ, Lin MW, Tsai HL, Kuo SS, Chen JW, et al. Microsatellite polymorphism in promoter of heme oxygenase-1 gene is associated with susceptibility to coronary artery disease in type 2 diabetic patients. Hum Genet 2002, Jul;111(1):1-8.
93. Yamada N, Yamaya M, Okinaga S, Nakayama K, Sekizawa K, Shibahara S, Sasaki H. Microsatellite polymorphism in the heme oxygenase-1 gene promoter is associated with susceptibility to emphysema. Am J Hum Genet 2000, Jan;66(1):187-95.
94. Herbert A, Rich A. The biology of left-handed Z-DNA. J Biol Chem 1996;271(20):11595.
95. Taha H, Skrzypek K, Guevara I, Nigisch A, Mustafa S, Grochot-Przeczek A, et al. Role of heme oxygenase-1 in human endothelial cells: Lesson from the promoter allelic variants. Arterioscler Thromb Vasc Biol 2010, Aug;30(8):1634-41.
96. Brunt KR, Fenrich KK, Kiani G, Tse MY, Pang SC, Ward CA, Melo LG. Protection of human vascular smooth muscle cells from h2o2-induced apoptosis through functional codependence between HO-1 and AKT. Arterioscler Thromb Vasc Biol 2006, Sep;26(9):2027-34.
97. Ashino T, Yamanaka R, Yamamoto M, Shimokawa H, Sekikawa K, Iwakura Y, et al. Negative feedback regulation of lipopolysaccharide-induced inducible nitric oxide synthase gene expression by heme oxygenase-1 induction in macrophages. Mol Immunol 2008, Apr;45(7):2106-15.
98. Miyazaki T, Kirino Y, Takeno M, Samukawa S, Hama M, Tanaka M, et al. Expression of heme oxygenase-1 in human leukemic cells and its regulation by transcriptional repressor bach1. Cancer Sci 2010, Jun;101(6):1409-16.
99. Abbas AK, Lichtman AH, Pillai S. Cellular and molecular immunology. 7, illustrated ed. Philadelphia: Elsevier - Health Sciences Division; 2011.

100. Johnston RB, Lehmeyer JE, Guthrie LA. Generation of superoxide anion and chemiluminescence by human monocytes during phagocytosis and on contact with surface-bound immunoglobulin G. J Exp Med 1976, Jun 1;143(6):1551-6.

101. Bailly S, Ferrua B, Fay M, Gougerot-Pocidalo MA. Differential regulation of IL 6, IL 1 A, IL 1 beta and TNF alpha production in lps-stimulated human monocytes: Role of cyclic AMP. Cytokine 1990, May;2(3):205-10.

102. Passlick B, Flieger D, Ziegler-Heitbrock HW. Identification and characterization of a novel monocyte subpopulation in human peripheral blood. Blood 1989, Nov 15;74(7):2527-34.

103. Belge KU, Dayyani F, Horelt A, Siedlar M, Frankenberger M, Frankenberger B, et al. The proinflammatory CD14+CD16+DR++ monocytes are a major source of TNF. J Immunol 2002, Apr 1;168(7):3536-42.

104. Szaflarska A, Baj-Krzyworzeka M, Siedlar M, Weglarczyk K, Ruggiero I, Hajto B, Zembala M. Antitumor response of CD14+/CD16+ monocyte subpopulation. Exp Hematol 2004, Aug;32(8):748-55.

105. Randolph GJ, Sanchez-Schmitz G, Liebman RM, Schäkel K. The CD16(+) (fcgammariii(+)) subset of human monocytes preferentially becomes migratory dendritic cells in a model tissue setting. J Exp Med 2002, Aug 19;196(4):517-27.

106. Ancuta P, Moses A, Gabuzda D. Transendothelial migration of CD16+ monocytes in response to fractalkine under constitutive and inflammatory conditions. Immunobiology 2004;209(1-2):11-20.

107. Merino A, Buendia P, Martin-Malo A, Aljama P, Ramirez R, Carracedo J. Senescent CD14+CD16+ monocytes exhibit proinflammatory and proatherosclerotic activity. J

Immunol 2010, Dec 29.

108. Cros J, Cagnard N, Woollard K, Patey N, Zhang SY, Senechal B, et al. Human cd14dim monocytes patrol and sense nucleic acids and viruses via TLR7 and TLR8 receptors. Immunity 2010, Sep 24;33(3):375-86.

109. Heimbeck I, Hofer TP, Eder C, Wright AK, Frankenberger M, Marei A, et al. Standardized single-platform assay for human monocyte subpopulations: Lower CD14+CD16++ monocytes in females. Cytometry A 2010, Sep;77(9):823-30.

110. Ho DD, Rota TR, Hirsch MS. Infection of monocyte/macrophages by human T lymphotropic virus type III. Journal of Clinical Investigation 1986;77(5):1712.

111. Centlivre M, Legrand N, Steingrover R, van der Sluis R, Grijsen ML, Bakker M, et al. Altered dynamics and differential infection profiles of lymphoid and myeloid cell subsets during acute and chronic HIV-1 infection. J Leukoc Biol 2011, May;89(5):785-95.

112. Cassol E, Malfeld S, Mahasha P, van der Merwe S, Cassol S, Seebregts C, et al. Persistent microbial translocation and immune activation in hiv-1-infected south africans receiving combination antiretroviral therapy. J Infect Dis 2010, Sep 1;202(5):723-33.

113. Hunt PW, Martin JN, Sinclair E, Bredt B, Hagos E, Lampiris H, Deeks SG. T cell activation is associated with lower CD4+ T cell gains in human immunodeficiency virus-infected patients with sustained viral suppression during antiretroviral therapy. J Infect Dis 2003, May 15;187(10):1534-43.

114. Almeida M, Cordero M, Almeida J, Orfao A. Abnormal cytokine production by circulating monocytes and dendritic cells of myeloid origin in art-treated HIV-1+ patients relates to CD4+ t-cell recovery and HCV co-infection. Curr HIV Res 2007, May;5(3):325-36.

115. Tilton JC, Johnson AJ, Luskin MR, Manion MM, Yang J, Adelsberger JW, et al.

Diminished production of monocyte proinflammatory cytokines during human immunodeficiency virus viremia is mediated by type I interferons. J Virol 2006, Dec;80(23):11486-97.

116. Funderburg NT, Mayne E, Sieg SF, Asaad R, Jiang W, Kalinowska M, et al. Increased tissue factor expression on circulating monocytes in chronic HIV infection: Relationship to in vivo coagulation and immune activation. Blood 2010, Jan 14;115(2):161-7.

117. Crowe SM, Westhorpe CL, Mukhamedova N, Jaworowski A, Sviridov D, Bukrinsky M. The macrophage: The intersection between HIV infection and atherosclerosis. J Leukoc Biol 2010, Apr;87(4):589-98.

118. Valcour VG, Shiramizu BT, Shikuma CM. HIV DNA in circulating monocytes as a mechanism to dementia and other HIV complications. J Leukoc Biol 2010, Apr;87(4):621-6.

119. Thieblemont N, Weiss L, Sadeghi HM, Estcourt C, Haeffner-Cavaillon N. Cd14Lowcd16High: A cytokine-producing monocyte subset which expands during human immunodeficiency virus infection. Eur J Immunol 1995, Dec;25(12):3418-24.

120. Locher C, Vanham G, Kestens L, Kruger M, Ceuppens JL, Vingerhoets J, Gigase P. Expression patterns of fc gamma receptors, HLA-DR and selected adhesion molecules on monocytes from normal and hiv-infected individuals. Clin Exp Immunol 1994, Oct;98(1):115-22.

121. Allen JB, Wong HL, Guyre PM, Simon GL, Wahl SM. Association of circulating receptor fc gamma riii-positive monocytes in AIDS patients with elevated levels of transforming growth factor-beta. J Clin Invest 1991, May;87(5):1773-9.

122. Kim WK, Sun Y, Do H, Autissier P, Halpern EF, Piatak M, et al. Monocyte heterogeneity underlying phenotypic changes in monocytes according to SIV disease stage. J

Leukoc Biol 2010, Apr;87(4):557-67.

123. Bazil V, Strominger JL. Shedding as a mechanism of down-modulation of CD14 on stimulated human monocytes. J Immunol 1991, Sep 1;147(5):1567-74.

124. Pedron T, Girard R, Chaby R. Variation of lps-binding capacity, epitope expression, and shedding of membrane-bound CD14 during differentiation of human monocytes. J Immunol 1995, Aug 1;155(3):1460-71.

125. Levere RD, Staudinger R, Loewy G, Kappas A, Shibahara S, Abraham NG. Elevated levels of heme oxygenase-1 activity and mrna in peripheral blood adherent cells of acquired immunodeficiency syndrome patients. Am J Hematol 1993, May;43(1):19-23.

126. Chauveau C, Rémy S, Royer PJ, Hill M, Tanguy-Royer S, Hubert FX, et al. Heme oxygenase-1 expression inhibits dendritic cell maturation and proinflammatory function but conserves IL-10 expression. Blood 2005, Sep 1;106(5):1694-702.

127. Mizuno K, Toma T, Tsukiji H, Okamoto H, Yamazaki H, Ohta K, et al. Selective expansion of cd16highccr2- subpopulation of circulating monocytes with preferential production of haem oxygenase (HO)-1 in response to acute inflammation. Clin Exp Immunol 2005, Dec;142(3):461-70.

128. Ancuta P, Liu KY, Misra V, Wacleche VS, Gosselin A, Zhou X, Gabuzda D. Transcriptional profiling reveals developmental relationship and distinct biological functions of CD16+ and CD16- monocyte subsets. BMC Genomics 2009;10:403.

129. Devadas K, Hewlett IK, Dhawan S. Lipopolysaccharide suppresses HIV-1 replication in human monocytes by protein kinase c-dependent heme oxygenase-1 induction. J Leukoc Biol 2010, May;87(5):915-24.

130. Slusher TM, Zipursky A, Bhutani VK. A global need for affordable neonatal jaundice

technologies. Semin Perinatol 2011, Jun;35(3):185-91.

131. Wiener AS, Brody M. Pathogenesis of kernicterus. Obstetrical & Gynecological Survey 1946;1(5):665.

132. Kappas A. A method for interdicting the development of severe jaundice in newborns by inhibiting the production of bilirubin. Pediatrics 2004, Jan;113(1 Pt 1):119-23.

133. Bharucha AE, Kulkarni A, Choi KM, Camilleri M, Lempke M, Brunn GJ, et al. First-In-Human study demonstrating pharmacological activation of heme oxygenase-1 in humans. Clin Pharmacol Ther 2010, Feb;87(2):187-90.

134. Zhong W, Xia Z, Hinrichs D, Rosenbaum JT, Wegmann KW, Meyrowitz J, Zhang Z. Hemin exerts multiple protective mechanisms and attenuates dextran sulfate sodium-induced colitis. J Pediatr Gastroenterol Nutr 2010, Feb;50(2):132-9.

135. Orozco-Ibarra M, Estrada-Sánchez AM, Massieu L, Pedraza-Chaverrí J. Heme oxygenase-1 induction prevents neuronal damage triggered during mitochondrial inhibition: Role of CO and bilirubin. Int J Biochem Cell Biol 2009, Jun;41(6):1304-14.

136. Lee IT, Luo SF, Lee CW, Wang SW, Lin CC, Chang CC, et al. Overexpression of HO-1 protects against tnf-alpha-mediated airway inflammation by down-regulation of tnfr1-dependent oxidative stress. Am J Pathol 2009, Aug;175(2):519-32.

137. Gan HT, Chen JD. Induction of heme oxygenase-1 improves impaired intestinal transit after burn injury. Surgery 2007, Mar;141(3):385-93.

138. Attuwaybi BO, Kozar RA, Moore-Olufemi SD, Sato N, Hassoun HT, Weisbrodt NW, Moore FA. Heme oxygenase-1 induction by hemin protects against gut ischemia/reperfusion injury. J Surg Res 2004, May 1;118(1):53-7.

139. Hayashi S, Takamiya R, Yamaguchi T, Matsumoto K, Tojo SJ, Tamatani T, et al.

Induction of heme oxygenase-1 suppresses venular leukocyte adhesion elicited by oxidative stress: Role of bilirubin generated by the enzyme. Circ Res 1999, Oct 15;85(8):663-71.

140. Devadas K, Dhawan S. Hemin activation ameliorates HIV-1 infection via heme oxygenase-1 induction. J Immunol 2006, Apr 1;176(7):4252-7.

141. Giorgi JV, Hultin LE, McKeating JA, Johnson TD, Owens B, Jacobson LP, et al. Shorter survival in advanced human immunodeficiency virus type 1 infection is more closely associated with T lymphocyte activation than with plasma virus burden or virus chemokine coreceptor usage. J Infect Dis 1999, Apr;179(4):859-70.

142. Wainberg MA, Dascal A, Blain N, Fitz-Gibbon L, Boulerice F, Numazaki K, Tremblay M. The effect of cyclosporine A on infection of susceptible cells by human immunodeficiency virus type 1. Blood 1988, Dec;72(6):1904-10.

143. Andrieu JM, Lu W, Levy R. Sustained increases in CD4 cell counts in asymptomatic human immunodeficiency virus type 1-seropositive patients treated with prednisolone for 1 year. J Infect Dis 1995, Mar;171(3):523-30.

144. Pettersen FO, Torheim EA, Dahm AE, Aaberge IS, Lind A, Holm M, et al. An exploratory trial of cyclooxygenase type 2 inhibitor in HIV-1 infection: Downregulated immune activation and improved T cell-dependent vaccine responses. J Virol 2011, Jul;85(13):6557-66.

145. Burt TD, Seu L, Mold JE, Kappas A, McCune JM. Naive human T cells are activated and proliferate in response to the heme oxygenase-1 inhibitor tin mesoporphyrin. J Immunol 2010, Nov 1;185(9):5279-88.

146. Han J, Wang B, Han N, Zhao Y, Song C, Feng X, et al. CD14(high)CD16(+) rather than CD14(low)CD16(+) monocytes correlate with disease progression in chronic hiv-infected

patients. J Acquir Immune Defic Syndr 2009, Dec;52(5):553-9.

147. Fischer-Smith T, Tedaldi EM, Rappaport J. CD163/CD16 coexpression by circulating monocytes/macrophages in HIV: Potential biomarkers for HIV infection and AIDS progression. AIDS Res Hum Retroviruses 2008, Mar;24(3):417-21.

148. Paul G, Bataille F, Obermeier F, Bock J, Klebl F, Strauch U, et al. Analysis of intestinal haem-oxygenase-1 (HO-1) in clinical and experimental colitis. Clin Exp Immunol 2005, Jun;140(3):547-55.

149. Becker JC, Fukui H, Imai Y, Sekikawa A, Kimura T, Yamagishi H, et al. Colonic expression of heme oxygenase-1 is associated with a better long-term survival in patients with colorectal cancer. Scand J Gastroenterol 2007, Jul;42(7):852-8.

150. Takagi T, Naito Y, Mizushima K, Nukigi Y, Okada H, Suzuki T, et al. Increased intestinal expression of heme oxygenase-1 and its localization in patients with ulcerative colitis. J Gastroenterol Hepatol 2008, Dec;23 Suppl 2:S229-33.

151. Lederer S, Favre D, Walters KA, Proll S, Kanwar B, Kasakow Z, et al. Transcriptional profiling in pathogenic and non-pathogenic SIV infections reveals significant distinctions in kinetics and tissue compartmentalization. Plos Pathog 2009, Feb;5(2):e1000296.

152. Pandrea I, Gaufin T, Brenchley JM, Gautam R, Monjure C, Gautam A, et al. Cutting edge: Experimentally induced immune activation in natural hosts of simian immunodeficiency virus induces significant increases in viral replication and CD4+ T cell depletion. J Immunol 2008, Nov 15;181(10):6687-91.

153. Kaufmann GR, Furrer H, Ledergerber B, Perrin L, Opravil M, Vernazza P, et al. Characteristics, determinants, and clinical relevance of CD4 T cell recovery to< 500 cells/μl in HIV type 1-infected individuals receiving potent antiretroviral therapy. Clinical Infectious

Diseases 2005;41(3):361-72.

154. Kelley CF, Kitchen CM, Hunt PW, Rodriguez B, Hecht FM, Kitahata M, et al. Incomplete peripheral CD4+ cell count restoration in hiv-infected patients receiving long-term antiretroviral treatment. Clin Infect Dis 2009, Mar 15;48(6):787-94.

155. Petrache I, Otterbein LE, Alam J, Wiegand GW, Choi AM. Heme oxygenase-1 inhibits tnf-alpha-induced apoptosis in cultured fibroblasts. Am J Physiol Lung Cell Mol Physiol 2000, Feb;278(2):L312-9.

156. Doberer D, Haschemi A, Andreas M, Zapf TC, Clive B, Jeitler M, et al. Haem arginate infusion stimulates haem oxygenase-1 expression in healthy subjects. Br J Pharmacol 2010, Aug 13.

157. Hunt PW. Role of immune activation in HIV pathogenesis. Curr HIV/AIDS Rep 2007, Feb;4(1):42-7.

158. Dolin R. HIV vaccine trial results□an opening for further research. New England Journal of Medicine 2009;361(23):2279-80.

159. Rerks-Ngarm S, Pitisuttithum P, Nitayaphan S, Kaewkungwal J, Chiu J, Paris R, et al. Vaccination with ALVAC and AIDSVAX to prevent HIV-1 infection in thailand. N Engl J Med 2009, Dec 3;361(23):2209-20.

160. Abdool Karim Q, Abdool Karim SS, Frohlich JA, Grobler AC, Baxter C, Mansoor LE, et al. Effectiveness and safety of tenofovir gel, an antiretroviral microbicide, for the prevention of HIV infection in women. Science 2010, Sep 3;329(5996):1168-74.

161. Vermund SH, Van Damme L. HIV prevention in women: Next steps. Science 2011;331(6015):284.

162. Michael NL. Oral preexposure prophylaxis for HIV□another arrow in the quiver? New

England Journal of Medicine 2010;363(27):2663-5.

163. Grant RM, Lama JR, Anderson PL, McMahan V, Liu AY, Vargas L, et al. Preexposure chemoprophylaxis for HIV prevention in men who have sex with men. N Engl J Med 2010, Dec 30;363(27):2587-99.

164. Cohen MS, Chen YQ, McCauley M, Gamble T, Hosseinipour MC, Kumarasamy N, et al. Prevention of HIV-1 infection with early antiretroviral therapy. N Engl J Med 2011, Jul 18.

165. Allers K, Hütter G, Hofmann J, Loddenkemper C, Rieger K, Thiel E, Schneider T. Evidence for the cure of HIV infection by CCR5Δ32/Δ32 stem cell transplantation. Blood 2011, Mar 10;117(10):2791-9.

166. Parker R, Sereti I. The power of 1 in HIV therapeutics. Blood 2011, Mar 10;117(10):2746-7.

I

Functional studies of heme oxygenase-1 in mice

and humans

"The General Experience" (5th Floor, Building 3, SF General Hospital)

Dan Jumanan (Artist)

Title: Metalloporphyrin administration in mice leads to altered T cell maturation and antigen presenting cell phenotype in lymphoid organs

Abstract:

Background

Metalloporphyrins were administered to mice to determine the effects of HO-1 activity on immune cells of lymphoid organs. Specifically, we hypothesized that inhibition of HO-1 *in vivo* by SnMP would result in T cell activation and proliferation while induction by CoPP would result in a reciprocal effect.

Methods

To determine how HO-1 pharmacological agents affect peripheral lymphoid tissue, wild-type adult mice were injected intraperitoneally with either saline, the HO-1 inducer CoPP (8 umoles/kg), or SnMP (6 umoles/kg). Mice were sacrificed at days 1, 3, and 7, and lymph nodes (pooled inguinal, axillary, and brachial lymph nodes) and spleen were harvested. *Results*

On day 3, mice injected with either metalloporphyrin displayed increased $CD3^+$ T cell apoptosis (Annexin V^+) in their lymph nodes, and had fewer naïve $CD4^+$ and $CD8^+$ T cells in both lymph nodes and spleen. Mice injected with either metalloporphyrin displayed decreased levels of the co-stimulatory marker CD86 and the murine major histocompability receptor on $CD11c^+$ cells in both lymph nodes and spleen.

Conclusions

These results demonstrate that pharmacological inhibition of HO-1 results in enhanced T cell maturation and apoptosis as well as in decreased expression of co-stimulatory markers on antigen-presenting cells.

Introduction

Heme oxygenase is a key enzyme in the catabolic conversion of intracellular heme and the overall maintenance of iron stores and carbon monoxide release. It is the rate limiting enzyme in the breakdown of heme to its stoichiometric reaction products CO, Fe^{2+}, and biliverdin (1).

Recently HO-1 has been implicated as an immune modulator with anti-proliferative, anti-oxidant, and anti-apoptotic effects (2). Studies with the HO-1 (-/-) mouse show that during activation (with either LPS or αCD3/αCD28), mouse macrophages deficient in HO-1 displayed increased production of TNFα, IFNα, IL-6, as well as IL-2 (3). Furthermore, HO-1 (-/-) mice displayed splenomagaly, lymphadenopathy, leukocytosis, hepatic inflammatory infiltrates, glomerulonephritis, as well as iron overload.

Studies have shown that HO-1 inhibits the expression of the pro-inflammatory cytokine TNFα while maintaining or augmenting the expression of the anti-inflammatory cytokine, IL-10. Notably, these observations were made in the myeloid lineage cells such as dendritic cells and macrophages (4-6). The mechanism of cytoprotection by HO-1 is primarily attributed to the actions of carbon monoxide, and exogenous administration of CO most closely mimics its effects. Administration of CO to Mkk3 (-/-) mice augmented IL-10 expression and inhibited TNFα expression via a mitogen-activated protein kinase pathway within macrophages (7).

In the NOD mouse model of type-1 diabetes, induction of HO-1 with cobalt protoporphyrin IX (CoPP) resulted in the rescue of normal insulin production well after autoimmune pancreatitis and islet destruction. This effect was attributed to HO-1 activity, as the administration of HO-1 inhibitor, SnMP, reversed these effects (8).

One reported clinical case study of an individual who was deficient for HO-1 reported growth retardation, anemia, leukocytosis, thrombocytosis, elevated serum haptoglobin, ferritin, and heme, low bilirubin concentration, hemolysis, an abnormal coagulation system, inflammation, high levels of heme, high levels of cold reactive protein, dysmorphic monocytes, lymphadenopathy and persistent endothelial damage with an increase in adhesion molecules such as von Willebrand factor, ICAM1, and selectins. (9,10).

To determine how peripheral lymphoid tissue were affected by pharmacological alteration of HO-1, mice were intraperitoneally injected with the inducer (CoPP) and the inhibitor (SnMP) over the course of a week. Various immune cell subsets were analyzed in a time course experiment for activation, proliferation, and maturation profiles.

Methods:

Research design

Adult female Balb/c mice (3 months) were given intreperitoneal injections of PBS (200 uL sterile 1x PBS), SnMP (6 umoles/kg, or 0.18 umoles) or CoPP: (8 umoles/kg, or 0.24 umoles). Mice were analyzed in triplicate for each sample collection (days 1, 3, and 7) for a total of 27 mice.

Tissue preparation

Pooled lymph nodes (pooled inguinal, axillary, and brachial lymph nodes) and spleen were harvested by crushing isolated organs over 70um mesh filter in RPMI-10 media (RPMI 1640 supplemented with 10% FBS, 1% penicillin/streptomycin, and 2 mM L-glutamine (Mediatech). Cells were counted on a hemacytometer to allow for uniform antibody staining.

Staining for Flow cytometry:

All cells were stained with a live/dead marker Amine-Aqua/Am-Cyan Live/Dead to exclude dead cells from analysis. For flow cytometry analysis, cells were washed in staining buffer [PBS with 2% FBS and 2 mM ethylenediamine tetra-acetic acid – EDTA] and then incubated for 30 minutes at 4°C in the presence of directly-conjugated fluorescent mAbs. All cells were stained with a live/dead marker (Amine-Aqua/Am-Cyan Live/Dead; Invitrogen) so that dead cells could be excluded from analysis. The cells were washed in staining buffer, and then fixed and permeabilized in Becton Dickinson Cytofix/Cytoperm according to the manufacturer's protocol for intracellular staining. Data were acquired with an LSR-II flow cytometer (BD Biosciences) and analyzed with FlowJo software (Treestar, Ashland, OR).

T cell maturation panel

Extracellular staining: the following antibodies were ordered from BD Biosciences (concentration, clone): CD25 Apccy7 (concentration 1:50, clone PC61), CD44 APC

(1:50, IM7), CD62L Pe-cy7 (1:150, MEL-14), CD3-Pacific Blue (1:100, 500A2); from eBioscience: MHC Class II (I-A/I-E) (1:150, M5/114.15.2); from Invitrogen: CD4 Qdot605 (final 1:150), Live Dead - AmCyan (final 1:300), CD8 Pecy5.5 (final 1:150, MCD0818)

Intracellular staining: The following antibodies were ordered from BD biosciences: Ki67-FITC (1:150, B56) and Foxp3 PE (1:150, MF23)

Dendritic cell maturation panel

Extracellular staining: the following antibodies were ordered from BD Biosciences (concentration, clone): CD3-Pacific Blue (1:100, 500A2), Gr1 Apccy7 (1:100, RB6-8C5); from eBioscience: CD14 PE (1:150, Sa2-8), MHC Class II (I-A/I-E) (1:150, M5/114.15.2), CD86 Pecy5 (1:100, GL-1), CD45R PE-Texas Red (1:150, RA3-6B2), CD80 FITC (1:50, 16-10A1), CD11c Pecy7 (1:100, N418), CD11b A647 (1:100, M1/70); from Invitrogen: Live Dead - AmCyan (final 1:300)

Results

The schematic for the intraperitoneal administration of metallorporphyrins into mice is summarized in Figure 1. Significant associations were made starting day 3 of the experimental course and were not observed at day 7 of the study. These results suggest that the kinetics of metalloporphyrin effects *in vivo* occurs several days after administration and disappear by week 1.

Mice injected with either metalloporphyrin displayed increased $CD3^+$ T cell apoptosis (Annexin V^+) in their lymph nodes ($p=0.0008$, 2-way ANOVA) (Figure 2), and had fewer

naïve ($CD44^{-}CD62L^{+}$) $CD4^{+}$ and $CD8^{+}$ T cells in both lymph nodes (p= 0.0043 and p= 0.0418, respectively by 2-way ANOVA) and a trending effect in the spleen (p=0.059 and p=0.0744 by 2-way ANOVA) (Figure 3).

Mice injected with either metalloporphyrin displayed decreased levels of the co-stimulatory marker CD86 and the murine major histocompability class II receptor on $CD11c^{+}$ cells in the spleen (p= 0.0305 and p=0.0143) (Figure 5).

Conclusions

Metalloporphyrin administration in mice led to decreased naïve $CD4^{+}$ and $CD8^{+}$ T cells ($CD44^{-}CD62L^{+}$) as well as increased percentages of pro-apoptotic cells ($AnnexinV^{+}$) in both lymph nodes and spleen. These results from the SnMP administration are directly in line with evidence from PBMCs from our *in vitro* human studies (11).

Analyses of antigen-presenting cells in these same animals showed that they displayed decreased expression of the CD86 co-stimulatory receptor and MHC Class II receptor on $CD11c^{+}$ dendritic cells in spleen.

These results show that *in vivo* administration of pharmacological HO-1 compounds in mice largely recapitulate the *in vitro* studies in human PBMCs. The results from these *in vivo* studies in mice will allow us to make more informed decisions concerning dosing, pharmacokinetics, and outcome measures for any future clinical intervention studies of these metalloporphyrins.

References

1. Ryter SW, Alam J, Choi AM. Heme oxygenase-1/carbon monoxide: From basic science to therapeutic applications. Physiol Rev 2006, Apr;86(2):583-650.

2. Wagener FA, Volk HD, Willis D, Abraham NG, Soares MP, Adema GJ, Figdor CG. Different faces of the heme-heme oxygenase system in inflammation. Pharmacol Rev 2003, Sep;55(3):551-71.

3. Kapturczak MH, Wasserfall C, Brusko T, Campbell-Thompson M, Ellis TM, Atkinson MA, Agarwal A. Heme oxygenase-1 modulates early inflammatory responses: Evidence from the heme oxygenase-1-deficient mouse. Am J Pathol 2004, Sep;165(3):1045-53.

4. Lee TS, Chau LY. Heme oxygenase-1 mediates the anti-inflammatory effect of interleukin-10 in mice. Nat Med 2002, Mar;8(3):240-6.

5. Rémy S, Blancou P, Tesson L, Tardif V, Brion R, Royer PJ, et al. Carbon monoxide inhibits tlr-induced dendritic cell immunogenicity. J Immunol 2009, Feb 15;182(4):1877-84.

6. Tamion F, Richard V, Renet S, Thuillez C. Protective effects of heme-oxygenase expression against endotoxic shock: Inhibition of tumor necrosis factor-alpha and augmentation of interleukin-10. J Trauma 2006, Nov;61(5):1078-84.

7. Otterbein LE, Bach FH, Alam J, Soares M, Tao Lu H, Wysk M, et al. Carbon monoxide has anti-inflammatory effects involving the mitogen-activated protein kinase pathway. Nat Med 2000, Apr;6(4):422-8.

8. Li M, Peterson S, Husney D, Inaba M, Guo K, Kappas A, et al. Long-Lasting expression of HO-1 delays progression of type I diabetes in NOD mice. Cell Cycle 2007, Mar 1;6(5):567-71.

9. Koizumi S. Human heme oxygenase-1 deficiency: A lesson on serendipity in the discovery of the novel disease. Pediatr Int 2007, Apr;49(2):125-32.

10. Yachie A, Niida Y, Wada T, Igarashi N, Kaneda H, Toma T, et al. Oxidative stress causes enhanced endothelial cell injury in human heme oxygenase-1 deficiency. J Clin Invest 1999, Jan;103(1):129-35.

11. Burt TD, Seu L, Mold JE, Kappas A, McCune JM. Naive human T cells are activated and proliferate in response to the heme oxygenase-1 inhibitor tin mesoporphyrin. J Immunol 2010, Nov 1;185(9):5279-88.

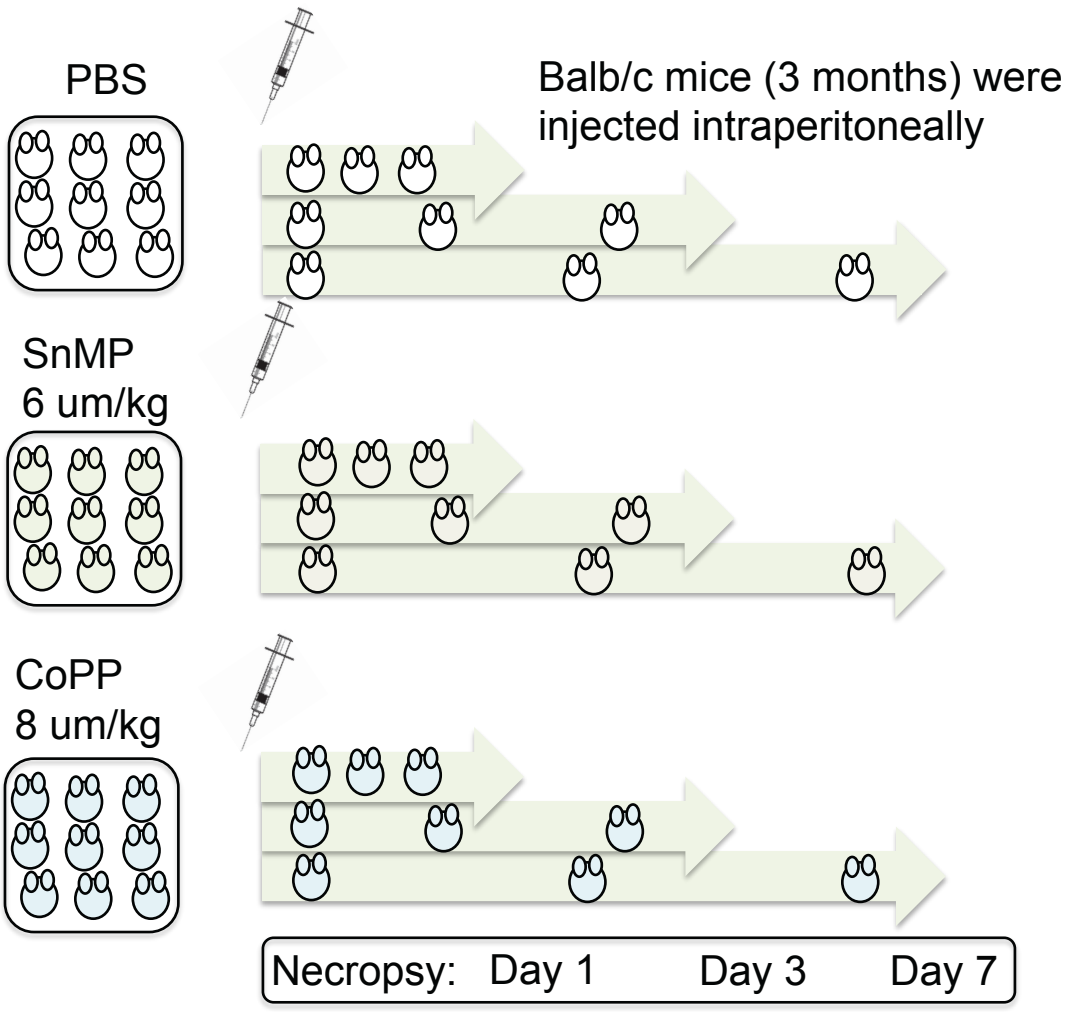

Figure 1: Schematic of metalloporphyrin administration to mice

Figure 2: T cell apoptosis, proliferation, and cell maturation in lymph nodes

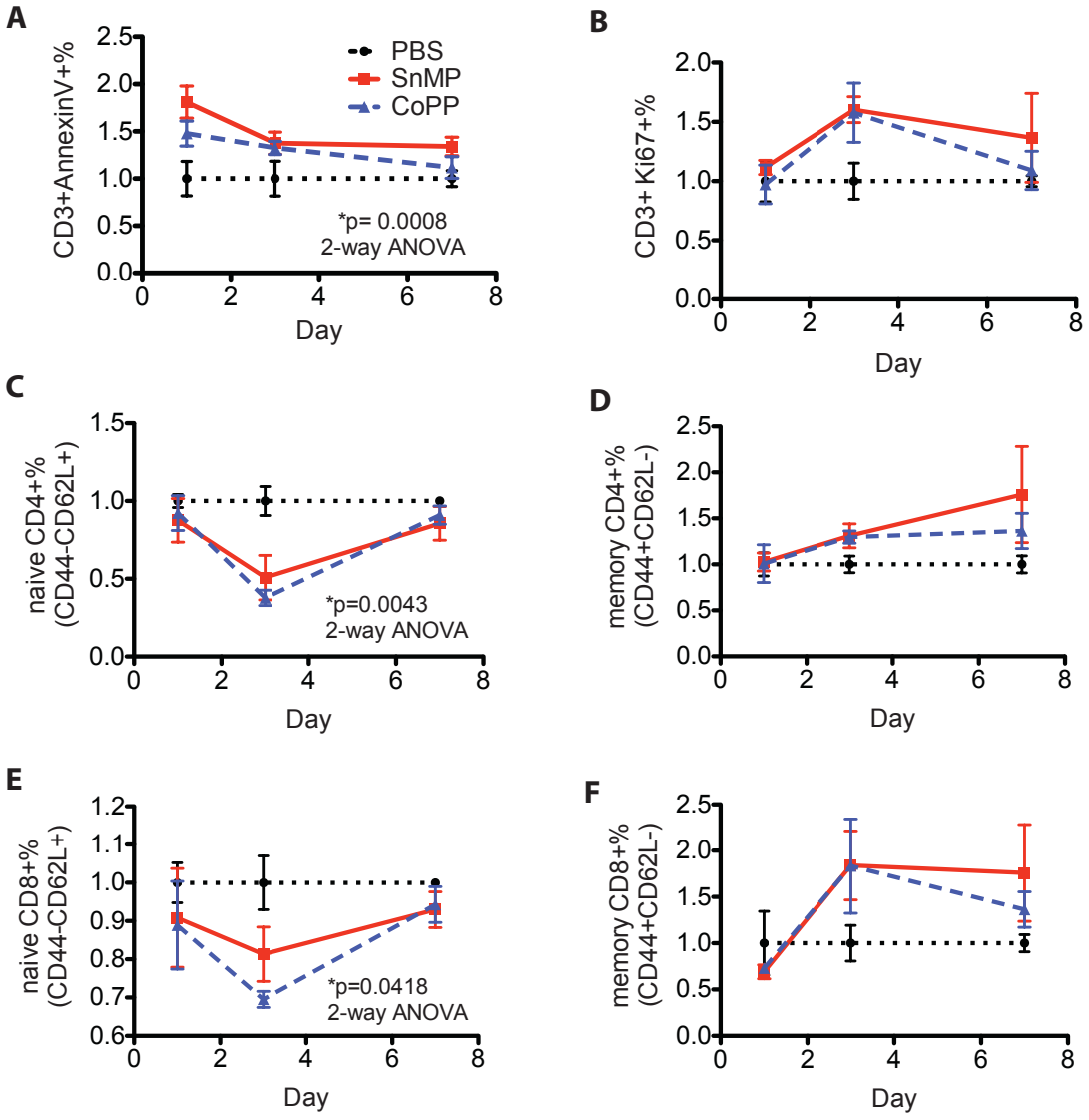

Figure 3: Antigen presenting cell maturation profiles in lymph node

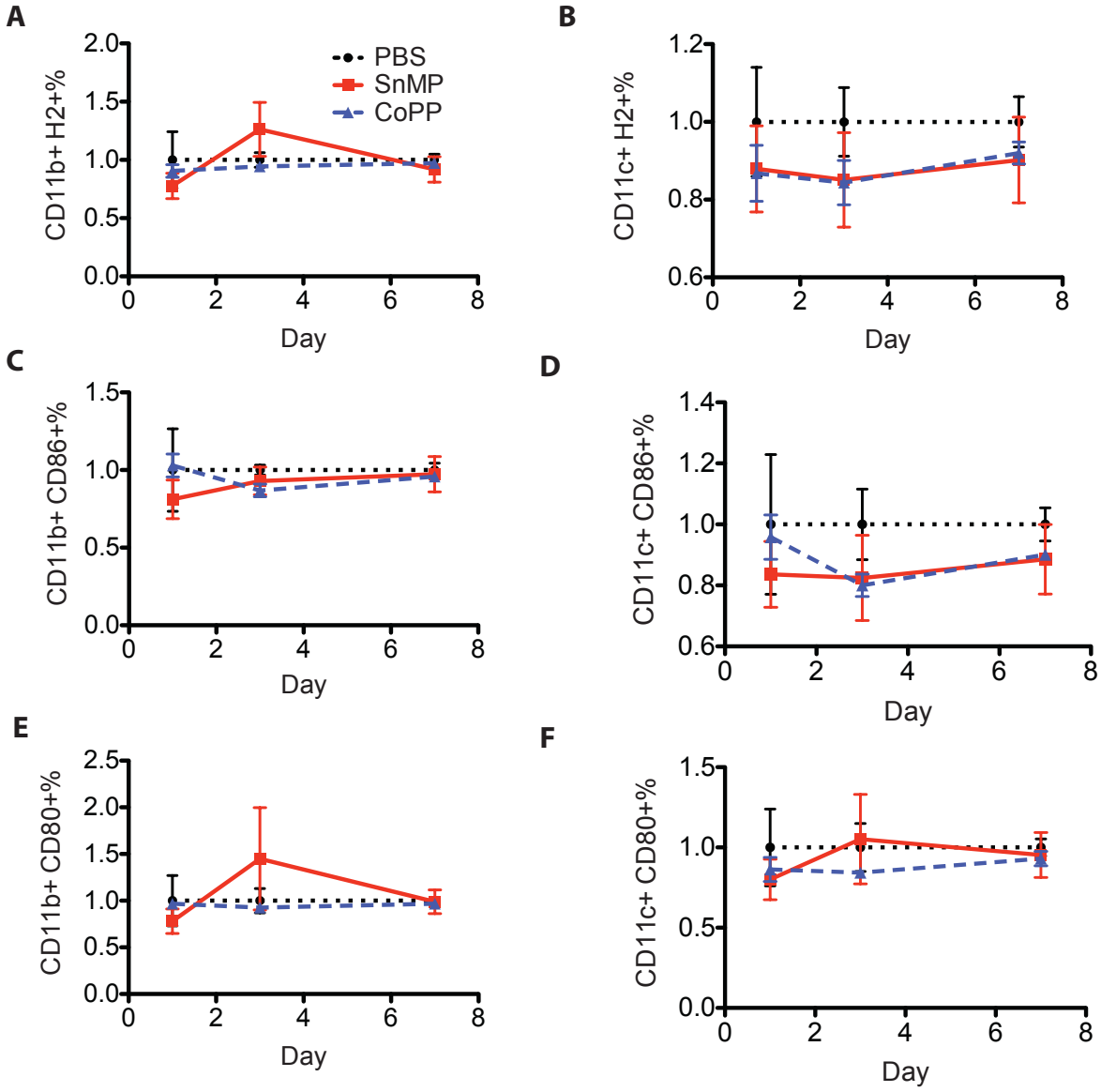

Figure 4: T cell apoptosis, proliferation, and cell maturation in spleen

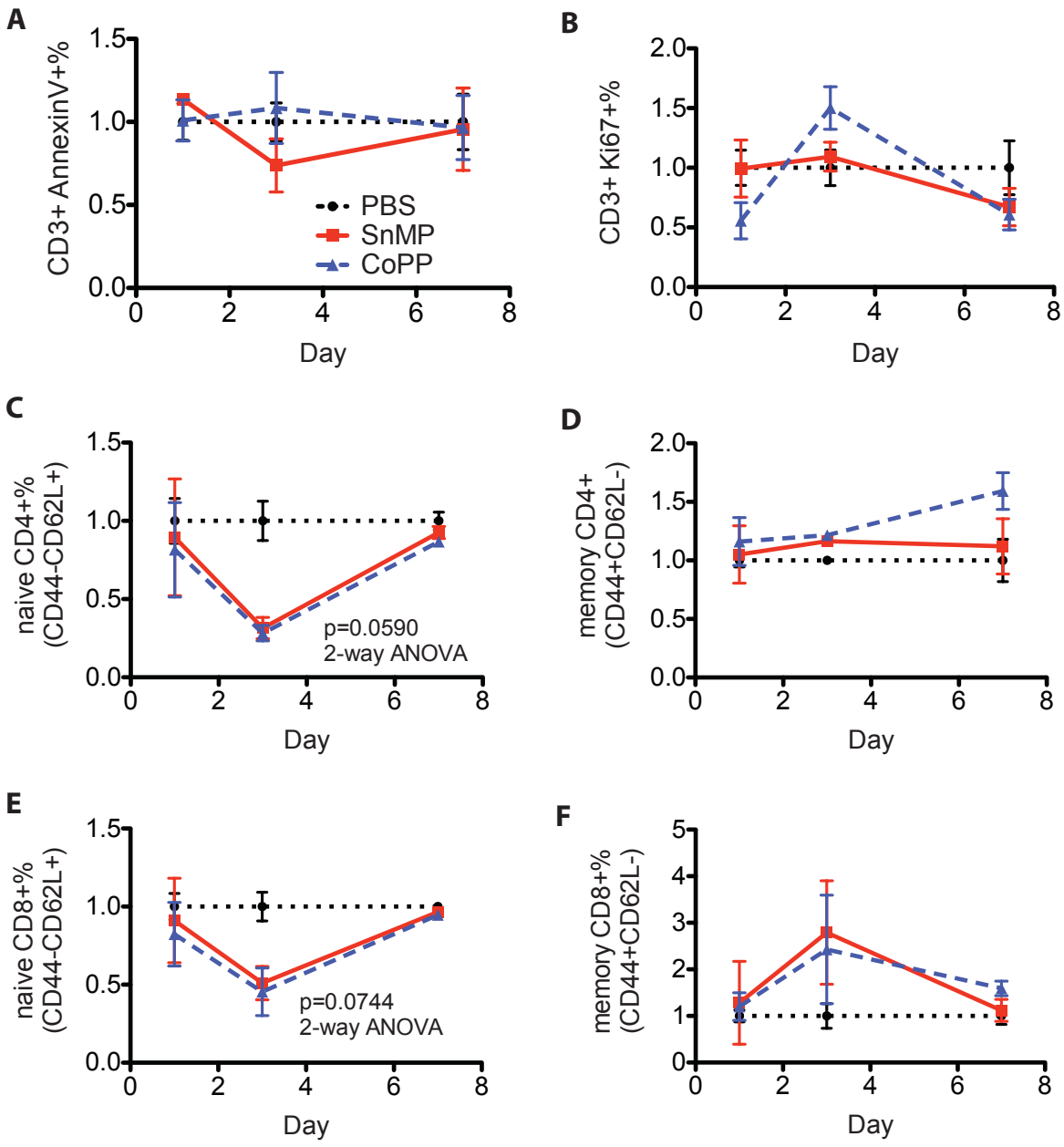

Figure 5: Antigen presenting cell maturation profiles in spleen

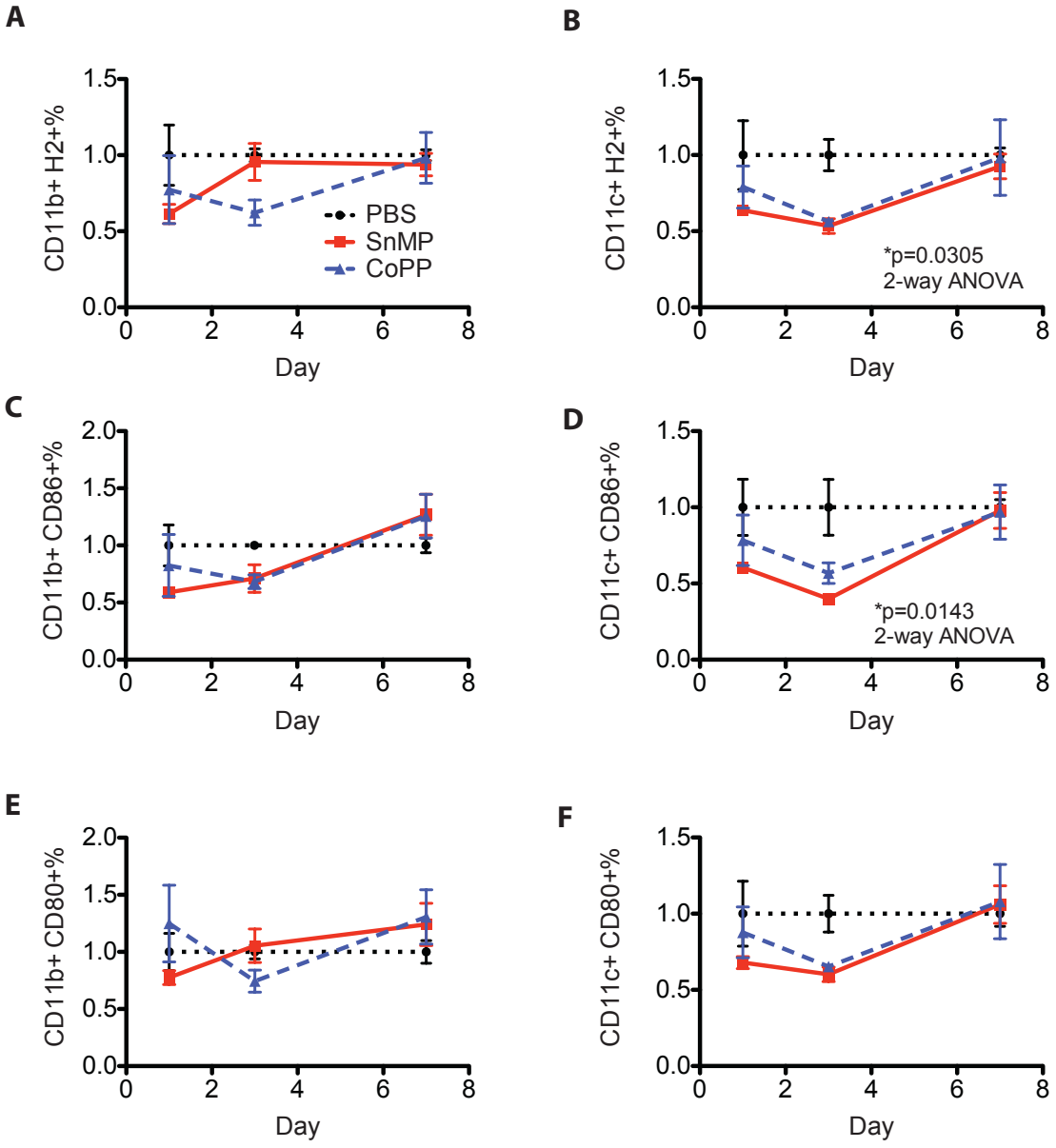

The Journal of Immunology

Naive Human T Cells Are Activated and Proliferate in Response to the Heme Oxygenase-1 Inhibitor Tin Mesoporphyrin

Trevor D. Burt, Lillian Seu, Jeffrey E. Mold, Attallah Kappas and Joseph M. McCune

J. Immunol. published online Oct 4, 2010; doi:10.4049/jimmunol.0903127

The Journal of Immunology is published twice each month by The American Association of Immunologists, Inc., 9650 Rockville Pike, Bethesda, MD 20814-3994.

Print ISSN: 0022-1767 Online ISSN: 1550-6606.

Published October 4, 2010, doi:10.4049/jimmunol.0903127

Naive Human T Cells Are Activated and Proliferate in Response to the Heme Oxygenase-1 Inhibitor Tin Mesoporphyrin

Trevor D. Burt,*,† Lillian Seu,†,‡ Jeffrey E. Mold,† Attallah Kappas,§ and Joseph M. McCune†,¶

Heme oxygenase-1 (HO-1) and its catabolic by-products have potent anti-inflammatory activity in many models of disease. It is not known, however, if HO-1 also plays a role in the homeostatic control of T cell activation and proliferation. We demonstrate here that the HO-1 inhibitor tin mesoporphyrin (SnMP) induces activation, proliferation, and maturation of naive $CD4^+$ and $CD8^+$ T cells via interactions with $CD14^+$ monocytes in vitro. This response is dependent upon interactions of T cells with MHC class I and II on the surface of $CD14^+$ monocytes. Furthermore, $CD4^+CD25^+FoxP3^+$ regulatory T cells were able to suppress this proliferation, even though their suppressive activity was itself impaired by SnMP. Given the magnitude of the Ag-independent T cell response induced by SnMP, we speculate that HO-1 plays an important role in dampening nonspecific T cell activation. Based on these findings, we propose a potential role for HO-1 in the control of naive T cell homeostatic proliferation. ***The Journal of Immunology*****, 2010, 185: 000–000.**

Heme oxygenase-1 (HO-1) catalyzes the breakdown of heme from intracellular hemoproteins and erythrocyte-derived hemoglobin into biliverdin, ferrous iron (Fe^{2+}), and carbon monoxide (CO) (1, 2). In addition to its crucial role as a catabolic enzyme, HO-1 is also a potent stress-response protein, induced by free-radical and oxidative stress caused by heavy metal exposure, bacterial LPS, inflammatory cytokines, hypoxia, and hyperoxia (2–8). Under varying circumstances, it has antiproliferative, antioxidant, and antiapoptotic effects (2, 9–11). The ability of HO-1 to be induced by such a great number and variety of stimuli underscores its importance as a cytoprotective and homeostatic factor.

*Division of Neonatology, Department of Pediatrics and †Division of Experimental Medicine, Department of Medicine, San Francisco General Hospital; ‡Department of Bioengineering and Therapeutic Sciences and ¶Department of Microbiology and Immunology, University of California San Francisco, San Francisco, CA 94110; and §Rockefeller University Hospital, The Rockefeller University, New York, NY 10021

Received for publication September 23, 2009. Accepted for publication August 30, 2010.

This work was supported in part by National Institutes of Health Awards U01 AI43641 and R37 AI40312 to J.M.M., who is the recipient of the Burroughs Wellcome Fund Clinical Scientist Award in Translational Research and of the National Institutes of Health Director's Pioneer Award Program, part of the National Institutes of Health Roadmap for Medical Research, through Grant DPI OD00329. During the period in which this work was carried out, T.D.B. was a fellow of the Pediatric Scientist Development Program and was supported by the American Pediatric Society, the American Academy of Pediatrics, and the March of Dimes. L.S. was supported by a California HIV Research Program Dissertation Fellowship Award (D09-SF-313). A.K. was supported by a grant from the Beatrice Renfield Foundation.

Address correspondence and reprint requests to Dr. Joseph M. McCune, Division of Experimental Medicine, Department of Medicine, University of California San Francisco, 1001 Potrero Avenue, Building 3, Room 601, San Francisco, CA 94110. E-mail address: mike.mccune@ucsf.edu

The online version of this article contains supplemental material.

Abbreviations used in this paper: BDCA-2, blood dendritic cell Ag 2; CoPP, cobalt protoporphyrin; DC, dendritic cell; FoxP3, forkhead box protein 3; HO-1, heme oxygenase-1; MHC-I, MHC class I; MHC-II, MHC class II; Mono, monocytes; SnMP, tin mesoporphyrin; T_{CM}, central memory T; $T_{CM}CD27^{high}$, T_{CM} cells with high CD27 expression; T_{EM}, effector memory T; T_{EMRA}, $CD45RA^+$ T_{EM} cells; T_N, naive T; Treg, regulatory T cell.

Recent studies have focused on the role that HO-1 serves as an immune mediator. In keeping with its antioxidant and antiproliferative effects in certain cell types, HO-1 appears to be predominantly suppressive of immune responses and to have anti-inflammatory effects. For example, in the NOD mouse model of type 1 diabetes, induction of HO-1 with cobalt protoporphyrin (CoPP) reversed established autoimmune pancreatitis and ongoing islet destruction, restored insulin production and normoglycemia, and was associated with fewer infiltrating $CD11c^+$ dendritic cells (DCs) and cytotoxic $CD8^+$ T cells (12). These effects were specifically associated with HO-1 activity and were blocked by the HO-1 inhibitor tin mesoporphyrin (SnMP). Such immunosuppressive effects have been observed in multiple other animal models, including those demonstrating the importance of HO-1 in allograft tolerance (13). In addition, there is evidence that HO-1 may play a role in the maintenance of immune homeostasis. For example, mice deficient in HO-1 develop an inflammatory state characterized by splenomegaly, lymphadenopathy, abnormal CD4/CD8 cell ratios, and T cell hyperresponsiveness to ex vivo stimuli (14–16). Likewise, HO-1 deficiency in humans is associated with leukocytosis, abnormalities in secondary lymphoid organs (e.g., asplenia and lymphadenopathy), and evidence of severe persistent endothelial damage (17, 18). There is also a large body of work now demonstrating that relatively common promoter polymorphisms in the HO-1 gene, thought to influence the magnitude and rate of induction, can have a profound effect on a wide variety of inflammatory disorders (reviewed in Ref. 19).

HO-1 is upregulated upon T cell activation, and both HO-1 and CO can inhibit T cell proliferation, suggesting that the induction of HO-1 may play an important role in the regulation of T cell activation and homeostasis (11, 20). Previous studies have shown that proliferation of $CD3^+$ T cells stimulated though the TCR can be inhibited by exposure to low concentrations of CO and that this effect acts through $p21^{cip}$-dependent activation of caspase-8 (11). Other investigators have shown that the antiproliferative effects of CO on $CD4^+$ T cells depend upon inhibition of the ERK pathway, leading to decreased production of IL-2 (20). Although these studies demonstrate the ability of HO-1 and its products to prevent

cellular activation, it remains unclear whether HO-1 exerts an antiproliferative effect at baseline and/or whether relief of such inhibition leads to T cell activation.

SnMP is a potent inhibitor of HO-1–mediated heme catabolism that has now been provided to many patients for the treatment of both neonatal jaundice and inherited hyperbilirubinemia syndromes (21). It was developed to possess unique structural and photophysical properties that make it a particularly potent and bioavailable in vivo inhibitor suitable for clinical use in newborns (22, 23), and studies to date have revealed a very favorable therapeutic profile with no significant adverse side effects. Given the potential immunomodulatory effects of HO-1 in health and disease, we tested the possibility that pharmacologic inhibition of HO-1 by SnMP would also lead to the activation of human T cells. Specifically, we hypothesized that inhibition of HO-1 in PBMCs in vitro by SnMP would result in T cell activation and proliferation.

Materials and Methods

Cells, Abs, and reagents

Human PBMCs were isolated from healthy adult donors by density gradient centrifugation of whole blood on cell separation medium (Histopaque-1077; Sigma-Aldrich, St. Louis, MO). PBMCs were collected, washed in PBS (Life Technologies, Rockville, MD), counted, and resuspended in RPMI 10 (RPMI 1640 medium; Life Technologies) with 10% heat-inactivated FBS (Hyclone Laboratories, Rockford, IL), 2 mM L-glutamine (Mediatech, Washington, DC), and 100 U/ml penicillin/streptomycin (Mediatech). Only freshly isolated cells were used for primary culture experiments. All samples were obtained in accordance with guidelines and under protocols approved by the Committee on Human Research at the University of California, San Francisco. CoPP and SnMP were purchased in powdered form from Frontier Scientific (Park City, UT), dissolved in 0.1 mM NaOH, and titrated to a pH of 7.6. The following fluorophore-conjugated mAbs were used for detection of cell surface markers: CD3 (SP34-2, Alexa 700, or Pacific blue), CD4 (RPA-T4, Alexa 700, or Pacific blue), CD11c (B-ly6, allophycocyanin, or V450), CD16 (B73.1, Pecy7), CD19 (H1B19, A700), CD20 (2H7, PE), CD38 (HB7, allophycocyanin), CD25 (M-A251, PE-Cy7, or allophycocyanin-Cy7), CD56 (B159, A700), CD69 (HB50, PE-Cy7), CD86 (FUN-1, allophycocyanin), CD127 (hIL-7R-M21, PE), HLA-DR (L243, APC-Cy7) (all from BD Biosciences, San Jose, CA), CD8 (3b5, PE-Cy5.5; Caltag Laboratories, Burlingame, CA), CD14 (RMO52, ECD; Beckman Coulter, Fullerton, CA), CD45RA (2H4, ECD; Beckman Coulter), CD27 (O323, APC–Alexa 750; eBioscience, San Diego, CA), CD163 (6H1, PE; eBioscience), and blood DC Ag 2 (BDCA-2) (AC144, FITC; Miltenyi Biotec, Auburn, CA). The following mAbs were used alone or in combination for detection of intracellular Ags: Forkhead box protein 3 (FoxP3) (PCH101, allophycocyanin, eBioscience), Ki-67 (B56, FITC; BD Biosciences), and HO-1 (rabbit polyclonal ab13243, unconjugated; Abcam, Cambridge, MA). HO-1 primary Ab was detected using F(ab′)2 anti-rabbit IgG conjugate (Q-11401MP, Qdot605; Invitrogen, Carlsbad, CA).

Cell preparation and Ab labeling

PBMCs were cultured on Upcell 96F MicroWell plates (Nunc, Rochester, NY) under various treatment conditions for indicated periods of time, and adherent cells were detached from the plates by incubating the plates at 25˚C for 20 min. For flow cytometry analysis, cells were washed in staining buffer (PBS with 2% FBS and 2 mM EDTA; Sigma), incubated at 4˚C in the presence of directly conjugated fluorescent mAbs for 30 min, washed in staining buffer, and then fixed in 2% paraformaldehyde. All cells were stained with a live/dead marker (Amine-Aqua/Am-Cyan or Amine-Violet/Pacific Blue Live/Dead; Invitrogen) so that dead cells could be excluded from analysis. FoxP3 staining was carried out according to the manufacturer's protocol, with slight modifications (eBioscience). Briefly, cells were washed after incubation with primary Abs, resuspended in FoxP3 fixation/permeabilization buffer (eBioscience), and then incubated for 1 h at 4˚C, washed twice in FoxP3 permeabilization buffer (eBioscience), and stained with anti-FoxP3 mAb in FoxP3 permeabilization buffer for 1 h at 4˚C. Cells were then washed twice in FoxP3 permeabilization buffer and resuspended in 2% paraformaldehyde. Data were acquired with an LSR-II flow cytometer (BD Biosciences) and analyzed with FlowJo software (Tree Star, Ashland, OR). HO-1 and Ki-67 staining were carried out using the BD Cytofix/Cytoperm kit according to the manufacturer's protocols (BD Biosciences).

Magnetic separation of cells

For in vitro assays involving cell depletion or selection, cells were washed and resuspended in MACS buffer (PBS with 0. 5% BSA and 2 mM EDTA). For depletion of cells expressing CD25, CD14, CD4, CD8, or CD45RA, PBMCs were incubated with the appropriate beads (e.g., CD25 Microbeads II, CD14 Microbeads, CD4 Microbeads, CD8 Microbeads, or CD45RA Microbeads, respectively, all from Miltenyi Biotec) for 30–45 min at 4˚C. Labeled cells were washed with staining buffer and run through magnetic columns (MS or LS Columns; Miltenyi Biotec). The unbound fraction was kept as the "depleted fraction", and cells that were retained in the column were isolated as the "positive fraction". In the case of CD25 beads, this fraction was found to be consistently 50–70% $FoxP3^+$ and was used for regulatory T cell (Treg) add-back assays. For mock depletions, cells were processed in parallel, incubated with anti-biotin magnetic beads (Miltenyi Biotec), and isolated using the same procedure. For isolation of purified $CD3^+$ T cells and $CD14^+$ cells, PBMCs were incubated with cocktails of biotin-conjugated Abs (designed to bind to all PBMCs except those positive for CD3 and/or CD14; Miltenyi Biotec) for 30 min at 4˚C, washed in MACS buffer, and then incubated with anti-biotin magnetic beads (Miltenyi Biotec) according to the manufacturer's protocol. Labeled cells were washed once more in staining buffer and passed over magnetic columns (MS or LS columns; Miltenyi). The unbound fraction (i.e., cells positive for CD3 and/or CD14) was retained for further use. All cells enriched in this manner by magnetic separation were monitored for purity by flow cytometry, comparing them against mock-depleted and unfractionated PBMCs using an appropriate phenotyping panel. Sorted cells were counted with a hemacytometer by trypan blue exclusion to determine the number of live cells and resuspended in appropriate buffer.

HO-1 Western blotting

PBMCs were cultured with vehicle control, CoPP, or SnMP (10 μM) for 7 d and then harvested as described earlier. For some experiments, unmanipulated harvested cells were lysed and used for protein analysis, whereas in other experiments, CD3 or CD14 isolation/depletion was performed prior to cell lysis. Cells were washed in PBS, then lysed in radioimmunoprecipitation assay buffer containing PMSF (1 mM), pepstatin A (1 μg/ml), aprotinin (2 μg/ml), and leupeptin (5 μg/ml) (Sigma). Protein was quantified using bicinchoninic acid assay as per the kit manufacturer's instructions (Pierce, Rockford, IL). Cell protein lysates were mixed with sample loading buffer (NuPAGE LDS Sample Buffer, NuPAGE Reducing Agent; Invitrogen) according to the manufacturer's instructions and heated at 70˚C for 10 min. Samples (20 μg protein) were loaded onto gels (NuPAGE Novex 4–12% Bis-Tris; Invitrogen) and subjected to electrophoresis (200 V, 45 min) (XCell *SureLock* Mini Cell; Invitrogen) under reducing conditions. Proteins were then transferred to polyvinylidene fluoride membranes (Immobilon P; Millipore, Billerica, MA) and blocked for 1 h in 5% nonfat milk in TBS (100 mM Tris-Cl, pH 7.5; 0.9% NaCl) containing 0.1% Tween, followed by incubation for 1 h at with anti–HO-1 (1:2000; SPA895; rabbit anti-human polyclonal; Assay Designs/Enzo Life Sciences, Plymouth Meeting, PA) and anti-GAPDH (1:2000; mAbcam 9484; mouse anti-human monoclonal; AbCam) primary Abs for 1 h. After three washes with TBS containing 0.1% Tween, the blots were incubated for 45 min with anti-rabbit and anti-mouse secondary Abs (Dako, Carpinteria, CA) conjugated with polymeric HRP. Finally, the bands were detected using a luminescence detection system (Amersham ECL Plus; GE Healthcare, Piscataway, NJ) and autoradiographic film (Amersham Hyperfilm ECL, GE Healthcare).

In vitro proliferation assays with carboxyfluorescein diacetate succinimidyl ester

For proliferation assays, cells were first labeled with 5 μM CFSE (Sigma) in PBS at 37˚C for 10 min, followed by three washes in RPMI-10. Cells were typically plated in RPMI-10 at a density of 1 million to 2 million cells/ml in 96-well U-bottom plates or 1 million to 4 million cells/ml in 6-well flat-bottom plates. Cells were exposed to metalloporphyrins in culture for 5–7 d at 37˚C, 5% CO_2 with no additional stimuli or growth factors. Upon harvesting, cells were washed in MACS buffer, labeled for flow cytometry, and analyzed as previously described (24). The frequency of $CFSE^{low}$ cells was used as a measurement of total T cell proliferation. For $CD14^+$ add-back assays, negatively selected CFSE-labeled $CD3^+$ T cells were incubated with a range of dilutions of negatively selected $CD14^+$ cells (to avoid stimulation of $CD14^+$ cells by positive selection with CD14 beads).

For CD25- and CD45RA-depletion experiments, PBMCs were labeled with CFSE and then subjected to either CD25, CD45RA, or mock depletion as described earlier, using anti-CD25, anti-CD45RA, or anti-biotin microbeads (Miltenyi Biotec). Depleted and mock-depleted cells were cultured with or without metalloporphyrins for 7 d.

CD25$^+$ Treg suppressor assays

Culture plates (96-well flat-bottom) were coated with anti-CD3 mAb (SP34-2; BD Biosciences) at a concentration of 5 μg/ml for 4 h at 37°C. After washing coated plates thoroughly in PBS, 150,000 CFSE-labeled CD25$^-$ responder cells were incubated with a range of dilutions of enriched CD25$^+$ cells. In different experiments, CD25$^+$ cells were isolated either from PBMCs or from PBMCs that had been cultured with SnMP or CoPP (10 μM) for 7 d. Anti-CD3 stimulated cells were collected after 5 d in culture, washed in MACS buffer, labeled for flow cytometry, and analyzed as described earlier. Control wells with no anti-CD3 mAb and no CD25$^+$ Tregs were used for all stimuli.

Transwell membrane and MHC blocking experiments

For Transwell (Corning, Corning, NY) membrane experiments, CFSE-labeled responder T cells were placed in the upper well of the chamber of a 1-μm pore-size cell culture insert (Corning), and negatively selected CD14$^+$ cells were placed either in the upper or lower chamber of the well. Cells were incubated with or without SnMP (10 μM) in RPMI-10 at 37°C for 7 d, harvested, labeled with florescent mAbs, and analyzed for proliferation by flow cytometry. For proliferation assays in the presence of MHC-blocking Abs, the following purified mAbs were used without azide and endotoxin: anti–HLA-A, -B, -C (W6/32) (obtained from Biolegend, San Diego, CA), anti–HLA-DR, -DP, -DQ (Tü39), and isotype controls (obtained from BD Pharmingen, San Diego, CA). The mAbs were first added to CFSE-labeled PBMCs 30 min before SnMP (10 μM) and were

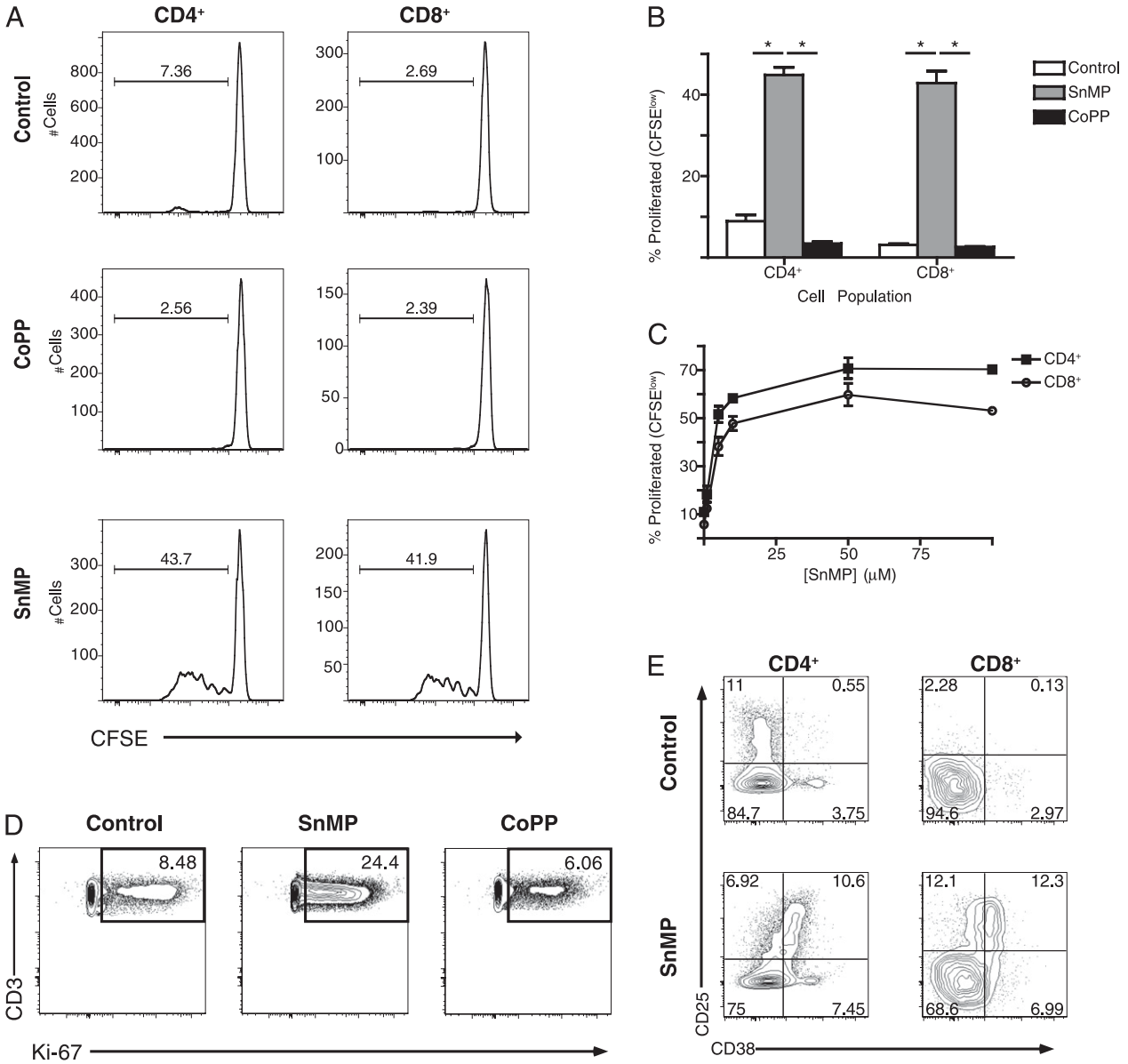

FIGURE 1. HO-1 inhibition by SnMP causes T cells in human PBMC cultures to proliferate. *A*, Representative flow cytometry histograms for a single donor demonstrating proliferation of CFSE-labeled CD4$^+$ and CD8$^+$ T cells in human PBMC cultures by CFSE dilution after 7 d in culture with SnMP, CoPP, or vehicle control (10 μM). Measurement bars and numbers represent the percentage of cells that are CFSE^{low} (i.e., proliferating). *B*, Comparison of the mean proliferation by CFSE dilution for four individual donors. Error bars represent SEM. Proliferation was significantly greater in the SnMP group compared with both the control and CoPP groups (10 μM). $*p < 0.001$. *C*, Dose-response curve demonstrating the relationship between T cell proliferation and SnMP concentrations ranging from 1 to 100 μM. *D* and *E*, Flow cytometry plots showing intracellular staining for Ki-67 in all CD3$^+$ cells (*D*) and extracellular staining for CD25 and CD38 (*E*) in CD3$^+$CD4$^+$ or CD3$^+$CD8$^+$ T cells after treatment of PBMCs with SnMP (25 μM).

then added again on day 3 of culture. Cells were harvested on day 7, stained for flow cytometry, and analyzed as described earlier.

Proliferation analysis of fluorescence-activated cell sorting–purified memory subsets

PBMCs were isolated, and $CD3^+$ T cells were purified by negative immunomagnetic selection, as previously described (Miltenyi Biotec). $CD3^+$ T cells were then labeled with CFSE and stained with a live/dead marker as well as with fluorescent mAbs against CD3, CD20, CD14, CD4, CD8, CD45RA, and CD27. Live naive ($CD20^-CD14^-CD3^+CD45RA^+CD27^+$) and central memory ($CD20^-CD14^-CD3^+CD45RA^-CD27^+$) T cells were sorted by FACS on a BD FACSAria (BD Biosciences). Sorted naive, central memory, and nonsorted cells were then co-incubated with $CD14^+$ cells isolated by negative immunomagnetic selection, using a dose range of SnMP. Cells were harvested at the end of 7 d, stained for flow cytometry, and analyzed as described above.

Results

Culture of PBMCs with SnMP results in activation and proliferation of T cells

Previous studies have shown that HO-1 expression in T cells inhibits CD3-dependent activation and proliferation (20). To investigate whether inhibition of HO-1 might result in activation of T cells, we cultured PBMCs from healthy adult donors either in the presence of the HO-1 inhibitor SnMP or of the HO-1 inducer CoPP. CoPP was chosen as an HO-1 inducer rather then heme because, unlike heme, it cannot be broken down enzymatically, allowing for a more constant concentration in culture. In the absence of any other activating stimulus, both $CD4^+$ and $CD8^+$ $CD3^+$ T cells were found to proliferate after incubation with SnMP (Fig. 1*A*), an effect that was reproducible in PBMC cultures from multiple donors (Fig. 1*B*). The magnitude of proliferation was positively correlated with the concentration of SnMP, reaching maximum levels at ~50 μmol for both $CD4^+$ and $CD8^+$ cells (Fig. 1*C*). There was no significant change in T cell viability at concentrations used in these experiments (0–50 μM; Supplemental Fig. 1). Using the FlowJo proliferation software platform, it was calculated that up to 25% of the original population of T cells underwent proliferation at an SnMP concentration of 50 μmol. SnMP exposure was associated with increased T cell expression of the proliferation marker Ki-67 and of the activation markers CD38 and CD25 (Fig. 1*D*, 1*E*, respectively). Of note, the HO-1 inducer CoPP did not induce T cell proliferation but conversely reduced baseline levels of $CD4^+$ cell proliferation and overall $CD3^+$ cell Ki-67 expression seen in control samples (Fig. 1*A*, 1*B*, 1*D*).

Activation and proliferation of T cells induced by SnMP requires interaction with $CD14^+$ PBMCs

In contrast with the proliferative response observed in PBMC cultures, isolated $CD3^+$ T cells did not become activated or proliferate when exposed to SnMP (Fig. 2*A*). Based on published evidence that HO-1 can alter the stimulatory activity of myeloid cells (25), we hypothesized that SnMP-induced T cell proliferation may involve interaction with cells of the myeloid lineage. We used $CD14^+$ peripheral blood monocytes (prepared by negative selection) as a representative myeloid cell type and confirmed by flow cytometry that these enriched cells expressed CD14, CD11c, and HLA-DR (MHC class II), consistent with the phenotype of human peripheral blood monocytes (Ref. 26; data not shown). When isolated T cells were cocultured with such $CD14^+$ monocytes, SnMP-induced T cell activation and proliferation was restored (Fig. 2A, *right panels*). Similar to PBMC cultures, proliferation of T cells in these T cell–monocyte cocultures was dependent on the concentration of SnMP (Fig. 2*B*). To establish whether there is a relationship between the frequency of

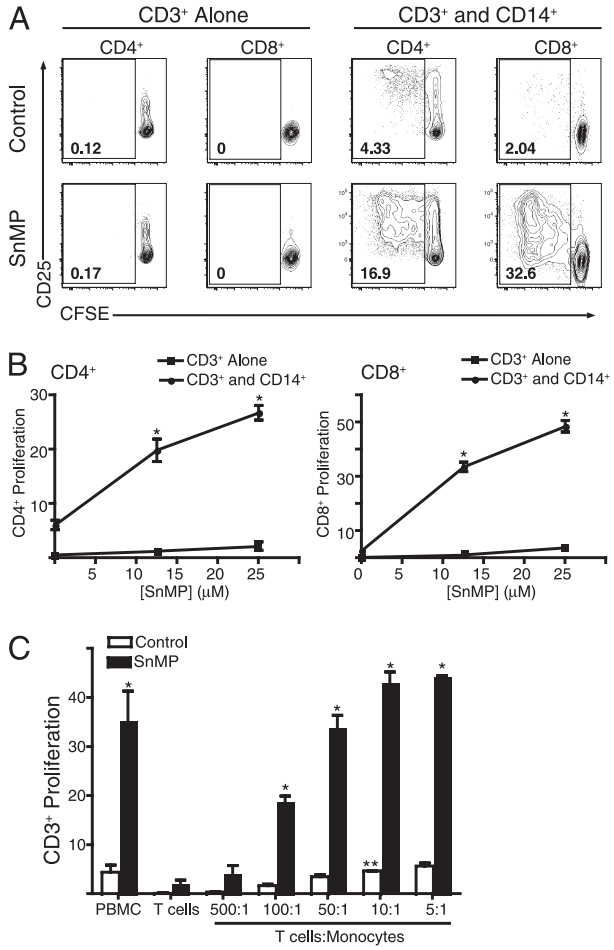

FIGURE 2. T cells require the presence of $CD14^+$ monocytes to proliferate in response to SnMP. $CD3^+$ T cells were isolated and cultured alone or in the presence of enriched autologous $CD14^+$ monocytes, with or without SnMP. *A*, Representative CFSE-dilution flow plots for a single SnMP concentration (10 μM). *B*, Compiled results shown for a concentration range of SnMP (0–25 μM). In each case, $CD4^+$ T cells are shown on the *left* and $CD8^+$ T cells are shown on the *right*. The percentage of $CFSE^{low}$ cells was used as a measure of $CD4^+$ or $CD8^+$ proliferation. Error bars represent SEM, and this figure represents the results of three separate experiments. $*p < 0.001$. *C*, $CD3^+$ T cells from a single donor were cultured alone or with increasing frequencies of autologous $CD14^+$ monocytes in the presence or absence of SnMP (10 μM). Unmanipulated PBMCs were used as controls. The percentage of $CFSE^{low}$ cells was used as a measure of $CD3^+$ proliferation. Significance is indicated for difference from T cell alone for SnMP treated and untreated. Samples were run in duplicate from each donor, and error bars represent the SEM. This figure represents the results of three separate experiments. $*p < 0.001$; $**p < 0.01$.

$CD14^+$ cells in culture and the extent of T cell proliferation, add-back experiments were carried out with varying ratios of T cells and monocytes. These experiments showed that the percentage of $CD14^+$ cells added back into culture correlates directly with the magnitude of SnMP-induced T cell proliferation (Fig. 2*C*), reaching maximal levels at a T cell/monocyte ratio of ~10:1.

SnMP alters monocyte expression of multiple markers of myeloid differentiation and activation

To explore what phenotypic changes were induced in monocytes by exposure to SnMP and CoPP, we performed flow cytometric analysis of multiple cell surface proteins known to be important markers of myeloid differentiation and activation, as well as

intracytoplasmic staining for HO-1 (Supplemental Figs. 2, 3). In preliminary experiments, T cell proliferation was not observed until day 4 of PBMC culture (data not shown), leading us to postulate that phenotypic changes in monocytes associated with T cell activation might be present prior to day 4. We found that on day 3, HO-1 protein was upregulated in monocytes by CoPP and, to a lesser extent, by SnMP, which is an expected result based on previous experiments using metalloporphyrins in myeloid cells (25). HO-1 protein expression was not significantly altered in T cells either by SnMP or CoPP. SnMP resulted in decreased expression of CD11c and CD16, whereas expression of the C-type lectin BDCA-2 and the coactivating molecule CD86 (B7-2) were increased. Like SnMP, CoPP reduced CD16 expression. In contrast with SnMP, CoPP had no effect on CD11c expression and decreased expression of CD86 and BDCA-2. CoPP also decreased expression of HLA-DR (MHC class II). In control cells, there was a broad range of expression of the heme scavenger receptor, CD163. CoPP decreased CD163 expression, whereas SnMP increased CD163 expression, such that the difference in CD163 expression was significant between the two conditions.

SnMP-induced T cell proliferation requires direct cell-to-cell contact with CD14$^+$ monocytes and is dependent on both MHC class I and II

To determine whether SnMP-induced T cell proliferation requires direct contact between CD3$^+$ T cells and CD14$^+$ monocytes, enriched preparations of these two populations were cultured either on the same side or on the opposite sides of semipermeable Transwell membranes. As shown in Fig. 3*A*, cell-to-cell contact was required for the SnMP effect on T cell proliferation. Because peripheral blood monocytes express MHC class I (MHC-I) and MHC class II (MHC-II) Ags that might interact with the TCR on T cells, monocytes and T cells were cultured together with SnMP in the presence of monoclonal anti-MHC Abs known to block such interactions. There was a trend toward reduced proliferation with either MHC-I or MHC-II blockade, and a statistically significant ablation of the proliferative response occurred even at low Ab concentrations when both MHC-I and MHC-II were blocked (Fig. 3*B*). This observation suggests that the SnMP-induced T cell proliferative response involves engagement of both MHC-I and MHC-II on CD14$^+$ monocytes.

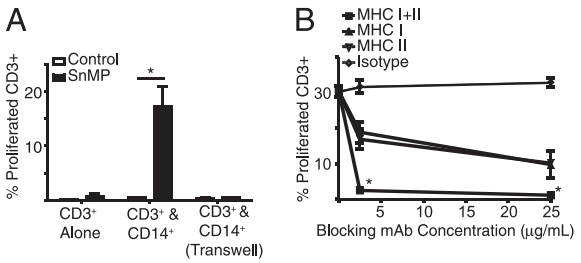

FIGURE 3. T cells require direct surface contact and MHC-dependent interaction with monocytes to proliferate in response to SnMP. *A*, CFSE-labeled CD3$^+$ T cells (1×10^6) were cocultured with 1×10^5 CD14$^+$ monocytes, either on the same side or on the opposite sides of semipermeable Transwell membranes in a 24-well plate for 7 d in the presence or absence of SnMP (10 μM). The percentage of CFSE^{low} cells was used as a measure of CD3$^+$ proliferation. In SnMP-containing cultures, there was a significant difference between proliferation of T cells cultured on the same side or on opposite sides of the Transwell membrane as monocytes. Error bars are representative of SEM, and data in *A* are representative of two separate experiments. $*p < 0.01$. *B*, CFSE-labeled CD3$^+$ cells (2×10^5) were cultured with 2×10^4 CD14$^+$ monocytes in a 96-well plate with SnMP (10 μM) with a titration of mAbs known to block MHC-I, MHC-II, or isotype. The blocking and isotype control mAb concentration refers to the total concentration of Ab per well. When mAbs were mixed, the proportion of each Ab was equal. A control well with no SnMP did not show significant proliferation (data not shown). The percentage of CFSE^{low} cells was used as a measure of CD3$^+$ proliferation. Significant difference from the no-Ab point is indicated by an asterisk next to a data point. Error bars represent the SEM, and *B* represents the results of three separate experiments. $*p < 0.05$.

Proliferating CD4$^+$ and CD8$^+$ T cells arise from CD45RA$^+$ T cells

To identify the cell populations that proliferate in response to SnMP, PBMC cultures were stained for multiple cell-surface maturation markers after a week in culture, with or without SnMP. Flow cytometry plots (Fig. 4*A*, *left*) demonstrate that SnMP induced a notable decrease in the percentage of naive (T_N: CD45RA$^+$ CD27$^+$) CD4$^+$ and CD8$^+$ T cells and a reciprocal increase in the percentage of central memory (T_{CM}: CD45RA$^-$CD27$^+$) CD4$^+$ and CD8$^+$ T cells, many of which (delineated by circles in the flow plots) had high levels of CD27 expression ($T_{CM}CD27^{high}$). Meanwhile, the relative fractions of effector memory (T_{EM}: CD45RA$^-$CD27$^-$) and CD45RA$^+$ effector memory T cells (CD45RA$^+$CD27$^-$) remained unchanged. The SnMP-induced decrease in T_N cells and increase in T_{CM} cells was dose dependent (Fig. 4*A*, *right*). Phenotypic analysis was then carried out on CFSE-labeled cells exposed to SnMP to determine the maturational phenotype of proliferating (CFSE^{low}) cells. No proliferating CD4$^+$ or CD8$^+$ T cells had a naive phenotype but were rather found to be predominantly of the T_{CM} (CD27$^+$ or CD27^{high}) phenotype, with fewer proliferating T_{EM} cells (Fig. 4*B*).

The concomitant decrease in the frequency of naive cells and increase in the frequency of proliferating cells with memory phenotypes suggested that the proliferating cells were derived from the CD45RA$^+$ naive T cell compartment. To test this possibility, PBMCs were either depleted of CD45RA$^+$ T cells or mock depleted, prior to culture with SnMP. As shown in Fig. 4*C*, minimal proliferation was detected in CD45RA-depleted cultures. To confirm that CD45RA$^+$CD27$^+$ T_N cells represent the predominant cell type proliferating in response to SnMP, these cells and T_{CM} cells were isolated by FACS and then cultured with CD14$^+$ monocytes in the presence or absence of SnMP. Both CD4$^+$ and CD8$^+$ T_N cells were found to proliferate and to upregulate CD25 in response to SnMP, whereas T_{CM} cells did not (Fig. 4*D*, *left*), and the proliferation of T_N cells was dose dependent (Fig. 4*D*, *right*). In aggregate, these experiments show that SnMP induces activation and maturation of naive CD45RA$^+$CD27$^+$ CD4$^+$ and CD8$^+$ T cells, leading to their maturation into memory cells.

CD4$^+$CD25$^+$FoxP3$^+$ Tregs suppress SnMP-induced T cell activation, and SnMP reduces the suppressive capacity of Tregs

We next evaluated the function of Tregs in SnMP-treated PBMC cultures. When Tregs were depleted from PBMCs prior to culture with SnMP, a statistically significant 2- to 3-fold increase in proliferation was observed (Fig. 5*A*), suggesting that Tregs are able to suppress the SnMP-induced proliferative response. This was confirmed by Treg add-back assays, demonstrating that SnMP-induced proliferation could be suppressed when Tregs were present at higher frequencies prior to SnMP exposure (Fig. 5*B*).

Given recent studies demonstrating that normal Treg development and suppressive function requires the activity of HO-1 in APCs (26), we next investigated whether SnMP had an inhibitory effect on Treg function. CD25$^+$ cells were isolated from PBMCs that had been cultured for a week with vehicle control, CoPP, or

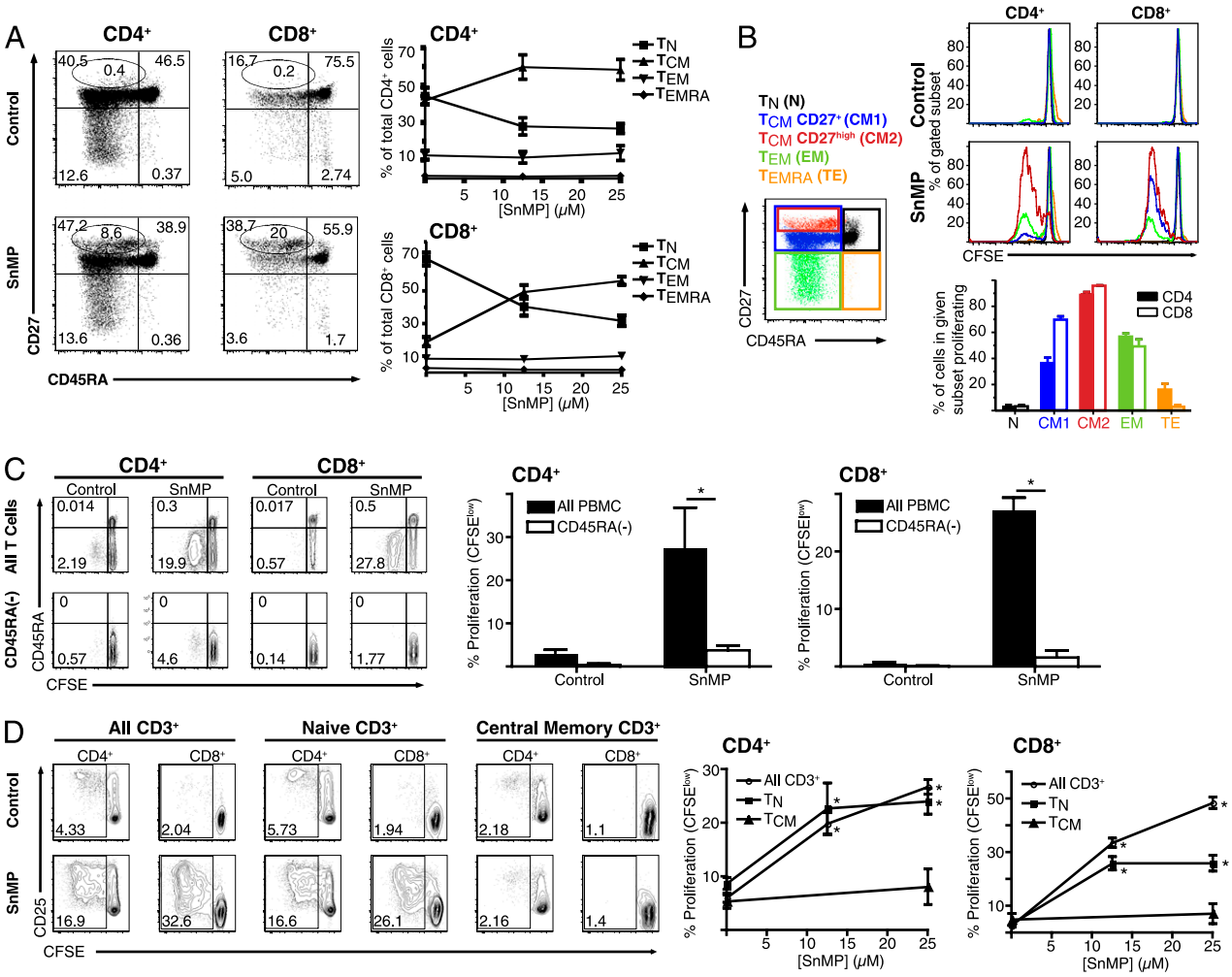

FIGURE 4. SnMP induces naive T cells to proliferate and to adopt a central memory phenotype. *A*, CFSE-labeled PBMCs were cultured with SnMP (0–25 μM) for 7 d and stained for flow cytometry with maturation markers. Representative plots from a single experiment are shown on the *left*, including treated (25μM) and untreated samples gated on $CD4^+$ and $CD8^+$ T cells. The plots on the *right* show cumulative data from a single donor over a dose range of SnMP and demonstrate the frequency of different naive/memory $CD4^+$ and $CD8^+$ subsets as a percentage of total $CD4^+$ and $CD8^+$ cells. *A* represents the mean of four separate experiments, and error bars represent the SEM. *B*, CFSE-labeled PBMCs were cultured with SnMP (25 μM) for 7 d and stained for flow cytometry with maturation markers. Gates were drawn to differentiate naive/memory subsets, each of which is shown on representative CFSE-dilution histogram to demonstrate the extent to which proliferation was induced by SnMP. Results of four separate experiments are compiled in the colored bar-graph, demonstrating the mean (±SEM) of the percentage of cells in a given subset gate that are proliferating. *C*, CFSE-labeled PBMCs were depleted of naive $CD45RA^+$ T cells prior to culture with SnMP (25 μM) using anti-CD45RA immunomagnetic beads or were mock-depleted with anti-biotin beads. After 7 d in culture, cells were harvested and stained for flow cytometry, and the extent of proliferation was determined by measuring the percentage of $CFSE^{low}$ cells. Representative flow cytometry plots from one experiment are shown in the flow cytograms on the *left*; the graphs on the *right* show the results of a single experiment with three donors; error bars represent SEM. Significant differences are indicated for comparisons between undepleted and CD45RA-depleted samples. Similar results were obtained in a second experiment with two donors. $*p < 0.01$. *D*, CFSE-labeled PBMCs were labeled with fluorescent mAbs and sorted by FACS to purify naive ($CD45RA^+CD27^+$) and central memory ($CD45RA^-CD27^+$) cells, which were subsequently cultured for 7 d in a dose range of SnMP (0–25 μM). Representative flow plots (SnMP 12.5 μM) (*left*) and cumulative data for two experiments using different donors (*right*) are shown. Error bars represent SEM. SnMP-treated samples for a given cell population were compared with the untreated samples for the same cell population, and significant differences are indicated with an asterisk. $*p < 0.05$. T_N cells; T_{CM} cells (CM1); T_{CM} cells with high CD27 expression ($T_{CM}CD27^{high}$; CM2); T_{EM} cells; and $CD45RA^+$ T_{EM} cells (T_{EMRA}).

SnMP. The frequency of purified $CD4^+CD25^+$ T cells expressing FoxP3 was similar in all treatment groups (52–59% $FoxP3^+$; Fig. 5*C*). The suppressive capacity of these purified metalloporphyrin-treated Tregs was then evaluated by adding them to cultures of CFSE-labeled, anti-CD3 stimulated autologous T cells. SnMP-treated Tregs were significantly less effective at suppressing responder T cell proliferation than Tregs isolated from cultures treated with CoPP or vehicle control (Fig. 5*D*). Together, these findings suggest that Tregs have a suppressive effect on SnMP-induced T cell activation but that SnMP counteracts this effect by reducing the suppressive capacity of Tregs.

Discussion

Numerous studies have demonstrated the importance of HO-1 and its enzymatic products as anti-inflammatory mediators in various disease states (12, 27–32). Compared with wild-type mice, HO-1 knockout mice develop a progressive inflammatory state, and splenocytes from these mice respond to TCR activation with increased production of proinflammatory cytokines such as IL-2, IFN-γ, TNF-α, GM-CSF, and IL-6 (16). Such effects have been observed in human cells as well, where HO-1 and CO inhibit T cell proliferation in response to activation through the TCR in vitro (11, 20). Furthermore, HO-1 activity in APCs such as

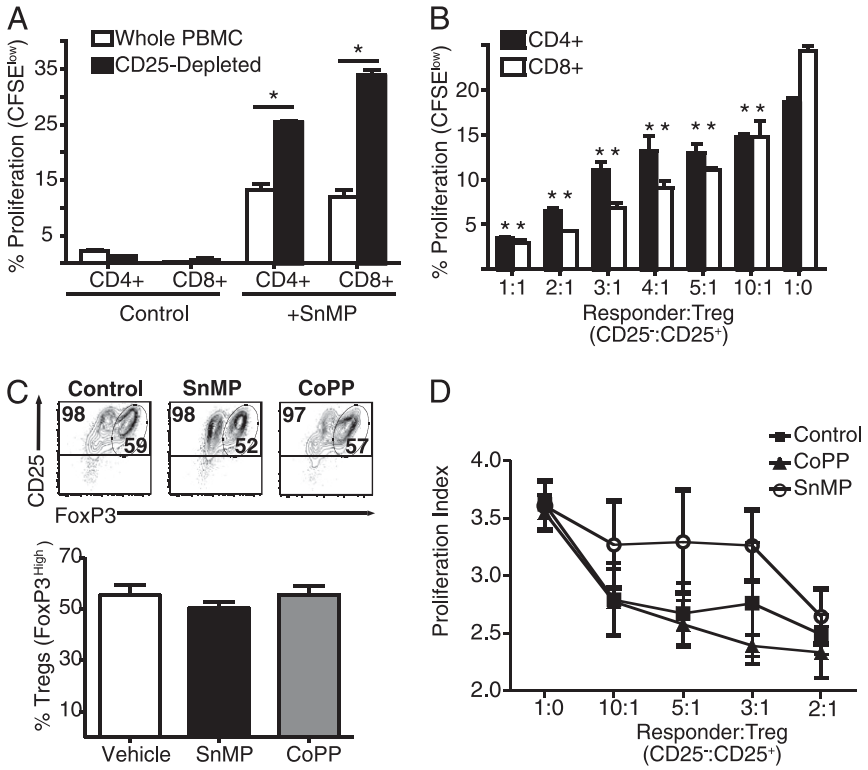

FIGURE 5. CD25$^+$ Tregs inhibit SnMP-induced T cell proliferation, and SnMP inhibits Treg suppressive function. *A*, CFSE-labeled PBMCs were depleted of CD25$^+$ cells using anti-CD25 immunomagnetic beads or were mock-depleted using anti-biotin beads and then cultured for 7 d with or without SnMP (25 μM). The graph includes results from three separate experiments. Error bars represent SEM, and CD25-depleted samples proliferated significantly more than mock-depleted samples. $*p < 0.01$. *B*, CFSE-labeled PBMCs were depleted of Tregs using anti-CD25 immunomagnetic beads, yielding a population of CD25$^-$ cells. Isolated CD25$^+$ cells were added back to the CD25$^-$ cells in increasing ratios and then cultured for 7 d with SnMP (10 μM). Proliferation was assessed as the percentage of CFSE^{low} cells. *B* includes results of two individual donors and is representative of two separate experiments. Error bars represent SEM. Proliferation of CD4$^+$ and CD8$^+$ cells from add-back samples was evaluated and compared with proliferation of CD4$^+$ and CD8$^+$ cells (respectively) in responder-only samples. Significant differences are indicated. $*p < 0.05$. *C* and *D*, PBMCs were cultured for 7 d in control media, SnMP, or CoPP (10 μM), harvested, and CD25$^+$ cells were then isolated using immunomagnetic beads. *C*, Representative flow cytometry staining showing FoxP3 staining of purified CD25$^+$ cells and demonstrating the percentage of FoxP3$^+$ Tregs. The results of three experiments are shown in the bar graph; error bars represent the SEM, and there were no significant differences. *D*, CD25$^+$ cells treated with metalloporphyrins or vehicle control (shown in *C*) were added to autologous CD25-depleted, CFSE-labeled PBMCs in increasing ratios and cultured on plates coated with an activating anti-CD3 Ab for 5 d. Cells were then harvested and stained for flow cytometry, and proliferation was assessed by determining the proliferation index of CD8$^+$ T cells using the Proliferation Analysis Platform of FlowJo. Results of a three separate experiments are shown; error bars represent SEM. Proliferation in the SnMP group was found to be significantly higher ($p < 0.01$) by two-way ANOVA.

DCs and cells of the monocyte/macrophage lineage can significantly influence the outcome of their interactions with T cells (25, 33–35). For example, splenocytes from HO-1 knockout mice display enhanced production of IL-6, TNF-α, IFN-γ, and IL-12 in response to LPS stimulation ex vivo (16). Chauveau et al. (25) showed that induction of HO-1 expression in rat and human DCs led to impaired LPS-induced activation and maturation and impaired ability to stimulate allogeneic T cell proliferation. Recent work by Tzima et al. (35) has also demonstrated a role for myeloid-expressed HO-1 in triggering innate immunity: mice carrying a myeloid-specific ablation of the HO-1 gene had impaired production of IFN-β in response to viral and bacterial infection and a more severe disease course after induction of experimental autoimmune encephalomyelitis. Together, these results suggest that HO-1 in myeloid cells may play a complex and important role in T cell activation and differentiation. Given that HO-1 overexpression and CO exposure can inhibit T cell activation via the TCR (11, 20) and that HO-1 can inhibit T cell activation by APCs (25), we considered whether HO-1 might exert some function at baseline in maintaining T cell quiescence. Specifically, we asked whether exposure to the potent pharmacologic HO-1 inhibitor SnMP would result in T cell activation.

In this study, we demonstrate that the HO-1 inhibitor SnMP induces activation, proliferation, and maturation of naive CD4$^+$ and CD8$^+$ T cells via interactions with CD14$^+$ monocytes in vitro. Notably, SnMP did not induce proliferation in isolated T cells but only in cultures where CD14$^+$ cells were also present. Although this observation does not rule out a direct effect of HO-1 on T cells, it does indicate that such an effect is not sufficient to induce activation. Proliferation occurred in the presence of very few monocytes, and there was a direct correlation between the frequency of monocytes present in culture and the extent of proliferation. Experiments using Transwell membranes and blocking Abs demonstrated that SnMP-induced T cell activation requires direct cell-to-cell MHC-I–dependent and MHC-II–dependent interactions between T cells and monocytes. Both MHC-I and MHC-II blockade inhibited SnMP-induced proliferation, and there was an amplified effect of dual blockade, with abrogation of proliferation even at low Ab concentrations.

Given that MHC-dependent interaction of monocytes with T cells plays a crucial role in this in vitro system, we analyzed the phenotypic changes that occur in CD14$^+$ cells on day 3 of culture, prior to observed T cell proliferation. In the absence of additional cytokines, monocytes in PBMC culture normally stick to plastic

plates and differentiate into monocyte-derived macrophages, which we see occurring in vehicle control samples, where $CD14^+$ cells are also $CD11c^+$, $CD16^+$, and $HLA\text{-}DR^+$. We noted several differences in $CD14^+$ cells that were cultured in SnMP. Among the effects noted were a decrease in the expression of both CD11c and CD16. Most notably, SnMP induced upregulation of the coactivating molecule CD86 (B7-2), which plays an important role in the MHC–TCR immunological synapse by providing crucial secondary signals that modulate T cell activation. We postulate that this upregulation may enhance the ability of monocyte-derived $CD14^+$ cells to activate T cells via TCR–MHC interactions. The C-type lectin BDCA-2, which is typically expressed on plasmacytoid DCs, was also significantly upregulated in SnMP-treated $CD14^+$ cells. Together, these changes demonstrate that the $CD14^+$ population undergoes several phenotypic changes in response to HO-1 inhibitor exposure, some of which have the potential to confer activating function, and HO-1 induction by CoPP is associated with changes that are associated with a noninflammatory phenotype (i.e., a decrease in the expression of CD86 and HLA-DR).

We found that SnMP-induced T cell proliferation can be inhibited by $CD25^+FoxP3^+$ Tregs but that, reciprocally, SnMP can inhibit the suppressive function of Tregs. Tregs from HO-1–deficient mice have no intrinsic defect in their ability to suppress T cell activation, but it is now known that their ability to do so maximally and efficiently requires interactions with wild-type APCs that have intact HO-1 activity (26, 36). Accordingly, we suggest that inhibition of HO-1 activity in APCs in human PBMC cultures results in impaired Treg function. It is widely accepted that Tregs can induce changes in APCs to downregulate their Ag-presenting functions (37, 38). Conversely, both immature DCs and alternatively activated macrophages can induce Treg development de novo, whereas classically activated macrophages and mature DCs can have negative effects on Treg function (39). The mechanism by which HO-1 activity supports Treg function remains a matter for speculation. CO produced by HO-1 in APCs could act in a paracrine fashion to support Tregs by suppressing T cell proliferation or by inducing transcriptional changes in the Tregs themselves, leading to enhanced survival or suppressor activity. Catabolic products of heme breakdown could also work in an autocrine fashion to drive APC differentiation toward a phenotype that supports Treg survival or function.

Based on the results of our experiments, we suggest the model shown in Fig. 6 to describe the interactions leading to T cell activation and proliferation in PBMC cultures upon HO-1 inhibition by SnMP. In this model, unopposed baseline endogenous HO-1 activity supports the quiescent state of monocytes. There may be an endogenous effect of HO-1 in both naive T cells and Tregs, but it is also likely that the effects of HO-1 are exerted via interactions with quiescent monocytes that promote Treg survival and function. In this baseline state, antiproliferative signals prevail, and interaction with self-MHC allows for T cell survival and low-level baseline rates of proliferation. Exposure to SnMP results in HO-1 inhibition, leading to proactivating phenotypic changes in monocytes, naive T cells, or both. The primary observed effect resulting from this is the MHC-dependent induction of T cell proliferation. HO-1 inhibition also results in monocyte-mediated impairment of Treg function, indirectly augmenting the extent of naive T cell proliferation. Together, these effects are sufficient to induce proliferation of a surprisingly large fraction of T cells present in PBMC cultures.

Although we base our model on the assumption that the enzymatic activity of HO-1 is responsible for the observed effect, it is important to consider the alternative possibility that nonenzymatic

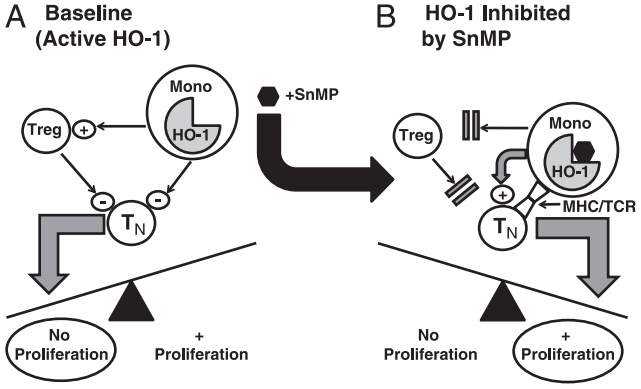

FIGURE 6. Model of SnMP-induced T cell activation and proliferation. *A*, At baseline, active HO-1 in monocytes (Mono) exerts an inhibitory influence on $CD45RA^+CD27^+$ T_N cells and simultaneously supports function of $CD4^+CD25^+FoxP3^+$ Tregs. Tregs also exert an inhibitory influence on T_N cell activation, ultimately resulting in a quiescent and nonproliferating T_N cell compartment. *B*, Upon addition of SnMP, HO-1 is inhibited, resulting in altered monocyte function and interaction with T_N cells. Through MHC-dependent contact, monocytes activate T_N cells via the TCR to mature and proliferate. With HO-1 inhibited by SnMP, monocytes are no longer able to support Treg function or may actively inhibit Treg activity, thereby diminishing Treg suppressive influence on T_N cells. Together, these effects result in T_N cell activation, maturation, and proliferation.

functions of HO-1 play a role. Recent work has shown that HO-1 possesses important transcriptional modifying activity that is completely independent of its catalytic function. In NIH 3T3 cells exposed to hypoxia or heme, HO-1 underwent cleavage of a C-terminal domain, leading to nuclear translocation of the N-terminal domain of HO-1 and subsequent transcriptional regulation by this cleaved portion (40). Furthermore, HO-1 protein that has been made to be catalytically inactive through site-directed mutagenesis participates directly in its own transcriptional autoregulation despite the absence of an active catalytic site (41). Thus, the phenotypic changes observed in response to SnMP may also be related to transcriptional changes induced by the presence of non-catalytically active (i.e., inhibited) HO-1 protein. This possibility is especially intriguing because HO-1 expression is induced by SnMP, resulting in a relative excess of inhibited HO-1. Of note, we attempted to carry out spectrophotometric HO-1 enzyme activity assays to confirm induction and inhibition of HO-1 (data not shown) but were limited by the number of cells available from an individual donor. Usually, this assay is carried out on tissue or cell-line lysates, from which protein yield is not normally limiting. We were unable to generate sufficient quantities of microsomal protein from single volunteer human donors to carry out this assay successfully and so were unable to demonstrate directly that SnMP inhibits HO-1 activity in our system. There is ample evidence from the literature that synthetic metalloporphyrin inducers and inhibitors of HO-1 are active in hematopoietic cells, and specifically in cells of the monocyte/macrophage lineage (42–44), and so it is reasonable to assume that SnMP acts as an inhibitor in our system.

The findings of this in vitro study suggest that HO-1 plays a role in controlling naive T cell activation, maturation, and proliferation, and in vivo studies are clearly warranted to validate the physiologic relevance of our findings. The goal of such studies would be to determine if HO-1 activity represents a safeguard mechanism to prevent nonspecific T cell activation by APCs, and whether removal of this safeguard by HO-1 downregulation or inhibition plays a role in promoting T cell activation and maturation under

physiologic or pathologic circumstances. Activation of T cells in vitro by SnMP required interaction with MHC-I and MHC-II, presumably via the TCRs on responding T cells. This is notable in that the observed response almost certainly represents a TCR-mediated response to self-MHC. Normally, T cells do not undergo widespread activation and proliferation in response to self-MHC, which is crucial for the maintenance of tolerance to self and prevention of autoimmunity. There are many mechanisms in place to ensure that T cell activation occurs only in appropriate settings (e.g., upon exposure to dangerous pathogens or upon detection of malignancy) and not in response to self-Ags. Chief among these mechanisms is the thymic deletion of autoreactive T cells through negative selection (45) and, in the peripheral immune system, the maintenance of tolerance by regulatory cells such as $CD4^+CD25^+$ $FoxP3^+$ Tregs (46, 47). These regulatory cells also participate in the tuning and modulation of immune responses to ensure their appropriate activation and termination. In the absence or relative paucity of these regulatory mechanisms, the immune response may proceed unchecked, causing collateral damage to the host (46, 47). Given the extent of proliferation observed after HO-1 inhibitor exposure, we posit that HO-1 may also serve as a safeguard mechanism to prevent inappropriate T cell activation. In many animal disease models, absence of HO-1 activity results in excess inflammation that contributes to pathology, including models of diabetes, asthma, multiple sclerosis, cerebral malaria, and transplant rejection (12, 27–32). The work presented here provides further support for a potential role of HO-1 in preventing inappropriate T cell activation in humans.

Naive T cells in the periphery undergo low levels of homeostatic proliferation until they encounter cognate Ag in the context of activating signal, at which point they go on to become effector and memory cells (48). This homeostatic proliferation is now thought to occur almost exclusively in lymph nodes, where T cells move through the parenchyma and come into contact with fibroblastic reticular cells (49). Among the signals that are crucial for naive T cell survival and proliferation, one of the most important is contact with MHC molecules on supporting accessory cells (48). In addition to the influence of critical growth factors, low-avidity interactions between the TCR on naive T cells and MHC provide survival signals that allow these cells to continue to proliferate at low levels, thereby maintaining a diverse and appropriately quiescent naive T cell population. Our experiments suggest that myeloid HO-1 activity may represent a "braking" mechanism for naive T cell proliferation, allowing for low-level proliferation in response to self-MHC while preventing uncontrolled activation and proliferation. If so, its absence could lead to dysregulated homeostasis. Indeed, mice that are deficient in HO-1 have clear evidence of dysfunctional lymphocyte homeostasis, including splenomegaly, lymphadenopathy, altered CD4/CD8 ratio, and disorganized lymph node and splenic architecture (14–16). They also have a higher frequency of activated T cells (15). This suggests that HO-1 plays a role in the regulation and maintenance of the peripheral T cell pool and/or in the prevention of inappropriate activation.

Our study suggests that HO-1 plays a role in T cell homeostasis, and support for this hypothesis is found most convincingly in our examination of the maturational profile of cells treated with SnMP. The experiments shown in Fig. 4 clearly demonstrate that proliferating cells are primarily naive T cells that adopt memory cell phenotypes, a phenomenon that is observed in some models of homeostatic T cell proliferation (50–53). For example, naive T cells transferred into syngeneic lymphopenic hosts repopulate the host's peripheral immune system by undergoing robust self-MHC–dependent proliferation, during which they take on the phenotype and characteristics of memory cells (50–53). It may be that the naive cells that become proliferating memory cells in our experiments are undergoing a similar homeostatic proliferative response. It remains to be seen whether comparable responses may occur in vivo during inhibition of HO-1. Certainly, this type of response would seem more likely to occur in secondary lymphoid organs, where T cells come in contact with myeloid cells for an extended period of time. Furthermore, variations in HO-1 activity that would theoretically lead to more or less T cell proliferation could occur in specialized subanatomic regions, possibly influenced by concentration gradients of natural HO-1 inducers such as heme.

HO-1 has been shown in many instances to be antiproliferative and to downregulate potentially harmful inflammatory responses. The experiments presented here raise another possible role for HO-1 in T cell homeostasis; namely, that unopposed HO-1 in myeloid cells provides homeostatic signals to T cells, allowing them to remain in a nonactivated state. In the absence of HO-1, or in the presence of inhibited HO-1, a different set of signals (or perhaps merely the absence of antiproliferative signals) may then lead to T cell activation and proliferation. This effect may also represent a mechanism to alleviate suppression of T cells in settings where activation is needed, such as infection or malignancy. In aggregate, these findings demonstrate that HO-1 can alter human T cell activation, maturation, and proliferation in vitro and suggest that this multifunctional protein may play a role in controlling lymphoid development and homeostasis in vivo. They also suggest the possibility that SnMP, or other pharmacologic HO-1 inhibitors, could be used as clinical modulators of T cell maturation, which would have potential use in settings requiring immune reconstitution such as chemotherapy and after initiation of highly active antiretroviral therapy for HIV.

Acknowledgments

We thank the volunteer blood donors who participated in this study, Dr. Nader Abraham for helpful technical advice, Terrence Ho and the Division of Experimental Medicine Flow Cytometry Core for assistance with flow cytometry and cell sorting, Dr. Jeffrey Bluestone and Dr. Mark Anderson for helpful discussions regarding Ab blockade experiments, and Dr. Jennifer Babik and Dr. Louise Swainson for thoughtful discussion and for careful review of the manuscript.

Disclosures

The authors have no financial conflicts of interest.

References

1. Ryter, S. W., J. Alam, and A. M. Choi. 2006. Heme oxygenase-1/carbon monoxide: from basic science to therapeutic applications. *Physiol. Rev.* 86: 583–650.
2. Abraham, N. G., and A. Kappas. 2008. Pharmacological and clinical aspects of heme oxygenase. *Pharmacol. Rev.* 60: 79–127.
3. Lee, P. J., S. L. Camhi, B. Y. Chin, J. Alam, and A. M. Choi. 2000. AP-1 and STAT mediate hyperoxia-induced gene transcription of heme oxygenase-1. *Am. J. Physiol. Lung Cell. Mol. Physiol.* 279: L175–L182.
4. Keyse, S. M., and R. M. Tyrrell. 1989. Heme oxygenase is the major 32-kDa stress protein induced in human skin fibroblasts by UVA radiation, hydrogen peroxide, and sodium arsenite. *Proc. Natl. Acad. Sci. USA* 86: 99–103.
5. Taketani, S., H. Kohno, T. Yoshinaga, and R. Tokunaga. 1988. Induction of heme oxygenase in rat hepatoma cells by exposure to heavy metals and hyperthermia. *Biochem. Int.* 17: 665–672.
6. Terry, C. M., J. A. Clikeman, J. R. Hoidal, and K. S. Callahan. 1998. Effect of tumor necrosis factor-alpha and interleukin-1 alpha on heme oxygenase-1 expression in human endothelial cells. *Am. J. Physiol.* 274: H883–H891.
7. Murphy, B. J., K. R. Laderoute, S. M. Short, and R. M. Sutherland. 1991. The identification of heme oxygenase as a major hypoxic stress protein in Chinese hamster ovary cells. *Br. J. Cancer* 64: 69–73.
8. Camhi, S. L., J. Alam, L. Otterbein, S. L. Sylvester, and A. M. Choi. 1995. Induction of heme oxygenase-1 gene expression by lipopolysaccharide is mediated by AP-1 activation. *Am. J. Respir. Cell Mol. Biol.* 13: 387–398.
9. Abuarqoub, H., R. Foresti, C. J. Green, and R. Motterlini. 2006. Heme oxygenase-1 mediates the anti-inflammatory actions of 2′-hydroxychalcone in

RAW 264.7 murine macrophages. *Am. J. Physiol. Cell Physiol.* 290: C1092–C1099.
10. Kim, H. J., H. S. So, J. H. Lee, J. H. Lee, C. Park, S. Y. Park, Y. H. Kim, M. J. Youn, S. J. Kim, S. Y. Chung, et al. 2006. Heme oxygenase-1 attenuates the cisplatin-induced apoptosis of auditory cells via down-regulation of reactive oxygen species generation. *Free Radic. Biol. Med.* 40: 1810–1819.
11. Song, R., R. S. Mahidhara, Z. Zhou, R. A. Hoffman, D. W. Seol, R. A. Flavell, T. R. Billiar, L. E. Otterbein, and A. M. Choi. 2004. Carbon monoxide inhibits T lymphocyte proliferation via caspase-dependent pathway. *J. Immunol.* 172: 1220–1226.
12. Li, M., S. Peterson, D. Husney, M. Inaba, K. Guo, A. Kappas, S. Ikehara, and N. G. Abraham. 2007. Long-lasting expression of HO-1 delays progression of type I diabetes in NOD mice. *Cell Cycle* 6: 1886–1895.
13. Yamashita, K., R. Ollinger, J. McDaid, H. Sakahama, H. Wang, S. Tyagi, E. Csizmadia, N. R. Smith, M. P. Soares, and F. H. Bach. 2006. Heme oxygenase-1 is essential for and promotes tolerance to transplanted organs. *FASEB J.* 20: 776–778.
14. Poss, K. D., and S. Tonegawa. 1997. Reduced stress defense in heme oxygenase 1-deficient cells. *Proc. Natl. Acad. Sci. USA* 94: 10925–10930.
15. Poss, K. D., and S. Tonegawa. 1997. Heme oxygenase 1 is required for mammalian iron reutilization. *Proc. Natl. Acad. Sci. USA* 94: 10919–10924.
16. Kapturczak, M. H., C. Wasserfall, T. Brusko, M. Campbell-Thompson, T. M. Ellis, M. A. Atkinson, and A. Agarwal. 2004. Heme oxygenase-1 modulates early inflammatory responses: evidence from the heme oxygenase-1-deficient mouse. *Am. J. Pathol.* 165: 1045–1053.
17. Kawashima, A., Y. Oda, A. Yachie, S. Koizumi, and I. Nakanishi. 2002. Heme oxygenase-1 deficiency: the first autopsy case. *Hum. Pathol.* 33: 125–130.
18. Yachie, A., Y. Niida, T. Wada, N. Igarashi, H. Kaneda, T. Toma, K. Ohta, Y. Kasahara, and S. Koizumi. 1999. Oxidative stress causes enhanced endothelial cell injury in human heme oxygenase-1 deficiency. *J. Clin. Invest.* 103: 129–135.
19. Exner, M., E. Minar, O. Wagner, and M. Schillinger. 2004. The role of heme oxygenase-1 promoter polymorphisms in human disease. *Free Radic. Biol. Med.* 37: 1097–1104.
20. Pae, H. O., G. S. Oh, B. M. Choi, S. C. Chae, Y. M. Kim, K. R. Chung, and H. T. Chung. 2004. Carbon monoxide produced by heme oxygenase-1 suppresses T cell proliferation via inhibition of IL-2 production. *J. Immunol.* 172: 4744–4751.
21. Kappas, A. 2004. A method for interdicting the development of severe jaundice in newborns by inhibiting the production of bilirubin. *Pediatrics* 113: 119–123.
22. Drummond, G. S., R. A. Galbraith, M. K. Sardana, and A. Kappas. 1987. Reduction of the C2 and C4 vinyl groups of Sn-protoporphyrin to form Sn-mesoporphyrin markedly enhances the ability of the metalloporphyrin to inhibit in vivo heme catabolism. *Arch. Biochem. Biophys.* 255: 64–74.
23. Delaney, J. K., D. Mauzerall, G. S. Drummond, and A. Kappas. 1988. Photophysical properties of Sn-porphyrins: potential clinical implications. *Pediatrics* 81: 498–504.
24. Michaëlsson, J., J. E. Mold, J. M. McCune, and D. F. Nixon. 2006. Regulation of T cell responses in the developing human fetus. *J. Immunol.* 176: 5741–5748.
25. Chauveau, C., S. Rémy, P. J. Royer, M. Hill, S. Tanguy-Royer, F. X. Hubert, L. Tesson, R. Brion, G. Beriou, M. Gregoire, et al. 2005. Heme oxygenase-1 expression inhibits dendritic cell maturation and proinflammatory function but conserves IL-10 expression. *Blood* 106: 1694–1702.
26. George, J. F., A. Braun, T. M. Brusko, R. Joseph, S. Bolisetty, C. H. Wasserfall, M. A. Atkinson, A. Agarwal, and M. H. Kapturczak. 2008. Suppression by CD4+ CD25+ regulatory T cells is dependent on expression of heme oxygenase-1 in antigen-presenting cells. *Am. J. Pathol.* 173: 154–160.
27. Pamplona, A., A. Ferreira, J. Balla, V. Jeney, G. Balla, S. Epiphanio, A. Chora, C. D. Rodrigues, I. P. Gregoire, M. Cunha-Rodrigues, et al. 2007. Heme oxygenase-1 and carbon monoxide suppress the pathogenesis of experimental cerebral malaria. *Nat. Med.* 13: 703–710.
28. Otterbein, L. E., M. P. Soares, K. Yamashita, and F. H. Bach. 2003. Heme oxygenase-1: unleashing the protective properties of heme. *Trends Immunol.* 24: 449–455.
29. Listopad, J., K. Asadullah, C. Sievers, T. Ritter, C. Meisel, R. Sabat, and W. D. Döcke. 2007. Heme oxygenase-1 inhibits T cell-dependent skin inflammation and differentiation and function of antigen-presenting cells. *Exp. Dermatol.* 16: 661–670.
30. Chora, A. A., P. Fontoura, A. Cunha, T. F. Pais, S. Cardoso, P. P. Ho, L. Y. Lee, R. A. Sobel, L. Steinman, and M. P. Soares. 2007. Heme oxygenase-1 and carbon monoxide suppress autoimmune neuroinflammation. *J. Clin. Invest.* 117: 438–447.
31. Sato, K., J. Balla, L. Otterbein, R. N. Smith, S. Brouard, Y. Lin, E. Csizmadia, J. Sevigny, S. C. Robson, G. Vercellotti, et al. 2001. Carbon monoxide generated by heme oxygenase-1 suppresses the rejection of mouse-to-rat cardiac transplants. *J. Immunol.* 166: 4185–4194.
32. Xia, Z. W., W. W. Zhong, L. Q. Xu, J. L. Sun, Q. X. Shen, J. G. Wang, J. Shao, Y. Z. Li, and S. C. Yu. 2006. Heme oxygenase-1-mediated CD4+CD25high regulatory T cells suppress allergic airway inflammation. *J. Immunol.* 177: 5936–5945.
33. Rémy, S., P. Blancou, L. Tesson, V. Tardif, R. Brion, P. J. Royer, R. Motterlini, R. Foresti, M. Painchaut, S. Pogu, et al. 2009. Carbon monoxide inhibits TLR-induced dendritic cell immunogenicity. *J. Immunol.* 182: 1877–1884.
34. Moreau, A., M. Hill, P. Thebault, J. Y. Deschamps, E. Chiffoleau, C. Chauveau, P. Moullier, I. Anegon, B. Alliot-Licht, and M. C. Cuturi. 2009. Tolerogenic dendritic cells actively inhibit T cells through heme oxygenase-1 in rodents and in nonhuman primates. *FASEB J.* 23: 3070–3077.
35. Tzima, S., P. Victoratos, K. Kranidioti, M. Alexiou, and G. Kollias. 2009. Myeloid heme oxygenase-1 regulates innate immunity and autoimmunity by modulating IFN-beta production. *J. Exp. Med.* 206: 1167–1179.
36. Zelenay, S., A. Chora, M. P. Soares, and J. Demengeot. 2007. Heme oxygenase-1 is not required for mouse regulatory T cell development and function. *Int. Immunol.* 19: 11–18.
37. Zhen, Y., J. Zheng, and Y. Zhao. 2008. Regulatory CD4+CD25+ T cells and macrophages: communication between two regulators of effector T cells. *Inflamm. Res.* 57: 564–570.
38. Wing, K., Y. Onishi, P. Prieto-Martin, T. Yamaguchi, M. Miyara, Z. Fehervari, T. Nomura, and S. Sakaguchi. 2008. CTLA-4 control over Foxp3+ regulatory T cell function. *Science* 322: 271–275.
39. Mahnke, K., T. Bedke, and A. H. Enk. 2007. Regulatory conversation between antigen presenting cells and regulatory T cells enhance immune suppression. *Cell. Immunol.* 250: 1–13.
40. Lin, Q., S. Weis, G. Yang, Y. H. Weng, R. Helston, K. Rish, A. Smith, J. Bordner, T. Polte, F. Gaunitz, and P. A. Dennery. 2007. Heme oxygenase-1 protein localizes to the nucleus and activates transcription factors important in oxidative stress. *J. Biol. Chem.* 282: 20621–20633.
41. Lin, Q. S., S. Weis, G. Yang, T. Zhuang, A. Abate, and P. A. Dennery. 2008. Catalytic inactive heme oxygenase-1 protein regulates its own expression in oxidative stress. *Free Radic. Biol. Med.* 44: 847–855.
42. Wyse, C. A., C. Nixon, M. McLaughlin, F. J. Dowell, and A. W. Philbey. 2006. Evidence for the expression and enzymatic activity of haem oxygenase-1 in the lungs of horses. *Vet. Rec.* 158: 795–797.
43. Lutton, J. D., S. Jiang, G. S. Drummond, N. G. Abraham, and A. Kappas. 1999. Comparative pharmacology of zinc mesoporphyrin and tin mesoporphyrin: toxic actions of zinc mesoporphyrin on hematopoiesis and progenitor cell mobilization. *Pharmacology* 58: 44–50.
44. Yoshida, T., P. Biro, T. Cohen, R. M. Müller, and S. Shibahara. 1988. Human heme oxygenase cDNA and induction of its mRNA by hemin. *Eur. J. Biochem.* 171: 457–461.
45. Gallegos, A. M., and M. J. Bevan. 2006. Central tolerance: good but imperfect. *Immunol. Rev.* 209: 290–296.
46. Sakaguchi, S., T. Yamaguchi, T. Nomura, and M. Ono. 2008. Regulatory T cells and immune tolerance. *Cell* 133: 775–787.
47. Sakaguchi, S. 2004. Naturally arising CD4+ regulatory t cells for immunologic self-tolerance and negative control of immune responses. *Annu. Rev. Immunol.* 22: 531–562.
48. Surh, C. D., and J. Sprent. 2008. Homeostasis of naive and memory T cells. *Immunity* 29: 848–862.
49. Link, A., T. K. Vogt, S. Favre, M. R. Britschgi, H. Acha-Orbea, B. Hinz, J. G. Cyster, and S. A. Luther. 2007. Fibroblastic reticular cells in lymph nodes regulate the homeostasis of naive T cells. *Nat. Immunol.* 8: 1255–1265.
50. Schluns, K. S., W. C. Kieper, S. C. Jameson, and L. Lefrançois. 2000. Interleukin-7 mediates the homeostasis of naïve and memory CD8 T cells in vivo. *Nat. Immunol.* 1: 426–432.
51. Goldrath, A. W., and M. J. Bevan. 1999. Low-affinity ligands for the TCR drive proliferation of mature CD8+ T cells in lymphopenic hosts. *Immunity* 11: 183–190.
52. Ernst, B., D. S. Lee, J. M. Chang, J. Sprent, and C. D. Surh. 1999. The peptide ligands mediating positive selection in the thymus control T cell survival and homeostatic proliferation in the periphery. *Immunity* 11: 173–181.
53. Tan, J. T., E. Dudl, E. LeRoy, R. Murray, J. Sprent, K. I. Weinberg, and C. D. Surh. 2001. IL-7 is critical for homeostatic proliferation and survival of naive T cells. *Proc. Natl. Acad. Sci. USA* 98: 8732–8737.

Supplemental Figure 1

T cell viability does not change over a range of SnMP concentrations. PBMC were cultured for 7 days in SnMP at various concentrations (0,12.5, 25 and 50 μM), stained for surface markers, and T cells were identified by CD3-expression. An amine-reactive dye was used to identify dead and dying cells. The graph shown includes results from four separate experiments, and error bars represent the SEM. Variance was analyzed using a one-way ANOVA, and there was no significant difference in viability detected at any SnMP concentration.

Supplemental Figure 2

HO-1 protein expression is induced in CD14+ cells, but not T cells, by CoPP and SnMP. (A-D) PBMC were cultured on Upcell™ plates for 3 days in vehicle control, SnMP or CoPP (10 μM), harvested by incubating plates at 25°C (which releases adherent cells), and stained for cell surface markers and HO-1. Lineage (Lin)+ (CD3+, CD19+, CD56+) cells were gated separately from Lin-CD14+ cells, and the mean fluorescence intensity (MFI) of HO-1 was determined. (A) and (C) are single representative histograms representing HO-1 MFI in Lin+ and Lin-CD14+ cells, respectively, while (B) and (D) show the mean of six individual donors. Error bars represent SEM, and significance was analyzed by Mann-Whitney test (* $P<0.01$). In the histograms, the black lines represent vehicle controls, the blue lines represent CoPP and the red lines represent SnMP. Intracellular HO-1 staining was confirmed to be specific by western blot analysis of FACS sorted HO-1-positive and negative cells, and secondary antibody-only controls were included in all experiments (data not shown). (E) PBMC cultures with SnMP or

vehicle control were harvested, as described above. CD3+ and CD14 + cells were isolated by negative magnetic bead selection, lysed, and analyzed for HO-1 protein expression by western blot; a single representative blot is shown.

Supplemental Figure 3

SnMP and CoPP alter monocyte expression of multiple markers of myeloid differentiation and activation. PBMC were cultured on Upcell™ plates for 3 days in vehicle control, SnMP or CoPP, harvested by incubating plates at 25°C (which also releases adherent cells), and stained for cell surface markers. Cells were gated on Lin- (CD3-CD19-CD56-) CD14+ cells, and mean fluorescence intensity was measured for CD11c, CD16, CD86, CD163, HLA-DR, and BDCA-2. In representative flow cytometry histrograms (A), the thick-lined, unshaded histogram represents vehicle control samples; the thin-lined unshaded histogram represents CoPP-treated samples; and the thick-lined shaded histogram represents SnMP-treated samples. The mean MFI for six individual donors are shown (B) and error bars represent SEM. Significance was determined by Mann-Whitney test, and *$P<0.01$, ** $P<0.05$

Supplemental Figure 1

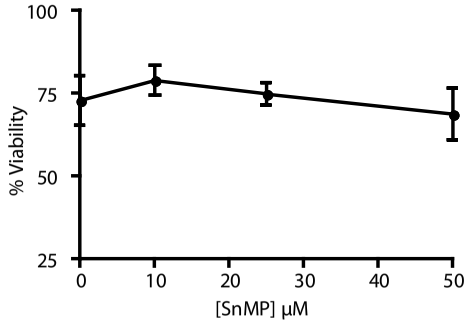

Supplemental Figure 2

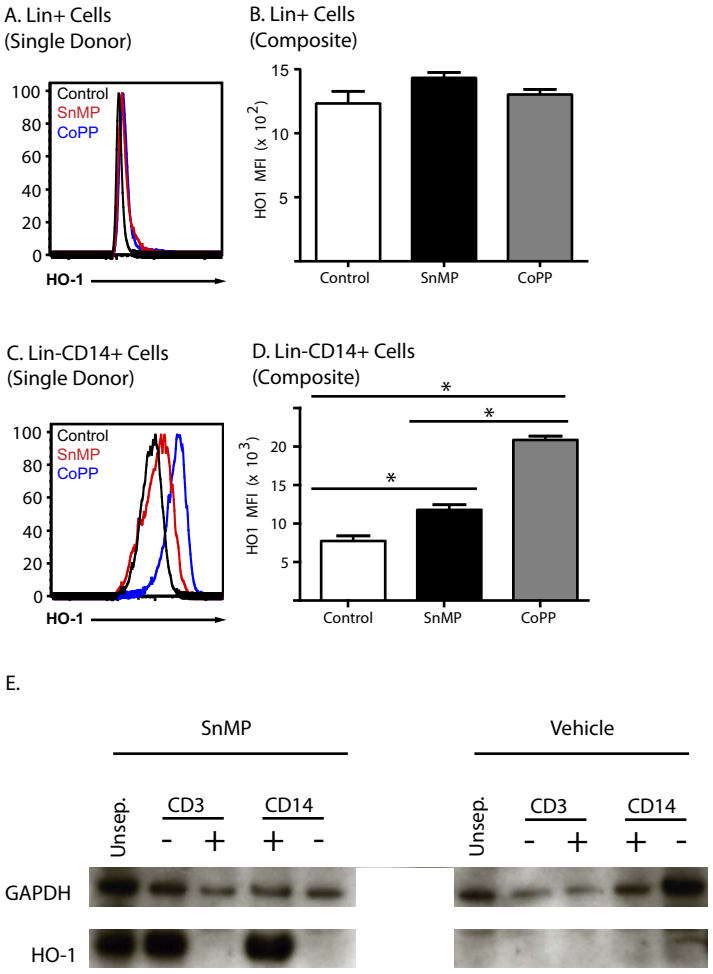

E.

Supplemental Figure 3

A. CD14+ Cells (Single Donor)

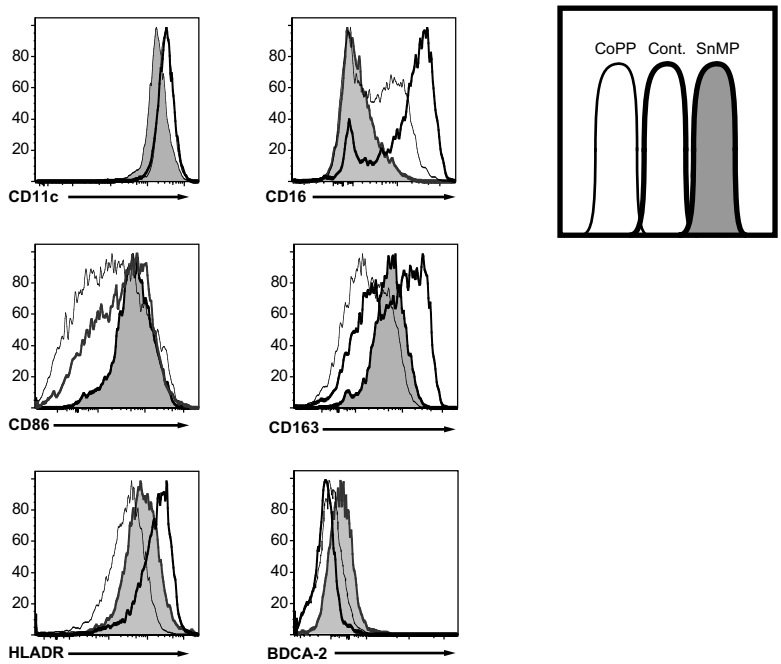

B. CD14+ Cells (Composite)

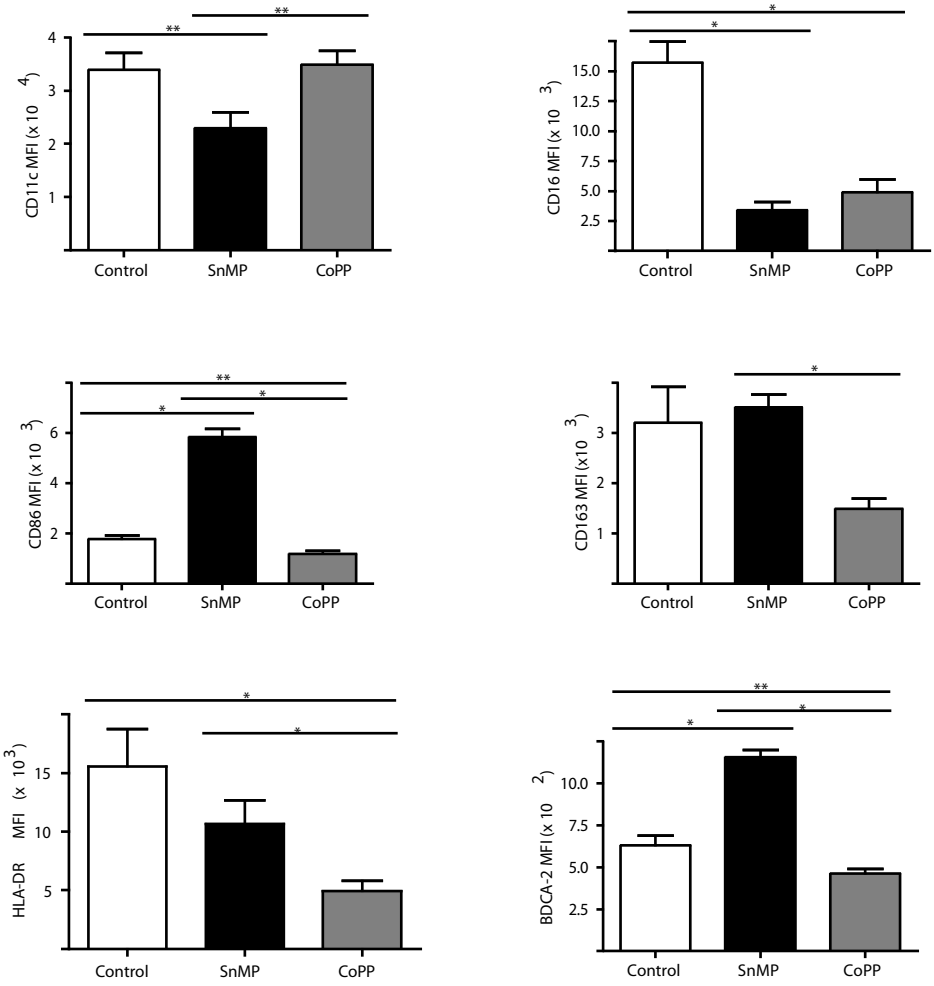

* P<0.01

**P<0.05

II

Variations in the heme oxygenase-1 microsatellite polymorphism are associated with plasma CD14 and viral load in HIV-infected African Americans

"Division of Experimental Medicine" (6th Floor, Building 3, SF General Hospital)

Dan Jumanan (Artist)

Full Title: Variations in the heme oxygenase-1 microsatellite polymorphism are associated with plasma CD14 and viral load in HIV-infected African Americans

Running title: HO-1 microsatellite polymorphisms during HIV

Authors: Lillian Seu,[1,2] Trevor D. Burt,[2,3] John S. Witte,[4,5] Jeffrey N. Martin,[5] Steven G. Deeks,[6] Joseph M. McCune[2]

[1]Department of Bioengineering and Therapeutic Sciences, University of California, San Francisco, CA 94110

[2]Division of Experimental Medicine, Department of Medicine, University of California, San Francisco, CA 94110

[3]Division of Neonatology, Department of Pediatrics, University of California, San Francisco, CA 94143

[4]Institute for Human Genetics, University of California, San Francisco, CA 94110

[5]Department of Epidemiology and Biostatistics, University of California, San Francisco, CA 94110

[6]Positive Health Program, Department of Medicine, University of California, San Francisco, CA 94110

ABSTRACT

Heme oxygenase-1 (HO-1) is an anti-inflammatory enzyme that maintains homeostasis during cellular stress. Given previous findings that shorter length variants of a HO-1 promoter-region GT_n microsatellite polymorphism are associated with increased HO-1 expression in cell lines, we hypothesized that shorter variants would also be associated with increased levels of HO-1 expression, less inflammation, and lower levels of inflammation-associated viral replication in HIV-infected subjects. Healthy donors (n=20) with shorter GT_n repeats had higher HO-1 mRNA transcript in peripheral blood mononuclear cells stimulated with lipopolysaccharide (LPS) ($r= -0.38$, $p=0.05$). The presence of fewer GT_n repeats in subjects with untreated HIV disease was associated with higher HO-1 mRNA levels in peripheral blood ($r= -0.41$, $p=0.02$); similar observations were made in $CD14^+$ monocytes from antiretroviral-treated subjects ($r= -0.36$, $p=0.04$). In African-Americans, but not Caucasians, greater GT_n repeats were correlated with higher soluble CD14 (sCD14) levels during highly active antiretroviral therapy (HAART) ($r= 0.38$, $p=0.007$) as well as higher mean viral load off-therapy ($r= 0.24$, $p=0.04$). These data demonstrate that the HO-1 GT_n microsatellite polymorphism is associated with higher levels of HO-1 expression and that this pathway may have important effects on the association between inflammation and HIV replication.

Keywords

Heme oxygenase-1, microsatellite, polymorphism, HIV, soluble CD14, monocytes

INTRODUCTION

Although host immune activation is critical for the eradication of infectious agents, the inflammatory response can also enhance pathogenesis. An example of this delicate balance is revealed by human immunodeficiency virus (HIV) disease: progressive and pathogenic infection is associated with chronic immune activation, including heightened destruction and diminished production of T lymphocytes (1), an increased frequency of T cells with an activated phenotype (2), increased T cell induction of the pro-inflammatory transcription factors, NFκB and NF-AT (3), and increased serum levels of pro-inflammatory cytokines (e.g., TNFα, IL-1 and IL-6) (4,5).

The impact of chronic inflammation on HIV (and simian immunodeficiency virus; SIV) disease progression has been well studied in both humans and non-human primates. Experiments in non-human primate models of acute SIV infection have demonstrated that increased bystander immune activation heightens viral cellular transmission by increasing the T cell target to T cell effector ratio (6). T lymphocyte activation as measured by cell surface markers has also been associated with viral load "set-point" in untreated HIV disease (7) and is associated with disease progression in both untreated and treated HIV infection (8,9).

Multiple mechanisms likely contribute to HIV-associated inflammation, including the direct effects of the virus. Recent studies have shown that circulating lipopolysaccharide (LPS) resulting from microbial translocation from gut associated lymphoid tissue (GALT) sites is a cause of systemic immune activation in chronic HIV infection (10), and is present even in HAART-suppressed subjects with undetectable viremia (11). An extension of this finding was the discovery that soluble CD14, the portion of the LPS-receptor that gets cleaved upon binding to its ligand, is elevated in HIV disease and strongly associated with

enhanced mortality in chronically HIV-infected subjects (12), and is a major force driving chronic inflammation during HAART in this cohort (13).

Given the impact of immune activation/inflammation on the pace of HIV disease progression, we hypothesized that host factors controlling inflammation might be protective. In this study, we focused on heme oxygenase-1 (HO-1), the rate-limiting enzyme that initiates heme degradation and maintains cellular homeostasis during stress through its depletion of pro-oxidant heme, through generation of cytoprotective carbon monoxide and biliverdin, and through induction of ferritin by Fe^{2+} release. Among the three isoforms, only HO-1 is induced by a myriad of stress signals including oxidative stress, ultraviolet (UVA) radiation, and the pro-inflammatory cytokines IL-1, IL-6, TNFα (14). Furthermore, we have recently demonstrated that the HO-1 inhibitor, tin mesoporphyrin IX (SnMP), induces activation, proliferation, and maturation of naïve human T cells via interactions with $CD14^+$ monocytes (15).

Given the important role that HO-1 has as an anti-inflammatory mediator, numerous studies have linked proximal promoter HO-1 polymorphisms to disease states that are driven by inflammation (e.g., graft versus host disease, ischemic stroke, coronary artery disease, etc.) [reviewed in (16)]. The GT_n microsatellite polymorphism is the best-characterized HO-1 genetic locus to date. Previous studies using promoter-luciferase assays in cell lines have shown an association between GT_n microsatellites with a small number of repeats and enhanced transcription of the HO-1 gene (17-20). Likewise, a recent study using primary endothelial cells isolated from newborns showed that HO-1 induction was more robust in the context of fewer ($GT_{n<23}$) than greater ($GT_{\geq 29}$) repeats (21). Although many candidate gene studies have detected associations between the short HO-1 GT_n microsatellite variant and

control of inflammatory disease states, no study has examined its functional role in regulating gene expression in primary immune cells that directly influence pathogenic outcomes in HIV-infected subjects.

Here, we have studied the influence of the promoter GT_n microsatellite repeat number on HO-1 transcript expression in peripheral blood mononuclear cells (PBMCs) of healthy adults after *in vitro* stimulation and in PBMCs isolated from HIV-infected subjects on and off antiretroviral therapy. Next, we conducted a candidate genotyping study for two biomarkers of HIV disease progression: mean viral load and soluble CD14. Lastly, we determined the association between HO-1 expression and CD14 expression on primary blood $CD14^+$ monocytes from healthy donors stimulated *in vitro* with LPS. In aggregate, our results suggest that the HO-1 GT_n microsatellite polymorphism is a functional determinant of HO-1 expression in primary immune cells and is associated with important biomarkers of HIV disease outcome.

RESULTS

Heme oxygenase-1 (HO-1) promoter description across HIV-infected subjects of different ethnicities

The HO-1 promoter region analyzed extends from the nucleotide position 1876 base pairs upstream and +75 base pairs downstream of the transcription start site at position +1 (Fig. 1a). This promoter region contains the GT_n dinucleotide repeat and two common SNPs (-413AT/rs2071746 and -1195AG/rs3761439) that have been analyzed in previous studies of the HO-1 gene (19,22). Two common insertion/deletion variants (dbSNP ID rs72441698 and rs58433947) with GT_7 repeats may explain the large frequency of GT_{23} and GT_{30} variants seen across all populations of HIV-infected subjects (n=717, median age ± interquartile range = 46.2 ± 10.2, 85.5% male, 28.6% African American, 55.2% Caucasian) (Suppl. Fig. 1). The GT_n repeats in the African-Americans follow a tri-modal distribution in contrast to the bi-modal distribution seen in Caucasians (Box III in Fig. 1b). The addition of this GT_7 insertion results in greater repeat numbers in African Americans (mean 31.5 ± 0.27, n=205) than in Caucasians (mean 28.1 ± 0.14, n=396) ($p<0.001$) (Fig. 1b) and in other ethnic groups (Suppl. Fig. 1a). Allele frequencies for these SNPs were also calculated across these ethnic groups (Suppl. Fig. 1b).

Prior studies of the HO-1 promoter region examined the association between the -413AT/rs2071746 and the -1195AG/rs3761439 SNPs with coronary artery disease outcomes and cardiac function during exercise (19,22). These SNPs were not in significant linkage disequilibrium with the most common GT_{23} and GT_{30} repeats in both African American and Caucasian populations (Fig. 1c), with r^2 values below 0.4. These results suggest limited linkage disequilibrium present at this locus.

Heme oxygenase-1 additive GT_n repeats negatively correlate with gene expression in PBMCs and $CD14^+$ monocytes from healthy donors

To extend these studies to primary cells that might be involved in the immune response to HIV, fresh peripheral blood mononuclear cells (PBMCs) (n=20) or enriched $CD14^+$ monocytes from healthy donors (n=6) (subsets of donors from those listed in Table 1) were analyzed for HO-1 relative transcript expression after stimulation with the HO-1 chemical inducers cobalt protoporphyrin IX (CoPP), hydrogen peroxide (H_2O_2), and lipopolysaccharide (LPS). Compared to the phosphate buffered saline (PBS) control, stimulation with CoPP led to a 46-fold increase in relative transcript abundance of HO-1 ($p<0.0001$, paired t-test) whereas H_2O_2 stimulation led to a 1.3-fold increase ($p=0.005$) and LPS to a 1.3-fold decrease ($p=0.007$) (Fig. 2a). Since prior studies have reported an important role of HO-1 in the function of $CD14^+$ monocytes (15,23), enriched $CD14^+$ monocytes were analyzed after *in vitro* stimulation with CoPP, H_2O_2, or LPS, which led to a 30-fold increase ($p<0.0001$), a 1.2-fold increase ($p=0.02$), and a 1.4-fold decrease ($p=0.02$), respectively (paired t-test, Fig. 2b).

Using an HO-1 promoter-reporter gene assay in HEK293T cells, the additive sum of an individual's GT_n repeat number ($GT_n^{\text{locus 1}} + GT_n^{\text{locus 2}}$) was found to be an informative variable for subsequent functional analyses of this polymorphism (i.e., the greater the repeat number the lower the level of HO-1 expression) (Suppl. Fig. 2). Healthy donors were genotyped for the HO-1 GT_n polymorphism and transcript levels in PBMCs were measured. Multiple regression analysis (controlling for self-identified ethnicity) of normalized HO-1 transcript level and additive GT_n repeats showed statistically significant negative correlations

in PBMCs from healthy donors stimulated with LPS (r= -0.38, β= -0.024, p=0.05) (Fig. 2c). The same analyses in PBMCs stimulated with CoPP (r= -0.30, β= -0.98, p=0.06) and H_2O_2 (r= -0.36, β= -0.076, p=0.08) showed trends towards negative correlations (Fig. 2c). Consistent with previous findings, the HO-1 transcript levels in unstimulated PBMCs did not show a correlation with an individual's additive GT_n repeat number (20) (Suppl. Fig. 3). These results are consistent with our gene expression results in the HEK293T cell lines as well as prior reports showing that greater GT_n repeats lead to decreased gene expression (17-19).

Finally, given prior evidence that the -413AT/rs2071746 may be associated with HO-1 expression in cell lines (19), we tested whether this SNP was associated with HO-1 induction in primary PBMCs exposed to CoPP, LPS, or H_2O_2 (Suppl. Fig. 4a-c, respectively). ANOVA analysis showed no significant association between HO-1 gene expression with this SNP or another common SNP (-1195AG/rs3761439). In summary, these results show that the GT_n microsatellite polymorphism is associated with the regulation of HO-1 gene transcription in primary immune cells.

Heme oxygenase-1 additive GT_n repeats negatively correlate with gene expression in PBMCs and $CD14^+$ monocytes from HIV-infected subjects

Prior studies have shown that HIV infection leads to up-regulation of HO-1 mRNA levels in peripheral blood cells (24). To determine whether HIV-infected subjects with a greater number of additive GT_n repeats displayed lower HO-1 expression, we harvested thawed PBMCs and measured relative HO-1 transcript abundance. Multiple regression analysis with ethnicity as a covariate was performed to determine the relationship between

the number of additive GT_n repeats and HO-1 relative transcript levels in "viral non-controllers" (prototypic HIV-infected adults with plasma HIV RNA levels above 10 000 copies RNA/mL, n=34) (Table 2a) and "viral controllers" (HIV-infected adults able to fully or partially control HIV replication with plasma HIV RNA level below 1 000 copies RNA/mL in the absence of therapy, n=30) (Table 2a). Among non-controllers, there was a significant correlation between additive GT_n repeats and the HO-1 relative transcript level (Fig. 3a) ($r= -0.41$, $\beta= -3.08$, $p=0.02$). There was no association between these factors in the controllers ($r=0.03$, $\beta= -0.36$, $p=0.4$).

Further phenotyping analyses in PBMCs from HIV-infected subjects on highly active antiretroviral therapy (HAART) showed that HO-1 was expressed to the highest extent in $CD14^+$ monocytes. Among individuals with a favorable response to HAART (as defined by having a plasma viral loads with <75 copies RNA/mL) (Table 2b), there was a negative correlation in $CD14^+$ monocytes ($r= -0.36$, $\beta= -30.45$, $p=0.04$) (Fig. 3b). These results suggest that the GT_n microsatellite polymorphism is an important correlate of HO-1 expression within peripheral immune cells during the course of HIV disease, especially in those subjects with progressive disease and high viremia.

HO-1 additive GT_n repeats are correlated with levels of soluble CD14 and viremia in African American HIV-infected subjects

Given recent studies linking high levels of soluble CD14 with enhanced mortality in chronically HIV-infected subjects on HAART (12) and the functional role that HO-1 plays in $CD14^+$ monocyte biology, we measured levels of plasma sCD14 levels in a larger cohort of African American and Caucasian HIV-infected, HAART-suppressed subjects (Table 3a).

Greater HO-1 additive GT_n repeats correlated with higher levels of sCD14 in African American HAART subjects (n=50, r= 0.38, p=0.007) (Table 3a) (Fig. 4a). Furthermore, each unit increase in additive GT_n repeats correlated with a sCD14 level increase of 2.3 ± 0.8 x 10^4 pg/mL (regression coefficient β= 2.3). Greater additive GT_n repeats also correlated with higher mean plasma HIV RNA levels in African American subjects that were during the chronic phase of infection (n=74, r=0.24, p=0.04) (Fig. 4b). Furthermore, each unit increase in additive GT_n repeats correlated with a mean viral load increase of 3 805.13 ± 1 803.7 HIV RNA copies/mL (regression coefficient β= 3 805.13). Neither the soluble CD14 levels during suppressive HAART (n=123, r= 0.0016, β=0.80, p=1.0) nor the mean viral load level in the absence of therapy (n=177, r= -0.02, β=3 119.26, p=0.2) were statistically different in Caucasian subjects with greater HO-1 additive GT_n repeat numbers.

In summary, these data suggest that the genetically determined level of HO-1 expression in $CD14^+$ monocytes may play a role in HIV disease outcome in African-Americans.

Higher levels of HO-1 expression in primary human $CD14^{hi}$ monocytes correlate with decreased loss of cell surface CD14 after LPS stimulation

CD14 is expressed on the cell surface of monocytes and is the receptor for LPS, a cell wall component of gram-negative bacteria. Upon binding to LPS, a cleaved form of CD14 is shed into the circulation (25,26). Given the finding that greater numbers of HO-1 additive GT_n repeats are positively correlated with higher levels of sCD14 (Fig. 4a), we tested the possibility that HO-1 expression in CD14+ monocytes predicts their ability to retain CD14 cell surface expression upon LPS stimulation. HO-1 protein levels were quantified in PBMCs

from 22 healthy donors (Table 1) by multiparameter flow cytometry analysis (Fig. 5a). As previously demonstrated (15,23), HO-1 was most highly expressed at baseline in PBMCs within the $CD14^{+}$ blood monocyte population. Upon exposure to CoPP, HO-1 was up-regulated to a greater extent within monocytes that are $CD14^{hi}$ than in "non-classical" $CD14^{dim}CD16^{+}$ monocytes (55 226 vs. 13 448 in geometric mean fluorescence intensity (gMFI); $p<1x10^{-8}$). By contrast, $CD3^{+}$ T cells displayed very low HO-1 expression, even after induction with 25 uM CoPP (Fig. 5a).

We measured HO-1 expression after LPS stimulation and saw a significant decrease in expression of HO-1 gMFI within $CD14^{hi}$ monocytes (paired t-test, p=0.04) (Fig. 5b). Since HO-1 is generally considered to be anti-inflammatory, we hypothesized that induction of HO-1 in $CD14^{hi}$ monocytes after LPS stimulation might positively correlate with the ability of these cells to retain cell surface CD14. To test this hypothesis, the relationship between the change in staining intensities for HO-1 and for CD14 (normalized ΔCD14 gMFI and ΔHO1 gMFI) were determined in $CD14^{hi}$ blood monocytes of healthy donors upon *in vitro* LPS stimulation (Fig. 5c). Multiple regression analysis (covariates included ethnicity, age, and gender) showed an association between the expression of HO-1 and retention of cell surface CD14 in LPS-stimulated $CD14^{hi}$ monocytes. (n=22, r=0.54, β=0.60, p=0.05). Notably, $CD14^{hi}$ monocytes from individuals with very high GT repeat numbers (>60) generally had less induction of HO-1 and greater loss of CD14 when stimulated with LPS (boxed data points, Fig. 5c).

These results suggest that the ability to induce HO-1 in $CD14^{hi}$ monocytes upon exposure to LPS is protective against loss of CD14 from the cell-surface, which itself is a favorable predictor of outcome in HIV disease.

Discussion

Since high levels of immune activation and inflammation predict a more rapid pace of HIV disease progression (7,9,12), host immunoregulatory factors that blunt immune activation and inflammation may contribute to delayed disease progression. Amongst such factors, HO-1 is an important anti-inflammatory enzyme that has been implicated in multiple disorders in the past. In these studies, we have performed an assessment of HO-1 promoter polymorphism genetics, HO-1 expression, and two biomarkers associated with HIV disease outcome in a large cohort of well-characterized HIV-infected and -uninfected adults. Our data show that HO-1 GT_n microsatellite genotypes predict HO-1 expression in primary cells, and that there is a consistent association between HO-1 promoter genotype and HO-1 expression. We also show that greater additive GT_n repeats correlate with higher viral loads and higher levels of the inflammatory sCD14 biomarker in HIV-infected African Americans. Finally, we show that higher levels of HO-1 induction in monocytes correlate with retention of CD14 on the cell surface after LPS stimulation. In light of these data, we speculate that induction of the anti-inflammatory enzyme HO-1 may play a role in limiting the injurious effects of immune activation in chronic HIV disease, e.g., that caused upon microbial translocation and circulation of LPS (10,12). This is in line with evidence that HO-1 induces tolerogenic properties in monocyte-derived antigen presenting cells (15,23). By influencing monocyte maturation and activation, HO-1 may accordingly represent an anti-inflammatory control mechanism for monocyte-mediated inflammation induced by LPS.

It has long been recognized that individuals with HIV have a higher proportion of circulating $CD14^{dim}CD16^{+}$ inflammatory monocytes than do uninfected controls (27-29). Reciprocally, we have observed that initiation of suppressive HAART therapy in chronically

HIV-infected subjects is associated with a decrease in the percentage of circulating $CD14^{dim}CD16^{+}$ inflammatory monocytes and an increase in the percentage of $CD14^{hi}$ 'conventional' monocytes (unpublished data). Shedding of CD14 from the surface of non-inflammatory $CD14^{hi}$ monocytes upon exposure to an activating stimulus (e.g., LPS) may represent an important part of their transition into pro-inflammatory $CD14^{dim}CD16^{+}$ monocytes, and further studies exploring this possibility are underway.

We also demonstrate that higher copy numbers within the HO-1 GT_n repeat promoter polymorphism correlate with higher mean viral load during chronic HIV infection in African American subjects, suggesting that HO-1 activity can modulate viral load. For this analysis, we focused on individuals with high mean viral loads due to the fact that HO-1 expression is not induced to as high an extent in individuals that are able to control viral loads (Figs. 3a and 3b). HO-1 induction may limit bystander immune activation during the acute stage of HIV infection, and thereby reduce the harmful T cell target to T cell effector ratio that leads to heightened viral transmission leading into the chronic stage of infection (6).

Our data show that having fewer GT_n repeats within the microsatellite polymorphism of the HO-1 promoter region is associated with higher levels of HO-1 gene expression in primary immune cells. The alternating purine-pyrimidine repeats within the GT_n microsatellite form a left-handed helical Z-DNA conformation and may affect gene transcription through the inhibition of RNA polymerase-mediated transcription (30). The HO-1 GT_n microsatellite locus is unique in being able to influence gene transcription under multiple cellular stress conditions. Our study shows that additive GT_n repeats influence HO-1 expression upon CoPP, H_2O_2, and LPS stimulation, confirming the findings of a recent study analyzing this polymorphism in primary human endothelial cells of newborns (21). The

central mediator implicated in this pathway is the Nrf2 transcription factor during HO-1 induction with CoPP and H_2O_2 (31,32) and HO-1 down-regulation with LPS stimulation (33).

In this study, we report an association between greater additive GT_n repeats and plasma sCD14 in HAART-suppressed subjects and mean viral load in chronically HIV-infected, untreated African American subjects. Interestingly, this association was not observed in Caucasians, a discrepancy that might be explained by the fact that individuals of African ancestry have a greater average number of HO-1 GT_n repeats within the microsatellite polymorphisms than do other ethnic groups (Suppl. Fig. 1). The prevalence of higher GT_n repeat numbers in individuals with African ancestry may reflect an interplay between HO-1 activity and the various hemolytic conditions that are prevalent in this population (e.g., about 75% of the global incidence of hemoglobinopathy is in sub-Saharan Africa) (34). Indeed, there is evidence showing positive selection for the genomic region specific to African ancestral populations, with this group showing a positive Cross Population Expression Haplotype Homozygosity (XP-EHH) coefficient of 1.8 as opposed to other populations showing negative XP-EHH coefficients (Human Genome Diversity Project: http://hgdp.uchicago.edu/) (Suppl. Fig. 5) (35). To better understand the basis of the association with African American subjects, it will be important to carry out larger cross-population comparisons of the HO-1 genetic locus as well as of up-stream mediators of HO-1 gene induction in the future.

Given the results of this study, pharmacological augmentation of HO-1 may represent a strategy for the treatment of diseases such as HIV, in which unchecked immune activation results in deleterious clinical outcomes. Given the increased burden of HIV disease in African and African American subjects, such a strategy might prove to be particularly useful

in these populations. Our study demonstrates that there are population-specific genetic variations of a GT_n dinucleotide polymorphism involved in the control of HO-1 gene expression in immune cells that have an important role in HIV disease outcome. A recent clinical study reported that the synthetic metalloporphyrin Hematin (Fe^{2+} protoporphyrin IX) (Panhematin ®, Lundbeck Inc.) can induce a 15-fold increase in HO-1 activity (36). Further investigations HO-1 GT_n microsatellite genetic locus may help us better understand the clinical pharmacogenetics of these interventions.

In summary, our data show that the HO-1 GT_n microsatellite promoter polymorphism predicts expression of HO-1 in primary immune cells that play an important role in host interactions with HIV. We show that that greater additive GT_n repeats correlate with higher levels of the inflammatory sCD14 biomarker in African Americans on HAART and of the mean viral load in subjects off therapy. Finally, we show that the genetically-determined level of HO-1 expression in monocytes correlates with the extent of LPS-induced loss of cell-surface CD14 expression within healthy donors. This study highlights the potential role of the HO-1 GT_n genetic locus as a predictive biomarker for disease outcome in HIV-infected subjects on and off antiretroviral therapy.

Materials and Methods

Human subjects

Peripheral blood samples were collected from HIV-infected and -uninfected adults after written informed consent was obtained under protocols approved by the University of California at San Francisco Committee on Human Research (San Francisco, CA). Healthy adults (n=22) were recruited from the San Francisco Bay Area (Table 1). HIV-positive subjects were recruited from the San Francisco Bay Area into the UCSF-based Study of the Consequences of the Protease Inhibitor Era (SCOPE) Cohort, a clinic-based cohort of >1500 adults with chronic HIV infection (Table 2 and Table 3). Participants undergo clinical laboratory monitoring and have their biological specimens banked. HIV controllers are defined as HIV-infected subjects that are off antiretroviral therapy for at least the latest 12 month period for which follow-up is available, with at least three plasma HIV RNA levels taken during this time below 1 000 copies/mL. HIV viral non-controllers are defined as individuals with HIV RNA levels over 10 000 copies RNA/ml (by bDNA, Chiron Diagnostics, Emeryville, USA) or 20 000 copies RNA/mL (by Abbott RealTime HIV-1 PCR, Abbott Park, Illinois, USA) at some point in the past, regardless if during a period of treatment or no treatment.

Measurement of plasma CD14 in HAART-suppressed subjects and mean viral loads in HIV-infected patients off therapy

For sCD14 measurement in HAART-suppressed subjects (Table 3a), a commercially available enzyme-linked immunosorbent assay was used according to the manufacturer's protocol (R&D Systems, Minneapolis, MN). The mean viral loads measured in HIV-infected

patients (Table 3b) were defined as the mean of all viral load determinations known to have been measured in the absence of therapy. All experiments were performed in a blinded manner without prior knowledge of an individual's genotype.

Primary cell isolation and culture conditions

PBMCs were isolated from whole blood drawn into sodium heparin tubes by density centrifugation using Histopaque®-1077 (Sigma Aldrich, Saint Louis, MO), and the MACS® Monocyte Isolation Kit II (Miltenyi, Auburn, CA) was used to enrich $CD14^+$ monocytes from PBMCs (mean 95% purity, as assessed by multiparameter flow cytometry). PBMCs or $CD14^+$ monocytes were cultured in RPMI 1640 (Life Technologies, Rockville, MD) supplemented with 10% FBS (Gemini Bio-Products, Woodland, CA), 1% penicillin/ streptomycin (Mediatech, Washington, DC), and 2 mM L-glutamine (Mediatech) (hereafter referred to as R10 medium) on Upcell™ 96F MicroWell plates (Thermo Scientific, Rochester, NY). Cobalt protoporphyrin IX (CoPP) was purchased in powdered form (Frontier Scientific, Park City, Utah), dissolved in 0.1 mM NaOH, and titrated to a pH of 7.6. Lipopolysaccharides (LPS) from Escherichia coli 055:B5 (Sigma Aldrich) were reconstituted in water to a final stock concentration of 1 mg/mL. 3% (w/w) hydrogen peroxide (H_2O_2) (Sigma Aldrich) was diluted in water for a final stock concentration of 2 mM. PBMCs or $CD14^+$ monocytes were incubated at a final concentration of 25 uM of CoPP, 100 ng/mL LPS, or 100 uM H_2O_2 in RPMI-10 at 37° for 48 hours. Adherent cells were detached from the Upcell™ plates by incubating the plates at 25°C for 20 minutes.

Cell preparation and antibody labeling

All cells were stained with a live/dead marker Amine-Aqua/Am-Cyan Live/Dead (Invitrogen) to exclude dead cells from analysis. The following fluorophore-conjugated monoclonal antibodies (mAbs) were used to detect cell surface markers: CD3-APC-Cy7 (SP34-2, BD Biosciences, Franklin Lakes, NJ), CD14-Qdot605 (Q10013, Invitrogen), and CD16-APC (3G8, Caltag-Invitrogen). The following antibodies were used for detection of intracellular antigens: HO-1 rabbit polyclonal (ab13243, unconjugated, Abcam, Cambridge, MA) and a secondary goat anti-rabbit IgG conjugate (554020, FITC, BD Biosciences). For flow cytometry analysis, cells were washed in staining buffer [PBS with 2% FBS and 2 mM ethylenediamine tetra-acetic acid – EDTA (Sigma)] and then incubated for 30 minutes at 4°C in the presence of directly-conjugated fluorescent mAbs. All cells were stained with a live/dead marker (Amine-Aqua/Am-Cyan Live/Dead; Invitrogen) so that dead cells could be excluded from analysis. The cells were washed in staining buffer, and then fixed and permeabilized in BD Cytofix/Cytoperm (BD Biosciences) according to the manufacturer's protocol for intracellular staining. The cells were incubated for 1 hour at 4°C in the presence of a rabbit polyclonal antibody specific for HO-1 (ab13243, unconjugated, Abcam) and a secondary goat anti-rabbit IgG conjugate (554020, FITC, BD Biosciences). The cells were washed in staining buffer and then fixed in 1% paraformaldehyde (PFA). Data were acquired with an LSR-II flow cytometer (BD Biosciences) and analyzed with FlowJo software (Treestar, Ashland, OR).

DNA isolation and genotyping

DNA was isolated from the cell pellets of both healthy donors and HIV-infected subjects using the DNeasy Blood and Tissue Kit (Qiagen, Valencia, CA), according to the

manufacturer's instructions. HO-1 microsatellite genotyping was performed by the UCSF Genomics Core Facility. Primers were designed with the Primer3 algorithm http://fokker.wi.mit.edu/primer3/input.htm. The primer set was "MS-Primer1" 5'-FAM-CCAGCTTTCTGGAACCTTCTG and "MS-Primer2" 5'-GAAACAAAGTCTGGCCATAGGA. The samples were amplified on a touchdown PCR protocol. The resulting products were run on the 3730xl DNA Analyzer (Applied Biosystems, Foster City, CA) and analyzed with GeneMapper (Applied Biosystems). The TaqMan® SNP Genotyping Assay was used to discriminate the allelic composition for the HO-1 SNPs at positions -1195AG/rs3761439 and -413AT/rs2071746. Unlabeled forward and reverse flanking PCR primers (900 nM final concentration) and two allele-specific probes labeled with either VIC or FAM reporter dye (200 mM final concentration) were added to 20 ng DNA in a 20-ml reaction containing TaqMan Universal PCR Mix. The sequence for the rs2071746 SNP probe was 5'-AGTTCCTGATGTTGCCCACCAGGCT[A/T]TTGCTCTGAGCAGCGCTGCCTCCCA (Assay ID: C__15869717_10, Applied Biosystems, Carlsbad, CA) and for the rs3761439 SNP probe was 5'-CATAGGGAGACCC[T/C]GTCT (Custom assay, Applied Biosystems). Samples were run on the StepOnePlus™ Real-Time PCR system, and the results were analyzed using Step One v2.0 (Applied Biosystems)

Quantitative PCR

For quantitative PCR analysis, cells were harvested and RNA was isolated using TRIzol ® Reagent (Invitrogen, Carlsbad, CA). Total cellular RNA (0.2 μg) was used for cDNA synthesis with Oligo-dT primers and reverse transcriptase from Omniscript (Qiagen).

Relative expression levels of HO-1 mRNA were measured by quantitative RT-PCR using validated Taqman® Gene Expression assay mixes for HO-1 (Assay ID: Hs00157965_m1, Applied Biosystems) and the reference gene, human hypoxanthine-guanine phosphoribosyl transferase (HPRT) (Assay ID: Hs99999909_m1, Applied Biosystems), according to the manufacturer's protocol. The StepOnePlus™ Real-Time PCR system (Applied Biosystems) was used for amplification and detection, and the efficiency corrected calculation ($2^{-\Delta CT}$) of the threshold cycle C(t) was used to measure HO-1 gene expression relative to the HPRT gene.

Transient transfection assay for Dual-glo gene expression assay

Transient co-transfection with the HO-1-luciferase fusion plasmid and the pRL-ef1alpha plasmid (Promega, Madison, WI, USA) was performed using the calcium phosphate method. For transfection, HEK293T cells were split 24 h before transfection and seeded in Dulbecco's Modified Eagle Medium (Gibco/Invitrogen, Carlsbad, CA) supplemented with 10% FBS (Gemini Bio-Products, Woodland, CA), 1% penicillin/ streptomycin (Mediatech, Washington, DC), and 2 mM L-glutamine (Mediatech). The 10x co-transfection mix was made up with 1 ug of HMOX1-pGL4.20 and 0.1 ug of pRL-ef1alpha plasmid DNA in 200 uM $CaCl_2$ in Hepes buffered saline and added dropwise to the wells. Cells were harvested at 48 hours, and the transfection efficiency and cell viability was analyzed by flow cytometric analysis of %GFP+ cells (mean 80% efficiency) Luciferase activity was analyzed using the Dual-Glo ® luciferase reporter assay system (Promega, Madison, WI, USA). Renilla luciferase activity in the lysates was used to normalize the activity of HMOX1 promoter driven firefly luciferase activity on a Spectramax M2 luminometer. (Molecular Devices,

Sunnyvale, CA)

Statistical and genetic analyses

Linkage disequilibrium analysis of the additive GT_n repeats and the SNPs -1195A/G (rs3761439) and -413A/T (rs2071746) was carried out using the "pwld" function (http://www.gene.cimr.cam.ac.uk/clayton). HO-1 GT_n repeat differences between African Americans and Caucasians (Fig. 1b), HO-1 relative qPCR levels before and after each stimulation condition using paired Student's T-test analysis (Fig. 2ab), and HO-1 gMFI levels in $CD14^{hi}$ monocytes before and after each stimulation condition using paired Student's T-test analysis (Fig. 5b) were all performed using GraphPad Prism v5.0d (Graphpad Software, La Jolla, CA, USA). We performed multiple linear regression of healthy donor HO-1 additive GT_n repeats and the HO-1 relative qPCR levels upon different stimulation conditions (Fig. 2c) of HIV-infected subject additive GT_n repeats and the HO-1 relative qPCR levels (Figs. 3a and 3b), for additive GT_n repeats compared to mean viral load and post-HAART soluble CD14, and for comparing the normalized delta CD14 gMFI to normalized delta HO-1 gMFI in $CD14^{hi}$ monocytes (Fig. 5c). For all correlation analyses, the Pearson r correlation and its p values are reported using GraphPad Prism v5.0d (Graphpad Software, La Jolla, CA, USA). For all multiple regression analyses, the regression coefficient β was calculated and adjusted for ethnicity, age, and gender when noted. All regression analyses were undertaken using STATA v11.2 (StataCorp LP, College Station, TX).

Acknowledgements

We would like to thank all participants from the San Francisco General Hospital and San Francisco Veteran Affairs Medical centers. We would like to thank Dr. David Williamson for his help in setting up the HO-1 SNP assay as well as curation of DNA samples. L.S. was supported by a pre-doctoral dissertation California HIV Research Program grant (#D09-SF-313). During the period in which this work was carried out, T.D.B. was a fellow of the Pediatric Scientist Development Program and was supported by the American Pediatric Society, the American Academy of Pediatrics, and the March of Dimes. J.M.M. was supported by NIH Awards U01 AI43641 and R37 AI40312, and is the recipient of the National Institutes of Health Director's Pioneer Award, part of the National Institutes of Health Roadmap for Medical Research, through Grant DPI OD00329. The SCOPE cohort was supported by the Centers for AIDS Research at UCSF (PO AI27763), CFAR Network of Integrated Systems (R24 AI067039), the UCSF CTSI (UL1 RR024131), NIAID (RO1 AI087145, K24AI069994, AI-76174, amfAR, and the Ragon Institute. The authors would also like to thank Christopher R. Gignoux for critical discussion during the preparation of the manuscript.

Conflict of Interest

The authors report no conflict of interest

Supplementary information is available at the Genes and Immunity website

1. Hellerstein M, Hanley MB, Cesar D, Siler S, Papageorgopoulos C, Wieder E, et al. Directly measured kinetics of circulating T lymphocytes in normal and hiv-1-infected humans. Nat Med 1999, Jan;5(1):83-9.

2. Hazenberg MD, Stuart JW, Otto SA, Borleffs JC, Boucher CA, de Boer RJ, et al. T-Cell division in human immunodeficiency virus (HIV)-1 infection is mainly due to immune activation: A longitudinal analysis in patients before and during highly active antiretroviral therapy (HAART). Blood 2000, Jan 1;95(1):249-55.

3. Kinoshita S, Su L, Amano M, Timmerman LA, Kaneshima H, Nolan GP. The T cell activation factor nf-atc positively regulates HIV-1 replication and gene expression in T cells. Immunity 1997;6(3):235-44.

4. Matsuyama T, Kobayashi N, Yamamoto N. Cytokines and HIV infection: Is AIDS a tumor necrosis factor disease? AIDS 1991;5(12):1405.

5. Poli G, FAUCI AS. The effect of cytokines and pharmacologic agents on chronic HIV infection. AIDS Res Hum Retroviruses 1992;8(2):191-7.

6. Haase AT. Early events in sexual transmission of HIV and SIV and opportunities for interventions. Annu Rev Med 2010, Jan 27.

7. Deeks SG, Kitchen CM, Liu L, Guo H, Gascon R, Narváez AB, et al. Immune activation set point during early HIV infection predicts subsequent CD4+ t-cell changes independent of viral load. Blood 2004, Aug 15;104(4):942-7.

8. Hunt PW, Martin JN, Sinclair E, Bredt B, Hagos E, Lampiris H, Deeks SG. T cell activation is associated with lower CD4+ T cell gains in human immunodeficiency virus-infected patients with sustained viral suppression during antiretroviral therapy. J Infect Dis 2003, May 15;187(10):1534-43.

9. Giorgi JV, Hultin LE, McKeating JA, Johnson TD, Owens B, Jacobson LP, et al. Shorter survival in advanced human immunodeficiency virus type 1 infection is more closely associated with T lymphocyte activation than with plasma virus burden or virus chemokine coreceptor usage. J Infect Dis 1999;179:859-70.

10. Brenchley JM, Price DA, Schacker TW, Asher TE, Silvestri G, Rao S, et al. Microbial translocation is a cause of systemic immune activation in chronic HIV infection. Nat Med 2006, Dec;12(12):1365-71.

11. Baroncelli S, Galluzzo CM, Pirillo MF, Mancini MG, Weimer LE, Andreotti M, et al. Microbial translocation is associated with residual viral replication in haart-treated HIV+ subjects with <50copies/ml HIV-1 RNA. J Clin Virol 2009, Dec;46(4):367-70.

12. Sandler NG, Wand H, Roque A, Law M, Nason MC, Nixon DE, et al. Plasma levels of soluble CD14 independently predict mortality in HIV infection. J Infect Dis 2011, Jan 20.

13. Cassol E, Malfeld S, Mahasha P, van der Merwe S, Cassol S, Seebregts C, et al. Persistent microbial translocation and immune activation in hiv-1-infected south africans receiving combination antiretroviral therapy. J Infect Dis 2010, Sep 1;202(5):723-33.

14. Ryter SW, Alam J, Choi AM. Heme oxygenase-1/carbon monoxide: From basic science to therapeutic applications. Physiol Rev 2006, Apr;86(2):583-650.

15. Burt TD, Seu L, Mold JE, Kappas A, McCune JM. Naive human T cells are activated and proliferate in response to the heme oxygenase-1 inhibitor tin mesoporphyrin. J Immunol 2010, Nov 1;185(9):5279-88.

16. Exner M, Minar E, Wagner O, Schillinger M. The role of heme oxygenase-1 promoter polymorphisms in human disease. Free Radic Biol Med 2004, Oct 15;37(8):1097-104.

17. Yamada N, Yamaya M, Okinaga S, Nakayama K, Sekizawa K, Shibahara S, Sasaki H. Microsatellite polymorphism in the heme oxygenase-1 gene promoter is associated with susceptibility to emphysema. Am J Hum Genet 2000, Jan;66(1):187-95.

18. Chen YH, Lin SJ, Lin MW, Tsai HL, Kuo SS, Chen JW, et al. Microsatellite polymorphism in promoter of heme oxygenase-1 gene is associated with susceptibility to coronary artery disease in type 2 diabetic patients. Hum Genet 2002, Jul;111(1):1-8.

19. Ono K, Mannami T, Iwai N. Association of a promoter variant of the haeme oxygenase-1 gene with hypertension in women. J Hypertens 2003, Aug;21(8):1497-503.

20. Hirai H, Kubo H, Yamaya M, Nakayama K, Numasaki M, Kobayashi S, et al. Microsatellite polymorphism in heme oxygenase-1 gene promoter is associated with susceptibility to oxidant-induced apoptosis in lymphoblastoid cell lines. Blood 2003, Sep 1;102(5):1619-21.

21. Taha H, Skrzypek K, Guevara I, Nigisch A, Mustafa S, Grochot-Przeczek A, et al. Role of heme oxygenase-1 in human endothelial cells: Lesson from the promoter allelic variants. Arterioscler Thromb Vasc Biol 2010, Aug;30(8):1634-41.

22. He Z, Hu Y, Feng L, Lu Y, Bao D, Xi Y, et al. Association between HMOX-1 genotype and cardiac function during exercise. Appl Physiol Nutr Metab 2008, Jun;33(3):450-60.

23. Chauveau C, Rémy S, Royer PJ, Hill M, Tanguy-Royer S, Hubert FX, et al. Heme oxygenase-1 expression inhibits dendritic cell maturation and proinflammatory function but conserves IL-10 expression. Blood 2005, Sep 1;106(5):1694-702.

24. Levere RD, Staudinger R, Loewy G, Kappas A, Shibahara S, Abraham NG. Elevated levels of heme oxygenase-1 activity and mrna in peripheral blood adherent cells of acquired immunodeficiency syndrome patients. Am J Hematol 1993, May;43(1):19-23.

25. Hiki N, Berger D, Prigl C, Boelke E, Wiedeck H, Seidelmann M, et al. Endotoxin binding and elimination by monocytes: Secretion of soluble CD14 represents an inducible mechanism counteracting reduced expression of membrane CD14 in patients with sepsis and in a patient with paroxysmal nocturnal hemoglobinuria. Infect Immun 1998, Mar;66(3):1135-41.

26. Bazil V, Strominger JL. Shedding as a mechanism of down-modulation of CD14 on stimulated human monocytes. J Immunol 1991, Sep 1;147(5):1567-74.

27. Locher C, Vanham G, Kestens L, Kruger M, Ceuppens JL, Vingerhoets J, Gigase P. Expression patterns of fc gamma receptors, HLA-DR and selected adhesion molecules on monocytes from normal and hiv-infected individuals. Clin Exp Immunol 1994, Oct;98(1):115-

28. Thieblemont N, Weiss L, Sadeghi HM, Estcourt C, Haeffner-Cavaillon N. Cd14Lowcd16High: A cytokine-producing monocyte subset which expands during human immunodeficiency virus infection. Eur J Immunol 1995, Dec;25(12):3418-24.

29. Pulliam L, Gascon R, Stubblebine M, McGuire D, McGrath MS. Unique monocyte subset in patients with AIDS dementia. Lancet 1997, Mar 8;349(9053):692-5.

30. Herbert A, Rich A. The biology of left-handed Z-DNA. J Biol Chem 1996;271(20):11595.

31. Ashino T, Yamanaka R, Yamamoto M, Shimokawa H, Sekikawa K, Iwakura Y, et al. Negative feedback regulation of lipopolysaccharide-induced inducible nitric oxide synthase gene expression by heme oxygenase-1 induction in macrophages. Mol Immunol 2008, Apr;45(7):2106-15.

32. Brunt KR, Fenrich KK, Kiani G, Tse MY, Pang SC, Ward CA, Melo LG. Protection of human vascular smooth muscle cells from h2o2-induced apoptosis through functional codependence between HO-1 and AKT. Arterioscler Thromb Vasc Biol 2006, Sep;26(9):2027-

33. Miyazaki T, Kirino Y, Takeno M, Samukawa S, Hama M, Tanaka M, et al. Expression of heme oxygenase-1 in human leukemic cells and its regulation by transcriptional repressor bach1. Cancer Sci 2010, Jun;101(6):1409-16.

34. Weatherall DJ, Clegg JB. Inherited haemoglobin disorders: An increasing global health problem. Bull World Health Organ 2001;79(8):704-12.

35. Sabeti PC, Varilly P, Fry B, Lohmueller J, Hostetter E, Cotsapas C, et al. Genome-Wide detection and characterization of positive selection in human populations. Nature 2007, Oct 18;449(7164):913-8.

36. Bharucha AE, Kulkarni A, Choi KM, Camilleri M, Lempke M, Brunn GJ, et al. First-In-Human study demonstrating pharmacological activation of heme oxygenase-1 in humans. Clin Pharmacol Ther 2010, Feb;87(2):187-90.

Table 1. Healthy donors	
Characteristics	Healthy donors for HO-1 phenotyping studies (n=22)
Age (median ± IQR)	33 ± 13
Gender (% Male)	45.4%
Ethnicity	
Caucasian	77.3%
African	4.5%
Asian	18.2%

Table 2a. Demographic and clinical characteristics of HIV-infected subjects off HAART		
Characteristics (median ± IQR)	Viral controllers (n=30)	Viral non-controllers (n=34)
Age	45 ± 9	44 ± 8
Gender (% male)	68.0%	91.2%
Plasma viral load (copies/mL)	75 ± 98	84 142 ± 112 100
CD4 (cells/uL)	745 ± 433	317 ± 264
Ethnicity (%African American)	40%	29.4%
HLA-DR+CD38+% of CD4+ T cells	3.12 ± 1.5	11 ± 11.4
HLA-DR+CD38+% of CD8+ T cells	8.4 ± 10.8	23.5 ± 11.4

Table 2b. Demographic and clinical characteristics of HIV-infected subjects on HAART	
Characteristics (median ± IQR)	HAART patients (n=25)
Age	45 ± 7
Gender (% male)	84.0%
Months on HAART	20.1 ± 6.7
Plasma viral load (copies/mL)	75 ± 25
CD4 (cells/uL)	300 ± 151
Ethnicity (% African American)	24.0%
HLA-DR+CD38+% of CD4+ T cells	9.7 ± 7.7
HLA-DR+CD38+% of CD8+ T cells	41.2 ± 26.4

Table 3a. Demographic and clinical characteristics of HIV-infected HAART suppressed subjects		
Characteristics (median ± IQR)	African American (n=50)	Caucasian (n=123)
Age	44.0 ± 8.8	43.8 ± 10.0
Gender (% male)	62.0%	88.6%
Soluble CD14 (median ± IQR)	260 ± 72	249 ± 66
Months on HAART	21.2 ± 27.0	23.0 ± 32.8
Pre-HAART VL (copies/mL)	29 809 ± 64 571	64 649 ± 149 040
Post-HAART VL (copies/mL)	75 ± 28	75 ± 25
Pre-CD4 T cell count (cells/uL)	162 ± 182	192 ± 242
Post-CD4 T cell count (cells/uL)	310.5 ± 398	430 ± 374

Table 3b. Demographic and clinical characteristics of HIV-infected subjects off therapy		
Characteristics (median ± IQR)	African American (n=74)	Caucasian (n=177)
Age	32.2 ± 9.0	46.8 ± 11.3
Gender (% male)	60.0%	89.8%
Mean VL (copies/mL)	63 935 ± 511 768	87 485 ± 161 380
CD4 T cell count (cells/uL)	330 ± 401.5	448 ± 344

Figure legends

Figure 1. Heme oxygenase-1 (HO-1) promoter description and variation across HIV-infected subjects of different ethnicities. (a) HO-1 promoter region (-1876 to +75) encompassing subcloning region, GT_n repeat, sequencing primers, and transcription start site (TSS) at position +1. The GT_n dinucleotide repeat is shown in the boxed area (extending from 260 base pairs to 200 base pairs upstream of the TSS) and two common SNPs (-413AT/ rs2071746 and -1195AG/ rs3761439) are shown. Two common insertion deletion variations (dbSNP ID rs72441698 and rs58433947) with GT_7 repeats are shown in bold font within the GT_n repeat. Microsatellite sequencing primers for capillary electrophoresis are denoted by "MS-Primer1" and "MS-Primer2." Subcloning primers for the promoter-reporter gene expression assay are denoted by "S-primer1" and "S-primer2." **(b)** GT_n allele frequencies within HIV-infected patients reported as (mean ± s.e.m.): African Americans (31.5 ± 0.27, n=205) and Caucasians (28.1 ± 0.13, n=396) (difference in mean length between ethnic groups, $p<0.0001$, Student's unpaired T-test). Boxes I, II, and III represent the distribution of the additive GT_n repeats with peaks at GT_{23}, GT_{30}, and GT_{37}. **(c)** The GT_n microsatellite repeats that are most represented in all populations (n=23 and 30) are not in linkage disequilibrium (LD) with -413AT/rs2071746 and -1195AG/rs3761439 in either Caucasians (n=396) or African Americans (n=205). The top two heat maps represent the pair-wise LD results for African American patients with GT_{23} (left) and GT_{30} (right), with the values in the legend corresponding to the r^2 values for each pair-wise comparison between the SNPs -413AT/ rs2071746, -1195AG/rs3761439, and the GT_n microsatellite repeat. The bottom two heat maps represent the same for Caucasian patients.

Figure 2. Heme oxygenase-1 additive GT_n repeats negatively correlate with relative gene expression in PBMCs and $CD14^+$ monocytes from healthy donors. Cells from healthy donors (n=20) were stimulated with CoPP (25 μM), H_2O_2 (100 uM), or LPS (100 ng/mL), and then harvested 48 hours later for HO-1 transcript analysis. Paired T-test analyses yield statistically significant increases in HO-1 relative transcript abundance normalized to HPRT in **(a)** PBMCs and **(b)** $CD14^+$ monocytes upon stimulation with CoPP or H_2O_2 and decreases upon stimulation with LPS. **(c)** PBMCs from healthy donors were stimulated with CoPP (25 uM), H_2O_2 (100 uM) or LPS (100 ng/mL) and genotyped for their HO-1 GT_n repeat polymorphism. Multiple regression and correlation analyses with ethnicity as a covariate showed a significant decline in normalized HO-1 transcript levels within LPS-stimulated cells as the additive GT_n repeats increased ($r= -0.38$, $\beta= -0.024$, $p=0.05$), and trends in PBMCs stimulated with CoPP ($r= -0.30$, $\beta= -0.98$, $p=0.06$) and H_2O_2 ($r= -0.36$, $\beta= -0.076$, $p=0.08$). The solid line represents a fitted linear regression line and dashed lines represent the 95% confidence interval band.

Figure 3. Heme oxygenase-1 additive GT_n repeats negatively correlate with gene expression in PBMCs and $CD14^+$ monocytes from HIV-infected subjects. PBMCs from HIV-infected subjects were analyzed for HO-1 transcript analysis. **(a)** Total mRNA was harvested from thawed PBMCs of HIV viral non-controllers and multiple regression analysis with ethnicity as a covariate yields a significant decline in normalized HO-1 transcript levels as the additive GT_n repeats increase ($n=34$, $r= -0.41$, $\beta= -3.08$, $p=0.02$). Total mRNA was harvested from thawed PBMCs of HIV viral controllers and multiple regression analysis with

ethnicity as a covariate does not lead to a significant decline in normalized HO-1 transcript levels as the additive GT_n repeats increase (n=30, r=0.03, β= -0.36, p=0.4). **(b)** Thawed PBMCs from HAART-suppressed subjects were analyzed by multiparameter flow cytometry for HO-1 expression within $CD14^+$ monocytes. Multiple regression analysis with ethnicity as a covariate yields a significant decline in normalized HO-1 gMFI as the additive GT_n repeats increase within $CD14^+$ monocytes (n=25, r= -0.36, β= -30.45, p=0.04). The solid line represents a fitted linear regression line and dashed lines represent the 95% confidence interval band.

Figure 4. Increased levels of soluble CD14 during HAART and mean viral load are detected in African American HIV-infected subjects with higher HO-1 additive GT_n repeats. Two important clinical parameters associated with accelerated HIV disease (high levels of circulating soluble CD14 and a mean viral load) were measured. **(a)** Plasma soluble CD14 levels were measured by ELISA in African American and Caucasian HAART-suppressed HIV-infected subjects. Greater HO-1 additive GT_n repeats correlated with higher levels of sCD14 in African American (n=50, r= 0.38, β= 2.3, p=0.007) but not Caucasian HIV-infected HAART subjects (n=123, r= 0.0016, β=0.80, p=1.0); this correlation remained after adjusting for gender as a covariate. **(b)** Mean viral loads were measured in African American and Caucasian subjects and in the chronic stage of infection before they were placed on HAART. Greater HO-1 additive GT_n repeats correlated with higher mean viral loads in African American but not Caucasian HIV-infected HAART subjects (n=74, r=0.24, β= 3 805.13, p=0.04), and stayed significantly associated after adjusting for gender as a covariate. The mean viral load level in the absence of therapy was not statistically associated

with the additive GT_n repeat numbers in Caucasian HIV subjects (n=177, r= -0.02, β=3 119.26, p=0.2). Mean viral loads are shown in logarithmic base 10 scale. The solid line represents a fitted linear regression line, and dashed lines represent the 95% confidence interval band.

Figure 5. A higher level of HO-1 expression in primary human $CD14^{hi}$ monocytes correlates with decreased loss of cell-surface CD14 after LPS stimulation. (a) Fresh PBMCs from healthy donors were stimulated with either 25 uM CoPP or PBS for 48 hours. Analysis was performed by sequentially gating on live cells, singlets (FSC-A/FSC-H), non-lymphocyte (SSC-A high/FSC-A high), and $CD3^-$ populations. Monocyte populations were further gated on CD14 and CD16. HO-1 was induced to a greater extent within $CD14^{hi}$ monocytes upon stimulation with 25uM CoPP as compared to $CD14^{dim}CD16^{pos}$ monocytes (55 226 3 ± 916.9 vs. 13 448 ± 2 458.4 in gMFI; unpaired Student's T-test $p<1x10^{-8}$). Histograms are shown depicting the intensity of HO-1 staining in CD3+ T cells, $CD14^{dim}CD16^+$ monocytes, or $CD14^{hi}$ monocytes (25 uM CoPP or PBS) as well as with the secondary antibody (goat anti-rabbit-FITC). **(b)** PBMCs were stimulated with either LPS (100 ng/mL) or PBS for 48 hours. HO-1 gMFI within $CD14^{hi}$ monocytes is reduced upon LPS stimulation (5 068 ± 256.5 vs. 4 481 ± 196.2 gMFI, p=0.04) paired Student's T-test). **(c)** Multiple linear regression with ethnicity, age, and gender as covariates showed that normalized delta HO-1 gMFI in $CD14^{hi}$ monocytes correlates with the normalized delta CD14 gMFI upon LPS stimulation (n=22, r=0.54, β=0.60, p=0.05). The solid line represents a fitted linear regression line and dashed lines represent the 95% confidence interval band. Boxed data points refer to individuals with $GT_{>60}$ repeats.

1a

```
-1920   CAGGAAAGATCAACCACTGG AGAGAGAAAGAGACTGGGAG TCATCACCAGACCCAGACAG
                                                                S-primer1
-1860   ATTTACCTGTTCTTCTGAGG ACAGTGCCAAGAGATTACCT GGGGGACTTTATCTGCCTAG
   /                                                                 /
   /                                                                 /
-1200   GAGACRGGGTCTCCCTATGT TGCCCAGGCCAGTCTCGAAC TCAAAGCAATCTTCCCACCT
        -1195AG/rs3761439
-1140   CGACTGGGCTCAAAGCGCTC TTCCCACCTCAACCTCCCAA AGTACTGGGACTACAGGTGT
   /                                                                 /
   /                                                                 /
 -480   GACATTTTAGGGAGCTGCAG ACAGCAGAGCCTGGGGTTGC TAAGTTCCTGATGTTGCCCA

 -420   CCAGGCTWTTGCTCTGAGCA GCGCTGCCTCCCAGCTTTCT GGAACCTTCTGGGACGCCTG
              -413AT/rs2071746                    MS-Primer1
 -360   GGGTGCATCAAGTCCCAAGG GGACACGGAGCAGAAGGGGG GGCTCTGGAAGGAGCAAAAT

 -300   CACACCCAGAGCCTGCAGCT TCTCAGATTTCCTTAAAGGT TTTGTGTGTGTGTGTGTGTG
                                                   rs72441698
 -240   TGTGTGTGTGTGTATGTGTG TGTGTGTGTGTGTGTGTGTG TGTTTTCTCTAAAAGTCCTA
                             rs58433947
 -180   TGGCCAGACTTTGTTTCCCA AGGGTCATATGACTGCTCCT CTCCACCCCACACTGGCCCG
        MS-Primer2
 -120   GGGCGGGCTGGGCGCGGGCC CCTGCGGGTGTTGCAACGCC CGGCCAGAAAGTGGGCATCA

  -60   GCTGTTCCGCCTGGCCCACG TGACCCGCCGAGCATAAATG TGACCGGCCGCGGCTCCGGC

   +1   AGTCAACGCCTGCCTCCTCT CGAGCGTCCTCAGCGCAGCC GCCGCCCGCGGAGCCAGCAC
                                                                S-primer2
  +61   GAACGAGCCCAGCACCGGCC GGATGGAGCGTCCGCAACCC GACAGGCAAGCGCGGGGCGC
```

1b

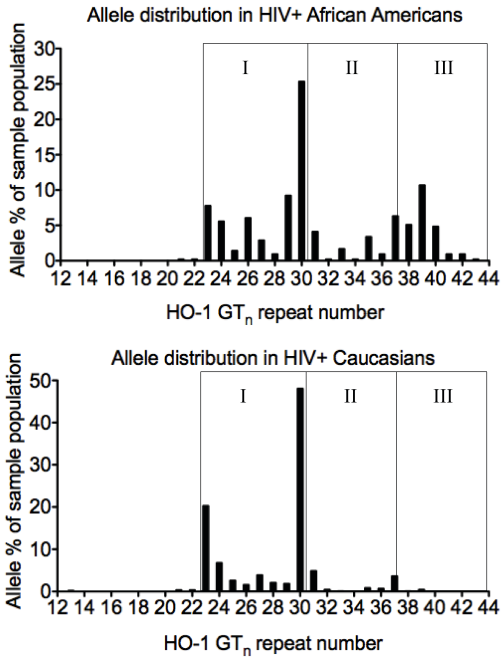

1c

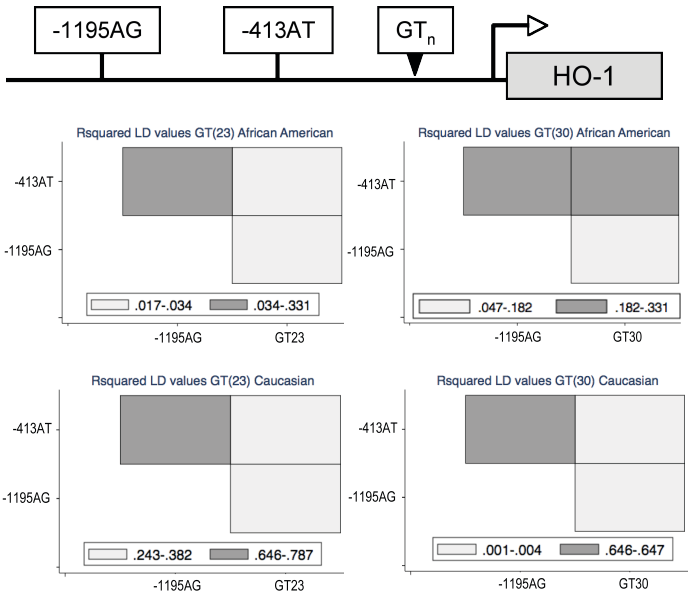

2a

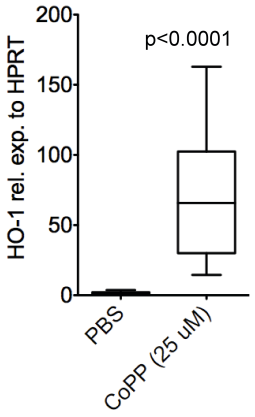
HO-1 rel. exp. to HPRT
200
150
100
50
0
p<0.0001
PBS
CoPP (25 uM)

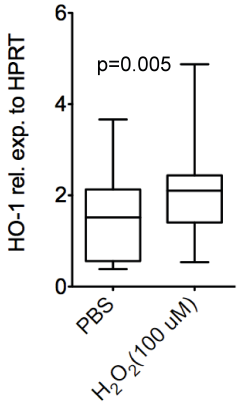
HO-1 rel. exp. to HPRT
6
4
2
0
p=0.005
PBS
H2O2(100 uM)

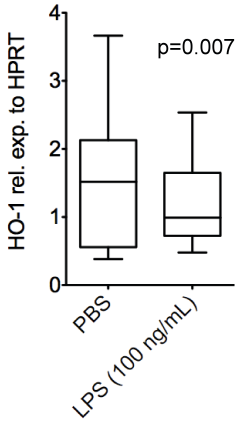
HO-1 rel. exp. to HPRT
4
3
2
1
0
p=0.007
PBS
LPS (100 ng/mL)

2b

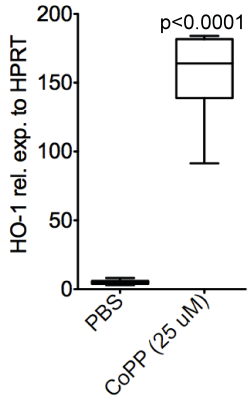
HO-1 rel. exp. to HPRT
200
150
100
50
0
p<0.0001
PBS
CoPP (25 uM)

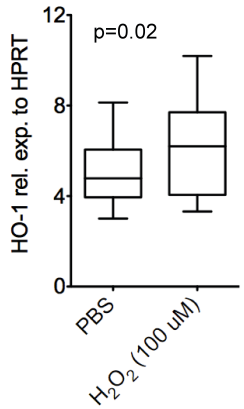
HO-1 rel. exp. to HPRT
12
8
4
0
p=0.02
PBS
H2O2 (100 uM)

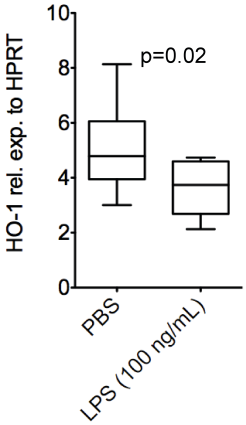
HO-1 rel. exp. to HPRT
10
8
6
4
2
0
p=0.02
PBS
LPS (100 ng/mL)

2c

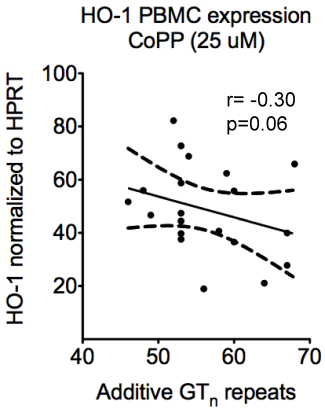
HO-1 PBMC expression
CoPP (25 uM)
HO-1 normalized to HPRT
100
80
60
40
20
r= -0.30
p=0.06
40
50
60
70
Additive GTn repeats

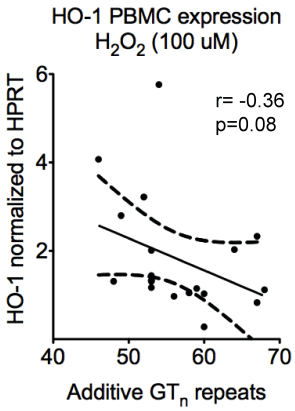
HO-1 PBMC expression
H2O2 (100 uM)
HO-1 normalized to HPRT
6
4
2
r= -0.36
p=0.08
40
50
60
70
Additive GTn repeats

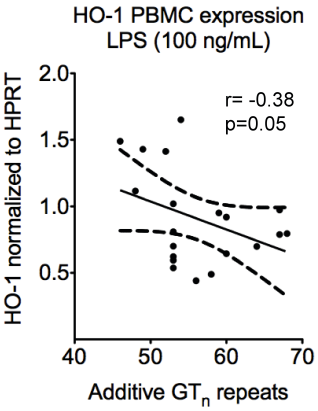
HO-1 PBMC expression
LPS (100 ng/mL)
HO-1 normalized to HPRT
2.0
1.5
1.0
0.5
r= -0.38
p=0.05
40
50
60
70
Additive GTn repeats

3a

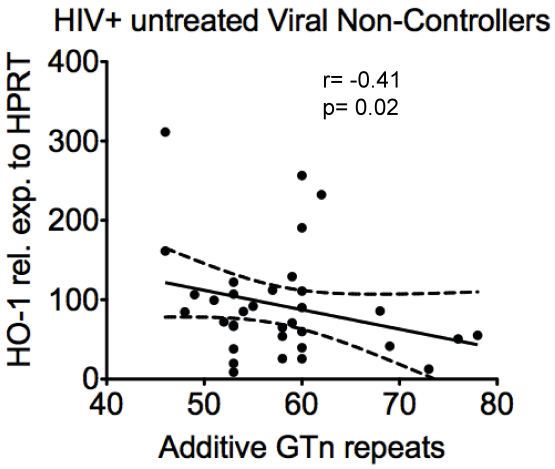
HIV+ untreated Viral Non-Controllers
HO-1 rel. exp. to HPRT
400
300
200
100
0
r= -0.41
p= 0.02
40
50
60
70
80
Additive GTn repeats

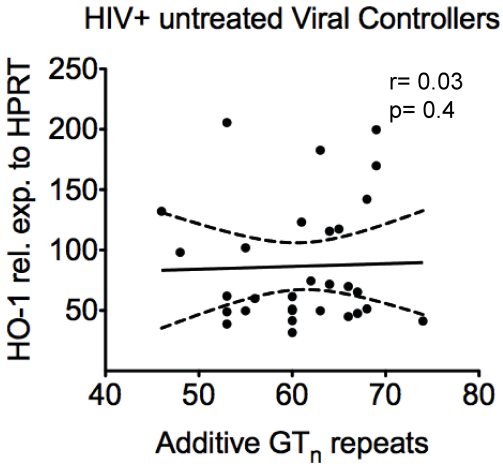
HIV+ untreated Viral Controllers
HO-1 rel. exp. to HPRT
250
200
150
100
50
r= 0.03
p= 0.4
40
50
60
70
80
Additive GTn repeats

3b

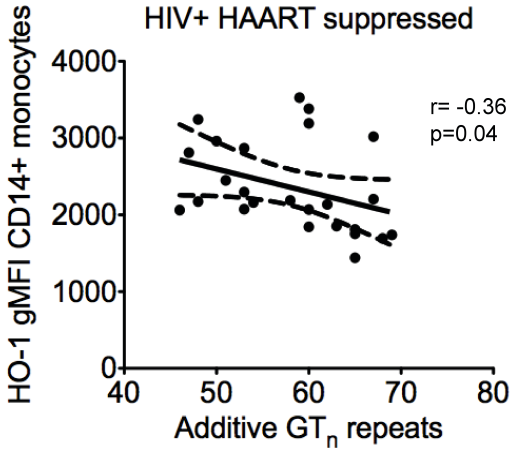
HIV+ HAART suppressed
HO-1 gMFI CD14+ monocytes
4000
3000
2000
1000
0
r= -0.36
p=0.04
40
50
60
70
80
Additive GTn repeats

4a

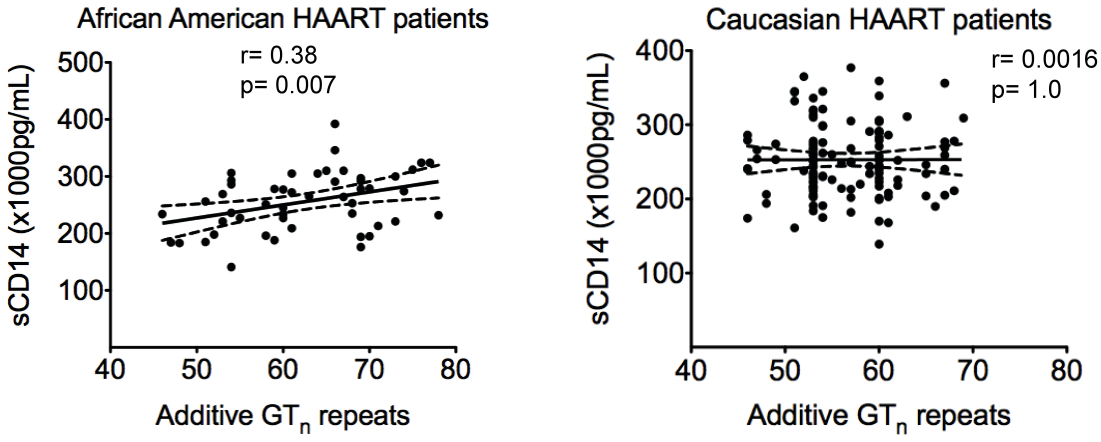
African American HAART patients
r= 0.38
p= 0.007
sCD14 (x1000pg/mL)
500
400
300
200
100
40
50
60
70
80
Additive GTn repeats
Caucasian HAART patients
r= 0.0016
p= 1.0
sCD14 (x1000pg/mL)
400
300
200
100
40
50
60
70
80
Additive GTn repeats

4b

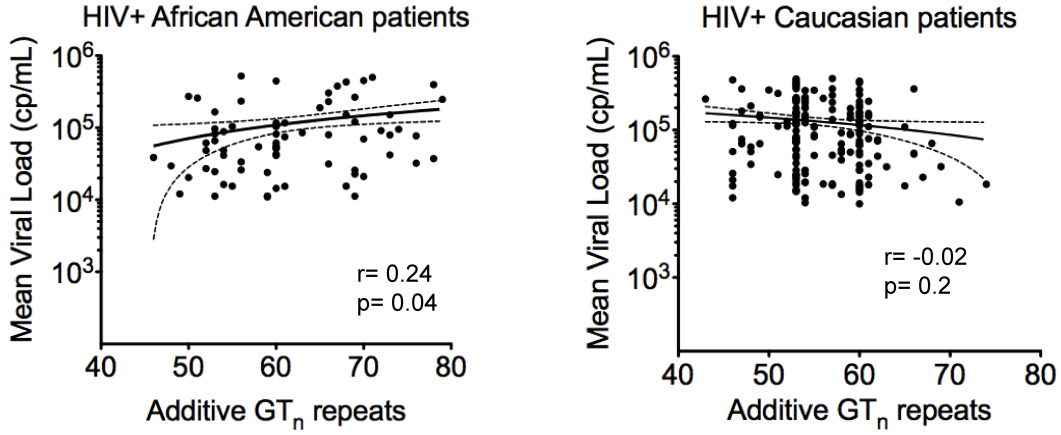
HIV+ African American patients
Mean Viral Load (cp/mL)
10^6
10^5
10^4
10^3
r= 0.24
p= 0.04
40
50
60
70
80
Additive GTn repeats
HIV+ Caucasian patients
Mean Viral Load (cp/mL)
10^6
10^5
10^4
10^3
r= -0.02
p= 0.2
40
50
60
70
80
Additive GTn repeats

5a

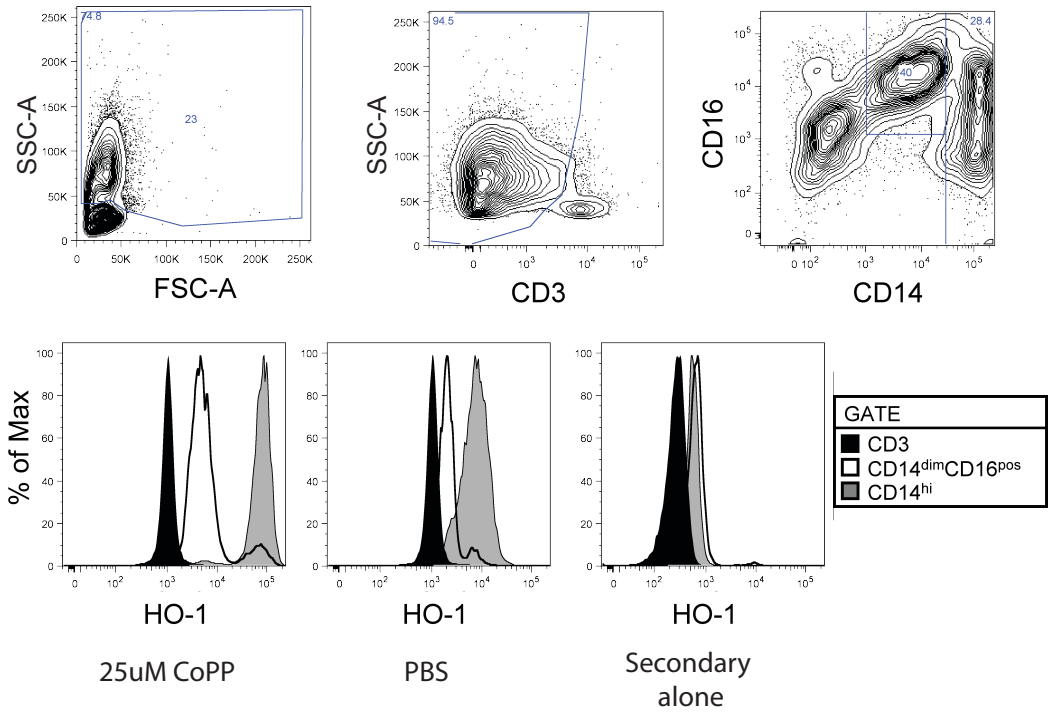
74.8
23
SSC-A
FSC-A
94.5
SSC-A
CD3
28.4
40
CD16
CD14
% of Max
HO-1
HO-1
HO-1
GATE
CD3
CD14dimCD16pos
CD14hi
25uM CoPP
PBS
Secondary alone

5b

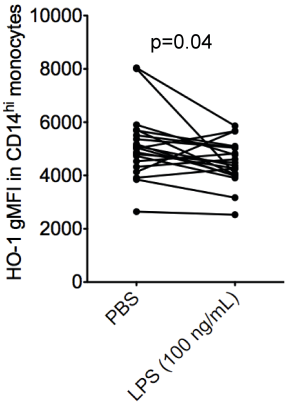
p=0.04
HO-1 gMFI in CD14hi monocytes
PBS
LPS (100 ng/mL)

5c

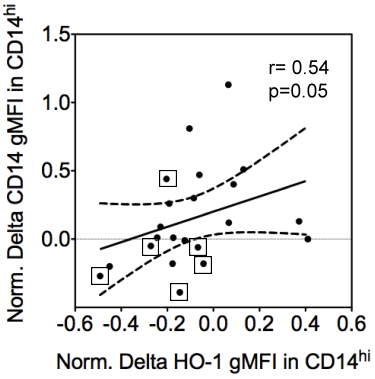
r= 0.54
p=0.05
Norm. Delta CD14 gMFI in CD14hi
Norm. Delta HO-1 gMFI in CD14hi

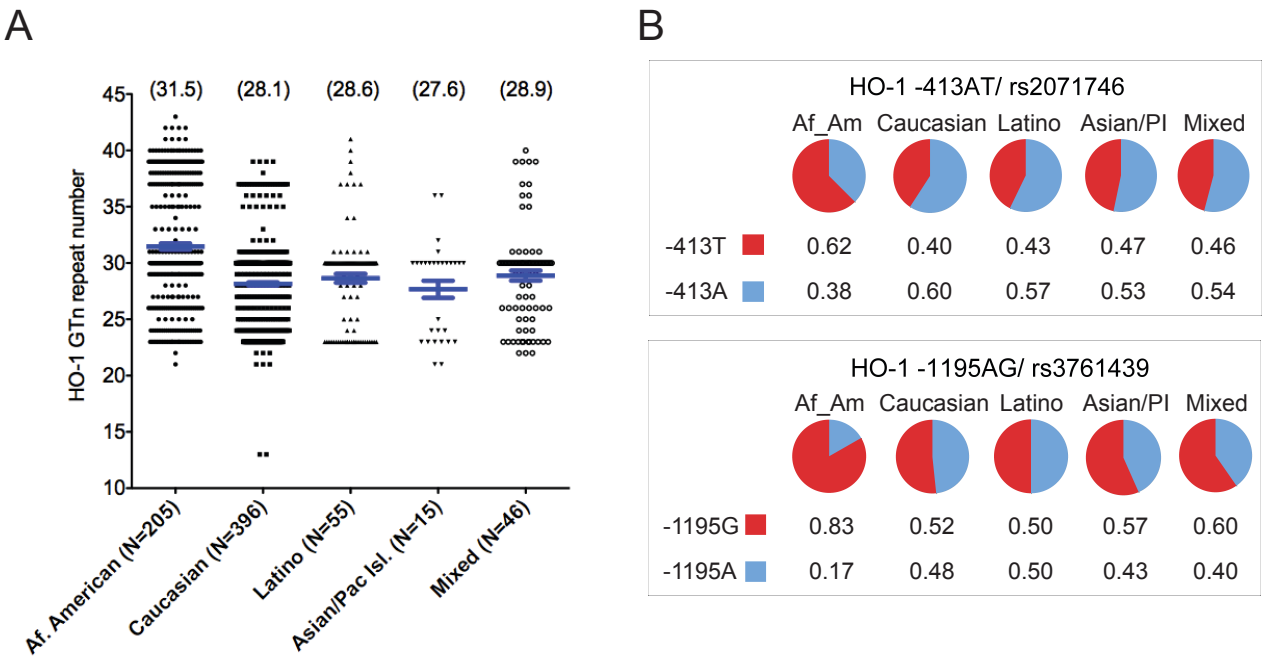

Suppl. Fig 1. HO-1 polymorphisms variations amongst HIV patients from the San Francisco Bay Area
(A) HO-1 GTn microsatellites and **(B)** two common SNPs (-413AT/rs2071746 and -1195AG/rs3761439). Numbers in parentheses in **(A)** represent the group mean ± s.e.m. GTn repeats. SNP allele frequencies are represented in the pie charts of **(B)**.

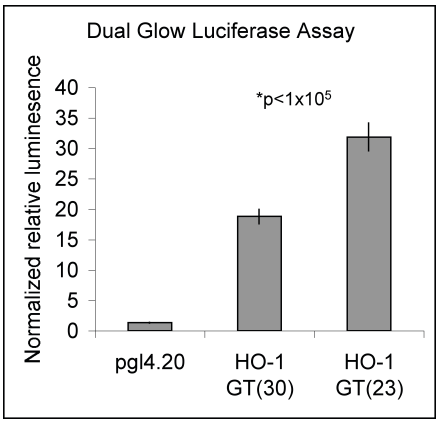

Suppl. Fig. 2. Differential expression from long (GT=30) and short (GT=23) HO-1 promoters. Hek293T cells were transfected with the promoter-reporter plasmid and harvested 48 hours later. The GT30 construct had lower normalized light units compared to the GT23 construct (18.8 vs 31.8, respectively; Student's unpaired two-tailed T-test p<1x10-5)

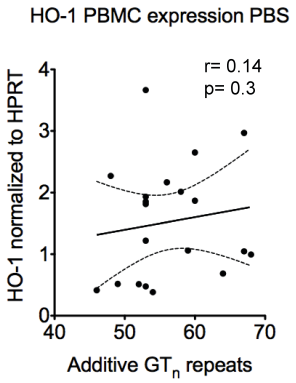

Suppl. Fig. 3. HO-1 additive GTn repeats and relative gene expression in unstimulated PBMCs
PBMCs from healthy donors (n=20) were cultured with phosphate buffered saline, and then harvested 48 hours later for HO-1 transcript analysis alongside the other stimulation conditions. Multiple regression and correlation analyses with showed no significant association in normalized HO-1 transcript levels as additive GTn repeats increased (r= 0.14, β= 0.002, p=0.3).

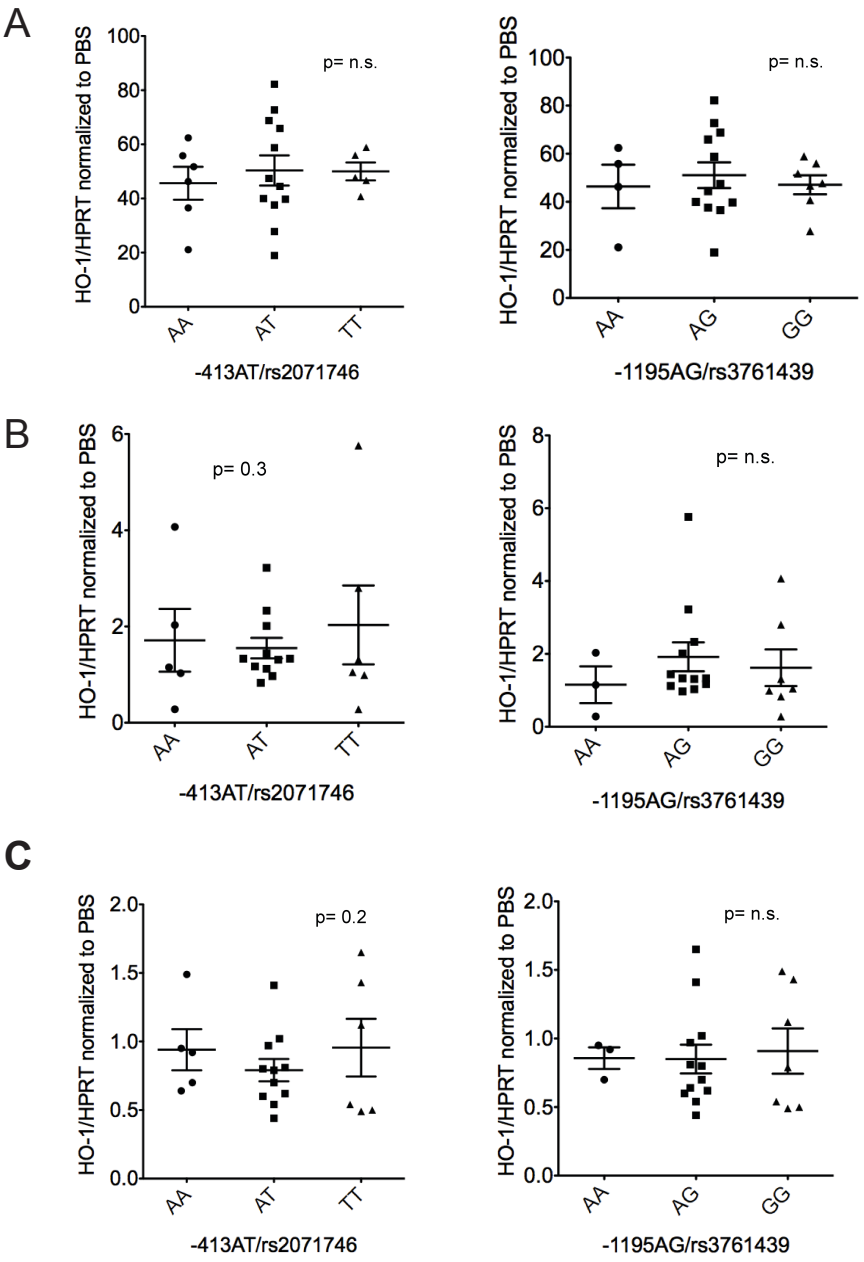

Suppl. Fig. 4. HO-1 promoter SNPs -413AT/rs2071746 and -1195AG/rs3761439 analysis
Healthy donors were genotyped (n=20) and their PBMCs were stimulated in vitro for 48 hours at 37ºC with **(A)** cobalt protoporphyrin IX, **(B)** hydrogen peroxide, or **(C)** lipopolysaccharide, and then analyzed for relative HO-1 transcript levels. Error bars represent mean ± s.e.m.

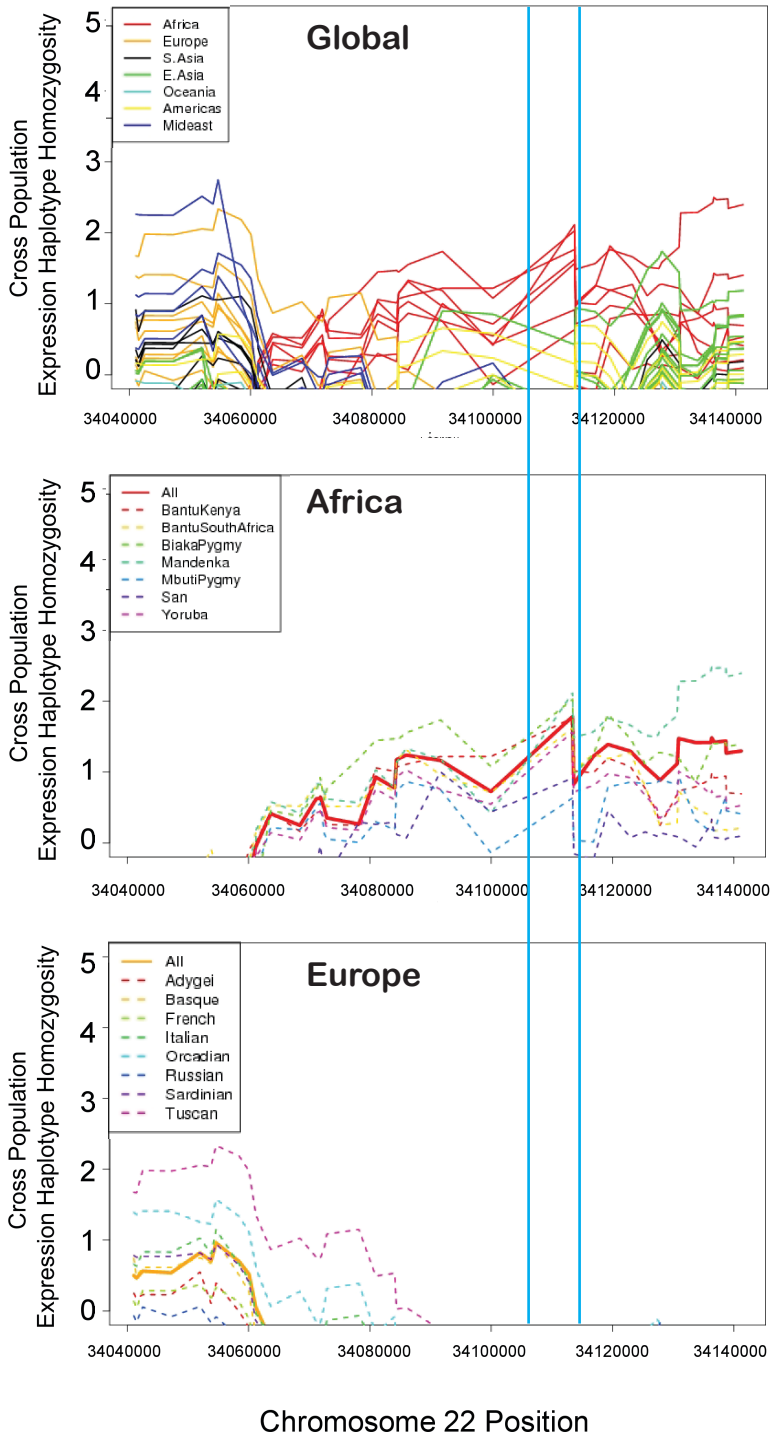

Suppl. Fig. 5. Positive selection in the HO-1 genomic region in African ancestral groups.
The area bounded by the two lines represents the general HO-1 genetic locus of all global, African, and European ancestral populations. African ancestral groups have a positive XP-EHH value of 1.8. Images from the Human Genome Diversity Project Selection Browser: http://hgdp.uchicago.edu/.

III

Circulating myeloid subpopulations differentially predict CD4 recovery in patients during early HAART

San Francisco Pride Parade 2011: Positive Health Program Banner (Lineup #134)

Circulating myeloid subpopulations differentially predict CD4 reconstitution in patients during early HAART

Lillian Seu[1, 2,]a, Gabriel M. Ortiz[2,3,]a, Trevor D. Burt[2,4], Yong Huang[1], Steven G. Deeks[5], Jeffrey N. Martin[5,6], Joseph M. McCune[2*]

[1]Department of Bioengineering and Therapeutic Sciences, University of California, San Francisco, CA 94110, USA

[2]Division of Experimental Medicine, Department of Medicine, University of California, San Francisco, CA 94110, USA

[3]Division of Infectious Diseases, Department of Medicine, University of California, San Francisco, CA 94143, USA

[4]Division of Neonatology, Department of Pediatrics, University of California, San Francisco, CA 94143

[5]Positive Health Program, Department of Medicine, University of California, San Francisco, CA 94110, USA

[6]Department of Epidemiology and Biostatistics, University of California, San Francisco, CA 94110, USA

a L.S. and G.M.O. contributed equally to this study

*Corresponding author

415-206-8101 (Fax Number) 415-206-8091 (Office number), mike.mccune@ucsf.edu

Abstract

Background

Myeloid cells likely contribute to multiple aspects of HIV pathogenesis. We measured peripheral blood myeloid cells ($CD14^{hi}CD16$-, $CD14^{dim}CD16^{+}$, and CD11c+ dendritic cells) from HIV patients on and off therapy.

Methods

A cross-sectional study of seronegatives, viral non-controllers (viral load >10,000 copies/mL), viral controllers (viral load <1000 copies/mL), and HAART suppressed (viral load <75 copies/mL, >1 year of therapy) was performed. CD4 reconstitution was analyzed to determine how myeloid cells measured at a time point during the first year of suppressive antiviral treatment predicted CD4 reconstitution.

Results

Myeloid cells are distinguished by their expression of CD11c, CD14 and CD16. We performed analyses of myeloid markers: heme oxygenase-1 (HO-1), HLA-DR, CD33, CD11b, and CD11c. In a cross-sectional analysis, we show that the non-classical $CD14^{dim}CD16^{+}$ monocytes were the highest in the viral non-controllers and lowest in seronegatives, with the opposite pattern seen in the classical $CD14^{hi}$ monocytes. HO-1 expression in classical monocytes had an inverse relationship with serum kynurenine/tryptophan ratios in elite controllers ($p=0.05$, $r=-0.37$). We show that the percentage of $CD11c^{+}$ dendritic cells was correlated with lower CD4 reconstitution ($p=0.021$, $r=-0.48$). Interestingly, the level of HO-1 expression on $CD14^{hi}$ monocytes correlated with higher CD4 reconstitution after four years of suppressive HAART ($p=0.028$, $r=0.46$).

Conclusions

These results suggest that different myeloid sub-populations may play important roles in the context of ongoing viremia and as well as CD4 reconstitution after HAART.

Keywords (3-7)

Monocytes, HAART, CD4 reconstitution, elite controllers, HIV, HLADR, HO-

Introduction

Immune activation and inflammation are predictive of a rapid pace of HIV disease progression, and host immunoregulatory factors that blunt immune activation and inflammation may contribute to delayed disease progression (1-5). Studies in non-human primates (NHP) and in infected humans have revealed that inflammation during SIV/HIV infection is tightly correlated with the generation of pro-inflammatory cytokines (6), T cell activation (7), increased microbial translocation of lipopolysaccharide products from the gut flora (8), and increased frequencies of inflammatory monocyte populations (9,10).

In humans, blood monocytes have been characterized on the basis of morphology, the activity of monocyte-specific esterase, and by flow cytometric detection of distinguishing light scatter properties that includes CD14 expression. The latter technology has also enabled the identification of a CD16 subpopulation that comprises about 10% of $CD14^{+}$ cells and about 13% of $CD16^{+}$ cells (11). This latter population is characterized by higher basal major histocompatibility complex (MHC) class II expression and higher TNFα production after stimulation by Toll-like receptor (TLR) ligands (12). Based on the fact that this latter $CD14^{dim}CD16^{+}$ monocyte population expresses surface markers resembling those found on tissue macrophages, it was designated the "non-classical monocyte" while the $CD14^{+}CD16^{-}$ were designated "classical monocytes." Further studies have shown non-classical monocytes have low IL-10 expression, high levels of TNFα, interleukin-12, and inducible nitric oxide synthase after stimulation (13).

It has long been recognized that individuals with HIV have 2 to 8-fold percent higher non-classical monocytes than uninfected controls (14-16). In an animal model of pathogenic

HIV infection, rhesus macaques infected with SIV were shown to have significantly elevated absolute numbers of monocytes expressing CD16 during acute and chronic infection. Also, a significant positive correlation was evident between the number of monocytes expressing CD16 and plasma viral load in the infected cohort (17).

A recent study showed that HAART-naive patients with elevated proportions of $CD14^{hi}CD16^{+}$ monocytes had increased viral loads and decreased $CD4^{+}$ T-cell counts, whereas the non-classical $CD14^{dim}CD16^{+}$ monocytes did not show such correlation with disease progression (18). This study suggests that blood monocyte populations may play a regulatory role in the extent of immune reconstitution during HIV disease.

Studies have shown that HO-1 inhibits the expression of the pro-inflammatory cytokine TNFα while maintaining or augmenting the expression of the anti-inflammatory cytokine, IL-10. Notably, these observations were made in the myeloid lineage cells such as dendritic cells and macrophages (19-21). Previous studies reported that pharmacological alterations of HO-1 induced a tolerogenic profile in antigen presenting cells of the monocytic lineage (22). Another study showed that blood monocytes that were $CD16^{+}CCR2^{-}$ had a preferential production of HO-1 at steady state (23).

To investigate how different myeloid populations correlate with parameters of immune inflammation, $CD4^{+}$ T cell reconstitution during HAART (highly active antiretroviral therapy) and $CD4^{+}$ T cell preservation in treatment naïve viral controllers, subpopulations of peripheral myeloid cells from HIV patients were analyzed. We show that $CD11c^{+}$ dendritic cells are predictive of lower CD4 reconstitution in the course of early HAART, and HO-1 expression in the classical $CD14^{hi}$ monocytes is predictive of higher CD4 reconstitution. We also show that there is a negative correlation with the extent of HO-1 expression in classical

monocytes and the $CD11c^+$ dendritic cell frequencies. Our results show that HO-1 expression in classical monocyte populations are predictive of decreased immune inflammation and enhanced $CD4^+$ T cell reconstitution.

Methods

Human subjects

Peripheral blood samples were collected from HIV-infected and -uninfected adults after written informed consent was obtained under protocols approved by the University of California at San Francisco Committee on Human Research (San Francisco, CA). Healthy adults (n=22) were recruited from the San Francisco Bay Area (Table 1). HIV-positive subjects were recruited from the San Francisco Bay Area into the UCSF-based Study of the Consequences of the Protease Inhibitor Era (SCOPE) Cohort, a clinic-based cohort of >1500 adults with chronic HIV infection (Table 2 and Table 3). Participants undergo clinical laboratory monitoring and have their biological specimens banked. HIV controllers are defined as HIV-infected subjects that are off antiretroviral therapy for at least the latest 12 month period for which follow-up is available, with at least three plasma HIV RNA levels taken during this time below 1,000 copies/mL. HIV viral non-controllers are defined as individuals with HIV RNA levels over 10,000 copies RNA/ml (by bDNA, Chiron Diagnostics, Emeryville, USA) or 20 000 copies RNA/mL (by Abbott RealTime HIV-1 PCR, Abbott Park, Illinois, USA) at some point in the past, regardless if during a period of treatment or no treatment.

Inclusion Criteria for early HAART phenotyping:

Patients included in the analysis for the early HAART phenotyping were included on the basis of the following criteria: (1) Slope of CD4 reconstitution curve drawn after viral suppression from >1000 copies/mL to <100 copies/mL. (2) During the duration of analysis (regression line), viral suppression <100 copies/mL is maintained with only one blip of >1000 copies/mL permissible

(3) The first "phenotyping" point is within 12 months of initial viral suppression

Primary cell and plasma isolation

Plasma was isolated from whole blood drawn into EDTA tubes. Blood was centrifuged and plasma was harvested and frozen at -80 degrees centigrade until time of use. Peripheral blood mononuclear cells (PBMCs) were isolated from whole blood drawn into sodium heparin tubes by density centrifugation using Histopaque®-1077 (Sigma Aldrich, Saint Louis, MO). PBMCs were washed with RPMI 1640 (Life Technologies, Rockville, MD) supplemented with 10% FBS (Gemini Bio-Products, Woodland, CA), 1% penicillin/streptomycin (Mediatech, Washington, DC), and 2 mM L-glutamine (Mediatech) (hereafter referred to as R10 medium). The PBMCs were then frozen in small aliquots in R10 medium with 10% DMSO (Sigma Aldrich, Saint Louis, MO) and stored in liquid nitrogen cryofreezer until time of use. On day of staining, PBMCs were rapidly thawed and washed in R10 medium. Viable PBMCs were counted under direct microscopic visualization using a hemacytometer and Trypan Blue exclusion (Sigma Aldrich, Saint Louis, MO). PBMCs were then pelleted and resuspended at an adequate cell number for subsequent experiments. For the HO-1 induction experiments, Cobalt protoporphyrin (CoPP) was purchased in powdered form from Frontier

Scientific (Park City, Utah), dissolved in 0.1 mM NaOH, and titrated to a pH of 7.6. PBMCs were cultured on Upcell^{TM} 96F MicroWell plates and were incubated with saline or 25uM cobalt protoporphyrin (CoPP) in R10 at 37° for 48 hours. Adherent cells were detached from the plates by incubating the plates at 25° for 20 minutes.

Flow cytometry antibody labeling

All cells were stained with a live/dead marker Amine-Aqua/Am-Cyan Live/Dead (Invitrogen) to exclude dead cells from analysis and fluorophore-conjugated monoclonal antibodies (mAbs) were used to detect cell surface markers. The following antibodies from BD Biosciences (Franklin Lakes, NJ): CD3-APC-Cy7 (SP34-2), CD11c V450 (B-ly6), CD11b Pecy7 (icrf44), CD56 APC (NCAM16.2), CD19 (HIB19), CD124 (hil4r-m57), HLA-DR (L243), CD33 (HIM3-4). The following were from Invitrogen: CD14-Qdot605 (Q10013) and CD16-APC (3G8, Caltag-Invitrogen). The following antibodies were used for detection of intracellular antigens: HO-1 rabbit polyclonal (ab13243, unconjugated, Abcam, Cambridge, MA) and a secondary goat anti-rabbit IgG conjugate (554020, FITC, BD Biosciences). For flow cytometry analysis, cells were washed in staining buffer [PBS with 2% FBS and 2 mM ethylenediamine tetra-acetic acid – (EDTA) (Sigma)] and then incubated for 30 minutes at 4°C in the presence of directly-conjugated fluorescent mAbs. All cells were stained with a live/dead marker (Amine-Aqua/Am-Cyan Live/Dead; Invitrogen) so that dead cells could be excluded from analysis. The cells were washed in staining buffer, and then fixed and permeabilized in BD Cytofix/Cytoperm (BD Biosciences), according to the manufacturer's protocol for intracellular staining. The cells were incubated for 1 hour at 4°C in the presence of a rabbit polyclonal antibody specific for HO-1 (ab13243, unconjugated,

Abcam) and a secondary goat anti-rabbit IgG conjugate (554020, FITC, BD Biosciences). The cells were washed in staining buffer and then fixed in 1% paraformaldehyde (PFA). Data were acquired with an LSR-II flow cytometer (BD Biosciences) and analyzed with FlowJo software (Treestar, Ashland, OR).

Measurement of tryptophan and kynurenine concentrations in plasma

Tryptophan and kynurenine concentrations in plasma were measured by high-performance liquid chromatography as described previously (24). Standard curves and quality control samples [phosphate-buffered saline–bovine serum albumin (BSA) (5%) with 50 μM tryptophan and 2.5 μM kynurenine were included in each run, and final concentrations were determined based on internal standards and standard curves.

Statistical analyses

Multiple 2-way ANOVA comparisons were performed on these myeloid sub-populations and the cross-sectional study of HIV patients, and on the comparisons of the geometric mean fluorescence intensities of the various myeloid markers. Delta CD4 calculations were made by subtracting the nadir CD4 count from the peak CD4 count on HAART. We performed linear regression of all of the biomarkers against the delta CD4 reconstitution (CD4 cells/uL) and correlation analyses (Pearson r correlation and its p values are reported) using GraphPad Prism v5.0d (Graphpad Software, La Jolla, CA, USA).

Results

Myeloid cells are defined by distinct cell surface receptors

We show that blood monocytes are comprised of several populations as defined by CD11c, CD14 and CD16 expression (Figure 1a). Three distinct lineage negative, HLADR+, CD11c+ populations are defined: $CD14^{hi}CD16$- "classical monocytes", $CD14^{dim}CD16^{+}$ cells "non-classical monocytes", and $CD14^{-}CD16^{-}$CD11c+ dendritic cells (25).

We performed a comprehensive analysis of the geometric mean fluorescence intensities (gMFI) of various myeloid markers in these populations: heme oxygenase-1, HLADR, CD11c, CD11b, and CD33 (Figure 1b). In both early-HAART patients (Table 1b) and HAART-naïve elite controllers (Table 1c), the $CD14^{hi}$ classical monocytes had the highest levels of CD11b and CD33 expression, whereas the $CD14^{dim}CD16^{+}$ non-classical monocytes had the highest levels of CD11c expression, and $CD11c^{+}$ dendritic cells had the highest levels of HLA-DR (Figure 1b). Early HAART patients had higher levels of HLA-DR and CD11b expression on their classical and non-classical monocyte populations compared to elite controllers.

These results show that three main myeloid sub-populations can be distinguished based on cell-surface phenotypes defined by CD11c, CD14, and CD16 expression, and that these sub-populations are further characterized by both intracellular and cell-surface myeloid markers.

Non-classical monocytes are associated with progressive HIV disease

Immune activation is not only associated with progressive HIV disease, but is actually predictive of the pace of HIV disease progression, even more so than plasma viral load. In particular, studies have shown that $CD8^{+}$ T cell expression of the surface "immune activation

marker," CD38, predicts survival times in chronic HIV disease, independently of viral load (26). A cross-sectional study of seronegatives, viral non-controllers (viral load >10,000 copies/mL), viral controllers (viral load <1000 copies/mL), and HAART suppressed patients (viral load <75 copies/mL, >1 year of therapy) was performed (Table 1a). We corroborated the previous findings that expression of CD38 and HLA-DR on $CD4^+$ and $CD8^+$ T lymphocytes is increased in the context of progressive HIV disease. To determine the extent of indoleamine 2, 3-dioxygenase (IDO1) activity, we analyzed the measured the kynurenine to tryptophan ratios. IDO1 has been shown to be up-regulated in circulating dendritic cells during HIV-induced inflammation (24), and is also expressed in a variety of monocytes and tissue macrophage subsets. We found that the pattern of IDO1 matched that of T cell activation across patients (Figure 2a). This supports the previous reports in the literature and suggests a potentially harmful role that myeloid dendritic cells may have during the course of HIV disease.

We found that the frequency of $CD14^{dim}CD16^+$ non-classical monocytes followed the same pattern as that of CD38 and HLA-DR on T lymphocytes. The frequencies of these cells were the highest in the HIV viral non-controllers and the lowest in HIV-seronegative individuals (Figure 2b). The population of $CD14^{hi}$ classical monocytes showed a pattern that was reciprocal to that of non-classical monocytes. These results confirm and extend existing reports (14,16,18,27) and suggest that blood monocyte populations may play a regulatory role in the extent of immune reconstitution and T cell activation during HIV disease.

Serum levels of IDO catabolites are directly correlated with T lymphocyte activation and inversely correlated with HO-1 expression in classical monocytes

Previously, IDO1 has been shown to be up-regulated in circulating dendritic cells during HIV-induced inflammation (24). We confirmed this previously reported correlation between IDO1 activity (serum kynurerenine/tryptophan levels) and HLA-DR+/CD38+ co-expression on both $CD4^+$ (r=0.50, p=0.0003) and $CD8^+$ (r=0.49, p=0.0003) T cell activation (Figure 3a).

To address whether the composition of monocyte populations may influence the extent of IDO1 activity, we compared the monocyte frequencies to serum kynurenine/tryptophan in all HAART-naïve patients regardless of viral loads (Table 1a, viral controllers and non-controllers). We show that frequencies of classical monocytes have a negative correlation with serum kynurenine/tryptophan (r=-0.22, p=0.052) (Figure 3b). $CD11c^+$ DC frequencies were not correlated with the kynurenine/tryptophan ratio (r=0.18, p=0.37, data not shown).

We next looked specifically within elite controllers (Table 1a) to see if HO-1 expression within the classical and non-classical monocyte population had a correlation with serum kynurenine/tryptophan. We show that HO-1 expression in classical monocytes, but not in non-classical monocytes, show a negative correlation with the kynurenine/tryptophan ratio (r=-0.37, p=0.05) (Figure 3c). HO-1 gMFI in $CD11c^+$ DCs was not correlated with the kynurenine/tryptophan ratio (r=-0.02, p=0.93, data not shown).

We then investigated in the elite controllers whether HO-1 expression in classical monocytes may be correlated with levels of $CD11c^+$ DCs. This sub-population represents the myeloid sub-population that has been shown to up-regulate IDO1 upon IFNγ stimulation (24). We show that HO-1 gMFI in both classical (r=-0.62, p=0.0002) and non-classical (r=-0.65, p<0.0001) monocytes are inversely correlated with the measured $CD11c^+$ DC frequencies.

These results show that serum IDO1 catabolites are a reliable measure of immune

inflammation based on their strong correlation to $CD4^+$ and $CD8^+$ T cell activation. We also show that HO-1 expression within monocyte populations are inversely correlated with both $CD11c^+$ DC frequencies as well as serum kynurenine/tryptophan levels. These results strongly suggest that there may be a reciprocal regulation of IDO1 activity and HO-1 expression.

Activated T cell frequencies are lowered while $CD14^{hi}$ monocytes frequencies are increased after prolonged HAART

We next examined how inflammatory cell types were altered during the course of suppressive HAART (Table 1b). Frequencies of $CD4^+$ and $CD8^+$ T lymphocytes that co-express CD38 and HLA-DR are decreased (mean of differences 7.12% and 15.62%, respectively) from early (3-12 months) to late HAART (2-3 years) time points (Figure 4a). Reciprocally, we showed that $CD14^{hi}$ classical monocyte frequencies are increased (mean of difference 6.95, p=0.011) over this same period (Figure 4b). These results in combination show that prolonged HAART leads to decreased immune activation, and that the percentages of circulating classical monocytes may reflect decreased turnover or increased production of this population.

CD11c+ dendritic cells are associated with decreased CD4 reconstitution, while HO-1 expression in $CD14^{hi}$ monocytes is associated with increased CD4 reconstitution in early HAART patients

HAART-suppressed patients were studied longitudinally while on treatment (n=23) (Table 1b). $CD4^+$ T cell reconstitution was measured by taking the peak and subtracting the

nadir $CD4^+$ T cell count (cells/uL) PBMC phenotyping was performed on an early time point between 3 to 12 months of HAART initiation to determine myeloid cell properties predictive of disease outcomes after 2 to 4 years of suppressive therapy (Figure 5a).

First, we show that in early HAART patients (3-12 months of therapy), HO-1 expression in classical (r=-0.48, p=0.02) and non-classical (r=-0.41, p=0.05) monocytes is negatively correlated with the $CD11c^+$ DC frequency (Figure 5b).

Next, we show that the percentage of $CD11c^+$ dendritic cells at this early HAART time point was correlated with lower CD4 reconstitution (p=0.021, r=-0.48), whereas there was no significant association with the other myeloid populations. Interestingly, the level of HO-1 expression on $CD14^{hi}$ classical monocytes correlated with higher CD4 reconstitution (p=0.028, r=0.46).

These results underscore the reciprocal effects that circulating myeloid cells have in predicting $CD4^+$ T cell reconstitution in patients several years subsequent to measurement.

Cobalt protoporphyrin (CoPP) induction of patient PBMCs leads to increased HO-1 induction in CD14+ monocytes and a more classical monocyte phenotype

Isolated PBMCs from early-HAART patients (Table 1b) were cultured with the HO-1 inducer CoPP (25uM) for 48 hours on UpCell^{TM} plates. Myeloid sub-populations were gated using the same gating strategy from Figure 1. However, because myeloid sub-populations displayed different expression patterns of CD14 and CD16 upon culturing, two main sub-populations of the $CD11c^+$ DC and $CD14^+$ monocytes were gated (Figure 6a). Analysis of the two subpopulations demonstrated that CoPP induction led to increased HO-1 gMFI in $CD14^+$ monocytes ($p<0.01$, 2-way ANOVA post-test) but not $CD11c^+$ DCs ($p<0.0001$, 2-way

ANOVA between subpopulations), as well as decreased CD16 ($p<0.01$, 2-way ANOVA post-test) and CD14 ($p<0.01$, 2-way ANOVA post-test) gMFI (Figure 6b amd 6c).

These functional experiments support our previous findings that selective HO-1 expression in classical monocytes of early HAART patients is predictive of longitudinal CD4 reconstitution. HO-1 induction also leads to a skewing of $CD14^+$ monocytes towards a more "classical" phenotype, and represents a potential functional link to why HO-1 expression may be predictive of enhanced CD4 reconstitution during HAART.

Discussion

Various myeloid cell subsets can be infected by HIV (28) and represent a source of the viral reservoir in HIV-infected patients (29). These cells may also be involved in the shuttling of virus to tissue sites where they contribute to the establishment of productive infection. They may also contribute to the basal amounts of immune activation observed even in the context of maximally suppressive combination ART regimens (30,31). During HIV infection, there are elevated levels of the monocyte pro-inflammatory cytokines such as IL-1, IL-6, and TNF-α (32,33). Infected blood monocytes may also function as the causative link to observed co-morbidities during treated and un-treated HIV disease, such as increased risk of thrombosis (34), cardiovascular diseases (35), and HIV-associated dementia (36). Here we show that non-classical monocytes are associated with progressive HIV disease, classical monocyte frequencies increase over time of on suppressive HAART, and CD11c+ dendritic cell frequencies inversely correlate while HO-1 expression within classical monocytes positively correlates with CD4 reconstitution after 2 to 4 years of continuous suppressive

HAART.

The role that myeloid cells play in HIV disease has been incompletely elucidated, partly due to the heterogeneous composition of the population. The best accepted paradigm for distinguishing myeloid cell subsets has been proposed in a recent publication (25). Based on this paradigm, the $CD14^{dim}CD16^{+}$ non-classical monocytes have been shown to develop into $CD1b^{+}$ DC with superior antigen-presenting as well endothelial adhesion and tissue migratory capabilities (37,38). These cells also exhibit pro-inflammatory and pro-atherosclerotic activity, with shortened telomere length as compared to the $CD14^{+}CD16^{-}$ monocytes (39). A recent study showed that human $CD14^{dim}CD16^{+}$ monocytes have the functional role of patrolling the endothelium of blood vessels and are weak phagocytes that do not produce ROS or cytokines in response to cell-surface Toll-like receptors. Instead, they are involved in the innate local surveillance of tissues and may contribute to the pathogenesis of autoimmune diseases (40). Consistent with this pro-inflammatory role, we have found that circulating frequency of non-classical monocytes is highest in HIV subjects with high viral loads. This also corroborates findings made by other groups (14,16,18,27) and suggest that blood monocyte populations may play a regulatory role in the extent of immune reconstitution and T cell activation during HIV disease.

Shedding of CD14 from the surface of non-inflammatory $CD14^{hi}$ monocytes upon exposure to an activating stimulus (e.g., LPS) may represent an important part of their transition into pro-inflammatory $CD14^{dim}CD16^{+}$ monocytes (41,42). The increase in the frequency of classical monocytes after suppressive HAART treatment may reflect decreases in systemic immune activation and decreased plasma LPS levels associated with suppressive HAART (43,44).

Heme-oxygenase-1 is an inducible enzyme expressed in response to inflammatory stimuli an doxidative stress, resulting in myeloid cells with decreased immune stimulatory properties. Previous studies reported that pharmacological alterations of heme oxygenase-1 induced a tolerogenic profile in antigen presenting cells of the monocytic lineage (22). Several other studies have shown that blood monocytes that are $CD16^{+}CCR2^{-}$ have preferential production of HO-1 at steady state (23,45). Our finding that increased HO-1 expression in $CD14^{+}$ classical monocytes during early HAART predicts subsequent CD4 T cell gains is suggestive that ability to increase tolerogenic/anti-inflammatory states during HAART treatment is associated with ability to reconstitute CD4 T cell counts.

In this report, we show that circulating myeloid cells are defined by distinct cell surface receptors (CD11c, CD14, and CD16) and have different expression patterns of CD11c, CD11b, HLA-DR, and CD33. We also show that $CD14^{dim}CD16^{+}$ cells are associated with progressive HIV disease and that $CD14^{hi}$ monocyte frequencies are increased after prolonged HAART. We measure CD4 reconstitution in early HAART patients, and show that $CD14^{-}$ $CD16^{-}$ cells are associated with decreased CD4 reconstitution, while HO-1 expression in $CD14^{hi}$ monocytes is associated with increased CD4 reconstitution in early HAART patients. We show that, unlike HAART patients, myeloid cells are not predictive of $CD4^{+}$ T cell preservation in HIV elite controllers. Rather, functional T cell subsets (Th17 and T regulatory cells) are predictive of CD4 preservation in this antiretroviral-naïve and aviremic HIV-positive population.

These findings can potentially contribute to improved clinical guidelines for the treatment of HIV HAART patients that may be at risk of failing therapy. Immunological Non-responders (INRs) are HIV patients that fail to restore CD4 counts above a level of 500

cells/uL despite years of suppressive HAART. Based on large cohort studies, INRs represent about 30% of HAART patients (46,47). Biomarkers that may predict the pace and capacity for CD4 reconstitution during early therapy can help predict, and then guide clinical decisions for the type of antiretroviral regimen that the patient should be administered. Our results show that different CD11c+ dendritic cells and HO-1 expression in classical monocytes may be important immune predictors of CD4 reconstitution after HAART, and may play important mechanistic roles in CD4 reconstitution.

Figure Legends

Figure 1- Myeloid cells are defined by distinct cell surface receptors

(a) Thawed PBMCs from HIV patients were stained with antibodies recognizing cell-surface and intracellular myeloid markers. Analysis was performed by sequentially gating on live cells, singlets (FSC-A/FSC-H), non-lymphocyte (SSC-A high/FSC-A high), lineage negative ($CD3^-$ $CD19^-$ $CD56^-$), and HLA-DR and CD11c positive populations. Myeloid cells were further defined by expression of CD14 and CD16 into three subsets ($CD14^{hi}$ "classical", $CD14^{dim}CD16^+$ "non-classical", and $CD11c^+$ dendritic cells). **(b)** Plots depict staining intensity (geometric mean fluorescence intensity) of various myeloid markers (HO-1, HLA-DR, CD11b, CD11c, and CD33) in the three myeloid sub-populations (column statistics performed by 2-way ANOVA, with asterisks representing the significance to the decimal place of the p value between cell subpopulations).

Figure 2- $CD14^{dim}CD16^+$ "non-classical" monocytes are associated with progressive HIV

disease

(a) Thawed PBMCs were analyzed in a cross-sectional study of seronegatives, viral non-controllers (viral load >10,000 copies/mL), viral controllers (viral load <1000 copies/mL), and HAART suppressed patients (viral load <75 copies/mL, >1 year of therapy) (Table 1a). CD38 and HLA-DR cell-surface staining was measured in $CD4^+$ and $CD8^+$ T cells, and plasma kynurenine/tryptophan measures levels were measured. Column statistics were performed by 1-way ANOVA. **(b)** Thawed PBMCs were analyzed in the same patient population for the presence of the myeloid cell-surface markers, CD14 and CD16. Frequencies of $CD14^{hi}$ "classical", $CD14^{dim}CD16^+$ "non-classical", and $CD11c^+$ dendritic cells in relation to the parent myeloid gate were calculated. Column statistics were performed by 1-way ANOVA. The nomenclature for $p<0.05$, $p<0.01$, $p<0.001$ are shown with the symbols *, **, ***, respectively.

Figure 3- Serum levels of IDO catabolites are correlated with parameters of inflammation

(a) Thawed PBMCs from all HAART-naïve patients (Table 1a) were analyzed for cell-surface co-expression of HLA-DR/CD38 on $CD4^+$ and $CD8^+$ T cells. Concurrent serum from the same were analyze for kynurenine/tryptophan levels. There was a positive correlation between HLA-DR+/CD38+% on $CD4^+$ T cells ($r=0.50$, $p=0.0003$) and $CD8^+$ T cells ($r=0.49$, $p=0.0003$).

(b) Myeloid sub-populations were analyzed in the same patients were analyzed for their correlation to kynurenine/tryptophan levels. There was a negative correlation with the classical monocyte frequencies ($r=0.22$, $p=0.052$) but not in non-classical monocyte frequencies ($r=0.13$, $p=0.26$). **(c)** HO-1 expression in the two myeloid sub-populations were

analyzed for their relationship to serum kynurenine/tryptophan levels. There was a negative correlation with the classical monocyte frequencies (r=-0.37, p=0.05) but not in non-classical monocyte frequencies (r=-0.29, p=0.13). **(d)** HO-1 expression in the two myeloid sub-populations was analyzed for their relationship to $CD11c^+$ DC frequencies. There was a negative correlation with the classical monocyte frequencies (r=-0.62, p=0.0002) as well as in non-classical monocyte frequencies (r=-0.65, p=0.0001). All statistics were performed using Pearson's correlation coefficient across normally distributed data, with p values reporting the strength of the r correlation coefficient.

Figure 4- Activated T cell frequencies are lowered while $CD14^{hi}$ monocytes frequencies are increased after prolonged HAART

(a) CD38 and HLA-DR cell-surface staining was measured in $CD4^+$ and $CD8^+$ T cells from thawed PBMCs of HIV HAART patients. Early ARV refers to a period from 3-12 months of treatment, whereas late ARV refers to a period from 2-3 years of treatment. Student's paired T-test analyses yield statistically significant decreases in CD38 and HLA-DR co-expression on $CD4^+$ T cells ($p<0.001$) and $CD8^+$ T cells ($p<0.0001$). **(b)** $CD14^{hi}$, $CD14^{dim}CD16^+$, and $CD14^-CD16^-$ cells were measured during early and late ARV in the same patient cohort. Student's paired T-test analyses yielded a statistically significant decrease $CD14^{hi}$ monocytes (p=0.011)

Figure 5- Myeloid cells predict CD4 reconstitution in early HAART patients

(a) $CD4^+$ T cell reconstitution was measured by taking the peak and subtracting the nadir

$CD4^+$ T cell count (cells/uL) from a subset of HAART patients followed longitudinally (Table 1b) Plasma viral load measurements (p24 RNA copies/milliliter) are depicted in the corresponding graph **(b)** There was a negative correlation with HO-1 gMFI in classical monocytes and $CD11c^+$ DC frequencies (r=-0.48, p=0.02) as well as in non-classical monocyte frequencies (r=-0.41, p=0.05). **(c)** Myeloid populations ($CD11c^+$ DCs, classical monocytes, and non-classical monocytes) were correlated to the delta CD4 levels. $CD11c^+$ DCs had a negative correlation with delta CD4 (r=-0.48, p=0.021) whereas there was no significant association with the classical monocytes, and non-classical monocytes. **(d)** HO-1 gMFI was measured and correlated to the delta CD4 levels. HO-1 gMFI in classical monocytes were positively correlated with delta CD4 (r=0.46, p=0.028) whereas it trended towards increased delta CD4 in non-classical monocytes (r=0.35, p=0.097). Pearson's correlation coefficient p is reported with its corresponding P-value.

Figure 6- Cobalt protoporphyrin (CoPP) induction of patient PBMCs leads to increased HO-1 induction in CD14+ monocytes and a more classical monocyte phenotype

(a) Thawed PBMCs from early HAART patients (Table 1b) were cultured with saline or 25uM CoPP for 48 hours on UpCell^{TM} plates and then stained with antibodies recognizing cell-surface and intracellular myeloid markers. Analysis was performed similarly to what is described in Figure 1a. Myeloid cells were further defined by $CD11c^+$ DCs and $CD14^+$ monocytes. Flow panels depict one early-HAART patient with PBMCs cultured with PBS (saline) or CoPP (25uM). **(b)** Histograms represent the fluorescence intensities of HO-1, CD14, CD16, and CD11c in both $CD11c^+$ DCs and $CD14^+$ monocytes with saline or CoPP treatment. **(c)** Graphical analyses show that CoPP induction leads to $CD14^+$ monocytes

specific up-regulation of HO-1 ($p<0.01$) and down-regulation of CD16 ($p<0.01$) and CD14 ($p<0.01$) (2-way ANOVA across cell types, $p<0.0001$).

References

1. Pantaleo G, Fauci AS. Immunopathogenesis of HIV infection. Annu Rev Microbiol 1996;50:825-54.

2. Lawn SD, Butera ST, Folks TM. Contribution of immune activation to the pathogenesis and transmission of human immunodeficiency virus type 1 infection. Clin Microbiol Rev 2001, Oct;14(4):753-77, table of contents.

3. Cannavo' G, Paiardini M, Galati D, Cervasi B, Montroni M, De Vico G, et al. Abnormal intracellular kinetics of cell-cycle-dependent proteins in lymphocytes from patients infected with human immunodeficiency virus: A novel biologic link between immune activation, accelerated t-cell turnover, and high levels of apoptosis. Blood 2001, Mar 15;97(6):1756-64.

4. Boasso A, Shearer GM. Chronic innate immune activation as a cause of HIV-1 immunopathogenesis. Clin Immunol 2008, Mar;126(3):235-42.

5. Douek DC, Roederer M, Koup RA. Emerging concepts in the immunopathogenesis of AIDS. Annu Rev Med 2009;60:471-84.

6. Manches O, Bhardwaj N. Resolution of immune activation defines nonpathogenic SIV infection. J Clin Invest 2009, Dec;119(12):3512-5.

7. Barbour JD, Ndhlovu LC, Xuan Tan Q, Ho T, Epling L, Bredt BM, et al. High CD8+ T cell activation marks a less differentiated HIV-1 specific CD8+ T cell response that is not altered by suppression of viral replication. Plos One 2009;4(2):e4408.

8. Pandrea I, Apetrei C. Where the wild things are: Pathogenesis of SIV infection in african

nonhuman primate hosts. Curr HIV/AIDS Rep 2010, Feb;7(1):28-36.

9. Hasegawa A, Liu H, Ling B, Borda JT, Alvarez X, Sugimoto C, et al. The level of monocyte turnover predicts disease progression in the macaque model of AIDS. Blood 2009, Oct 1;114(14):2917-25.

10. Sodora DL, Allan JS, Apetrei C, Brenchley JM, Douek DC, Else JG, et al. Toward an AIDS vaccine: Lessons from natural simian immunodeficiency virus infections of african nonhuman primate hosts. Nat Med 2009, Aug;15(8):861-5.

11. Passlick B, Flieger D, Ziegler-Heitbrock HW. Identification and characterization of a novel monocyte subpopulation in human peripheral blood. Blood 1989, Nov 15;74(7):2527-34.

12. Belge KU, Dayyani F, Horelt A, Siedlar M, Frankenberger M, Frankenberger B, et al. The proinflammatory CD14+CD16+DR++ monocytes are a major source of TNF. J Immunol 2002, Apr 1;168(7):3536-42.

13. Szaflarska A, Baj-Krzyworzeka M, Siedlar M, Weglarczyk K, Ruggiero I, Hajto B, Zembala M. Antitumor response of CD14+/CD16+ monocyte subpopulation. Exp Hematol 2004, Aug;32(8):748-55.

14. Allen JB, Wong HL, Guyre PM, Simon GL, Wahl SM. Association of circulating receptor fc gamma riii-positive monocytes in AIDS patients with elevated levels of transforming growth factor-beta. J Clin Invest 1991, May;87(5):1773-9.

15. Locher C, Vanham G, Kestens L, Kruger M, Ceuppens JL, Vingerhoets J, Gigase P. Expression patterns of fc gamma receptors, HLA-DR and selected adhesion molecules on monocytes from normal and hiv-infected individuals. Clin Exp Immunol 1994, Oct;98(1):115-22.

16. Thieblemont N, Weiss L, Sadeghi HM, Estcourt C, Haeffner-Cavaillon N. Cd14Lowcd16High: A cytokine-producing monocyte subset which expands during human immunodeficiency virus infection. Eur J Immunol 1995, Dec;25(12):3418-24.

17. Kim WK, Sun Y, Do H, Autissier P, Halpern EF, Piatak M, et al. Monocyte heterogeneity underlying phenotypic changes in monocytes according to SIV disease stage. J Leukoc Biol 2010, Apr;87(4):557-67.

18. Han J, Wang B, Han N, Zhao Y, Song C, Feng X, et al. CD14(high)CD16(+) rather than CD14(low)CD16(+) monocytes correlate with disease progression in chronic hiv-infected patients. J Acquir Immune Defic Syndr 2009, Dec;52(5):553-9.

19. Lee TS, Chau LY. Heme oxygenase-1 mediates the anti-inflammatory effect of interleukin-10 in mice. Nat Med 2002, Mar;8(3):240-6.

20. Rémy S, Blancou P, Tesson L, Tardif V, Brion R, Royer PJ, et al. Carbon monoxide inhibits tlr-induced dendritic cell immunogenicity. J Immunol 2009, Feb 15;182(4):1877-84.

21. Tamion F, Richard V, Renet S, Thuillez C. Protective effects of heme-oxygenase expression against endotoxic shock: Inhibition of tumor necrosis factor-alpha and augmentation of interleukin-10. J Trauma 2006, Nov;61(5):1078-84.

22. Chauveau C, Rémy S, Royer PJ, Hill M, Tanguy-Royer S, Hubert FX, et al. Heme oxygenase-1 expression inhibits dendritic cell maturation and proinflammatory function but conserves IL-10 expression. Blood 2005, Sep 1;106(5):1694-702.

23. Mizuno K, Toma T, Tsukiji H, Okamoto H, Yamazaki H, Ohta K, et al. Selective expansion of cd16highccr2- subpopulation of circulating monocytes with preferential production of haem oxygenase (HO)-1 in response to acute inflammation. Clin Exp Immunol 2005, Dec;142(3):461-70.

24. Favre D, Mold J, Hunt PW, Kanwar B, Loke P, Seu L, et al. Tryptophan catabolism by indoleamine 2,3-dioxygenase 1 alters the balance of TH17 to regulatory T cells in HIV disease. Sci Transl Med 2010, May 19;2(32):32ra36.

25. Ziegler-Heitbrock L, Ancuta P, Crowe S, Dalod M, Grau V, Hart DN, et al. Nomenclature of monocytes and dendritic cells in blood. Blood 2010, Oct 21;116(16):e74-80.

26. Giorgi JV, Hultin LE, McKeating JA, Johnson TD, Owens B, Jacobson LP, et al. Shorter survival in advanced human immunodeficiency virus type 1 infection is more closely associated with T lymphocyte activation than with plasma virus burden or virus chemokine coreceptor usage. J Infect Dis 1999;179:859-70.

27. Fischer-Smith T, Tedaldi EM, Rappaport J. CD163/CD16 coexpression by circulating monocytes/macrophages in HIV: Potential biomarkers for HIV infection and AIDS progression. AIDS Res Hum Retroviruses 2008, Mar;24(3):417-21.

28. Ho DD, Rota TR, Hirsch MS. Infection of monocyte/macrophages by human T lymphotropic virus type III. Journal of Clinical Investigation 1986;77(5):1712.

29. Centlivre M, Legrand N, Steingrover R, van der Sluis R, Grijsen ML, Bakker M, et al. Altered dynamics and differential infection profiles of lymphoid and myeloid cell subsets during acute and chronic HIV-1 infection. J Leukoc Biol 2011, May;89(5):785-95.

30. Hunt PW, Martin JN, Sinclair E, Bredt B, Hagos E, Lampiris H, Deeks SG. T cell activation is associated with lower CD4+ T cell gains in human immunodeficiency virus-infected patients with sustained viral suppression during antiretroviral therapy. J Infect Dis 2003, May 15;187(10):1534-43.

31. Cassol E, Malfeld S, Mahasha P, van der Merwe S, Cassol S, Seebregts C, et al.

Persistent microbial translocation and immune activation in hiv-1-infected south africans receiving combination antiretroviral therapy. J Infect Dis 2010, Sep 1;202(5):723-33.

32. Almeida M, Cordero M, Almeida J, Orfao A. Abnormal cytokine production by circulating monocytes and dendritic cells of myeloid origin in art-treated HIV-1+ patients relates to CD4+ t-cell recovery and HCV co-infection. Curr HIV Res 2007, May;5(3):325-36.

33. Tilton JC, Johnson AJ, Luskin MR, Manion MM, Yang J, Adelsberger JW, et al. Diminished production of monocyte proinflammatory cytokines during human immunodeficiency virus viremia is mediated by type I interferons. J Virol 2006, Dec;80(23):11486-97.

34. Funderburg NT, Mayne E, Sieg SF, Asaad R, Jiang W, Kalinowska M, et al. Increased tissue factor expression on circulating monocytes in chronic HIV infection: Relationship to in vivo coagulation and immune activation. Blood 2010, Jan 14;115(2):161-7.

35. Crowe SM, Westhorpe CL, Mukhamedova N, Jaworowski A, Sviridov D, Bukrinsky M. The macrophage: The intersection between HIV infection and atherosclerosis. J Leukoc Biol 2010, Apr;87(4):589-98.

36. Valcour VG, Shiramizu BT, Shikuma CM. HIV DNA in circulating monocytes as a mechanism to dementia and other HIV complications. J Leukoc Biol 2010, Apr;87(4):621-6.

37. Randolph GJ, Sanchez-Schmitz G, Liebman RM, Schäkel K. The CD16(+) (fcgammariii(+)) subset of human monocytes preferentially becomes migratory dendritic cells in a model tissue setting. J Exp Med 2002, Aug 19;196(4):517-27.

38. Ancuta P, Moses A, Gabuzda D. Transendothelial migration of CD16+ monocytes in response to fractalkine under constitutive and inflammatory conditions. Immunobiology

2004;209(1-2):11-20.

39. Merino A, Buendia P, Martin-Malo A, Aljama P, Ramirez R, Carracedo J. Senescent CD14+CD16+ monocytes exhibit proinflammatory and proatherosclerotic activity. J Immunol 2010, Dec 29.

40. Cros J, Cagnard N, Woollard K, Patey N, Zhang SY, Senechal B, et al. Human cd14dim monocytes patrol and sense nucleic acids and viruses via TLR7 and TLR8 receptors. Immunity 2010, Sep 24;33(3):375-86.

41. Pedron T, Girard R, Chaby R. Variation of lps-binding capacity, epitope expression, and shedding of membrane-bound CD14 during differentiation of human monocytes. J Immunol 1995, Aug 1;155(3):1460-71.

42. Bazil V, Strominger JL. Shedding as a mechanism of down-modulation of CD14 on stimulated human monocytes. J Immunol 1991, Sep 1;147(5):1567-74.

43. Sandler NG, Wand H, Roque A, Law M, Nason MC, Nixon DE, et al. Plasma levels of soluble CD14 independently predict mortality in HIV infection. J Infect Dis 2011, Jan 20.

44. Douek D. HIV disease progression: Immune activation, microbes, and a leaky gut. Top HIV Med 2007;15(4):114-7.

45. Ancuta P, Liu KY, Misra V, Wacleche VS, Gosselin A, Zhou X, Gabuzda D. Transcriptional profiling reveals developmental relationship and distinct biological functions of CD16+ and CD16- monocyte subsets. BMC Genomics 2009;10:403.

46. Kelley CF, Kitchen CM, Hunt PW, Rodriguez B, Hecht FM, Kitahata M, et al. Incomplete peripheral CD4+ cell count restoration in hiv-infected patients receiving long-term antiretroviral treatment. Clin Infect Dis 2009, Mar 15;48(6):787-94.

47. Kaufmann GR, Furrer H, Ledergerber B, Perrin L, Opravil M, Vernazza P, et al.

Characteristics, determinants, and clinical relevance of CD4 T cell recovery to< 500 cells/μl in HIV type 1-infected individuals receiving potent antiretroviral therapy. Clinical Infectious Diseases 2005;41(3):361-72.

The authors report no conflict of interest for this study

L.S. was supported by a pre-doctoral dissertation California HIV Research Program grant (#D09-SF-313). J.M.M. was supported by NIH Awards U01 AI43641 and R37 AI40312, and is the recipient of the National Institutes of Health Director's Pioneer Award, part of the National Institutes of Health Roadmap for Medical Research, through Grant DPI OD00329. The SCOPE cohort was supported by the Centers for AIDS Research at UCSF (PO AI27763), CFAR Network of Integrated Systems (R24 AI067039), the UCSF CTSI (UL1 RR024131), NIAID (RO1 AI087145, K24AI069994, AI-76174, amfAR, and the Ragon Institute. This work was also supported by the NIH grant P30AI027763 (UCSF-GIVI Center for AIDS Research) and the National Center for Research Resources (NCRR) grant UL1 RR024131.

Table 1a: Cross Sectional Analysis Clinical table

	VL copies/mL (Median ± I.Q.R.)	CD4/ul (Median ± I.Q.R.)	Mean Age (Median ± I.Q.R.)	Male %
Viral Controllers **(n=54)**	75 ± 52	716 ± 458.5	47 ± 10	76.9%
Viral Non-controllers **(n=28)**	101316 ± 140021	237.7 ± 220.2	39 ± 8	96.4%
HAART patients (>1 year) **(n=50)**	75 ± 19	373 ± 210	48 ± 7	84.0%
Seronegative **(n=30)**	NA	NA	42.7 ± 1.1	100.0%

Table 1b: Longitudinal HAART patients

	VL copies/mL (Median ± I.Q.R.)	CD4/ul (Median ± I.Q.R.)	Mean Age (Median ± I.Q.R.)	Male %	months on HAART (Median ± I.Q.R.)
HAART patients (n=23)	75 ± 25	323 ± 148	46 ± 6	91.30%	5.7 ± 3.9

Table 1c: Longitudinal elite controllers

	VL copies/mL (Median ± I.Q.R.)	CD4/ul (Median ± I.Q.R.)	Mean Age (Median ± I.Q.R.)	Male %
Elite Controllers (n=28)	40 ± 1.2	728 ± 432	48 ± 7.5	75.00%

Figure 1a

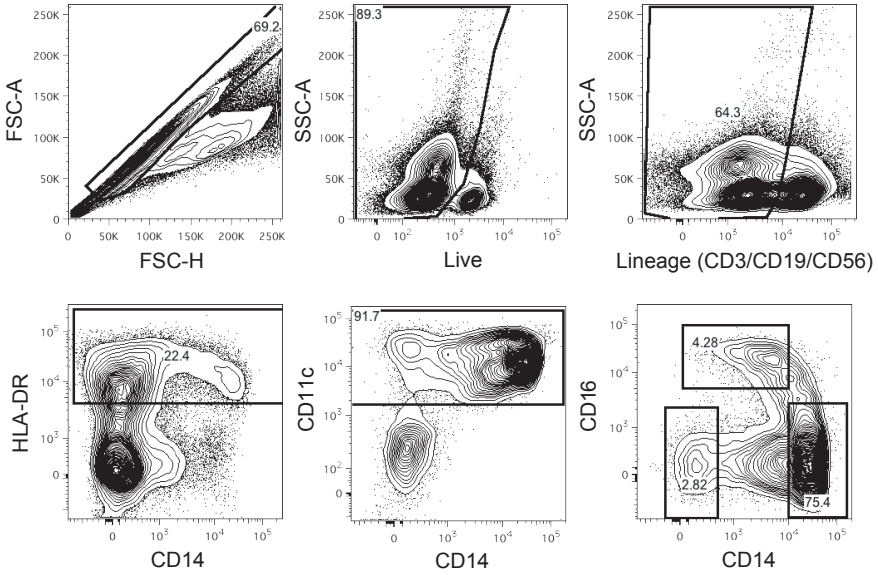

Figure 1b

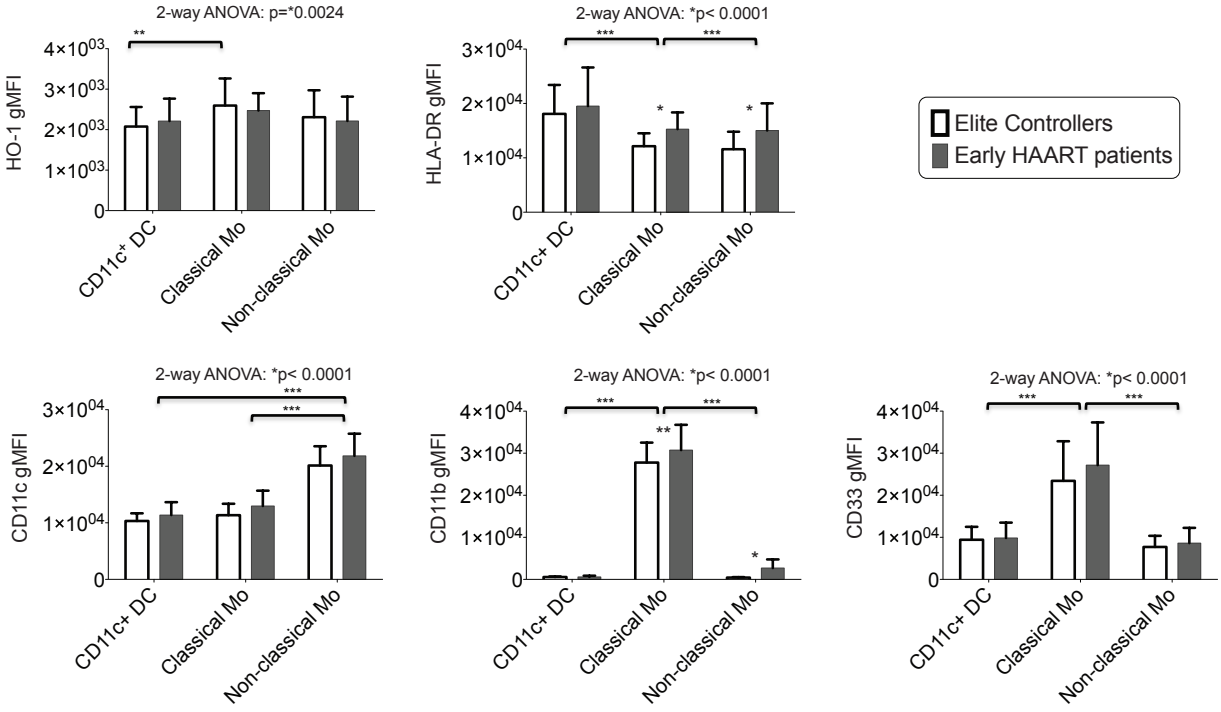

Figure 2a

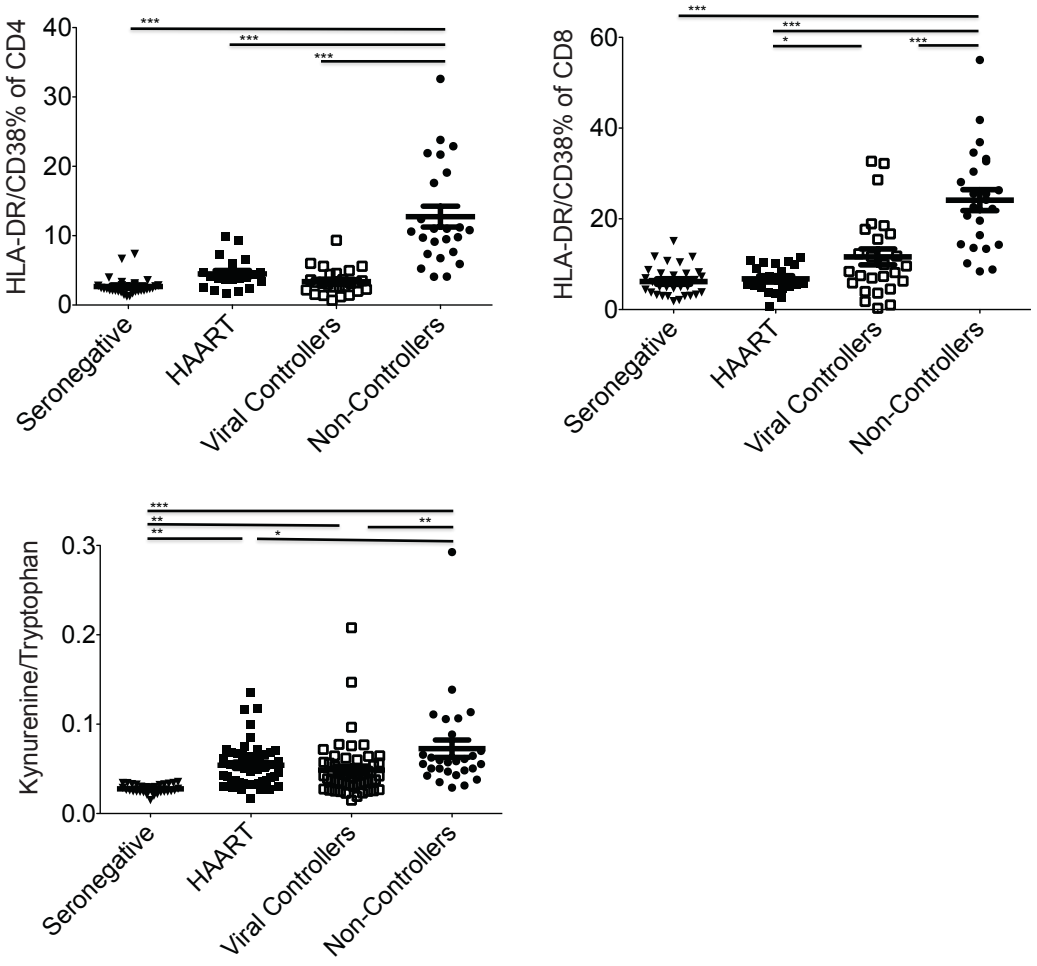

Figure 2b

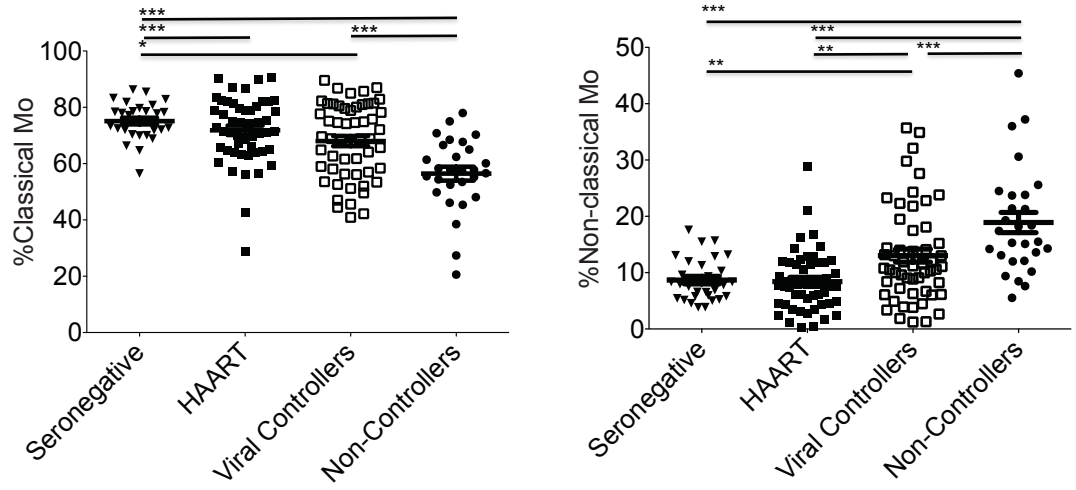

Figure 3a

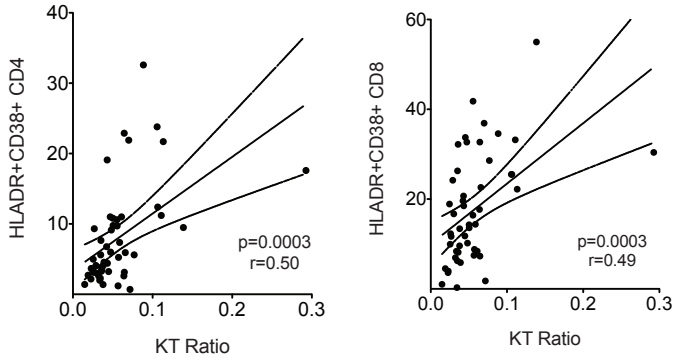

Figure 3b

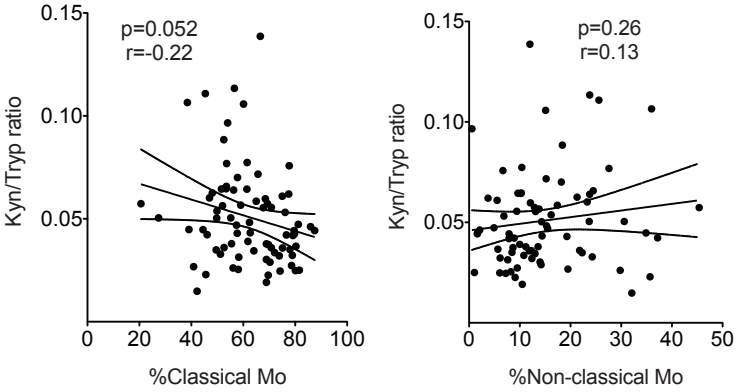

Figure 3c

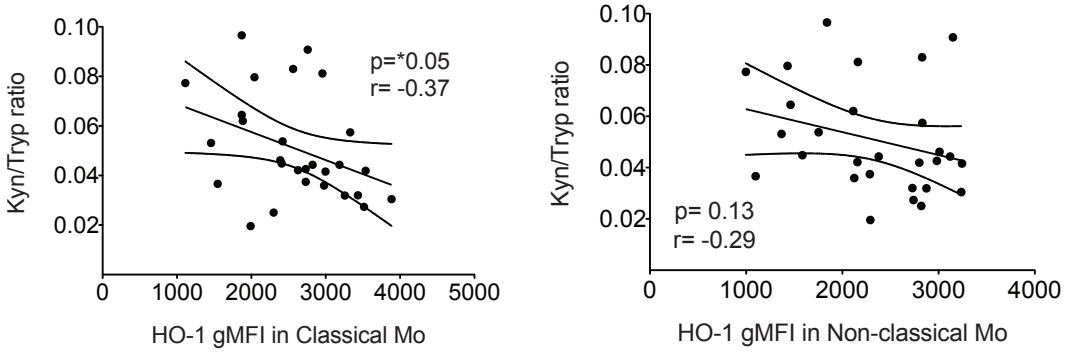

Figure 3d

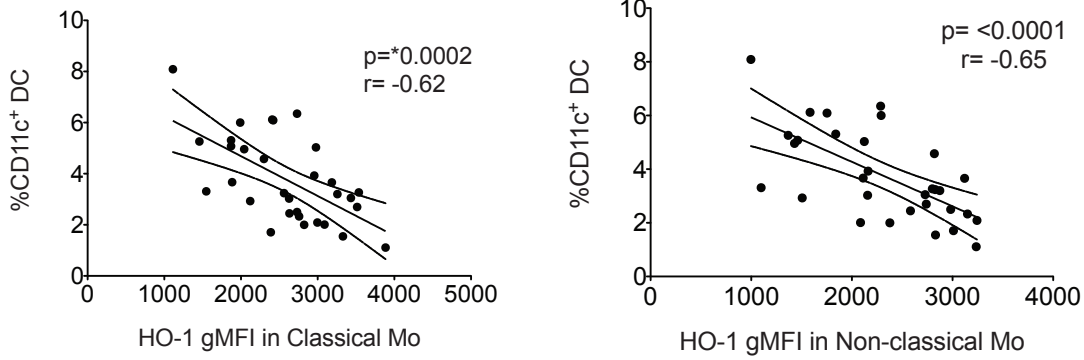

Figure 4a

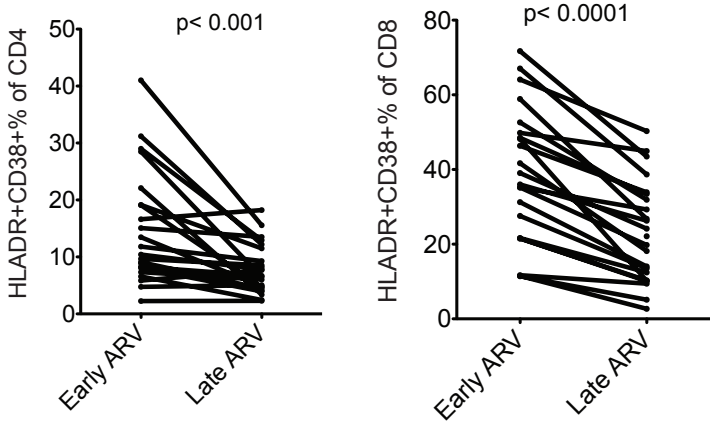

Figure 4b

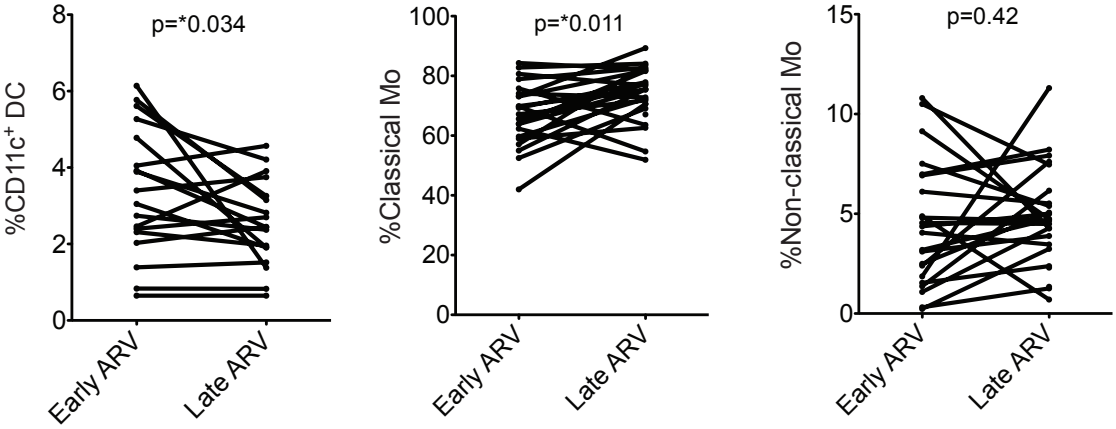

Figure 5a

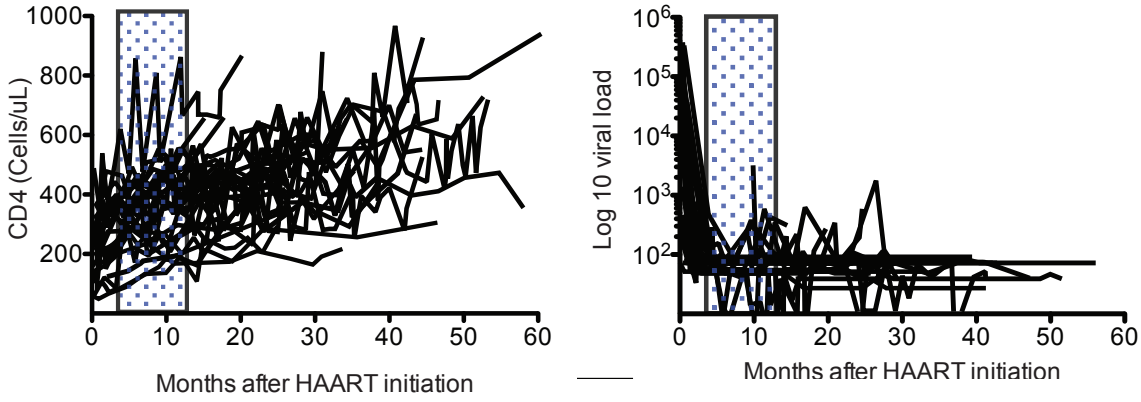

Figure 5b

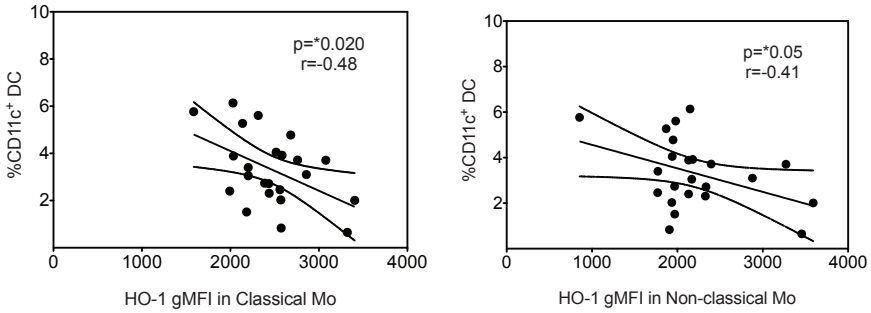

Figure 5c

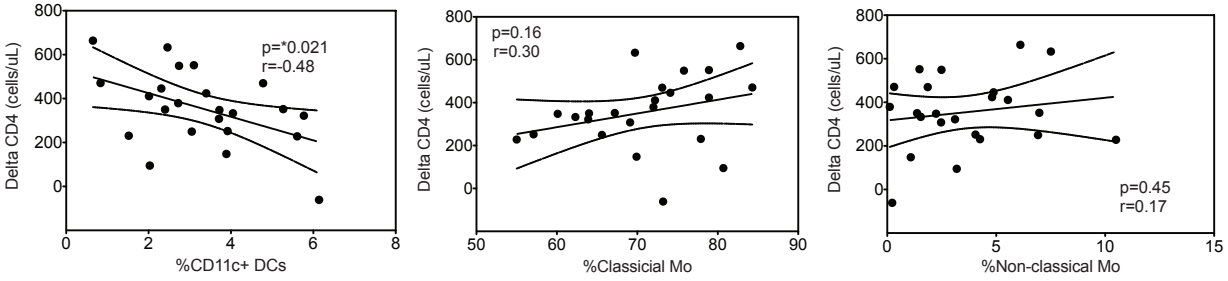

Figure 5d

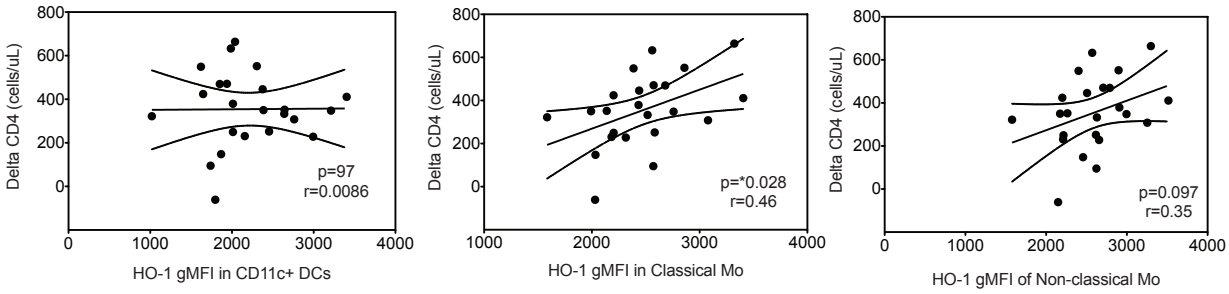

Figure 6a

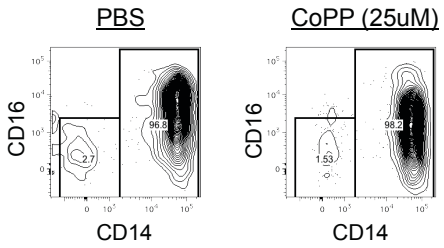

Figure 6b

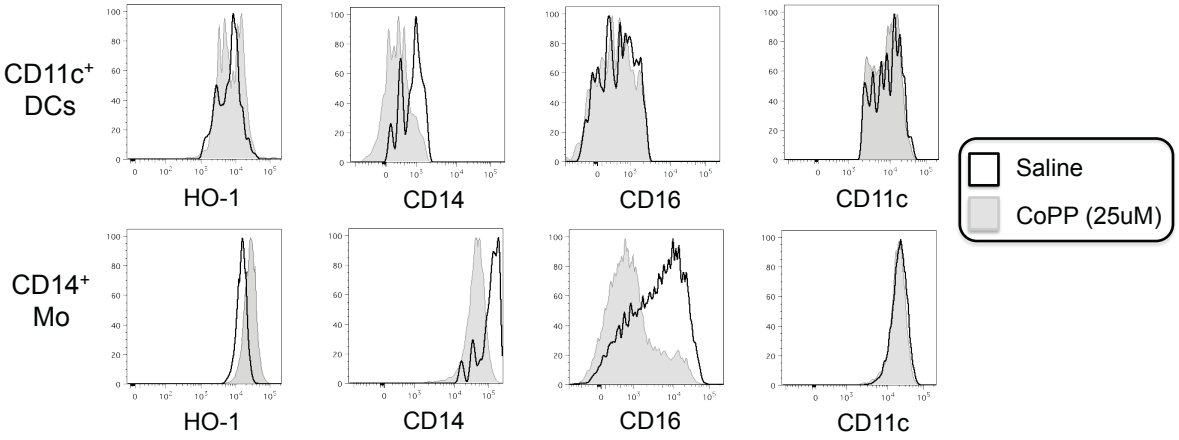

Figure 6c

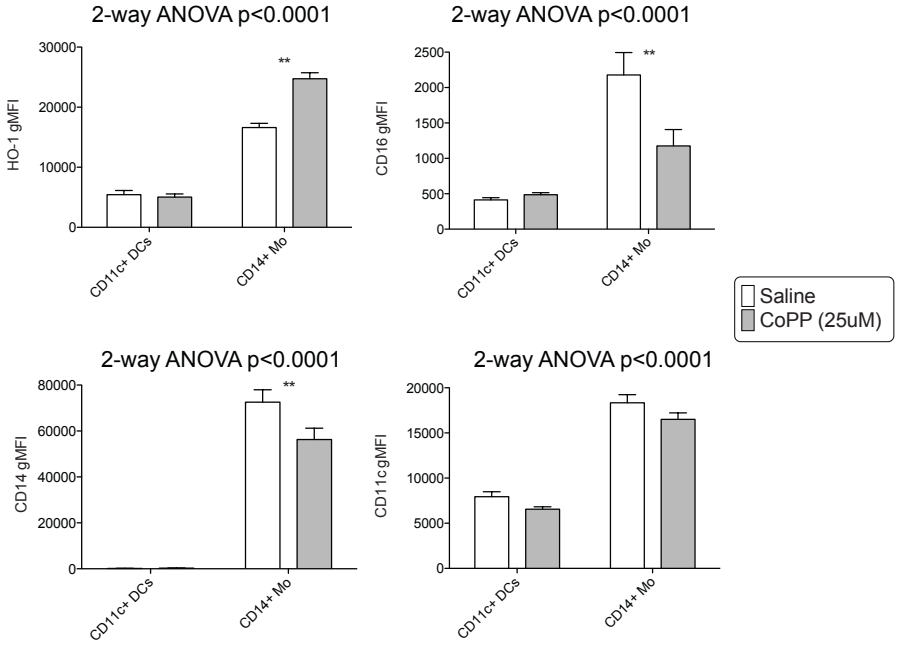

Supplementary Figure 1a

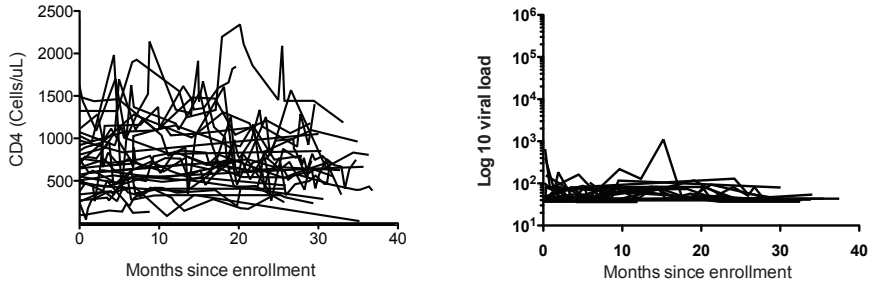

Supplementary Figure 1b

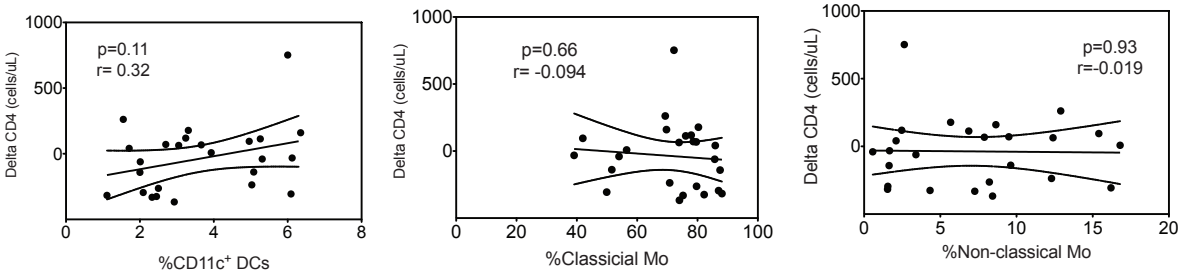

Supplementary Figure 1c

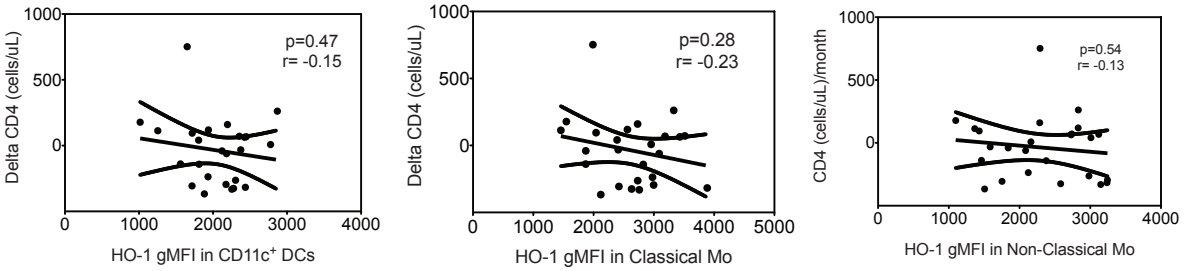

Supplemental Table 1a: Biomarkers predictive of CD4 reconstitution in early HAART patients

Correlation with Delta CD4	Patients	Pearson r	p value (2-tailed)
Blood myeloid cells			
CD14hi	23	0.3028	0.1602
CD14dimCD16+	23	0.1659	0.4494
CD14+CD16+	23	0.11	0.61
CD14-CD16-	23	-0.4781	*0.021
HO-1 in CD14hi	23	0.46	*0.028
HO-1 in CD14dimCD16+	23	0.35	0.097
HO-1 in CD14+CD16+	23	0.12	0.59
HO-1 in CD14-CD16-	23	0.0086	0.97
Th17/T regulatory cells			
Th17% of CD4+ T cells	18	-0.01	0.97
Tregs of CD4+ T cells	17	-0.1544	0.554
Th17/Treg	17	0.1795	0.4906
K/T ratio	28	-0.3485	0.0691
T cell anergy and activation			
FCRL3 Treg	17	0.166	0.5242
FCRL3 CD4	17	0.4367	0.0797
FCRL3 CD8	17	0.632	*0.0065
PD-1 on CD4	24	-0.0328	0.8791
PD-1 on CD8	24	0.2289	0.2821
HLADR+CD38+ on CD4	22	0.09339	0.6793
HLADR+CD38+ on CD8	22	0.142	0.5284

Supplemental Table 1b: Biomarkers predictive of CD4 preservation in HIV Elite Controllers

Correlation with Delta CD4	Patients	Pearson r	p value (2-tailed)
Blood myeloid cells			
CD14hi	25	-0.094	0.66
CD14dimCD16+	25	-0.019	0.93
CD14+CD16+	25	-0.025	0.91
CD14-CD16-	25	0.32	0.11
HO-1 in CD14hi	25	-0.23	0.28
HO-1 in CD14dimCD16+	25	-0.13	0.54
HO-1 in CD14+CD16+	25	-0.093	0.66
HO-1 in CD14-CD16-	25	-0.15	0.47
Th17/T regulatory cells			
Th17% of CD4+ T cells	28	0.4	*0.037
Tregs of CD4+ T cells	22	-0.14	0.54
Th17/Treg	22	0.62	*0.002
K/T ratio	25	-0.2	0.35
T cell anergy and activation			
FCRL3 Treg	22	0.24	0.29
FCRL3 CD4	22	0.35	0.11
FCRL3 CD8	22	0.19	0.39
PD-1 on CD4	28	0.37	0.054
PD-1 on CD8	28	0.11	0.59
HLADR+CD38+ on CD4	28	0.02	0.9
HLADR+CD38+ on CD8	28	-0.009	0.97

Supplemental Figure 1

(a) $CD4^+$ T cell preservation was measured by taking the last CD4 measurement and subtracting the baseline $CD4^+$ T cell count (cells/uL) from elite controllers followed longitudinally (Table 1c). Plasma viral load measurements (p24 RNA copies/milliliter) are depicted in the corresponding graph. **(b)** Myeloid populations ($CD11c^+$ DCs, classical monocytes, and non-classical monocytes) were correlated to the delta CD4 levels. There was no correlation between $CD11c^+$ DCs and delta CD4 ($r=0.32$, $p=0.11$), the classical monocytes ($r=-0.094$, $p=0.66$), or non-classical monocytes ($r=-0.019$, $p=0.93$). **(d)** HO-1 gMFI was measured and correlated to the delta CD4 levels. There was no correlation between HO-1 gMFI in $CD11c^+$ DCs and delta CD4 ($r=-0.15$, $p=0.47$), the classical monocytes ($r=-0.23$, $p=0.28$), or non-classical monocytes ($r=-0.13$, $p=0.54$). Pearson's correlation coefficient p is reported with its corresponding P-value.

Supplementary Figure 1a

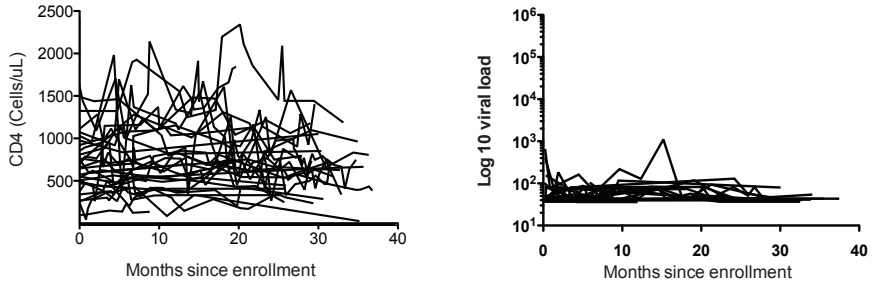

Supplementary Figure 1b

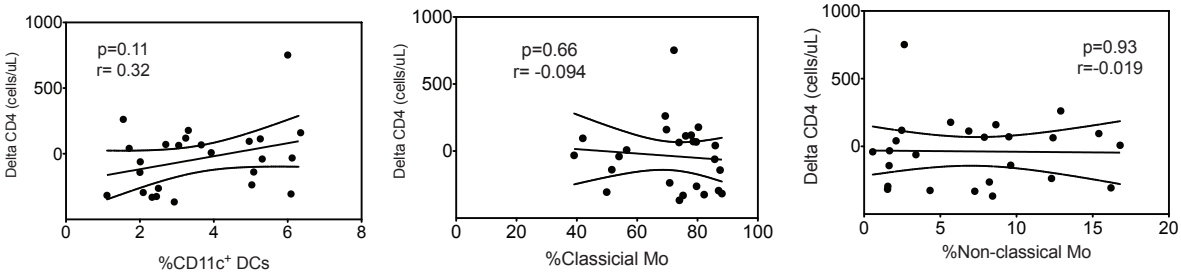

Supplementary Figure 1c

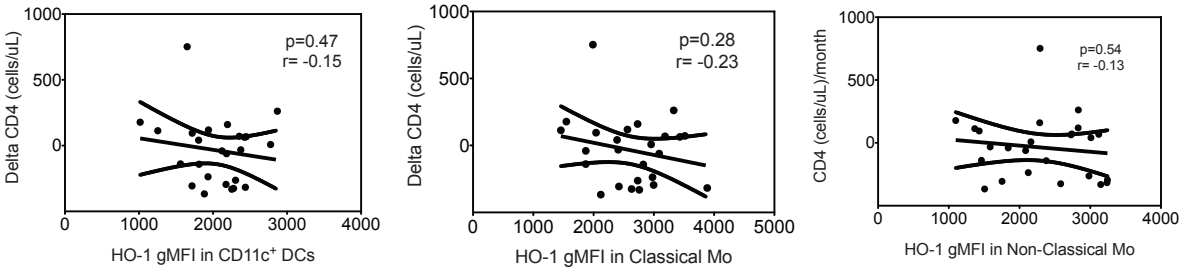

IV

Inhibition of heme oxygenase-1 in SIV-infected African Green Monkeys causes increased immune activation and viremia

San Francisco Gay Pride Parade 2011:

Positive Health Program float (Lineup #134)

Title: Inhibition of heme oxygenase in SIV-infected AGMs causes increased immune activation and viremia

Trevor D. Burt, **Lillian Seu**, Rebecca Botelho, David Favre, Yong Hong, Richard M. Dunham, Kristina Abel, Atallah Kappas, Joseph M. McCune (In Preparation)

Abstract:

Background

African Green Monkeys (AGMs) are non-human primates that are able to effectively control the inflammation that leads to worsened SIV disease progression. We hypothesized that inhibition of the anti-inflammatory stress response enzyme, HO-1, during SIV infection of these animals would subsequently lead to greater SIV disease.

Methods

AGMs were treated with the HO-1 inhibitor, tin mesoporphyrin, SnMP (5 animals) or saline (3 animals) longitudinally and then infected with Simian Immunodeficiency Virus (SIV) to determine the effect of HO-1 inhibition on viral pathogenesis.

Results

SnMP-treated animals were found to have a higher peak viral load during seroconversion and higher levels of T cell activation (CD8+ Ki-67% and HLA-DR%), consistent with the hypothesis that HO-1 activity normally plays a role in suppressing disease progression in this species. Interestingly, SnMP treated animals had higher absolute CD4+ T cell counts during SIV infection

Conclusions

Our results demonstrate that HO-1 inhibition leads to enhanced T cell proliferation and activation as well as viral replication. These events may lead to heightened T cell proliferation that may then lead to greater numbers of CD4 T cells. Further studies must be conducted to determine the maturation and functional capacity of these cells.

Introduction

Studies in non-human primates (NHP) and in infected humans have revealed that inflammation during SIV/HIV infection is tightly correlated with the generation of pro-inflammatory cytokines (1), T cell activation (2), increased microbial translocation of lipopolysaccharide products from the gut flora (3), and increased frequencies of inflammatory monocyte populations (4,5).

For instance, in some NHP species (e.g., the AGM, sooty mangabey, and chimpanzees), SIV infection is non-pathogenic and is consistently associated with lower levels of bystander immune activation than in species that develop pathogenic SIV disease (e.g., pigtail or rhesus macaques) (6). In one study, necropsy samples from SIV-infected pigtail macaques displayed increased expression of Ki67, a marker of cell proliferation and activation, compared to SIV-infected AGMs (7). These studies suggest that increased immune activation during the chronic stage of HIV and SIV infection can contribute to disease pathogenesis, and are consistent with the fact that the pro-inflammatory environment during chronic infection leads to the promotion of anergy and apoptosis of activated T lymphocytes as well as to increased proviral transcription via the transcription factors NFkB and NF-AT (8).

AGMs are natural non-human primate hosts of SIV that do not normally show

disease progression (9). A recent study experimentally induced immune activation in AGMs with LPS and with a Treg inhibitor (Ontak: Diphtheria toxin-Interleukin-2 fusion protein). In this study, animals treated with LPS had a minor transient increase in viral load as well as an increase in $CD4^+$ and $CD8^+$ T cells that were $Ki67^+$ (10).

Based on our prior discoveries in mice and humans showing that HO-1 pharmacological inhibition leads to enhanced T cell proliferation and activation as well as altered antigen-presenting capabilities of APCs (11), we sought out to determine how such inhibition might influence virological and immunological consequences in a non-pathogenic animal model of HIV infection. AGMs were treated with SnMP (5 animals) or saline (3 total) , and then infected with SIV longitudinally to determine the effects of HO-1 inhibition on viral pathogenesis. SnMP-treated animals were found to have a higher peak viral load during seroconversion and higher levels of T cell activation (CD8+ Ki-67% and HLA-DR%), consistent with the hypothesis that HO-1 activity normally plays a role in suppressing disease progression in this species. Interestingly, SnMP treated animals had higher absolute CD4+ T cell counts during SIV infection

Methods:

Viral load assay

Viral RNA was purified from plasma using QIAmp Viral RNA mini kit (Qiagen, Valencia, CA). An aliquot of EDTA plasma was isolated and eluted into known volumes so that later viral load calculations could be made. SIVagm.sab92018 RNA standards were produced *in vitro* (SP6/T7 transcription kit, Roche, Applied Science,

Indianapolis,IN) from the LTR template made out of RNA extracts of SIVagm.sab92018(#800) by RT-PCR (primers T7-LTR-4S (5' - TAA TAC GAC TCA CTA TAG GGA GAA CTG GGC GGT ACT GGG AGT GGC TT - 3') and LTR-2A (5' - ACC TAA GGC AAG ACT TTA TTG AGG - 3') from IDT), and subsequently purified (QIamp Viral RNA kit), DNA treated (Ambion) and controlled for RNA weight and purity (Nanodrop). RNA standards were made taking into account the mass of the amplicon (http://www.unitconversion.org/unit_converter/weight-ex.html) and the concentration of the sample (measured on Nanodrop).

RNA viral loads in plasma and tissues were measured by real-time quantitative PCR (ABI PRISM 7700, Applied Biosystem Foster City, CA) in a one step RT-PCR reaction (HoTaq One Step-RT PCR Mix; Molecular Cloning Laboratories, South San Francisco, CA). Primers and probe are: LTR - 5' J15S (5'-CTC GGT GTT CTC TGG TAA G-3'), 3' J15S (5'-CAA GAC TTT ATT GAG GCA AT-3'), and 15s probe (5'-FAM-CGA ACA CCC AGG CTC AAG CTG G-TAMRA-3') [all RNase-free and HPLC-purified products from Integrated DNA Technologies (Coralville, IA)].

Processing of cells for flow cytometry

Simian PBMCs were isolated from whole blood drawn into sodium heparin tubes by density centrifugation using Histopaque®-1077 (Sigma Aldrich, Saint Louis, MO), Cells were counted on a hemacytometer to allow for uniform antibody staining for flow cytometry. All cells were stained with a live/dead marker Amine-Aqua/Am-Cyan Live/Dead to exclude dead cells from analysis. For flow cytometry analysis, cells were washed in staining buffer [PBS with 2% FBS and 2 mM ethylenediamine tetra-acetic acid

– EDTA] and then incubated for 30 minutes at 4°C in the presence of directly-conjugated fluorescent mAbs. All cells were stained with a live/dead marker (Amine-Aqua/Am-Cyan Live/Dead; Invitrogen) so that dead cells could be excluded from analysis. The cells were washed in staining buffer, and then fixed and permeabilized in Becton Dickinson Cytofix/Cytoperm according to the manufacturer's protocol for intracellular staining. Data were acquired with an LSR-II flow cytometer (BD Biosciences) and analyzed with FlowJo software (Treestar, Ashland, OR).

Flow cytometry panel: T cell activation

Extracellular staining: the following antibodies were ordered from BD Biosciences (concentration, clone): CD3-Pacific Blue (concentration 1:100, clone SP34-2), HLA-DR PeCy7 (1:100, M-A251), CD38 APC (1:50, HB7); from Biolegend: CD4 APCCy7 (1:25, Sk3); from Beckman Coulter: CD14 ECD (1:50, 2H4); from Invitrogen: Live Dead - AmCyan (final 1:300), CD8 Pecy5.5 (final 1:200, 3b5)

Intracellular staining: The following antibodies were ordered from BD Biosciences: Ki67-FITC (1:150, B56); and from Stressgen: HO1 488 (1:50, 5090725)

Flow cytometry panel: Trucount staining of whole blood

To determine the absolute numbers of leukocyte populations in the blood of the treated animals, the BD Biosciences Trucount tubes were used (catalog # 340334). The protocol for FACS lyses were followed after incubation of the whole blood with the following antibodies.

The following antibodies from BD Biosciences were used: CD3-Pacific Blue (concentration 1:100, clone SP34-2), HLA-DR PeCy7 (1:100, M-A251), CD4 APC (1:25, Sk3), CD19 PE (1:25, HIB19); from Beckman Coulter: CD45RA ECD (1:50, 2H4); from Invitrogen: Live Dead - AmCyan (final 1:300), CD8 Pecy5.5 (final 1:200, 3b5); from eBiosciences: CD27 APC-A750 (1:100, O323)

Results:

AGMs nfected with Simian Immunodeficiency Virus (SIV) were treated with SnMP (5 animals) or with saline (3 animals) longitudinally to determine the effects of HO-1 inhibition on viral pathogenesis (Figure 1).

SnMP-treated animals were found to have a mean log10 peak viral of 1 greater than saline-treated animals that started at the acute stage of infection (days 3-21) and persisted into the chronic phase of infection until necropsy (days 3- 140) (Figure 2).

Interestingly, SnMP treated animals had different absolute CD4+ T cell counts during SIV infection than Saline treated animals as measured by repeat-measures ANOVA analysis (Figure 3). In support of our previous findings that HO-1 pharmacological inhibition leads to enhanced T cell activation, proliferation, and maturation in mice and humans (11), SnMP-treated animals displayed higher T cell activation (CD8+ Ki-67% and HLA-DR%) (Figure 4). The proliferation of CD8+ T cells occurred prior to SIV infection, and is consistent to what is observed in the murine studies. CD8+ T cell activation as measured by HLA-DR% was higher in SnMP-treated animals, and occurred after SIV infection (Figure 4). This finding supports the results from our study in human

peripheral immune cells: PBMCs cultured with SnMP led to enhanced T cell proliferation as measured by CFSE dye incorporation into proliferated subsets.

Table 1: Total CD4 cells/uL of blood

DATE (From timepoint of SIV infection)	SnMP (cells/uL)	Control (cells/uL)	Bonferroni post-test
0.0	158.2	105.5	P > 0.05
3.000	109.9	79.7	P > 0.05
9.000	99.1	75.79	P > 0.05
17.00	89.15	58.85	P > 0.05
28.00	68.6	57.53	P > 0.05
56.00	80.56	43.15	P > 0.05
86.00	115	76.35	P > 0.05
112.0	112.7	85.18	P > 0.05
140.0	118.5	76.23	P > 0.05
200.0	133.4	69.33	P > 0.05

Discussion:

This study showed that the HO-1 inhibitor, SnMP, was effective in increasing parameters of progressive disease: enhanced viral loads and T cell proliferation and activation. Interestingly, absolute CD4+ T cell counts were higher in SnMP-treated animals.

Although absolute CD4+ T cell counts are currently used as the primary clinical outcome measure for assessing HIV disease progression, understanding the quality and the type of cells that are newly proliferating during disease progression is important for projecting the disease course. For example, certain situations where there is a rapid increase of CD4+ T cells after initiation or change of an ARV regimen is termed Immune Reconstitution Inflammatory Syndrome (IRIS). IRIS is a term used to describe the paradoxical worsening or unmasking of infections or tumors after antiretroviral therapy (ART) initiation. Patients developing IRIS episodes displayed higher frequencies of effector memory, PD-1^+, HLA-DR^+, and $Ki67^+$ $CD4^+$ T cells than patients without IRIS and higher serum interferon-γ (12). Therefore, careful phenotyping of the type different T cell subsets that are increased in SnMP-treated animals in the context of SIV infection can address the true effects of this treatment.

References

1. Manches O, Bhardwaj N. Resolution of immune activation defines nonpathogenic SIV infection. J Clin Invest 2009, Dec;119(12):3512-5.

2. Barbour JD, Ndhlovu LC, Xuan Tan Q, Ho T, Epling L, Bredt BM, et al. High CD8+ T cell activation marks a less differentiated HIV-1 specific CD8+ T cell response that is not altered by suppression of viral replication. Plos One 2009;4(2):e4408.

3. Pandrea I, Apetrei C. Where the wild things are: Pathogenesis of SIV infection in african nonhuman primate hosts. Curr HIV/AIDS Rep 2010, Feb;7(1):28-36.

4. Hasegawa A, Liu H, Ling B, Borda JT, Alvarez X, Sugimoto C, et al. The level of monocyte turnover predicts disease progression in the macaque model of AIDS. Blood 2009, Oct 1;114(14):2917-25.

5. Sodora DL, Allan JS, Apetrei C, Brenchley JM, Douek DC, Else JG, et al. Toward an AIDS vaccine: Lessons from natural simian immunodeficiency virus infections of african nonhuman primate hosts. Nat Med 2009, Aug;15(8):861-5.

6. Silvestri G, Paiardini M, Pandrea I, Lederman MM, Sodora DL. Understanding the benign nature of SIV infection in natural hosts. J Clin Invest 2007, Nov;117(11):3148-54.

7. Favre D, Lederer S, Kanwar B, Ma ZM, Proll S, Kasakow Z, et al. Critical loss of the balance between th17 and T regulatory cell populations in pathogenic SIV infection. Plos Pathog 2009, Feb;5(2):e1000295.

8. Rosenberg ZF, Fauci AS. Immunology of AIDS: Approaches to understanding the immunopathogenesis of HIV infection. International Journal of Clinical & Laboratory Research 1989;19(1):189-209.

9. Lederer S, Favre D, Walters KA, Proll S, Kanwar B, Kasakow Z, et al. Transcriptional profiling in pathogenic and non-pathogenic SIV infections reveals significant distinctions in kinetics and tissue compartmentalization. Plos Pathog 2009, Feb;5(2):e1000296.

10. Pandrea I, Gaufin T, Brenchley JM, Gautam R, Monjure C, Gautam A, et al. Cutting edge: Experimentally induced immune activation in natural hosts of simian immunodeficiency virus induces significant increases in viral replication and CD4+ T cell depletion. J Immunol 2008, Nov 15;181(10):6687-91.

11. Burt TD, Seu L, Mold JE, Kappas A, McCune JM. Naive human T cells are activated and proliferate in response to the heme oxygenase-1 inhibitor tin mesoporphyrin. J Immunol 2010, Nov 1;185(9):5279-88.

12. Antonelli LR, Mahnke Y, Hodge JN, Porter BO, Barber DL, DerSimonian R, et al. Elevated frequencies of highly activated CD4+ T cells in HIV+ patients developing immune reconstitution inflammatory syndrome. Blood 2010, Nov 11;116(19):3818-27.

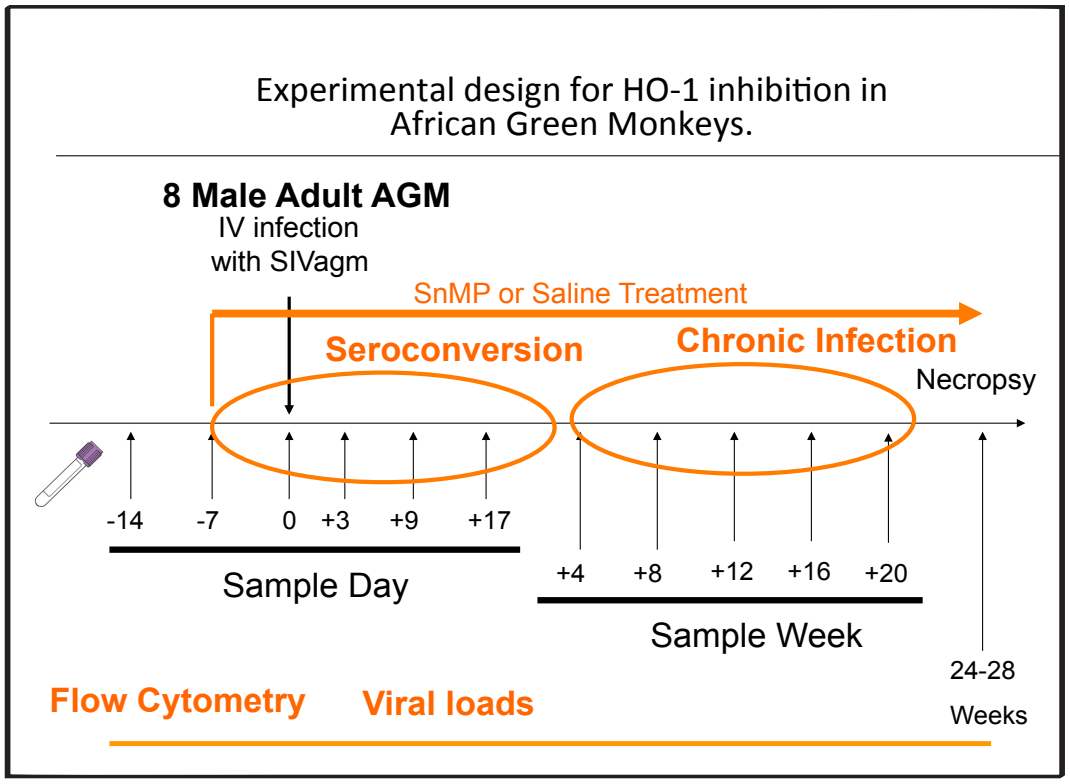

Figure 1: Schematic of drug administration in animals

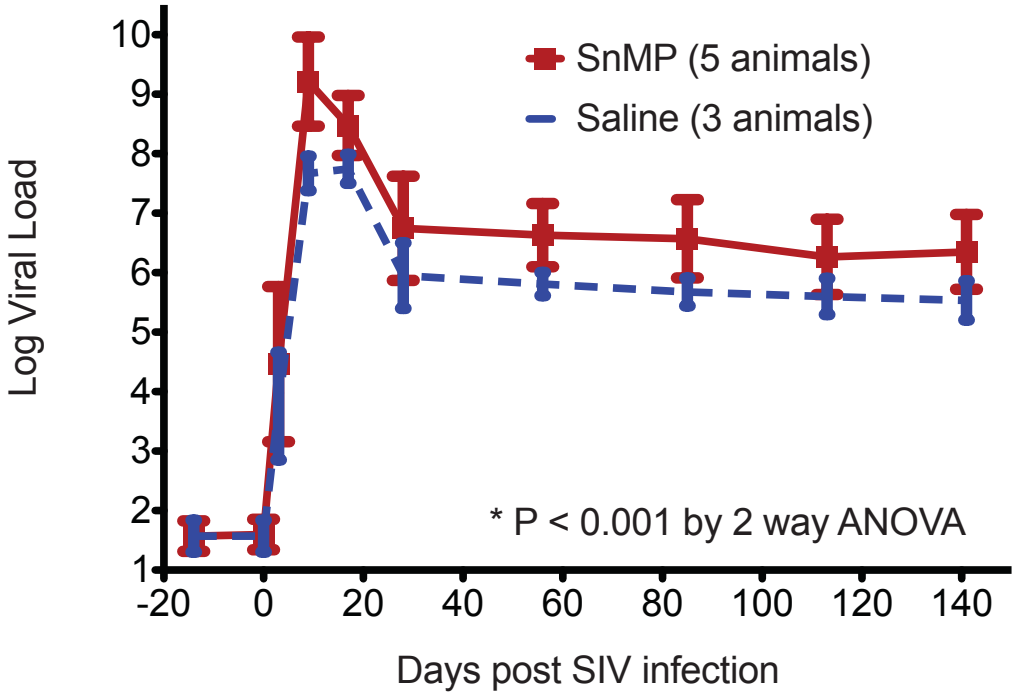

Figure 2: Viral load kinetics after SIV infection

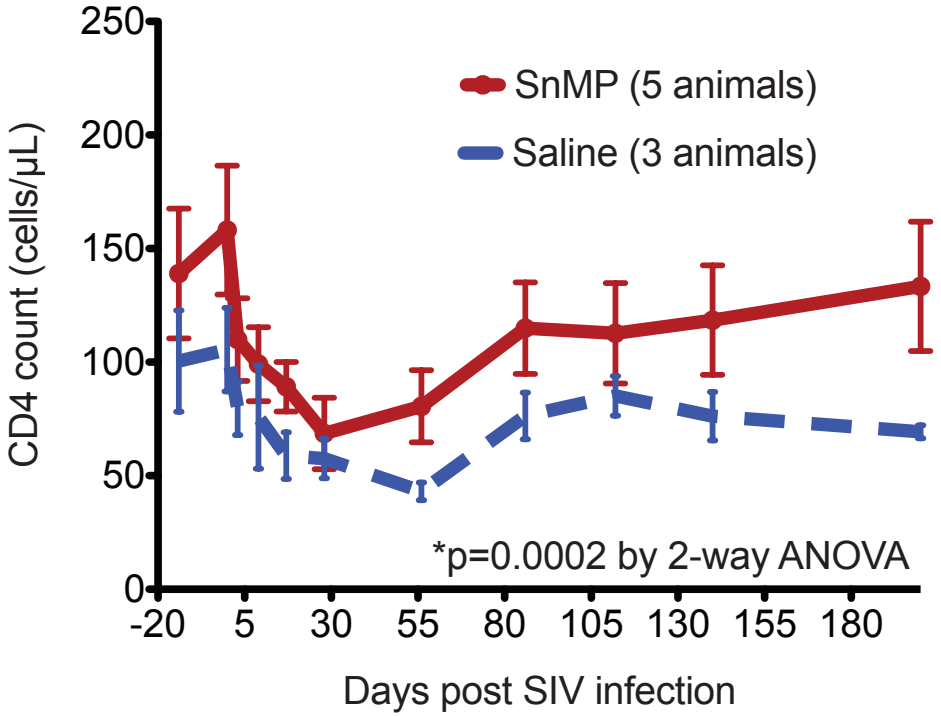

Figure 3: Absolute CD4+ T cell count (cells/uL) days post SIV infection

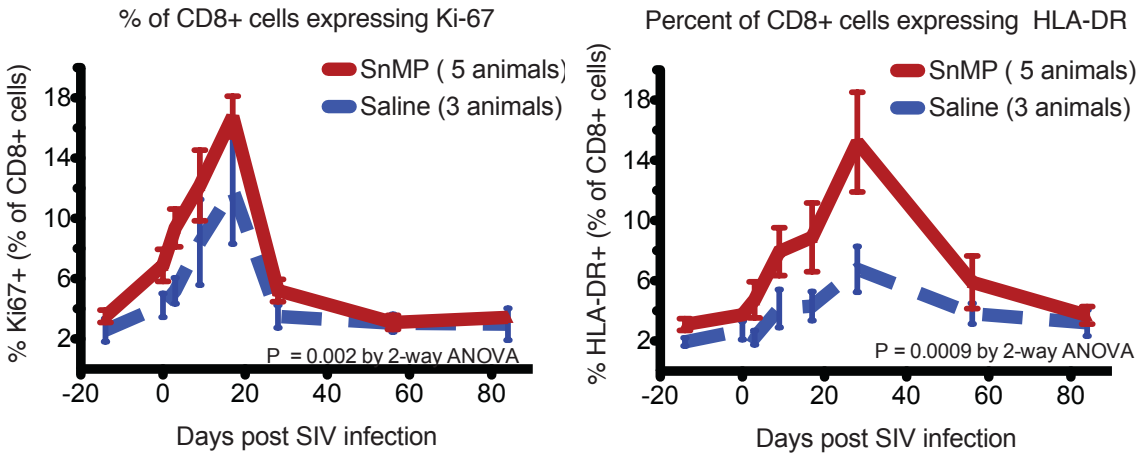

Figure 4: CD8+ T cell activation days post SIV infection

App. A

Heme oxygenase-1 immunohistochemistry staining in colon biopsy tissue of HIV patients off therapy

Building 80, San Francisco General Hospital

Immunohistochemistry of Heme Oxygenase-1 in Human tissue

Samples: Formalin-fixed, Paraffin embedded tissues were obtained from the following sources

1) Healthy Adult Spleen: Archived in SFGH Pathology Division (slides made on June 2011)

2) Healthy Adult Colon #1: Archived in SFGH Pathology Division (slides made on April 2011)

3) Healthy Adult Colon #2: From Positive Health Program. Patient ID #1812 (slides made on May 2011)

4) Healthy Adult Colon #3: From Positive Health Program. Patient ID #1871 (slides made on May 2011)

5) Inflammatory Bowel Disease patient with severe inflammation- Tissue Resection: Archived in SFGH Pathology Division (slides made on June 2011)

6) HIV patient pre-ARV therapy PID #1415 (slides made on May 2011)

7) HIV patient pre-ARV therapy PID #1600 (slides made on May 2011)

8) HIV patient pre-ARV therapy PID #1162 (slides made on May 2011)

9) HIV patient pre-ARV therapy PID #1386 seen on April 2010 (slides made on May 2011)

10) HIV patient post-ARV therapy PID #1386 seen on December 2010 (slides made on May 2011)

Methods:

Tissues were cut and mounted onto slides by the SFGH Pathology Division. Slides were prepared using a standard immunohistochemistry protocol, with rehydration steps in ethanol,

antigen retrieval in citrate buffer with 0.1% Tween pH 6.0, a peroxidase block incubation, and a further blocking experiment with goat serum in 1% BSA. Primary antibody were used in 1% BSA in TBS. The primary antibody was a murine monoclonal from Clontech (originally Takara) for heme oxygenase-1 (clone #GTS-1). Secondary was a goat-anti-mouse Horse Radish Peroxidase antibody cocktail (Dako Inc.) Staining was visualized with DAB chromogen substrate (Dako)

Results:

1) Healthy spleen: HO-1 staining is localized mainly to the perimeter of white pulp (lymphatic nodule) within the red pulp.

2) Healthy adult colon: HO-1 expression is highly expressed in cells that are interspersed throughout the lamina propria (these cells are consistent with a "granulocytic" morphology). There is little to absent staining in the epithelial/goblet cells lining crypts, even those surrounding regions of inflammatory lymphocytic infiltrates.

3) IBD patient with severe inflammation: HO-1 staining is localized to the apical epithelial cells of crypts that are adjacent to areas of inflammatory lymphocytic infiltration. In particular, HO-1 staining is highest in epithelial/goblet cells that are proximal to these infiltrates (even within the same crypt there is decreased staining further away from the infiltrates)

4) Pre-ARV therapy patient SCOPE 1415: minimal HO-1 staining in epithelial cells. Staining in large cells that are interspersed throughout the lamina propria.

5) Pre-ARV therapy patient SCOPE 1600: minimal HO-1 staining in epithelial cells. Staining in large cells that are interspersed throughout the lamina propria.

6) Pre-ARV therapy patient SCOPE 1162: HO-1 staining in epithelial cells bordering regions of inflammatory immune infiltrates. Staining in large cells that are interspersed throughout the lamina propria.

7) Pre-ARV therapy patient SCOPE 1386: HO-1 staining in epithelial cells bordering regions of inflammatory immune infiltrates. Staining in large cells that are interspersed throughout the lamina propria.

8) Post-ARV therapy patient SCOPE 1386 (8 months later): Based on sampling tissue, there is less HO-1 staining in epithelial cells bordering regions of inflammatory immune infiltrates. Also, there is a large region of fibrotic cells, and there is HO-1 staining within this region.

Discussion

Consistent with prior analyses (1-3), HO-1 appears to be present in macrophage-like cells interspersed throughout the lamina propria of the colon in healthy human tissue. Upon conditions of inflammation, HO-1 is induced in epithelial cells lining the crypts as well as in goblet cells. Interestingly, a common phenomenon observed in an IBD patient with severe inflammation as well as in pre-ARV HIV patients was HO-1 staining in epithelial cells lining crypts adjacent to regions of immune cell infiltration. Epithelial cells that are adjacent to these regions have the most HO-1 induction, which could be the result of gene up-regulation in these cell types upon stimulation with pro-inflammatory cytokines such as IFNγ and TNFα from infiltrating immune cells. Up-regulation of HO-1 in epithelial cells may serve as a protective mechanism combatting inflammation-led epithelial barrier breakdown and apoptosis. Prior studies administering the HO-1 inhibitor tin protoporphyrin (SnPP) aggravated TNBS-induced colitis in rats (4) and reciprocally, tranilast-induced expression of

HO-1 ameliorated acute colitis in mice (5).The protective role of HO-1 in a rat model of hemorrhagic shock was analyzed, and HO-1 was significantly increased at transcriptional and protein levels in mucosal epithelial cells in the duodenum, jejunum, and colon, whereas its expression in the ileum was hardly detectable and not increased at all by the treatment. In accordance with previous findings, inhibition of HO activity by tin-mesoporphyrin (SnMP) resulted in an aggravation of hemorrhagic shock -induced tissue inflammation and apoptotic cell death as measured by increases in ISOL (DNA fragmentation using *in situ* oligo ligation) and caspase-3 expression by flow cytometry and decreases in the anti-apoptotic Bcl-2 gene (6).

Conclusion

HO-1 is up-regulated in epithelial cells of colonic crypts during conditions of inflammation (e.g., viremic HIV and IBD). Notably, this epithelial expression shows a pattern of higher staining in regions that are adjacent to inflammatory infiltrates in the lamina propria. HO-1 induction in these regions could exert its cytoprotective mechanisms by combating inflammation and apoptosis in these tissue sites. These data have implications for HIV GALT biology: up-regulation of HO-1 may be a mechanism to protect epithelial cells from destruction that ultimately leads to microbial translocation and subsequent systemic immune activation.

References

1. Becker JC, Fukui H, Imai Y, Sekikawa A, Kimura T, Yamagishi H, et al. Colonic expression of heme oxygenase-1 is associated with a better long-term survival in patients

with colorectal cancer. Scand J Gastroenterol 2007, Jul;42(7):852-8.

2. Takagi T, Naito Y, Mizushima K, Nukigi Y, Okada H, Suzuki T, et al. Increased intestinal expression of heme oxygenase-1 and its localization in patients with ulcerative colitis. J Gastroenterol Hepatol 2008, Dec;23 Suppl 2:S229-33.

3. Paul G, Bataille F, Obermeier F, Bock J, Klebl F, Strauch U, et al. Analysis of intestinal haem-oxygenase-1 (HO-1) in clinical and experimental colitis. Clin Exp Immunol 2005, Jun;140(3):547-55.

4. Wang L, Lee JY, Kwak JH, He Y, Kim SI, Choi ME. Protective effects of low-dose carbon monoxide against renal fibrosis induced by unilateral ureteral obstruction. Am J Physiol Renal Physiol 2008, Mar;294(3):F508-17.

5. Sun X, Suzuki K, Nagata M, Kawauchi Y, Yano M, Ohkoshi S, et al. Rectal administration of tranilast ameliorated acute colitis in mice through increased expression of heme oxygenase-1. Pathol Int 2010, Feb;60(2):93-101.

6. Inoue K, Takahashi T, Uehara K, Shimuzu H, Ido K, Morimatsu H, et al. Protective role of heme oxygenase 1 in the intestinal tissue injury in hemorrhagic shock in rats. Shock 2008, Feb;29(2):252-61.

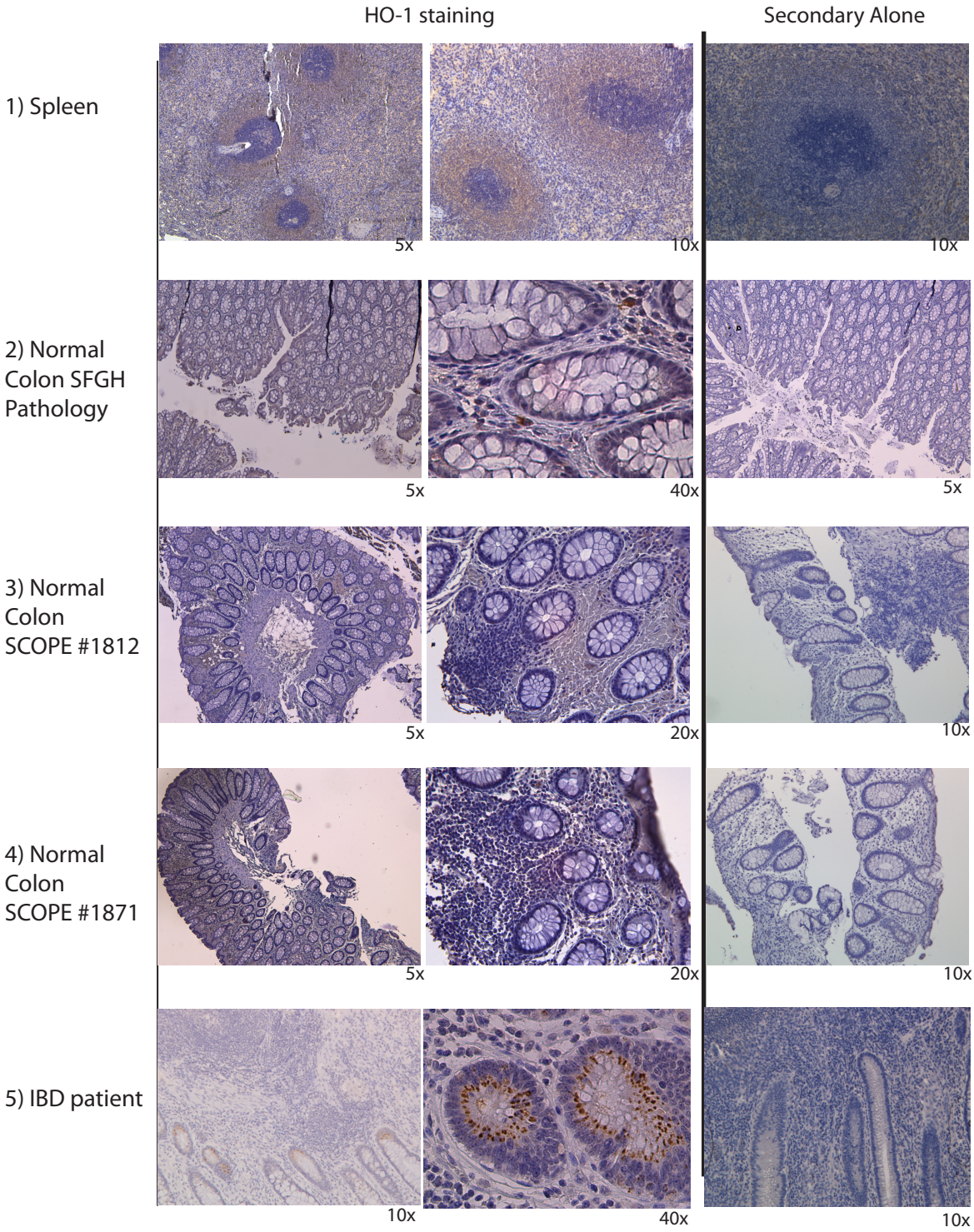
HO-1 staining
Secondary Alone
1) Spleen
5x
10x
10x
2) Normal Colon SFGH Pathology
5x
40x
5x
3) Normal Colon SCOPE #1812
5x
20x
10x
4) Normal Colon SCOPE #1871
5x
20x
10x
5) IBD patient
10x
40x
10x

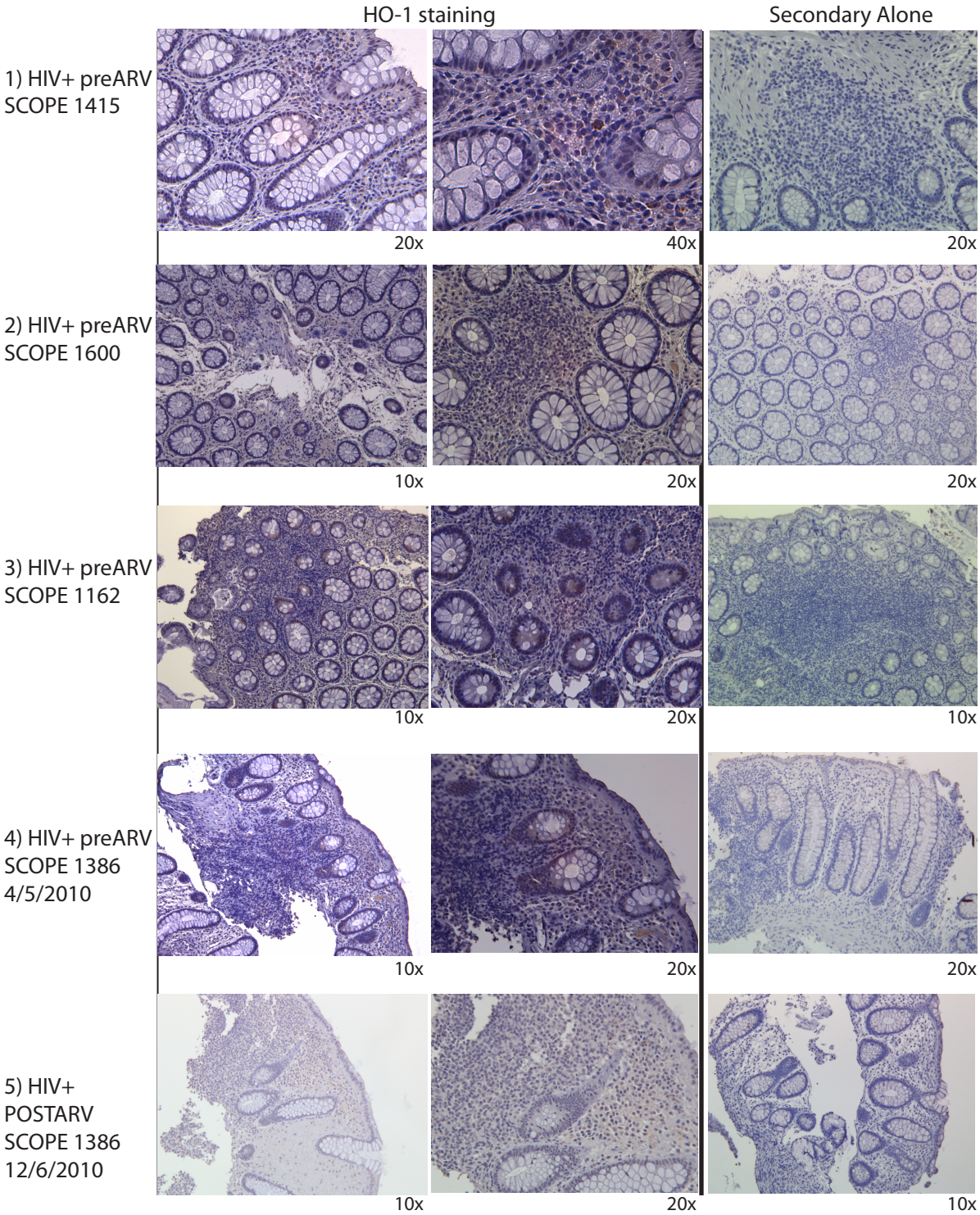
HO-1 staining
Secondary Alone
1) HIV+ preARV
SCOPE 1415
20x
40x
20x
2) HIV+ preARV
SCOPE 1600
10x
20x
20x
3) HIV+ preARV
SCOPE 1162
10x
20x
10x
4) HIV+ preARV
SCOPE 1386
4/5/2010
10x
20x
20x
5) HIV+
POSTARV
SCOPE 1386
12/6/2010
10x
20x
10x

App. B

Proposal for retrospective observational study of HO-1 promoter polymorphisms and cerebral malaria cases

Building 3, SF General Hospital

Host factors determining susceptibility to cerebral malaria- the role of HO-1 gene microsatellite polymorphisms

Research Question

Is there an association of longer Heme Oxygenase-1 genetic microsatellite polymorphisms among a cohort of patients presenting with Cerebral Malaria in Kampala, Uganda?

Significance

Cerebral malaria is a severe complication of malaria that affects up to 10% of the primarily pediatric patients infected with the P. *falciparum* parasite in regions of Sub-Saharan Africa [1]. Severe malaria in young children in malaria-endemic areas is dependent on age and level of transmission, and the risk of severe disease appears to be highest among populations exposed to low-moderate transmission. In these areas, the decreased exposure to the parasite fails to provide the same degree of partial immunity conferred by repeat infections experienced in areas of high transmission [2]. Symptoms of malaria usually start to appear 10-15 days after the bite of an infected mosquito, and can develop into a more severe form such as CM [3]. CM has potentially fatal outcomes with mortality rates of up to 18.6% [4]. The WHO clinically-defined criteria for CM is presentation with unarousable coma, exclusion of other encephalopathies, and confirmation of infection with the presence of asexual forms of P. *falciparum* demonstrated in peripheral blood. The standard of care for CM is resuscitation on admission, emergency management aims to rapidly correct severely abnormal metabolic states, and chemotherapy with anti-malarial quinines and intravenous fluids [5].

HO-1 is an inducible enzyme that metabolizes heme to its final clearance product bilirubin. In addition to its crucial role as a catabolic enzyme, HO-1 is also a potent stress-response protein and its expression can be induced by free-radical and oxidative stress as well as by increased amounts of its substrate heme [6].

HO-1 has been shown to be protective during episodes of high immune activation such as severe malaria by clearing the excess heme generated by erythrocytic turnover as well as by the generation of the immunosuppressive gas carbon monoxide. In a mouse model of experimental cerebral malaria, deletion of the *Hmox1* gene led to an increased incidence of disease [7]. The down-stream effects of HO-1 activity have been hypothesized to prevent blood-brain barrier (BBB) disruption, brain microvasculature congestion, and neuroinflammation and $CD8^+$ T-cell brain sequestration. Furthermore, genetic polymorphisms in the gene promoter regulatory region of HO-1 have been shown to influence its levels of expression, particularly the (GT) dinucleotide repeat. Shorter length repeats increase transcript levels while longer repeats diminish transcript levels due to an unfavorable Z confirmation of the DNA and the ensuing hindrance of transcription factors to bind in that region. [8]

Our hypothesis is that shorter HO-1 (GT) repeats will associate with protection against incidence of CM in patients that present with uncomplicated malaria due to its subsequent cytoprotective effects. For this study, we will conduct a case-control study of patients presenting with CM and compare them to patients presenting with uncomplicated malaria. A t-test will be performed on the mean length of microsatellite repeats between case and control groups.

Study Design

Because CM is a rare disease outcome, we have decided to pursue a case-control study.

We will be recruiting children that are consulted in the Malaria Clinic in the Mulago National Referral Hospital in Kampala, Uganda. Patient histories will be recorded from the Pediatric Department that details the extent of CM. Patients that had CM will be screened from those who presented with uncomplicated malaria. Patient consent will be obtained and a small volume (1-2 cc) of peripheral blood will be drawn for further genomic DNA isolation and PCR analysis of HO-1 alleles.

Subjects

1) Target and accessible populations:

The target population includes all children ≤5 years old who are native to Kampala, Uganda, and who have experienced episodes of CM.

The accessible population is pediatric patients ≤5 years old and will be recruited from the Malaria Study Clinic in the outpatient Malaria Clinic of the Mulago National Referral Hospital in Kampala, Uganda. In 2004, it was reported that about 20,000 children annually were admitted through the pediatric emergency unit of the hospital, of whom about 30% have malaria [9]. We hope to minimize the levels of genetic admixture by targeting individuals in this close geographical region, for purposes of the genotyping analysis.

2) Sampling:

We will use the WHO guidelines for diagnosing CM in patients admitted with malaria: the presence of unarousable coma by a Blantyre coma score of ≤2, exclusion of other encephalopathies, and confirmation of *P. falciparum* infection by the detection of asexual

parasites in the peripheral blood. Control subjects will be pediatric patients ≤5 years old that present with uncomplicated malaria in the same outpatient malaria clinic.

3) Recruitment:

Of the patients that came into the Malaria Study Clinic for treatment, we will monitor the progress of the course of disease as well as have them fill out questionnaires for their demographic information, medications they are on, prior malaria exposure, and knowledge of co-infections.

4) Inclusion and Exclusion Criteria:

Inclusion:

a) Willingness to give blood and understand the genetic research component of the research project. (Parental consent and Pediatric assent)

b) Residence in Kampala, Uganda

Exclusion:

a) Race: Non-Ugandan descent

Variables

1) Predictor variables: The length of the HO-1 GT repeat as measured on a discrete interval scale (repeat length can vary in any given population from 13 to 39 repeats. See Figure 1) . Special Considerations: In the past, statistical analysis at this locus has been conducted using the Chi-Square analysis with 3 nominal variables, where repeat lengths ≤26 or >26 have been used as a cut-off to denote the presence of a "Short" or "Long" allele, respectively. Thus, genotypes were analyzed via a 3x2 Chi-Square table (S/S, S/L, L/L). I propose that the better alternative for analyzing the data is to perform a T-test to compare the means, by looking at

the repeats on an interval scale. Although this would not take into account any given individual's genotype, it would improve the power calculations and reduce the sample size necessary to see a significant outcome. The best example of this is demonstrated in Duyao et al. 1993, where the authors analyzed trinucleotide glutamine-coding repeat units shown as a linear regression model of age of onset of Huntington's disease with a Pearson's correlation. [10]

2) Outcome variable: Binary measurements of presence or absence of CM detected after the incubation period and the manifestation of the primary symptoms of malaria (impaired consciousness, non-specific fever, and generalized convulsions)

3) Confounding variables/Covariates

a) Age

b) Gender

c) P. *falciparum* parasite load

d) Treatment histories

e) Access to care

f) Co-Morbidities/co-infections

g) Prior presentation with malaria

h) Other host genetic factors that may confer protection (ie, sickle cell disease, glucose-6-phosphate dehydrogenase deficiencies)

i) History of congenital or transfusion malaria

Statistical issues

Statistical test: T-test of data collected on an ordered discrete scale (0-40 repeats)

H_0: The mean values of the Heme Oxygenase-1 repeat in patients with uncomplicated malaria will not be different than those with Cerebral Malaria

Alternative Hypothesis: The mean values of the HO-1 repeat in patients with uncomplicated malaria will be significantly different than those with CM.

Specifications

a) Effect size: 5 HO-1 GT repeats. We chose an effect size that was shown in pilot experiments by others as well as ourselves to be important functionally in *in vitro* tissue culture studies.

b) Standard Deviation: 8 HO-1 GT repeats. Estimated from genotype analysis of self-identified African Americans living in the Bay Area. The limitations of using this data set is that this population has undergone considerable genetic admixture compared to the population in Kampala, Uganda (See Figure 2).

c) Sample size: We would like to power the study to determine a minimal effect size of 5 HMOX-1 GT repeats. Using a standardized effect size (E/S) = 5/8 = 0.625. Using the usual two-tailed α=0.05 and β=0.80, and effect size described above, the sample size was estimated at 45 per group.

Pretest plans

Prior analysis of HO-1 GT repeats in the Ugandan population has not yet been carried out. Although preliminary studies of self-identified African-Americans have been conducted, this is not the most relevant population of interest. I hope to collaborate with researchers who have stored samples of DNA from Mulago Hospital patients. I anticipate that this will require a modification to the original CHR protocol from UCSF.

Quality control and data management

The assay for HMOX-1 GT microsatellite polymorphism testing is conducted with capillary electrophoresis-based DNA sequencing. The Genomic Core Facility lab at UCSF is equipped with the machinery and technology to perform these studies, and data management will be performed using standard database and statistical software (Excel, Prism, Stata). I will be blinded to any patient-identifiers, and medical records will be coded and pared down to include only the salient clinical information for the study.

Ethical considerations

Consent forms will be drafted in language that is simple to understand and detailed to include all aspects of the research questions. Patients will be required to understand that their DNA will be stored for later genotyping studies. All patients will receive treatment in the clinic, and the inquiry about research participation will be made on an outpatient basis. All patient identifying information will be removed for subsequent analysis by the researchers by the clinicians treating the patients.

Feasibility considerations (comments from Grant Dorsey, M.D., Ph.D. of UCSF and Ben A. Gyan, Ph.D. of University of Ghana)

The challenge for this particular study will be the recruitment of cerebral malaria patients. Severe cases have reduced drastically due to the introduction of artesunate based antimalarials. Depending on the objective, considering severe malaria generally (ie CM.

severe anemia, hyperparasitemia, respiratory distress) would generate enough numbers over 2 to 3 years)

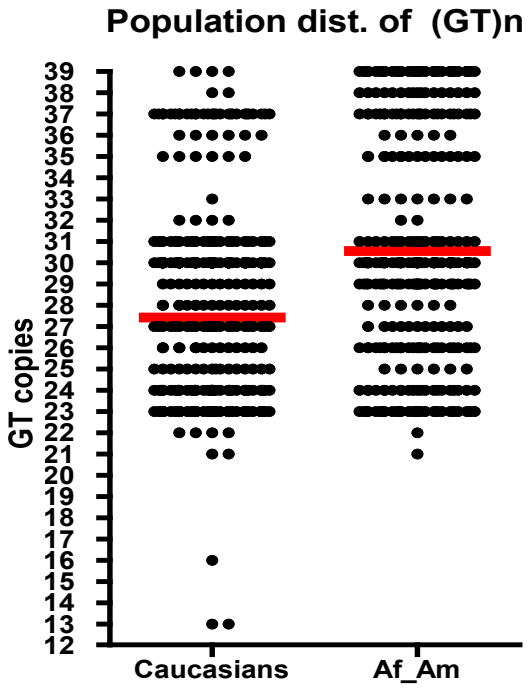

Figure 1: HMOX-1 GT repeats across two populations

References

1. Snow, R.W., et al., *The global distribution of clinical episodes of Plasmodium falciparum malaria.* Nature, 2005. **434**(7030): p. 214-7.

2. Snow, R.W., et al., *Relation between severe malaria morbidity in children and level of Plasmodium falciparum transmission in Africa.* Lancet, 1997. **349**(9066): p. 1650-4.

3. Idro, R., N.E. Jenkins, and C.R. Newton, *Pathogenesis, clinical features, and neurological outcome of cerebral malaria.* Lancet Neurol, 2005. **4**(12): p. 827-40.

4. Newton, C.R. and S. Krishna, *Severe falciparum malaria in children: current understanding of pathophysiology and supportive treatment.* Pharmacol Ther, 1998. **79**(1): p. 1-53.

5. *Severe falciparum malaria. World Health Organization, Communicable Diseases Cluster.* Trans R Soc Trop Med Hyg, 2000. **94 Suppl 1**: p. S1-90.

6. Ryter, S.W., J. Alam, and A.M. Choi, *Heme oxygenase-1/carbon monoxide: from basic science to therapeutic applications.* Physiol Rev, 2006. **86**(2): p. 583-650.

7. Pamplona, A., et al., *Heme oxygenase-1 and carbon monoxide suppress the pathogenesis of experimental cerebral malaria.* Nat Med, 2007. **13**(6): p. 703-10.

8. Exner, M., et al., *The role of heme oxygenase-1 promoter polymorphisms in human disease.* Free Radic Biol Med, 2004. **37**(8): p. 1097-104.

9. Idro, R. and J. Aloyo, *Manifestations, quality of emergency care and outcome of severe malaria in Mulago Hospital, Uganda.* Afr Health Sci, 2004. **4**(1): p. 50-7.

10. Duyao, M., et al., *Trinucleotide repeat length instability and age of onset in Huntington's disease.* Nat Genet, 1993. **4**(4): p. 387-92

App. C

Training in Clinical Research course: Proposal for randomized clinical trial of an HO-1 inducer in HAART patients

View of Sutro Tower from Building 3 of SF General Hospital

Increasing HAART-Induced Immune Restoration With Metalloporphyrins

Hypothesis and motivation for study:

Since high levels of immune activation are predictive of progressive HIV disease (1), host immunoregulatory factors that blunt immune activation may contribute to delayed disease progression. Heme oxygenase-1 (HO-1), the rate-limiting enzyme in heme catabolism, is a potent anti-inflammatory protein that may represent one such factor (2).

Immunological Non-responders (INRs) are HIV patients that fail to restore CD4 counts above a level of 500 cells/uL despite years of suppressive HAART. Based on large cohort studies, INRs represent about 30% of HAART patients (3,4). More specifically, one publication reported that 44% of HIV+ individuals who started therapy with a $CD4^+$ cell count of 100 cells/mm3 and 25% of those with 100-200 cells/mm3 were unable to achieve a $CD4^+$ cell count >500cells/mm3 by year 10 (3).

One measurable clinical feature seen in INRs is persistent T-cell hyperactivation and dysfunction. One report shows that T cell activation (cell surface marker expression of lymphocyte activation markers CD38 and HLADR) is associated with lower CD4+ T gains in HIV patients despite sustained viral suppression (median $CD4^+$ T cell count prior to HAART =210 cells/mm^3)

We propose an RCT using metalloporphyrin compounds that are known to alter the activity of HO-1 (5,6). The metalloporphyrin heme (synthesized endogenously and obtained through diet) and the xenobiotic cobalt protoporphyrin IX (CoPP) have been shown to induce greater levels of HO-1 expression from *in vivo* and *in vitro* studies (7,8). The first randomized control clinical study using hematin to induce HO-1 expression increased plasma

HO-1 protein concentration four- to fivefold and HO-1 activity ~15-fold relative to baseline at 24 and 48 h in treated patients (9). Another randomized control trial showed that administration of haem arginate led to increased HO-1 mRNA and protein over 48 hours (10)

We hypothesize that efficient up-regulation of HO-1 is associated with enhanced CD4 recovery in HIV patients undergoing HAART.

1. Research question

Does administration of Iron protoporphyrin IX enhance CD4 recovery among HIV immunological non-responders receiving (HAART)?

2. Type of randomized trial design

Randomized Interventional Trial (double-blinded)

a) Allocation: Randomized

1) Subject blinding: For the control participants, they will be receiving weekly IV injections in addition to their current HAART regimen that will be equivalent in color/ odor to the metalloporphyrin treatment.

2) Experimenter blinding: Physicians will be blinded to the treatment that is administered to the patients. Solutions will be made up prior to the patient visit and administered by blinded nurse/physicians

b) Endpoint Classification: Safety/Efficacy Study

c) Intervention Model: Treatment versus Placebo Assignment

1) HAART (2 nucleoside RT inhibitors + 1 protease inhibitor)

2) HAART (2 nucleoside RT inhibitors + 1 protease inhibitor)+ Hematin 3 mg/kg/week during the study duration

3. Subjects (target and accessible populations) and inclusion/exclusion criteria

a) Population: Projected n= 50 patients in each arm of intervention

Target population: HIV+ patients with CD4 T cell counts ≤ 500 cells/mm^3 (≥18 years old) on HAART

Accessible population: HIV+ patients with CD4 T cell counts ≤ 500 cells/mm^3 (≥18 years old) on HAART from HIV clinics in San Francisco (SF Veteran Affairs Medical Hospital and SF general hospital).

b) Inclusion/Exclusion Criteria:

Inclusion criteria:

1) Clinical status: HIV infected

2) Have a CD4 cell count between 100 cells/mm^3 and 500 cells/mm^3 within 30 days prior to study entry

3) Already initiated on HAART (2 nucleoside RT inhibitors + 1 protease inhibitor)

4) Have a viral load <1000 copies/ml within 30 days prior to study entry.

Exclusion:

1) Have an AIDS-related infection within 1 year of study entry.

2) Are pregnant or breast-feeding.

3) Weigh less than 88 lbs (40 kg).

4) Are allergic or sensitive to study HAART or porphyrins

5) Abuse drugs or alcohol.

6) Have autoimmune disease requiring immunosuppression.

7) Have kidney disease or insufficiency.

8) Have uncontrolled hypertension.

c) Control group:

We anticipate that findings from this study will allow for altered treatment guidelines for HIV+ Immunologic Non-responders that will include a co-administration of metalloporphyrins along with the standard HAART combination therapy. Due to the type of indication that we would like to develop, the control arm will be the cohort receiving the standard HAART regimen (i.e., there will be no control arms receiving metalloporphyrin only)

d) Maximization of adherence:

- Increase access to services such as health/sex education, syringe exchange services, peer counseling and group sessions, and monetary compensation for time/effort to enroll in the study
- Increase patient education to the disease
- Increase patient education to the phenomenon of Immunologic Non-response (and how it is particularly relevant to aging populations
- Create newsletters of the recent discoveries in the field as well as a "lay-man" essay of a peer-reviewed science manuscript that highlights the most

important findings.

- Hold a weekly or monthly seminar that brings together all of the clinicians, scientists, and patients to have a "town-hall" style meeting where patients get a detailed timeline of the research that will be conducted (and a rationale for the study) where the patients can act almost as a review board for the studies that they deem important and relevant.
- Incentivize the visits by sending birthday and holiday cards, and phone messages
- Technology-based clinic-visit reminders: email, text message, smartphone application
- Peer/focus groups to incentivize patients to talk about their condition as well as increase their knowledge of the disease.
- Holiday-related events that brings together all of the patients and the staff (mural-painting, potlucks, and raffles)

4. Outcome measures:

a) Primary: The change in CD4 count from baseline CD4 levels. CBC (complete blood count) will be recorded, viral loads measured (p24 RNA in plasma) and whole blood will be drawn from the following time points:

1) Baseline visit

2) 1 month

3) 3 months

4) 6 months

5) 1 year

b) Secondary (lab assays):

1) Parameters of generalized immune inflammation:

~Plasma: levels of the coagulation protein d-dimer, C-reactive protein, Inflammatory cytokines (TNFα, IL-6, IFN α/γ)

~Immune Cells: CD4:CD8 ratio, lymphocyte proliferation (Ki67), apoptosis (AnnexinV, caspase, Bip), lymphocyte cell surface activation markers (CD38, HLA-DR, CD95), monocyte cell surface activation markers (CD16, CD86/80, CD40, HLA-DR), monocyte cell surface adhesion markers (CD11b, CD11c)

2) Functional CD4 response: Elispot assays of Gag-specific CD4 responses (IFNγ production)

3) Antioxidant capacity of plasma: FRAP assay (Ferric Reducing Antioxidant Power)

5) Safety Monitoring

a) Adverse event and side effect measures:

1) Photosensitivity of skin: Pain, blistering, and swelling of sun-exposed skin

2) Abdominal pain

3) Vomiting

4) Acute neuropathy

5) Muscle weakness

6) Seizures

7) mental disturbances (hallucinations, anxiety, and paranoia)

8) Cardiac arythmia and tachycardia

9) Constipation and diarrhea

10) Jaundice

11) Increased serum iron and ferritin

b) Plans for interim monitoring

1) Establishing stopping rules:

i) Primary outcome measure: Change in CD4 counts from baseline. Mean ΔCD4 would be compared across all 3 groups. The trial would be stopped if there was no benefit observed by month 6.

ii) Secondary outcome measures: Known potential adverse effects such as photosensitivity, neuropathy, high serum iron/ferritin would be monitored and the trial would be stopped if the levels were high.

2) Statistical testing: I would use the O'Brien and Flemming statistical method for multiple comparisons testing (small ai for test at month 1, with a final a value of 0.05)

c) Ethical issues and management

1) Risk/Benefit ratio: Subjects with an appropriate risk/benefit ratio would be enrolled. In particular, these individuals are HAART patients that are both older and

have been on medications for many years. To justify the burden of clinic visits as well as the potential adverse affects from the metalloporphyrins, the risk benefit ratio will be carefully monitored over the course of the trial. Outliers that have a high risk/benefit ratio will be dropped from the study.

2) Equipoise: If, at some point along the study, it is clearly demonstrated that metalloporphyrin-induced HO-1 expression leads to enhanced recovery of CD4 cells, it would be unethical to continue placebo administration in patients with ever-declining CD4 cells.

Bibliography

1. Deeks SG, Kitchen CM, Liu L, et al. Immune activation set point during early HIV infection predicts subsequent CD4+ T-cell changes independent of viral load. *Blood.* 2004;104:942-947.

2. Ryter SW, Alam J, Choi AM. Heme oxygenase-1/carbon monoxide: from basic science to therapeutic applications. *Physiol Rev.* 2006;86:583-650.

3. Kelley CF, Kitchen CM, Hunt PW, et al. Incomplete peripheral CD4+ cell count restoration in HIV-infected patients receiving long-term antiretroviral treatment. *Clin Infect Dis.* 2009;48:787-794.

4. Kaufmann GR, Furrer H, Ledergerber B, et al. Characteristics, determinants, and clinical relevance of CD4 T cell recovery to< 500 cells/μL in HIV type 1-infected individuals receiving potent antiretroviral therapy. *Clinical infectious diseases.* 2005;41:361-372.

5. Inoue K, Takahashi T, Uehara K, et al. Protective role of heme oxygenase 1 in the intestinal tissue injury in hemorrhagic shock in rats. *Shock.* 2008;29:252-261.

6. Zhong W, Xia Z, Hinrichs D, et al. Hemin exerts multiple protective mechanisms and attenuates dextran sulfate sodium-induced colitis. *J Pediatr Gastroenterol Nutr.* 2010;50:132-139.

7. Petrache I, Otterbein LE, Alam J, Wiegand GW, Choi AM. Heme oxygenase-1 inhibits TNF-alpha-induced apoptosis in cultured fibroblasts. *Am J Physiol Lung Cell Mol Physiol.* 2000;278:L312-L319.

8. Attuwaybi BO, Kozar RA, Moore-Olufemi SD, et al. Heme oxygenase-1 induction by hemin protects against gut ischemia/reperfusion injury. *J Surg Res.* 2004;118:53-57.

9. Bharucha AE, Kulkarni A, Choi KM, et al. First-in-human study demonstrating

pharmacological activation of heme oxygenase-1 in humans. *Clin Pharmacol Ther.* 2010;87:187-190.

10. Doberer D, Haschemi A, Andreas M, et al. Haem arginate infusion stimulates haem oxygenase-1 expression in healthy subjects. *Br J Pharmacol.* 2010.

Publishing Agreement

It is the policy of the University to encourage the distribution of all theses, dissertations, and manuscripts. Copies of all UCSF theses, dissertations, and manuscripts will be routed to the library via the Graduate Division. The library will make all theses, dissertations, and manuscripts accessible to the public and will preserve these to the best of their abilities, in perpetuity.

Please sign the following statement:

I hereby grant permission to the Graduate Division of the University of California, San Francisco to release copies of my thesis, dissertation, or manuscript to the Campus Library to provide access and preservation, in whole or in part, in perpetuity.

Author Signature

8/17/2011
Date